The Identification and Characterisation of Novel Bioactive Peptides Derived from Porcine Liver and Placenta

A thesis submitted to the University of Huddersfield in the partial fulfillment of the requirements for the degree of Doctor of Philosophy

Nicholas Anthony Pearman

I) Dedication

I dedicate this thesis to my wife Zoë Louise Pearman, and my daughter Lucia Rose Pearman. I love you both more than even science.

II) Acknowledgements

I would like to thank my supervisors, Prof Alan Smith and Prof Gordon Morris for their guidance, scientific knowledge, and especially their understanding throughout this project, and Biofac, specifically Kristoffer Tømmeraas, Elena Ronander, Peter Rørvig and Helle Rørvig for giving me the opportunity to pursue a PhD and for the financial support of Biofac. I would also like to acknowledge the specialist advice and guidance given to me from Dr Muhammad Usman Ghori, Jim Rooney, Hayley Markham, Dr Richard Bingham, Prof Barbara Conway, and Dr Richard Hughes. Finally, I would like to acknowledge Prof Denis Shields and his team who developed and maintain the Peptide Ranker resource.

Through undertaking a PhD at Huddersfield I have made some great friends who have helped me in a multitude of ways. I would especially like to thank 'The office Brits' Dr Sam Moxon and Dr Glenn Robinson, and the ever dependable Dr Kartheek Sooda.

Finally, I would like to my family for their continued love and support, Neens and John, Dan and Will, and especially my beautiful Wife Zoë, and our amazing daughter Lucia.

Anyone else, you know who you are.

III) Abstract

Bioactive peptides are short (2-50 residues) sequences of amino acids that exhibit a single or multiple activities that can have an impact on biological systems. They can be derived from a variety of sources that include dietary proteins, which release peptides during digestion via digestive proteases *in-vivo*, or they can be isolated from various sources *ex vivo* such as plant-based proteins, animal proteins, or generated as a waste by-product from the meat industry. Many peptide sequences that could be bioactive are found in inactive states in larger proteins.

The objectives of this study were twofold; firstly, the physicochemical properties and bioactivity of porcine liver and placenta hydrolysates derived from waste material generated from the meat industry were investigated. The hydrolysates were manufactured and supplied by Biofac A/C (Denmark). Secondly, a method was developed to predict the presence of bioactive peptides, which was used in the generation of novel synthetic peptides, using the Biofac hydrolysates as the source.

The introduction and literature review (chapter 1) begins with general background information on bioactive peptides, including how peptides have been developed as pharmaceutical agents, nutraceutical peptides, and the types of bioactivities that can be demonstrated in peptides. Bioactive peptides that have been investigated in the literature generally are isolated from hydrolysates of proteins from the above sources, and analysed for activities such as antioxidant activity, regulation of blood pressure, wound healing, antimicrobial, and immunomodulation. Chapter 1 discusses the use of *in silico* methods used in the literature to characterise bioactive peptides that have been isolated. The use of online resources such as databases of known bioactive peptides, and where they were isolated from, is widely used in the literature. These databases, used in conjunction with *in silico* enzyme digestion tools, can be used to generate lists of peptides that theoretically exhibit bioactivity, which can then be run through algorithms that predict the likelihood of any given sequence being bioactive. Finally, the source of the hydrolysates used in this study, and how the work undertaken can be used by Biofac to increase the value of their product is discussed.

The first results chapter (chapter 3) investigated the physicochemical properties of the Biofac hydrolysates. These factors were analysed to provide information that could be utilised in the manufacturing process, and on how the product could be further processed, such as formulation. The morphology and flow properties of the powders were analysed using microscopy, particle size analysis, and particle flow analysis. Information on the molecular properties and composition of the powders were studied by analysing the solubility and saturation point, and the determination of the amount of carbohydrates present in the samples. Finally, the molecular weight (MW) of the constituent peptides were investigated using SEC-MALS. The placenta (P1) demonstrated much greater solubility than liver (L1), followed by the heart hydrolysate (H1). The composition of L2 hydrolysate showed the highest proportion of carbohydrate (4.32%), and P1 demonstrated the least (0.62).

Chapter 4 focused on the bioactivity of the hydrolysates (L1, L2, L3, P1, and P2), and the activity of fractions derived from the L2 sample after preparative HPLC. The bioactivities investigated in this chapter were antioxidant activity (using the DPPH assay, ORAC assay, lipid peroxidation assay, and a cellular antioxidant activity assay), cell proliferation (cell counts and MTT assay) and wound healing (scratch wound assay), and an ACE inhibition assay. It was found that the liver hydrolysates performed better overall as antioxidants, while placenta performed better as anti-ACE agents. Neither sets of hydrolysates were found to influence cell proliferation or wound healing. Furthermore, the peptides, which constitute the hydrolysates, were assessed using HPLC and an MTT assay over a seven-day period and found to be stable in solution.

The final results chapter (chapter 5) addressed the development of a high throughput screening method for bioactive peptides primarily using the online resources presented by the BIOPEP database, and the bioactivity prediction algorithm, Peptide Ranker. This set of work involved the isolation of individual peptides from the hydrolysates (L2 and P2) using reverse-phase HPLC so the amino acid sequence could be discovered using tandem mass spectrometry with *de-novo* sequencing. The sequences generated from this process were then used to discover the host protein they were from. These proteins were digested *in silico* using the enzyme papain, with the resulting peptides crosschecked against

databases of known bioactive peptides. Unreported peptides were then analysed using Peptide Ranker, and subsequently, four peptides that indicated a high probability of activity were selected to be synthesised. The synthesised peptides (FWG, MFLF, FFNDA, and SDPPLVFVG) were analysed using the same techniques as in chapter 4. It was found that FWG exhibited the greatest antioxidant activity followed by MFLG with FFNDA and SDPPLVFVG not demonstrating antioxidant activity at detectable levels. MFLG was found to be the most potent ACE inhibitor, followed by FWG, then FFNDA and SDPPLVFVG. None of the peptides exhibited any wound healing or cell proliferation activity.

Chapter 6 covers the general conclusions, and future work related to the study as well as analysing the usefulness of the screening method as a tool in predicting the presence of bioactive peptides before, and after the production of hydrolysates. The use of different enzymes to generate the peptides was explored along with utilising different algorithms for the prediction of specific bioactivity to increase the chance of identifying a peptide, and characterising the bioactivity. The future work section incorporates the theoretical use of the method to identify a possible anti-ACE peptide which could potentially be found in chickpeas.

IV) Abbreviations

The common amino acids, the single and three letter codes, and notes on their structure are represented in **Table IV-1**.

Table IV-1 Amino acid single, and three letter codes with a general description for each amino acid

Amino acid	One letter code	Three letter code	Structure
Alanine	A	Ala	Neutral, nonpolar side chain
Arginine	R	Arg	Basic, polar side chain
Asparagine	N	Asn	Neutral, polar side chain
Aspartate	D	Asp	Acidic, polar side chain
Cysteine	C	Cys	Neutral, polar side chain
Glutamate	E	Glu	Acidic, polar side chain
Glutamine	Q	Gln	Neutral, polar side chain
Glycine	G	Gly	Neutral, nonpolar side chain
Histidine	H	His	Basic, polar side chain
Isoleucine	I	Ile	Neutral, nonpolar side chain
Leucine	L	Leu	Neutral, nonpolar side chain
Lysine	K	Lys	Basic, polar side chain
Methionine	M	Met	Neutral, nonpolar side chain
Phenylalanine	F	Phe	Neutral, nonpolar side chain, aromatic
Proline	P	Pro	Neutral, nonpolar side chain
Serine	S	Ser	Neutral, polar side chain
Threonine	T	Thr	Neutral, polar side chain
Tryptophan	W	Trp	Neutral, polar side chain, aromatic
Tyrosine	Y	Tyr	Neutral, polar side chain, aromatic
Valine	V	Val	Neutral, nonpolar side chain

AAPH	-	2,2′-Azobis(2-Methylpropionamidine) Dihydrochloride
Abs	-	Absorbance
ABTS	-	2,2'-Azino-Bis(3-Ethylbenzothiazoline-6-Sulphonic Acid
ACE	-	Angiotensin Converting Enzyme
AUC	-	Area Under the Curve
BSEI	-	Back Scattered Electron Image
CAA	-	Cellular Antioxidant Activity
CEC	-	Capillary Endothelial Cells
CGM	-	Complete Growth Media
CID	-	Collision Induced Dissociation
DCF	-	2′, 7′-Dichlorofluorescein
DCFD	-	2′, 7′-Dichlorofluorescein Diacetate
DCFDA	-	2′, 7′-Dichlorodihydrofluorescein Diacetate
DMEM	-	Dulbecco’s Modified Eagle Medium
DMSO	-	Dimethyl Sulfoxide
DPPH	-	1, 1-Diphenyl-2-Picrylhydrazyl (α,α-Diphenyl-β-Picrylhydrazyl
DT	-	Doubling Time
ECM	-	Extra Cellular Matrix
ETD	-	Everheart Thornley Detector
FBS	-	Foetal Bovine Serum
FFC	-	Flow Function

FPLC	-	Fast Protein Liquid Chromatography
FRAP	-	Ferric Ion Reducing Antioxidant Parameter Assay
FTC	-	Ferric Thiocyanate
GI	-	Gastrointestinal
HA	-	Hippuric Acid
HAT	-	Hydrogen Atom Transfer
HBSS	-	Hank's Balanced Salt Solution
HCl	-	Hydrochloric Acid
HEPES	-	(4-(2-hydroxyethyl)-1-piperazineethanesulfonic acid)
HHL	-	Hippuryl Histidyl Leucine
HPLC	-	High Performance Liquid Chromatography
IC50	-	Inhibitory Concentration at 50 %
LDL	-	Low Density Lipoprotein
LM	-	Light Microscopy
MW	-	Molecular Weight
MS	-	Mass Spectrometry
MS/MS	-	Tandem Mass Spectrometry
MTT	-	3-(4,5-Dimethylthiazol-2-yl)-2,5-diphenyltetrazolium bromide
NADPH	-	Nicotinamide Adenine Dinucleotide Phosphate
LC-MS/MS	-	Liquid Chromatography with Tandem Mass Spectrometry
ORAC	-	Oxygen Radical Absorbance Capacity

PBS	-	Phosphate Buffered Saline
PDL	-	Population Doubling Level
PenStrep	-	Penicillin-Streptomycin
Prep HPLC	-	Preparative HPLC
RCF	-	Relative Centrifugal Force
ROO^{+}	-	Peroxide Radical
RSA	-	Radical Scavenging Activity (RSA)
RP-HPLC	-	Reverse Phase High Performance Liquid Chromatography
RNS	-	Reactive Nitrogen Species
ROS	-	Reactive Oxygen Species
SET	-	Single Electron Transfer
SEC	-	Size Exclusion Chromatography
SEC- MALS	-	Size Exclusion Chromatography Multi-Angle Light Scattering
SEM	-	Scanning Electron Microscopy
SHR	-	Spontaneously Hypertensive Rats
TE	-	Trolox Equivalence
TFA	-	Trifluoroacetic Acid
TRIS	-	Tris(Hydroxymethyl)Aminomethane
UV	-	Ultra-Violet
UV-Vis	-	Ultra-Violet/Visible Light Spectrophotometry

V) List of Figures

Figure 1-1 Mechanisms of hydrogen atom transfer (HAT), and single electron transfer (SET)antioxidant pathways. In SET an electron is transferred to the radical from the antioxidant, generating a radical cation, which can then form a radical. In the HAT pathway a hydrogen atom is donated from the antioxidant producing a radical. 35

Figure 1-2 Simplified renin/angiotensin pathway. The active form of angiotensin II is generated by the action of angiotensin II converting enzyme (ACE) on angiotensin I. The inhibition of ACE prevents the activation of angiotensin II receptors of vascular smooth muscles, preventing contraction..... 37

Figure 1-3 The three stages of wound healing after the initial damage (a) include inflammation where cells migrate into the wound area (b), tissue formation where granulation tissue forms, which is reinforced with collagen deposited by fibroblasts (c), and the remodelling phase where the wound is healed (d). 40

Figure 1-4 Biofac procedure for the production of porcine hydrolysates. 45

Figure 1-5 Preferential cleavage site for papain 46

Figure 1-6 Possible structure of peptide resulting from hydrolysation of a polypeptide by papain.... 46

Figure 3-1 Standard curve using different concentrations of liver 150615-1900 (L1) to determine the concentration of 150615-1900 (L1) at the saturation point at pH 1.2 (a), pH 5.8 (b), and pH 7.2 (c).. 61

Figure 3-2 Standard curve using different concentrations of heart 150615-1900 (H1) to determine the concentration of heart 150615-1900 (H1) at the saturation point at pH 1.2 (a), pH 5.8 (b), and pH 7.2 (c) 62

Figure 3-3 Standard curve using different concentrations of glucose (0 - 100 µg/mL) to determine the carbohydrate content of the peptide hydrolysates..... 64

Figure 3-4 : Microscopy images of hydrolysates heart 150615-1900 (H1) (A and D), liver 150615-1900 (L1) (B and E), and placenta 0-150625-1700 (P1) (C and F) by light microscopy A-C and scanning electron microscopy (SEM) D-F..... 66

Figure 3-5 Particle size distributions using wet laser diffraction for heart 150615-1900 (H1), liver 150615-1900 (L1) and 0-150625-1700 (P1) hydrolysate samples 67
Figure 3-6 Particle size distributions using dry powder laser diffraction for heart 150615-1900 (H1), liver 150615-1900 (L1) and placenta 0-150625-1700 (P1) hydrolysate samples. Where the distribution density is represented on the right y-axis and the cumulative distribution is represented on the left y-axis 68
Figure 3-7 Comparison of the three methods of particle size analysis, wet laser diffraction, dry powder laser diffraction, and sieve fractionation for heart 150615-1900 (H1), liver 150615-1900 (L1) and placenta 0-150625-1700 (P1) hydrolysate samples 69
Figure 3-8 Flow factor values for fractions generated from pharmaceutical sieves. Data could not be generated for the heart 150615-1900 (H1) peptide fractions 70
Figure 3-9 Mean saturation point concentrations for hydrolysate samples heart 150615-1900 (H1), and liver 150615-1900 (L1) (n=6) 71
Figure 3-10 Chromatograms for the size exclusion chromatography coupled with multi-angle light scattering (SEC-MALS) for heart 150615-1900 (H1) (a), liver 150615-1900 (L1) and liver 160126-0700 (L2) (b being L2) (b), placenta 0-150625-1700 (P1) and placenta 0-160330-1500 (P2) (b being P2) (c), and the combined graphs (d). 72
Figure 3-11 Molecular weight for the size exclusion chromatography coupled with multi-angle light scattering (SEC-MALS) for the Biofac hydrolysates 72
Figure 3-12 Total carbohydrate content (in relation to glucose) for the peptide hydrolysates 73
Figure 4-1 Conversion of the purple 1, 1-diphenyl-2-picrylhydrazyl (α,α-diphenyl-β-picrylhydrazyl radicl (DPPH·) to the yellow 1, 1-diphenyl-2-picrylhydrazyl (α,α-diphenyl-β-picrylhydrazyl (DPPH) by protonation 81
Figure 4-2 Mechanism for the cellular antioxidant assay. 2'-7' dichloro-dihydro-fluorescein diacetate (DCFH-DA) (non-polar) crosses the cell membrane where it is cleaved to form the more polar 2'-7' dichloro-dihydro-fluorescein (DCFH); DCFH cannot then diffuse out of the cell. 86

Figure 4-3 The nonpolar 2'-7' dichloro-dihydro-fluorescein diacetate (DCFH-DA) is converted into the polar 2'-7' dichloro-dihydro-fluorescein (DCFH) by cellular esterases. DCFH can then be oxidised into the fluorescent form of 2'-7' dichloro-dihydro-fluorescein (DCF) by (reactive oxygen species (ROS+) and peroxide radicals (ROO+). 87

Figure 4-4 An example of a wound created in a confluent monolayer of 3T3 fibroblasts (a), and the 'healed' wound (b) 93

Figure 4-5 Radical scavenging activity (RSA) of 0-150625-1700 (P1) hydrolysate, liver 150615-1900 (L1) hydrolysate, and heart 150615-1900 (H1) hydrolysate compared with the positive control ascorbic acid at 375 µg/mL (a) 0-150625-1700 (P1) hydrolysate at 5 mg/mL, and 50 mg/mL (b) 95

Figure 4-6 Radical scavenging activity (RSA) of heart 150615-1900 (H1) (a), liver 150615-1900 (L1) (b), and 0-150625-1700 (P1) (c) hydrolysates at different concentrations for 96 well plate assay 97

Figure 4-7 Radical scavenging activity (RSA) of liver 160126-0700 (L2), and placenta 0-160330-1500 (P2) for 96 well plate assay 98

Figure 4-8 Data plots generated from the fluorescent plate reader used to calculate the area under the curve (AUC) of Trolox (a), liver 150615-1900 (L1) (b), and 0-150625-1700 (P1) (c) hydrolysates . 99

Figure 4-9 area under the curve (AUC) against the concentration of Trolox (run in conjunction with liver 150615-1900 (L1), and 0-150625-1700 (P1) hydrolysates) plotted to form a standard curve to calculate Trolox equivalents (TE) 100

Figure 4-10 Data plots generated from the fluorescent plate reader used to calculate the area under the curve (AUC) of Trolox (a), and liver 160126-0700 (L2) (b), liver 170127-0815 (L3) (c), and placenta 0-160330-1500 (P2) (d) hydrolysates 101

Figure 4-11 area under the curve (AUC) against the concentration of Trolox (run in conjunction with liver 160126-0700 (L2), liver 170127-0815 (L3), and placenta 0-160330-1500 (P2) hydrolysates) plotted to form a standard curve to calculate Trolox equivalents (TE) 102

Figure 4-12 Absorbance at 500 nm as a result of the ferric thiocyannate assay (FTC) for liver 150615-1900 (L1), 0-150625-1700 (P1), and heart 150615-1900 (H1) plus ascorbic acid (positive control), and

the negative control (a), with the traces for the hydrolysates and ascorbic acid show in greater detail (b). 103
Figure 4-13 Percentage inhibition of lipid peroxidation at the reaction endpoint (48 h) 104
Figure 4-14 Fluorescence traces showing fluorescence against time (a-c) for liver 160126-0700 (L2) peptides (8 mg/mL, 4 mg/mL, and 2 mg/mL) (a), placenta 0-150625-1700 (P1) peptides (8 mg/mL, 4 mg/mL, and 2 mg/mL) (b), and Trolox (8 mg/mL, 4 mg/mL, and 2 mg/mL) (c). 105
Figure 4-15 Cellular antioxidant activity (percentage) derived from the traces shown in figure 4-13 106
Figure 4-16 Cell doubling time (DT), and population doubling level (PDL) measured using cell counts for liver 150615-1900 (L1) (a, and b), and 0-150625-1700 (P1) (c, and d) at concentrations ranging from 0 -200 µg/mL 107
Figure 4-17 Cell number (bars), and cell proliferation (dots) using (3-(4,5-Dimethylthiazol-2-yl)-2,5-Diphenyltetrazolium Bromide) (MTT) assay in comparison to the control for cells treated with liver 150615-1900 (L1) (a) and placenta 0-150625-1700 (P1) (b) 108
Figure 4-18 Analytical high performance liquid chromatography (HPLC) traces for liver 160126-0700 (L2) full chromatogram (a), with 0 – 8 minutes magnified (b), 8 – 18 minutes magnified (c), and 18 – 28 minutes magnified (d) 110
Figure 4-19 Analytical high performance liquid chromatography (HPLC) traces for placenta 0-160330-1500 (P2) full chromatogram (a), with 0 – 8 minutes magnified (b), 8 – 18 minutes magnified (c), and 18 – 28 minutes magnified (d) 111
Figure 4-20 High performance liquid chromatography (HPLC) chromatograms derived from preparative HPLC of liver 160126-0700 (L2). Run 1-4 (a - d) were loaded with 50 mg/mL peptide sample (2.2 mL), run 5 (e) was loaded with 25 mg/mL peptide sample (4.4 mL) 113
Figure 4-21 Comparison of analytical high performance liquid chromatography (HPLC) chromatograms of fractions F2R1 (a1), and F2R2 (b1) with areas of interest highlighted (F2R1 peaks indicated in a2, and F2R2 peaks indicated in b2) 116

Figure 4-22 Comparison of analytical high performance liquid chromatography (HPLC) chromatograms of fractions F1R1 (a1), and F1R2 (b1) with areas of interest highlighted (F1R1 peaks indicated in a2, and F1R2 peaks indicated in b2) 117
Figure 4-23 Comparison of analytical high performance liquid chromatography (HPLC) chromatograms of fractions F4R1a (a1), and F4R1b (b1) with areas of interest highlighted (F4R1a peaks indicated in a2, and F4R1b peaks indicated in b2) 118
Figure 4-24 Cell proliferation data derived from (3-(4,5-Dimethylthiazol-2-yl)-2,5-Diphenyltetrazolium Bromide) (MTT) assay for the fractions collected from prep high performance liquid chromatography (HPLC): Liver hydrolysate (L2) (a), F1R1 (b), and F1R2 (c) (fractions described in section 4.3.6.2). . 119
Figure 4-25Cell proliferation data derived from (3-(4,5-Dimethylthiazol-2-yl)-2,5-Diphenyltetrazolium Bromide) (MTT) assay for the fractions collected from prep high performance liquid chromatography (HPLC): F2R1 (a), F2R2 (b), and F4R1 (c) 120
Figure 4-26 Percentage wound closure for each sample over time showing the error bars for no peptide (c1) (a), full hydrolysate (b), and F1R1 (c) 121
Figure 4-27 Percentage wound closure for each sample over time showing error bars for F1R2 (a), F2R1 (b), and F2R2 (c) 122
Figure 4-28 Rate (µm2/h) of wound closure for negative control (C1), liver hydrolysate (L2) (Full), and the fractions generated from preparative high performance liquid chromatography (prep HPLC) (F1R1, F1R2, F2R1, and F2R2). 123
Figure 4-29 Radical Scavenging activity (RSA) of lyophilised liver peptide fractions measured by the 1, 1-diphenyl-2-picrylhydrazyl (α,α-diphenyl-β-picrylhydrazyl (DPPH) assay 124
Figure 4-30 Cell proliferation data derived from 1, 1-diphenyl-2-picrylhydrazyl (α,α-diphenyl-β-picrylhydrazyl (MTT) assay: placenta 0-160330-1500 (P2) 0h after preparation (a), placenta 0-160330-1500 (P2) 24h after preparation (b), placenta 0-160330-1500 (P2) 48h after preparation (c), placenta 0-160330-1500 (P2)72h after preparation (d), placenta 0-160330-1500 (P2) 96h after preparation,

placenta 0-160330-1500 (P2) 144h after preparation, and placenta 0-160330-1500 (P2) 168 h after preparation. 125

Figure 4-31 High performance liquid chromatography (HPLC) data obtained using an Ascentis® Express Peptide ES-C18, 2.7 Micron HPLC Column, showing data for placenta 0-160330-1500 (P2) in supplemented Dulbecco's Modified Eagle Medium (DMEM) 0h after preparation (a), 96h after preparation (b), and 168h after preparation (c) 126

Figure 4-32 Cell proliferation data derived from 1, 1-diphenyl-2-picrylhydrazyl (α,α-diphenyl-β-picrylhydrazyl (MTT) assay: liver 160126-0700 (L2)0h after preparation (a), liver 160126-0700 (L2) 24h after preparation (b), liver 160126-0700 (L2) 48h after preparation (c), liver 160126-0700 (L2) 72h after preparation (d), liver 160126-0700 (L2) 96h after preparation, liver 160126-0700 (L2) 144h after preparation, and liver 160126-0700 (L2) 168 h after preparation. 127

Figure 4-33 High performance liquid chromatography (HPLC) data obtained using an Ascentis® Express Peptide ES-C18, 2.7 Micron HPLC Column, showing data for liver 160126-0700 (L2) in supplemented Dulbecco's Modified Eagle Medium (DMEM) 0h after preparation (a), 96h after preparation (b), and 168h after preparation (c) 128

Figure 4-34: Percentage inhibition of angiotensin II converting enzyme (ACE) by the hydrolysates placenta 0-160330-1500 (P2), liver 160126-0700 (L2), and liver 170127-0815 (L3) 129

Figure 5-1 Chromatograms indicating the fraction that was collected for Liver 160126-0700 (L2) (peak at 6.017 min) (a), and the collected fraction loaded onto the column again to check for purity (peak at 6.217 min) (b)..... 150

Figure 5-2 Chromatograms indicating the fraction that was collected for placenta 0-160330-1500 (P2) (peak at 6.100 min) (a), and the collected fraction loaded onto the column again to check for purity (peak at 6.250 min) (b)..... 151

Figure 5-3 Structure of the peptide TPANEMTPTR with methionine sulfoxide..... 152

Figure 5-4 Structure of the peptide SAADKANVKAA..... 153

Figure 5-5 Structure of the peptide YSGTGQQQPER 153

Figure 5-6 Structure of the peptide NVINGGSHAGNK 154
Figure 5-7 The molecular structure of the peptide FFNDA 167
Figure 5-8 The molecular structure of the peptide FWG 167
Figure 5-9 The molecular structure of the peptide SDPPLVFVG 168
Figure 5-10 The molecular structure of the peptide MFLG 168
Figure 5-11 ORAC fluorescent traces for Trolox (a), LG (b), and FWG (c) 169
Figure 5-12ORAC fluorescent traces for MFLG (a), FFNDA (b), and SDPPLVFVG (c) 170
Figure 5-13 ORAC Trolox standard curve with the activity of the peptides at 12.5 µM plotted on the curve showing equivalence to Trolox concentration 171
Figure 5-14 Fluorescence over time for synthetic peptides. The cellular antioxidant activity (CAA) of each sample is derived by comparing the area under the curve (AUC) of the samples to the AUC of the negative control (c) 172
Figure 5-15 Cellular antioxidant activity (CAA) (%) of synthetic peptides with significant results highlighted 172
Figure 5-16 Cell proliferation data derived from (3-(4,5-Dimethylthiazol-2-yl)-2,5-Diphenyltetrazolium Bromide) (MTT) assay (percent proliferation relative to the control group) for synthetic peptides FWG (a), MFLG (b), SDPPLVFVG (c), and FFNDA (d) 173
Figure 5-17 Rate of scratch wound closure over 32 hours with control groups (c1, and c2) (no peptide); FWG, and MFLG with control (c1) (a), and SDPPLVFVG, and FFNDA with c2 (b) 174
Figure 5-18 Percentage inhibition of angiotensin II converting enzyme (ACE) by the synthetic peptides FWG, MFLG, SDPPLVFVG, and FFNDA 175

VI) List of Tables

Table IV-1 Amino acid single, and three letter codes with a general description for each amino acid . 7

Table 2-1 Description, batch number, and abbreviated form for the Biofac hydrolysates used in this study..... 48

Table 2-2 Sequences of the synthetic peptides derived from amino acid sequences found in the Biofac hydrolysates..... 48

Table 2-3 Specialist Equipment..... 49

Table 2-4 Specific materials and reagents 49

Table 3-1: Mass of fractions generated from sieving the hydrolysates heart 150615-1900 (H1), liver 150615-1900 (L1) and placenta 0-150625-1700 (P1). 67

Table 3-2 Total carbohydrate content (in relation to glucose) for the peptide hydrolysates 73

Table 4-1 Sample preparation for angiotensin II converting enzyme (ACE) inhibition assay..... 94

Table 4-2 Trolox equivalents for liver 150615-1900 (L1), and placenta 0-150625-1700 (P1) 100

Table 4-3 Trolox equivalents (TE) for liver 160126-0700 (L2), liver 170127-0815 (L3), and placenta 0-160330-1500 (P2)..... 102

Table 4-4 Times at which each fraction was taken for runs 1 to 5 using liver 160126-0700(L2). Fractions from run 2 to 5 were collated. Fraction from run 1 were kept separate 112

Table 4-5 Percentage of net proton donors present in the Biofac hydrolysates..... 132

Table 5-1 Known bioactive peptides that were predicted from the in silico digest of cytosol aminopepsidase with papain. Data taken from the BIOPEP database 156

Table 5-2 Known bioactive peptides that were predicted from the in silico digest of cytosol aminopepsidase with papain. Data taken from the BIOPEP database cont. 157

Table 5-3 Known bioactive peptides that were predicted from the in silico digest of cytosol aminopepsidase with papain. Data taken from the BIOPEP database cont. 158

Table 5-4 Known bioactive peptides that were predicted from the in silico digest of Haemoglobin subunit alpha with papain. Data taken from the BIOPEP database 159

Table 5-5 Known bioactive peptides that were predicted from the in silico digest of Type VI collagen alpha-1 chain, partial with papain. Data taken from the BIOPEP database 160
Table 5-6 Peptide Ranker scores for predicted papain digestion of cytosol aminopeptidase (1) 162
Table 5-7 Peptide Ranker scores for predicted papain digestion of cytosol aminopeptidase (2) 163
Table 5-8 Peptide Ranker scores for predicted papain digestion of Haemoglobin subunit alpha 164
Table 5-9 Peptide Ranker scores for predicted papain digestion of Type VI collagen alpha-1 chain, partial 165
Table 5-10 Predicted peptides with a predicted rank > 0.5 for all the digests (proteases and proteins). Green highlighted peptides were selected for synthesis, yellow highlighted peptides are repeats, and red highlighted peptides have been reported in the literature as bioactive peptides..... 166
Table 5-11 Trolox equivalent (TE) values for synthetic peptides..... 171
Table 5-12 Inhibitory Concentration at 50 %(IC_{50}) values for the synthetic peptides 179
Table 5-13 Examples of angiotensin II converting enzyme (ACE) Inhibitory Concentration at 50 % (IC_{50}) values for peptides derived from porcine muscle. Data in the review 'ACE Inhibitory Peptides Derived from Enzymatic Hydrolysates of Animal Muscle Protein' (Vercruysse et al., 2005)... 180
Table 6-1 Know bioactive peptides generated from trypsin digest of chickpea legumin 11S..... 188
Table 6-12 Un-reported peptides generated from trypsin digest of chickpea legumin 11S 189
Table 6-3 The probability of general activity (using Peptide Ranker (Mooney et al., 2012)), and anti-angiotensin II converting enzyme (ACE) activity of Selected peptides from the tryptic digest of chickpea legumin 11S , and three of the synthetic peptides produced for this study (yellow highlighted) using the AHTpin is an anti-ACE peptide predictor (Kumar et al., 2015) 190

Contents

I) Dedication 2
II) Acknowledgements 3
III) Abstract 4
IV) Abbreviations 7
V) List of Figures 11
VI) List of Tables 18
CHAPTER 1 Introduction and Literature Review 24
1.1 Project Aim and Background 24
1.2 General Protein Structure 24
1.3 Biologically Active Peptides 25
1.4 Pharmaceutical Peptides 26
1.5 Nutraceutical Peptides 27
1.6 Bioactive Peptides derived from Food Proteins and Meat Waste 28
1.7 Generation/isolation/identification of bioactive peptides 32
1.8 Assays used in the Analysis of Bioactive Peptides 34
1.8.1 Antioxidant activities of bioactive peptides 34
1.8.2 Blood pressure regulation 36
1.8.3 Wound healing 39
1.8.4 Antimicrobial 42
1.8.5 Immune modulation/adjuvants/innate immune response 43
1.9 In Silico Analysis 43
1.10 Biofac Hydrolysates 44
1.11 Rationale of Study 46
CHAPTER 2 Materials and General Methods 48
2.1 Materials 48
2.1.1 Biofac hydrolysates 48
2.1.2 Synthetic peptides 48
2.1.3 Equipment 49
2.1.4 General materials 49
2.1.5 Cell line 50
2.2 General Methods 50
2.2.1 Microscopy 50
2.2.2 Particle Size Analysis 50
2.2.3 Particle Flow Analysis 51

2.2.4 Size Exclusion Chromatography Multi-Angle Light Scattering 51
2.2.5 Phenol-Sulphuric Acid Assay 51
2.2.6 Antioxidant Assays 52
2.2.7 Cell Proliferation 53
2.2.8 Wound Healing Assay (Scratch Assay) 54
2.2.9 High Performance Liquid Chromatography (HPLC) 55
2.2.10 Lyophilisation 55
2.2.11 ACE Inhibition Assay 55
2.2.12 De-Novo Peptide Sequencing Using MS/MS 56
2.2.13 In silico Analysis of Bioactive Peptides 56
CHAPTER 3 Physicochemical analysis of possible bioactive hydrolysates derived from porcine hydrolysates 57
3.1 Introduction 57
3.2 Materials and methods 59
3.2.1 Microscopy of peptide samples 59
3.2.2 Particle size analysis 59
3.2.3 Particle flow analysis 60
3.2.4 Solubility and saturation point 60
3.2.5 SEC MALS analysis 63
3.2.6 Determination of Total Sugars Using the Phenol-Sulphuric Acid Assay 63
3.2.7 Statistical analysis 64
3.3 Results 66
3.3.1 Microscopy of peptide samples 66
3.3.2 Particle size and distribution 66
3.3.3 Particle flow analysis 70
3.3.4 Saturation point 70
3.3.5 SEC MALS analysis 71
3.3.6 Determination of Total Sugars Using the Phenol-Sulphuric Acid Assay 73
3.4 Discussion 74
3.5 Summary 77
CHAPTER 4 Bioactive properties of whole and fractionated hydrolysates 78
4.1 Introduction 78
4.2 Materials and methods 81
4.2.1 DPPH Radical Scavenging Activity (RSA) 81
4.2.2 ORAC Assay 83
4.2.3 Lipid peroxidation inhibition 85

4.2.4 Cellular antioxidant activity assay (CAA) 86
4.2.5 Cell proliferation 88
4.2.6 HPLC analysis of hydrolysates and fractionation of liver hydrolysate 89
4.2.7 Assays performed on prep HPLC fractions 91
4.2.8 Stability studies 93
4.2.9 ACE inhibition assay 93
4.3 Results 95
4.3.1 DPPH Radical Scavenging Activity (RSA) 95
4.3.2 ORAC Assay 99
4.3.3 Lipid peroxidation inhibition assay 102
4.3.4 Cellular antioxidant activity assay (CAA) 104
4.3.5 Cell proliferation 106
4.3.6 HPLC analysis of hydrolysates and fractionation of liver hydrolysate 109
4.3.7 HPLC analysis, and physical description of the fractions generated from prep HPLC 114
4.3.8 Stability studies of full hydrolysates 124
4.3.9 ACE inhibition assay 129
4.4 Discussion 130
4.4.1 Antioxidant activities of the whole hydrolysates 130
4.4.2 Cell proliferation and wound healing 135
4.4.3 HPLC analysis of hydrolysates and fractionation of liver hydrolysate L2 136
4.4.4 Stability Studies 141
4.4.5 ACE inhibition assay 141
4.5 Summary 141
CHAPTER 5 Generation of and bioactivity analysis of synthetic peptides derived from hydrolysates 143
5.1 Introduction 143
5.2 Materials and methods 146
5.2.1 Isolation of individual fractions for MS analysis 146
5.2.2 Peptide Sequencing Using MS/MS 146
5.2.3 In silico digestion, and activity prediction 147
5.2.4 Peptide synthesis and preparation 147
5.2.5 ORAC Assay 147
5.2.6 Cellular Antioxidant Activity Assay 148
5.2.7 MTT assay 148
5.2.8 Scratch assay 148
5.2.9 Angiotensin converting enzyme (ACE) inhibition assay 149

5.2.10 Statistical analysis 149
5.3 Results 150
5.3.1 Isolation of individual peaks for MS analysis 150
5.3.2 Peptide Sequencing Using MS/MS 151
5.3.3 In silico digestion, and activity prediction 155
5.3.4 ORAC assay 168
5.3.5 Cellular antioxidant activity assay (CAA) 171
5.3.6 MTT Cell proliferation assay 173
5.3.7 Scratch assay 173
5.3.8 ACE inhibition assay 175
5.4 Discussion 176
5.5 Summary 181
CHAPTER 6 General Discussion, Future Work and Conclusions 182
6.1 Original Project Aims 182
6.2 High throughput screening method development 183
6.3 Future Work 184
6.4 Theoretical digestion of proteins found within chickpeas 186
6.5 Conclusions 191
CHAPTER 7 References 192
VII) Appendices 199

CHAPTER 1 **Introduction and Literature Review**

1.1 Project Aim and Background

Recent trends in pharmaceutical development have seen an increased emphasis on biomolecules with regards to novel therapeutics. These biomolecules include proteins, monoclonal antibodies, and peptides (Prueksaritanont and Tang, 2012). With the increasing average age of the population, there is an ever-growing market for natural bioactive compounds with nutritional, functional and biological activities that are scientifically proven. Such compounds could be used as potential ingredients of health-promoting foods, nutraceuticals and other health supplements. Peptides are one class of compounds that have been shown to have a range of beneficial bioactive effects (Sánchez and Vázquez, 2017, Danquah and Agyei, 2012). In tandem with the discovery of novel compounds that exhibit bioactivities, the source is also of interest, specifically whether valuable compounds can be extracted from material that otherwise would be considered waste.

The aim of this research project was to evaluate hydrolysates derived from meat waste material for bioactivity. This project covers three major areas of investigation: the physicochemical structure of crude hydrolysates, the bioactivity demonstrated by the samples, and the analysis of the structure of the hydrolysates leading to the generation of novel synthetic peptides. This work was funded by Biofac A/C (Denmark), the manufacturer of the hydrolysates.

1.2 General Protein Structure

Proteins are organised into four levels of structure, primary, secondary, tertiary, and quaternary. Primary structure is the sequence of amino acids connected through covalent bonds known as peptide bonds. These chains of amino acids, or polypeptides, form into alpha helixes and beta sheets; these formations are termed secondary structure. The three-dimensional structures that result from the folding of a single polypeptide chain are called tertiary structures. The conformation of secondary and tertiary structures is bound together with bonds such as covalent disulphide bridges, hydrogen bonds, and van der Waals forces. The final level of structure is termed quaternary. Quaternary structures are the results

of multiple protein subunits (separate polypeptide chains) forming a complex. An example of a protein constituted in this fashion is haemoglobin, a protein that is made up of four globular protein subunits, and four haem groups (iron containing molecule that bind to oxygen) (Lukin et al., 2003, Alberts et al., 2008).

Proteins that constitute soft and connective tissues are of internet concerning this project because they are a common source of bioactive peptides (Mora et al., 2014). Skeletal, and cardiac muscle are both examples of striated muscle, which is composed of sarcomere. The main proteins that make up sarcomere are myosin and actin; these proteins form the filaments that allow the muscle tissue to contract (shorten) and to relax (lengthen). Collagen is the most abundant protein type in mammals, making up approximately 30% (Ricard-Blum, 2011). Collagen is constructed of polypeptide chains in a triple helix and is found in abundance in skin, tendons, and ligaments, but is also found in significant amounts in muscle tissue. The abundance of collagen in vertebrate tissue means that it is a likely source for bioactive peptides (Gómez-Guillén et al., 2011, Howell and Kasase, 2010)

1.3 Biologically Active Peptides

Peptides are short (2-50 residues) sequences of amino acids (Banga, 2015). Generally, amino acid sequences that are under 10 residues long are termed oligopeptides; sequences over 50 residues long are regarded as proteins. Many peptide sequences that are bioactive are found in larger proteins, but in an inactive state (Capriotti et al., 2015).

Bioactive peptides can be derived from a variety of sources; these could be from dietary proteins that are then broken down in the gastrointestinal tract to release bioactive peptides, or they can be isolated from various sources *ex vivo*. Sources include plant-based proteins such as soy, and chickpeas, and animal proteins such as from waste from the meat industry and fish skin (Himaya et al., 2012, Lassoued et al., 2015, Di Bernardini et al., 2011, Fu et al., 2017, Beermann et al., 2009, Capriotti et al., 2015, Xue et al., 2015, Xue et al., 2012, Howell and Kasase, 2010). Many studies have been carried out on bioactive peptides and their uses. Areas of greatest interest however, are where bioactive peptides can

be used in either treatment of a condition or aid in a biological process. Bioactivities that are of particular interest to this study are antioxidant activity, cell proliferation and wound healing, and regulation of blood pressure.

1.4 Pharmaceutical Peptides

There are three major groups of compounds that are routinely used in the treatment of diseases, small molecules, proteins, and peptides, with small molecules accounting for the majority of these therapeutics. That being said there has been a rise in the development of peptides as drug candidates in recent years (Otvos, 2008). Peptides have been used as pharmaceuticals for many years; peptide based vaccines against viral, and bacterial pathogens for example, were some of the earlier developed peptide based therapeutics. More recently, different types of conditions have subsequently been targeted with peptides (Otvos, 2008).

For the most part, small molecules have dominated drug development, with peptides regarded as a poorer target, due to their susceptibility to the large array of proteases found in the human body. The lack of oral availability of peptides is one of the major hurdles in development of drugs based on peptides and proteins, resulting in a more severe route of administration. Insulin for example, is injected instead of being delivered orally (Lau and Dunn, 2018). However, peptides and proteins are integral to many biological processes in the body including signalling between cells and within individual cells (de Mejia and Dia, 2010), and it has been noted that peptides that are naturally found in biological systems do exhibit greater stability than would be expected for this type of molecule (Uhlig et al., 2014). Nonetheless, altering a peptide chemically to remove certain disadvantages is an approach taken by researchers in drug discovery. This process is known as peptidomimetics, the rationale behind this is that while peptides may be potent active compounds in their own right, their structure leads them to have poor bioavailability. Thus, if an active peptide cannot reach the desired target site then it cannot perform its function.

Peptidomimetics involves the designing of molecules that mimic the active parts of peptides (in both structure and conformation), but removes or adds elements that lead to improved pharmacokinetics (Mizuno et al., 2017). An example of changes that can be made to peptides to improve their pharmacokinetics is the hydrocarbon stapling method that is used to improve the ability of a peptide to cross lipid bilayers (Chandrudu et al., 2013). The availability of peptide-based pharmaceuticals due to the advancements in development methods, and increasing limitations in the pursuit of small molecule candidates has therefore increased. Examples of commercially available peptide based drugs are Zoladex® (goserelin acetate), which targets breast, and prostate cancer, and Fuzeon® (enfuvirtide), which is used in the treatment of HIV (Chandrudu et al., 2013). The interest in therapeutic peptides has led to the investigations into other sources of active peptides, notably bioactive peptides found in proteins derived from food (Danquah and Agyei, 2012).

1.5 Nutraceutical Peptides

Bioactive peptides that are derived from proteins present in food are generally termed nutraceuticals. The term 'nutraceutical' is defined as food, or components of food that confer benefits to health as well as nutrition (de Mejia and Dia, 2010). The role of nutraceuticals in health is the subject of multiple studies that have investigated either the composition of peptides derived from food sources, or the effects certain diets or supplements have on certain conditions.

An example of the possible effects of a certain diet on health can be seen in the prevention of cardiovascular disease (Minuz et al., 2017). An example is the prevalence of extra virgin olive oil in the Mediterranean diet. Extra virgin olive oil has been shown to down regulate the enzyme nicotinamide adenine dinucleotide phosphate (NADPH) oxidase 2, the activity of which leads to the production of reactive oxygen species (ROS) (Carnevale et al., 2014). The production of ROS through NADPH oxidase 2 has been linked to atherosclerosis (caused by the build-up of plaque in the blood vessels); the down regulation of NADPH oxidase 2 therefore can help reduce the damage that leads to cardiovascular disease (Loffredo et al., 2017).

The role of bioactive peptides as nutraceuticals has been extensively investigated. In fact, peptides have been shown to be the most versatile group of molecules with regards to health benefits. Activities that have been demonstrated in nutraceutical peptides include antioxidant, antihypertensive, antimicrobial, anticancer, and anti-inflammatory (Girija, 2018). This wide variety of activities attributed to bioactive peptides found in nutraceuticals, and the fact that single peptides have been shown to convey more than one type of activity make them an interesting group of molecules to study. The study by Himaya et al (2012) is an example of an investigation where the authors discovered numerous types of activity that could be attributed to a peptide that they were researching. As well as angiotensin converting enzyme (ACE) inhibitory properties, they also investigated the protective effects of the peptide on cell membrane lipid peroxidation, cell membrane protein oxidation, and on cellular DNA oxidation. They also investigated the effects on cell viability using MRC-5, and RAW264.7 cells using the 3-(4,5-Dimethylthiazol-2-yl)-2,5-diphenyltetrazolium bromide (MTT) assay. The study indicated that the peptide was involved in the upregulation of mRNA expression for cellular antioxidative enzymes. This indicated that multiple effects can be attributed either to the same peptide, or from peptides extracted from one source.

1.6 Bioactive Peptides derived from Food Proteins and Meat Waste

There is a significant amount of literature on the benefits of bioactive peptides when used as dietary supplements. Much of this focuses on bioactive peptides derived from milk and soy proteins. These studies show that bioactive peptides are present in proteins found in foods, and via hydrolysis in the gastrointestinal tract, they are released from this non-functional state.

Two studies into bioactive peptides derived from food protein were carried out by Ahmed, et al (2015), and Corrêa, et al (2014). Both of these groups investigated bioactive peptides derived from milk proteins, with the former focusing on the release of bioactive peptides from the hydrolysis of goat milk proteins (specifically caseins and whey proteins) by digestive enzymes found in the gastrointestinal tract. The proteins were digested with pepsin, and then lyophilised. The protein digests were further processed using fast protein liquid chromatography (FPLC) and the fractions collected were assayed

for any antioxidant activity. Fractions that showed good antioxidant activities were separated using high performance liquid chromatography (HPLC), and analysed for sequence data using mass spectrometry.

Data from the study carried out by Ahmed, et al (2015) indicated that short peptides were found to be more antioxidant than longer chains, and that amphiphilic peptides seem to enhance antioxidant activity. It was suggested that amphiphilic peptides were more antioxidant because the hydrophobic residues within the peptide have high antioxidant activity, with the polar residues allowing greater solubility, therefore increasing the availability of the peptides in the assays. It is noted in the study that most of the isolated peptides are rich in hydrophobic residues, therefore the specific sequence in the more active peptides is directly related to their bioactivity (Ahmed et al., 2015).

The study carried out by Corrêa, et al (2014), investigated hydrolysates derived from whey produced as a by-product of cheese making, they hydrolysed the whey proteins using a protease isolated from bacteria (*Bacillus* sp. P7). The results showed that hydrolysed whey protein had an increased radical scavenging activity when compared to the non-hydrolysed protein when measured using the 2,2'-azino-bis(3-ethylbenzothiazoline-6-sulphonic acid) (ABTS) assay, a greater Fe^{2+}-chelating ability, along with an increase in hydrophobicity. The data in this study relates to other studies such as the one carried out by Ahmed, et al. (2015), because hydrolysis time was shown to be proportional to antioxidant activity (up to and including 6 hours), suggesting that smaller peptides are more active. One of the sequences discovered that displayed high antioxidant activity (isolated after 4 hours hydrolysis) was LAFNPTQLEGQCHV. Leu (1), Ala (2), and Phe (3) at the N-terminus are all hydrophobic residues. The sequence also contains four more hydrophobic residues (Pro (5), Thr (6), Leu (8), and Val (13)). The authors highlight the presence of Val at the C-terminus as being significant because radical scavenging activity of bioactive peptides could be related to the availability of non-polar amino acids. Structural data suggests that the hydrophobic residues (LAF) at the N-terminus are exposed, and therefore can contribute to radical scavenging activity. They also indicate that the CH at the C-terminus

are not hidden, and therefore contribute antioxidant activity due to these residues redox and metal chelating properties (Corrêa et al., 2014).

The two studies discussed both indicate that short peptide chains, when liberated from larger proteins, can have significant antioxidant properties. Furthermore, Ahmed, et al. (2015), used pepsin, an enzyme found in the gastrointestinal (GI) tract. This indicates that the bioactive peptides found within proteins in goats' milk can be liberated through digestion.

The study carried out by Jang and Lee (2005) investigated peptides isolated from hydrolysates derived from beef. They were particularly interested in peptides that could act as ACE inhibitors. Hydrolysates were extracted from sarcoplasmic proteins using the enzymes thermolysin, protease A, and protease type XIII. The homogenised meat samples were incubated with the enzymes over 24 hours, with time points for sampling at 0, 4, 8, 12, and 24 hours. The peptides were isolated using ultrafiltration, gel filtration, and reverse-phase HPLC. The purified peptide with the greatest ACE inhibition was sequenced using Edman degradation.

The study found that the peptides with the most potent ACE inhibitory activity were from the 4-hour time point of the hydrolysis, with thermolysin and protease A. The sequence of the peptide that was found to have the greatest ACE inhibitory activity was VLAQYK. The authors suggest that their peptide shows similar properties to another study, where the hydrophobic/aliphatic V at the N-terminus is important to ACE inhibitory activity (other examples of aliphatic amino acids are glycine (G), alanine (A), leucine (L), and isoleucine (I)). The same group evaluated their peptide in spontaneously hypertensive rats (SHR). They found that groups fed the peptide showed lower concentrations of total cholesterol, and low-density lipoprotein (LDL) cholesterol than the control groups. Systolic blood pressure was shown to be suppressed with increasing concentrations of the peptide (Jang and Lee, 2005).

An example of bioactive peptides discovered in plant-based material is an investigation carried out by Capriotti, et al (2015). This group looked at the release of bioactive peptides from simulated gastrointestinal digestion of proteins derived from soybeans. Proteins were isolated from different sources derived from soy, which were then sequenced using nano-liquid chromatography in conjunction with tandem mass spectrometry (nano-LC-MS/MS). The sequences generated from this process were then cross-referenced against databases of known peptides that show bioactivity. They were particularly interested in bioactive peptides that were predicted to demonstrate antimicrobial properties. The results indicated that bioactive peptides can be generated from simulated gastrointestinal digestion of proteins, and that three of the sequences they had found had been reported in previous studies. They also identified known bioactive peptide sequences that were contained in larger peptides. The three bioactive peptides identified that were present in the databases showed ACE inhibition, and antioxidant properties. The bioactive peptides that were identified to be contained in longer precursor sequences had been shown to have either ACE inhibition, or antioxidant properties, with one having immunomodulating activity (Capriotti et al., 2015). This study used bioinformatics to assess the peptides released from the digests. The authors tabled the most likely candidates that had predicted antimicrobial activity using the online database CAMP, which uses four machine-learning algorithms to analyse the peptides (Random Forests, Support Vector Machines, Artificial Neural Network, and Discriminant Analysis) (Thomas et al., 2010).

It was noted that nine of the peptides found with predicted antimicrobial activity were derived from the precursor proteins glycinin, and beta-conglycinin; these proteins have been previously reported to reduce the growth of three pathogenic bacteria that had been inoculated into raw milk. Gycinin was shown to significantly reduce the growth of the bacteria (Osman et al., 2013).

Another interesting point that this study made was that the peptide sequences generated from the soy products were slightly longer than those extracted from animal sources using similar digestion methods. It was suggested that the presence of protease inhibitors that can be found in plant seeds could be the reason for this (Capriotti et al., 2015).

The papers discussed here investigated the generation of bioactive peptides from longer amino acid sequences by simulating digestion of food derived proteins *in vitro*, using proteases. While the bioactive peptides were from different sources (dairy, meat, and plant), they all identified certain properties that were related. It is therefore, reasonable to assume that bioactive peptides found in Biofac hydrolysates may have antioxidant activity, ACE inhibition, and even antimicrobial activity. An important consideration when releasing bioactive peptides from protein samples is the choice of enzyme used for the hydrolysis. It has been demonstrated that the type of protease used in processing samples is related to the peptides produced. An example of this was highlighted by Arihara et al (2001), where they found that fractions produced from the digestion of porcine skeletal muscle by the enzyme thermolysin showed the greatest ACE inhibitory activity of the eight enzymes investigated (trypsin, alpha-chymotrypsin, pronase E, proteinase K, thermolysin ficin, papain, and pepsin) (Arihara et al., 2001, Toldrá et al., 2012, Di Bernardini et al., 2011).

This study is based on the analysis of hydrolysates derived from waste produced from the meat industry, and if any value can be extracted from such material. The approach to producing and analysing hydrolysates from meat waste is similar to that of projects looking at other sources. Typical by-products of meat production are meat trimmings, mechanically recovered meat, collagen, and blood. All of these are constituted of proteins, which can therefore be hydrolysed using proteases to release peptides (Mora et al., 2014). Regardless of the source of the proteins, the methods to extract them, and the resulting peptides should be the same whether they are extracted from waste, or food grade material. The difference should be from the method of hydrolysis, recovery of the hydrolysate, and the isolation of peptides.

1.7 Generation/isolation/identification of bioactive peptides

Bioactive peptides can be generated by processing raw materials that contain proteins, producing hydrolysates that contain peptides of various size and sequence (Sánchez and Vázquez, 2017). One of the more prevalent methods reported for generating bioactive peptides is the use of proteases to

hydrolyse lager proteins (Mora et al., 2014); this leads to peptides of differing length and structural conformations, that are related to their activity (Himaya et al., 2012). Different structures, that can alter activity, can form in peptides of sufficient length, for example, secondary structures forming where hydrophobic residues move to the centre of a structure, or hydrogen bonds can form between two non-adjacent amino acids (Möhle and Hofmann, 1998). Different proteases will cleave peptides at different sites therefore, by using a specific enzyme in a single digestion (or multiple), various peptide fragments can be generated that have varying bioactivity (Jang and Lee, 2005).

It is common for bioactive peptides to be generated from precursor proteins by enzymes that can be found in the gastrointestinal tract such as pepsin and trypsin, but proteases from other sources can also be used (such as cysteine proteases like papain). Peptides can be isolated from the protein digests using a number of methods either singularly or in combination with various methods of chromatography being widely used. Size exclusion chromatography (SEC) is often used as the first step in isolating peptides from their crude hydrolysates, the fractions generated from SEC can then be further processed using FPLC, and reverse phase high performance liquid chromatography (RP-HPLC). Fractions collected from chromatography can then be assayed for any bioactive properties. Fractions that show activity can then be further separated using HPLC, and sequenced by using mass spectrometry (MS) (Ahmed et al., 2015, Corrêa et al., 2014).

An example of using tandem mass spectrometry (MS/MS) for the characterisation of bioactive peptides in the literature is the study undertaken by Jang and Lee (2005). They used SEC to separate hydrolysates from the marine bivalve *Mactra veneriformis* (using sephadex G-25 gel filtration column). Five fractions were collected from the column and each were assayed for antioxidant activty. The two most active fractions were then sequenced using ultra high pressure liquid chromatography, linked to MS/MS, using positve electrospray ionisation and collision induced dissociation (CID) mode. From these two fractions, twenty one sequences were identified and the information used to synthesise these peptides. The synthetic sequences were then assayed to determine their hydroxyl radical scavenging activies. Using this method the authors were able to isolate, and identify specfifc bioactive peptides

that were antioxidants, they also highlighted that peptides rich in proton donor amino acids and hydrophobic amino acids can act as potent antioxidants (Jang and Lee, 2005).

Sequencing bioactive peptides that have been generated by the hydrolysis of larger peptides/proteins is a powerful tool in identifying the molecular mechanism of activity of bioactive peptides. Using chromatographic techniques, fractions of the hydrolysate can be generated, which contain peptides. These fractions can then be assayed for bioactivity, with active fractions undergoing MS/MS, and *de novo* sequencing to identify the sequence of the active peptide. This structural information can then be used to understand peptide bioactivity (Liu et al., 2015).

1.8 Assays used in the Analysis of Bioactive Peptides

Fractions generated using chromatography will normally be assayed for bioactivity to assess whether they are suitable candidates for further investigation through sequencing. To investigate bioactivity in these fractions, certain simple assays can be used. Fractions that display good activity can therefore be further explored. Once sequences are identified the peptides can be crosschecked with databases of known bioactive peptides and identify known bioactive peptide sequences that are contained in larger peptides. Examples of activities of bioactive peptides researched in this fashion are ACE inhibition, antioxidant activity, immunomodulating activity, and antimicrobial activity (Capriotti et al., 2015). The examples of assays discussed in this section represent the most common types of bioactivity investigated in relation to peptides in the literature.

1.8.1 Antioxidant activities of bioactive peptides

Oxidative stress in biological systems is a major factor relating to cellular damage. It is caused by ROS, which are by-products of some of the most important biological reactions, including respiration (Gagné, 2014). The reduction in oxidative stress induced damage is therefore an important consideration in leading a healthy lifestyle.

Antioxidant activity is one of the most prevalent bioactivities exhibited by peptides generated through hydrolysis of protein rich materials with proteases. Antioxidant assays can be divided into two major types, *in vitro*, and *in vivo*. The use of *in vitro* assays is useful for high throughput assays, but to discover if the samples being analysed are biologically available, an *in vivo* assay is required. A specific sample may show excellent antioxidant activity *in vitro*, but if it cannot interact with the biological target, it will not be effective (Vermeirssen et al., 2007). That being said, *in-vitro* assays are an important tool because they can screen potential targets using relatively inexpensive procedures before being analysed with more expensive and complex *in-vivo* methods. *In vitro* antioxidant assays can be further separated into hydrogen atom transfer (HAT), and single electron transfer (SET) assays depending on the type of chemical reaction involved (**Figure 1-1**) (Huang et al., 2005). Examples of antioxidant assays commonly used that involve the HAT pathway are the oxygen radical absorbance capacity assay (ORAC), and the lipid peroxidation assay. Examples of ET assays are the 1, 1-diphenyl-2-picrylhydrazyl (α,α-diphenyl-β-picrylhydrazyl (DPPH) radical scavenging assay, and the ferric ion reducing antioxidant parameter assay (FRAP).

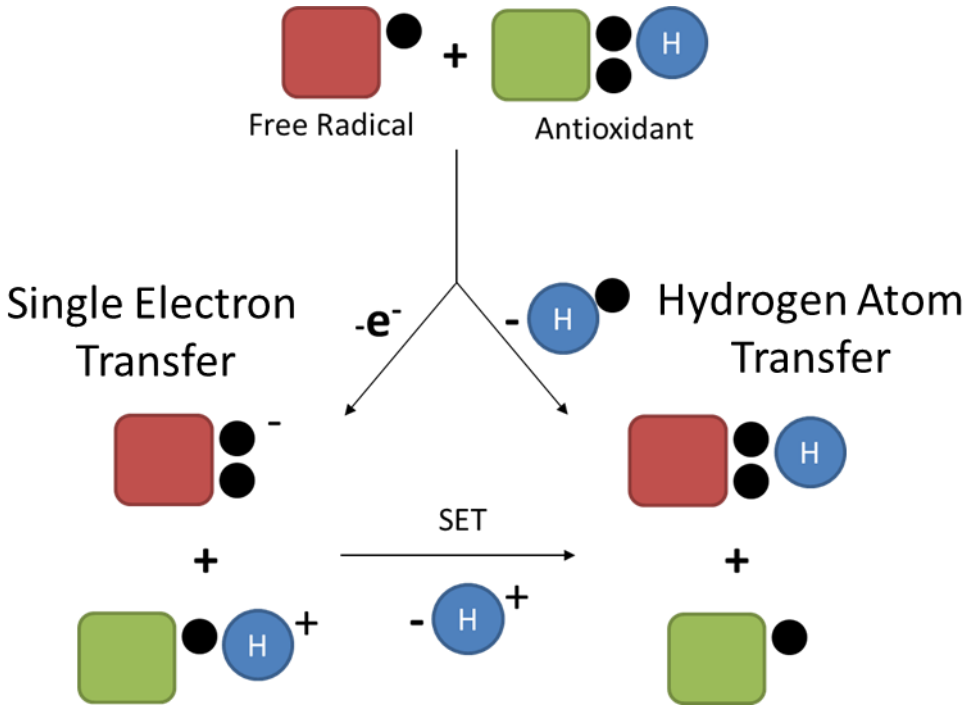

Figure 1-1 Mechanisms of hydrogen atom transfer (HAT), and single electron transfer (SET)antioxidant pathways. In SET an electron is transferred to the radical from the antioxidant, generating a radical cation, which can then form a radical. In the HAT pathway a hydrogen atom is donated from the antioxidant producing a radical.

The antioxidant properties of various bioactive peptides have been analysed in numerous studies. These studies use multiple assays to determine the antioxidative potential of different bioactive peptides. The studies by Corrêa et al (2014) and Ahmed et al (2015) that have previously been discussed here determined that small peptides hydrolysed form larger proteins could exhibit antioxidant properties.

Antioxidant properties of bioactive peptides can be assessed through various assays, some of which have been noted as being biologically significant to mammals. However, some antioxidant activities noted in certain papers were generated using assays that have been described as not being biologically relevant. In their review, Lopez-Alarcon and Denicola (2012) suggest that to thoroughly evaluate antioxidant ability of natural products, multiple chemical *in vitro* methods should be used including cell-based assays. It was found that there is not a strong correlation between chemical and cellular assays. The authors' stress that it is important to assess the samples in cellular based assays after initial screening has been carried out to evaluate their bioavailability. Antioxidant activity is not just related to the ability of a compound to scavenge ROS, and reactive nitrogen species (RNS), the up regulation of antioxidant enzymes is also important (López-Alarcón and Denicola, 2013). It is therefore important when investigating the antioxidant activity exhibited by peptides, to cover a broad range of antioxidant mechanisms by performing assays that utilise different pathways.

The information on antioxidant assays used to assess the capacity of peptides to reduce oxidative stress gathered from the literature suggests that to analyse the antioxidant activity of peptides requires the use of multiple assays. To reflect this, a selection of different antioxidant assays were used in this research. These will be discussed in section 2.26.

1.8.2 Blood pressure regulation

Hypertension is a condition that is of growing concern in modern global healthcare. It is the most important factor in relation to cardiovascular disease, with over 60% of adults over 60 years of age being affected (Delacroix, 2014). Angiotensin II is a peptide that is connected with common conditions associated with the cardiovascular system including hypertension, and coronary heart disease (Dostal

and Baker, 1999). The active form of angiotensin II, which causes the constriction of blood vessels, is generated by the action of ACE on angiotensin I. The inhibition of ACE is therefore an important therapeutic target (**Figure 1-2**).

ACE inhibitors were developed after the discovery of the antihypertensive effects of snake venom in the 1960s. Captopril, which was discovered in the 1970s, and its subsequent approval by regulatory bodies in the 1980s was the first commercially available ACE inhibitor (Cushman and Ondetti, 1991). In the following years, numerous ACE inhibitory peptides were isolated and derived from snake venom (Captopril being a prominent example), that have been developed into ACE inhibitors that improved upon Captopril in terms of selectivity and side effects. ACE inhibitory peptides have subsequently been found in food proteins (both animal and plant derived) and have been isolated by means of hydrolysis by proteases, and identified using HPLC and mass spectrometry(Himaya et al., 2012, Vercruysse et al., 2005, Hong et al., 2008).

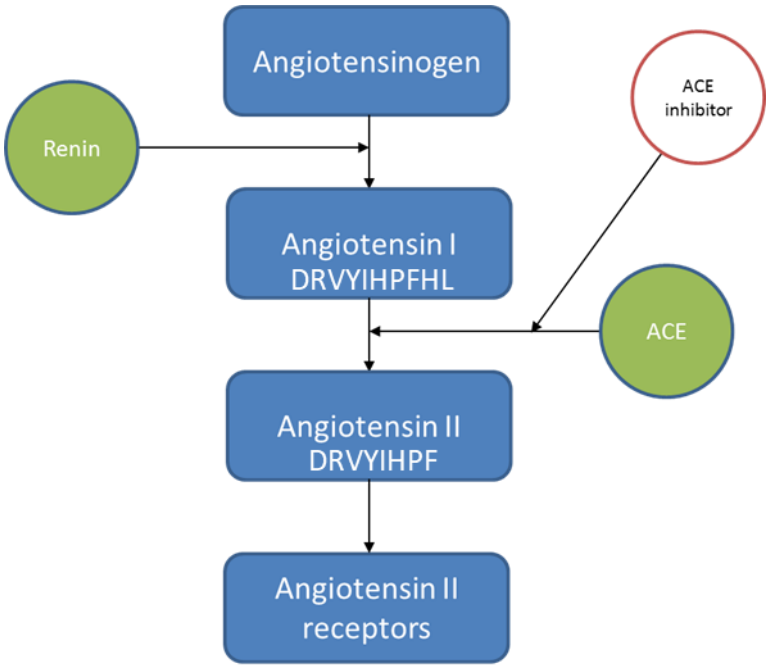

Figure 1-2 Simplified renin/angiotensin pathway. The active form of angiotensin II is generated by the action of angiotensin II converting enzyme (ACE) on angiotensin I. The inhibition of ACE prevents the activation of angiotensin II receptors of vascular smooth muscles, preventing contraction.

A number of studies have been performed on the ability of certain peptides to inhibit ACE *in vitro*. As discussed previously, Correa et al (2014), investigated hydrolysates derived from whey produced as a by-product of cheese making. One of the aspects of the peptides they assayed was their ability to inhibit ACE. Himaya et al (2012), and Jang and Lee (2005) investigated ACE inhibition caused by bioactive peptides.

Himaya et al (2012) isolated an active peptide from Pacific cod skin gelatin, a waste product of the fisheries industry, using gastrointestinal enzymes (pepsin, trypsin, and alpha-chymotrypsin) to hydrolyse the protein. The isolated peptide sequence was LLMLDNDLPP, which was shown to have potent non-competitive ACE inhibition, and showed antioxidant properties (Himaya et al., 2012). Their findings relate to other studies discussed previously in that peptides generated by hydrolysis using gastrointestinal enzymes contain hydrophobic residues at specific positions in the sequence. They highlight that the presence of branched chain aliphatic amino acids at the N-terminus (leucine and methionine), and that the proline and leucine residues at the C-terminus are what enables the peptide to be a potent ACE inhibitor. It is suggested that the lower molecular weight of digested peptides not only ensure that bioactive sequences are exposed, but that they are also more biologically available because they can easily be absorbed into the body (Himaya et al., 2012).

The findings of Himaya et al (2012) echo that of the one carried out by Jang and Lee (2005), analysing peptides derived from meat waste, discussed previously. They found that the sequence of the peptide with the greatest ACE inhibitory activity was VLAQYK, with the valine (a branched chain aliphatic amino acid) at the N-terminus enabling the ACE inhibitory activity of the peptide (Jang and Lee, 2005). The fact that the peptides isolated in each study end in hydrophobic residues appears to be the significant factor in activity. The large aromatic side chain of tyrosine could also cause steric interference, if the smaller aliphatic valine binds to the ACE.

The ACE inhibitory activity assessed by the two studies discussed here was determined using the Cheung and Cushman (1971) method, which utilises he ACE specific substrate hippuryl histidyl leucine

(HHL). The hydrolysis of HHL results in the product hippuric acid (HA) by ACE, is used to measure the activity of the enzyme by detecting the amounts of HA in relation to HHL by ultra-violet (UV) spectrophotometry. Reduction in HA production when the reaction mixture contains ACE inhibitors is used to assess their functional ability (Cushman and Cheung, 1971). Improvements to this assay have been undertaken in other studies, such as the use HPLC as the method of detection, increasing the sensitivity of the assay (Meng et al., 1995).

The study carried out by Lassoued et al (2015), investigated hydrolysates from thornback ray skin. Directing their research towards ACE inhibition and antioxidant activity, sequences isolated were assayed before being synthesised to confirm their activity *in vitro*. They found the most active ACE inhibitor to be GIPGAP (Lassoued et al., 2015).

The three peptides discussed here (LLMLDNDLPP, VLAQYK, GIPGAP) while appearing to be different in structure do show some similarities to each other that may determine their activity. LLMLDNDLPP and VLAQYK both have residues with hydrophobic sidechains at the N-terminus (LLML, and VLA), and LLMLDNDLPP and GIPGAP both have proline at the C-terminus. Proline is the particular amino acid is that conveys the activity of Captopril and has been noted to be important in the inhibition of ACE (Bhuyan and Mugesh, 2011). ACE has also been noted to preferably bind to peptides with hydrophobic residues at the C-terminus (Segura Campos et al., 2013). While VLAQYK ends in lysine, it does contain tyrosine next to the C-terminus, and considering the size of the peptide, the sidechain of tyrosine is likely to be available. This method of synthesising peptides derived from hydrolysates was adopted in work presented in chapter 5 of this thesis.

1.8.3 Wound healing

A prominent area of research involving bioactive peptides is that of wound healing. The process of repairing damage to tissues is performed, and controlled by various cell types, extracellular matrix molecules, mediators, and cytokines found at the site of the wound. Wound healing can be separated

into three distinct, but overlapping phases: Inflammation, tissue formation, and tissue remodelling (**Figure 1-3**).

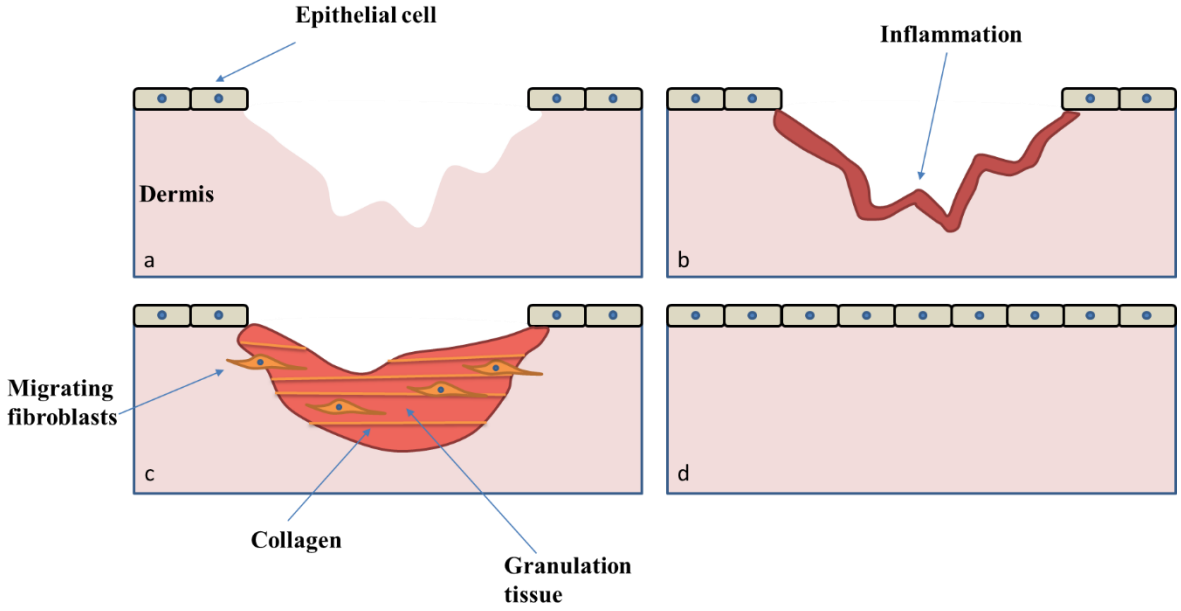

Figure 1-3 The three stages of wound healing after the initial damage (a) include inflammation where cells migrate into the wound area (b), tissue formation where granulation tissue forms, which is reinforced with collagen deposited by fibroblasts (c), and the remodelling phase where the wound is healed (d).

The inflammation stage involves the initial response to the trauma, including the aggregation of platelets to form a clot, the release of cytokines, and the arrival of leukocytes to the region. Tissue is then produced to cover over the wound site; this tissue is mainly made up of endothelial cells and fibroblasts. The tissue then undergoes remodelling to repair the wound (Eming et al., 2007).

Demidova-Rice et al (2011) derived bioactive peptides from vascular endothelial cell extracellular matrices (ECM). They proposed that the degradation of the ECM released bioactive peptides that stimulate cellular response to damage, and promote angiogenesis. ECM was degraded using collagenase from *C. histolyticum*. Peptides isolated from the hydrolysates were then synthesised, and assayed for their ability to stimulate the proliferation of capillary endothelial cells (CEC) in culture. They found that bioactive peptides derived from ECM could stimulate endothelial cell proliferation, and microvascular remodelling *in vitro* (Demidova-Rice, 2011).

A major factor involved in inflammation and tissue repair is the protease thrombin. This protein is part of a cascade that causes blood to clot. Prothrombin is cleaved to thrombin, which in turn cleaves fribrinogin to form fribin, an insoluble protein that forms the fibrous matrixes that limit the flow of blood (Brummel et al., 2002). Thrombin has also been shown to catalyse other important processes involved in wound healing (Stiernberg et al., 2000). In their study investigating the synthetic thrombin peptide, TP508 (AGYKPDEGKRGDACEGDSGGPFV), Stiernberg et al. (2000), demonstrated that the peptide accelerated wound closure (37% more than negative controls by day 7); importantly, the peptide does not promote the recruitment of platelets or cleave fibrinogin. The authors showed that wounds not only healed at a faster rate than the control, but they also had a greater breaking strength at the same point post treatment. The authors suggest that the mode of action of TP508 is related to how thrombin acts in the process of wound healing. In normal wound healing, products of thrombin degradation are released from the fibrin clots a few days after the injury, thus initiating a cascade. In this case, the application of TP508 would seem to initiate this cascade sooner.

The peptide (TP508) was assessed using an *in vivo* full thickness model. Adult male Harlan Sprague-Dawley rats had two full thickness dermal circles (2 cm) excised (down to the skeletal muscle). The wounds were treated either with saline or with saline containing TP508. The wounds were then left uncovered. The wounds were checked periodically to track wound closing. After the wounds had closed, the new tissue was excised and tested for breaking strength. Analysis of photomicrographs of the wound area indicated that the density of functional blood vessels was the same for each group; however, the number of larger vessels found in the TP508 treated groups were significantly greater than that of the control group. The authors suggest that the increased rate of wound closure is due to the increased early inflammatory cell recruitment, and the presence of blood vessels that are significantly larger than in the un-treated control group. The structure of the peptide is not discussed in this paper. They do state however, that the peptide binds to high-affinity thrombin receptors, and that in doing so mimics the natural activity of thrombin (Stiernberg et al., 2000). This indicates that the structure is specific to the receptor, and that during natural wound healing this part of the thrombin molecule will bind to the same receptors. The study by Stiernberg et al, 2000 highlights a useful *in vivo* wound healing

assay that could be used with active peptides derived from the Biofac samples if preliminary wound healing assays such as the scratch wound assay provide positive results. The fact that TP508 (though synthetic) is a fragment of a larger protein is interesting because it follows the precedent that active peptide sequences are located in longer inactive peptides. The discovery of active peptides by degradation of larger molecules *in-vitro* can therefore be linked with processes occurring *in-vivo* such as blood clotting. In comparison to the other sequences mentioned in this review, TP508 has affinity for a specific receptor so will not necessarily have similar sequence and structure.

1.8.4 Antimicrobial

Peptides can act as potent antimicrobial agents, many of which are large peptide sequences that can form into secondary structures, and have been shown to have a net negative charge with approximately 50% of the sequence being hydrophobic residues. The prevalence of the hydrophobic residues can lead to the peptide conforming into amphiphilic structures when interacting with cell membranes. Peptides that demonstrate antimicrobial activity contain alpha helical or beta sheet structures that are essential to function (Daoud et al., 2005, Marr et al., 2006, Powers and Hancock, 2003, Andreu and Rivas, 1998). The characteristics that make these peptides antimicrobial also account for toxicity towards eukaryotic cells (Chen et al., 2005).

Only two new classes of antibiotics have been developed, and approved in the past 20 years, neither of which are active on Gram-negative bacteria. While there are numerous targets still in development, only 15 out of 44 show any activity towards Gram-negative bacteria (Tacconelli et al., 2018). The systemic, pharmacodynamic and pharmacokinetic issues with peptides have not been overcome to date. Common issues arising include; *in vivo* half-life, susceptibility to mammalian proteases, dosing, and aggregation of peptides (Marr et al., 2006).

Daoud et al (2005) used hydrolysis to generate antimicrobial peptides derived from bovine haemoglobin. The antimicrobial activity was measured by the disc-diffusion method where activity is deduced from the diameter of the cleared area around the inoculation site in relation to a positive, and

a negative control. The peptide was shown to have antimicrobial activity against four species of bacteria, and was shown to not be haemolytic at relatively high concentrations (Daoud et al., 2005).

Antimicrobial properties of the Biofac samples could be evaluated in a similar way. However, sequence data of peptides contained in the samples would be important here because only sequences that can potentially form into the secondary structures are likely to confer antimicrobial activity, and would have to be released as a single peptide to become active.

1.8.5 Immune modulation/adjuvants/innate immune response

Immunomodulation is the process of modifying the immune system. Modification can be achieved either by the use of prophylactics (*e.g*. vaccines) or therapeutics (Gea-Banacloche, 2006). Many antimicrobial peptides found in a wide selection of organisms show direct antimicrobial action. There is evidence that these peptides also play an important role in modulating the innate immune response, can act as adjuvants, and promote wound healing (Brown and Hancock, 2006).

Cationic amphipathic peptides can be defined as peptides with between 12 and 50 residues. Within this sequence, between 2 and 9 will be a positively charged residues (either lysine or arginine), and up to half will be hydrophobic residues (Brown and Hancock, 2006). Cationic host defence peptides have been shown to be active against microbial infection and have immune modulating effect on the innate immune response. These peptides are one of the most conserved aspects of innate immunity in organisms and are expressed by either a response to pathogen associated molecular pattern molecules, or in response to inflammatory mediators, such as certain cytokines (Bowdish et al., 2005). LL-37 is an example of a human cationic host defence peptide that has been demonstrated to have a potent immunomodulating activity.

1.9 In Silico Analysis

Bioinformatics is a powerful tool in the analysis of peptides released from protein digests because of the great number of sequences that can be isolated from peptides. Thus *in silico* analysis of peptides

can therefore, lead to the more rapid discovery of novel bioactive peptides. A number of online tools are available that predict possible cleavage sites, for example the BIOPEP database (Minkiewicz et al., 2008) can be used to predict the peptides released from proteins after digestion with a selected enzyme. This information can be used in conjunction with experimental data, to predict the type of sequences that are in a particular hydrolysate. Therefore, an *in silico* approach to selecting the enzyme to hydrolyse precursor proteins can be a useful tool (Cheung et al., 2009). The predicted peptides that are generated by the *in silico* digests can then be further analysed by online tools that can predict bioactivity. The example of the resource used in the present study was the Peptide Ranker tool by Bioware (Mooney et al., 2012). This program assigns a rank to the likelihood of a peptide sequence being bioactive (0.0 being highly unlikely, 1.0 being highly likely). Further details on how the Peptide Ranker tool works is presented in chapter 5.

An example where peptide databases were used in the discovery of bioactive peptides was the study performed by Cheung et al. (2009). This group utilised the BIOPEP database to predict which enzyme would produce the most bioactive peptides from oat proteins that could inhibit ACE. The group then used the information gathered to compare with experimental data to validate their method. The results indicated that an *in silico* approach to selecting the enzyme to hydrolyse precursor proteins can be a useful tool. Another group that utilised the BIOPEP database was that of Lafarga et al (2014). The group used *in silico* techniques to predict the release of bioactive peptides from proteins derived from haemoglobin, collagen, and serum albumin. Peptides that were identified to be bioactive (in this case antihypertensive) were synthesised and assayed *in vitro* (Lafarga et al., 2014).

1.10 Biofac Hydrolysates

This project was based on investigating the bioactive properties of hydrolysates of porcine liver, and placenta provided by the company Biofac. These were produced by processing the raw material (liver or placenta) before hydrolysis is carried out with the cysteine protease papain. The procedure used to produce the hydrolysates is described in **Figure 1-4**. Briefly, the raw material generated from meat waste was homogenised before the addition of water and heating to 85°C. Hydrogen peroxide was then

added to the mix, and the batch was heated to 63-68°C, at this point papain was added and the reaction mixture was left for 10-14 hours. The temperature was then increased to 85°C for 30 minutes to inactivate the enzyme, after which several filtration steps were undertaken to purify the sample. The sample was then dried through evaporation, and spray dried before the final sieving process.

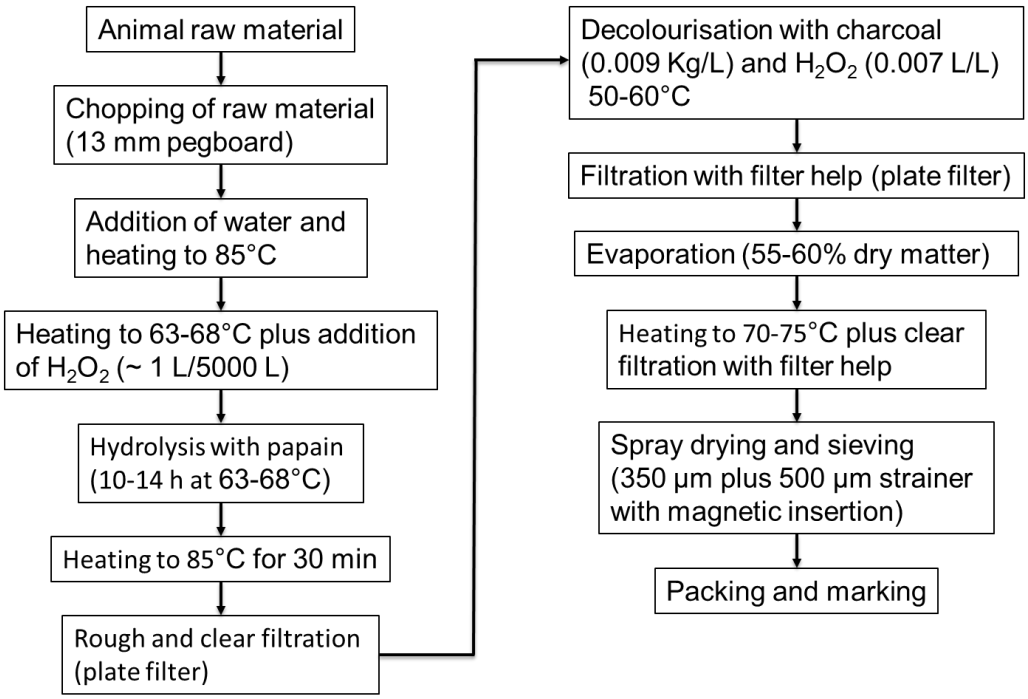

Figure 1-4 Biofac procedure for the production of porcine hydrolysates.

The use of papain as the proteolytic enzyme results in multiple peptides of varying length (Storer and Ménard, 2013). Papain preferentially hydrolyses polypeptides as illustrated in **Figure 1-5** with the resulting peptides having a structure as shown **Figure 1-6**. The enzyme however, can also cleave at the carboxyl side of a number of different residues that can exhibit basic, acidic, and neutral characteristic, along with aliphatic and aromatic residues (Kimmel, 1954). These factors indicate that hydrolysates generated through papain digestion will contain many small and varied peptides.

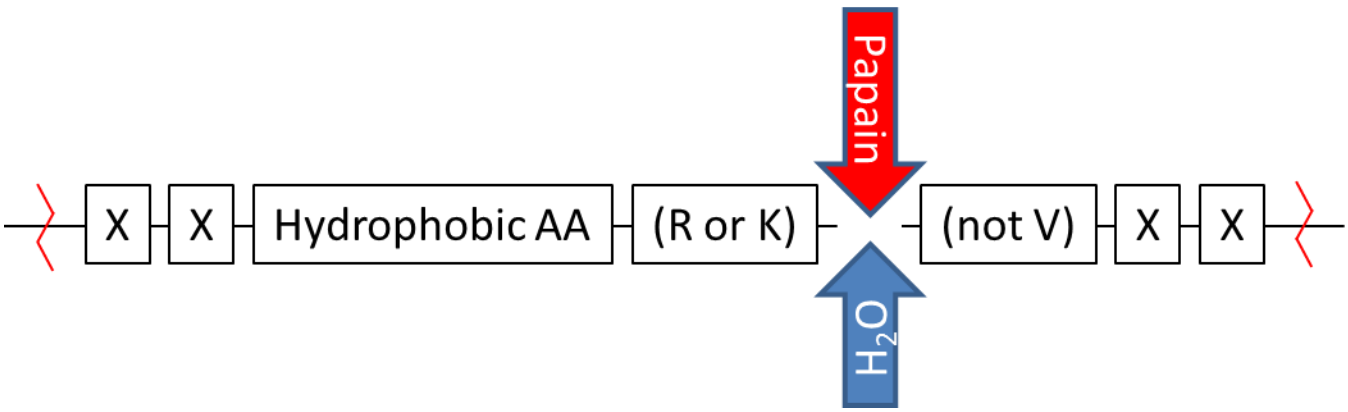

Figure 1-5 Preferential cleavage site for papain

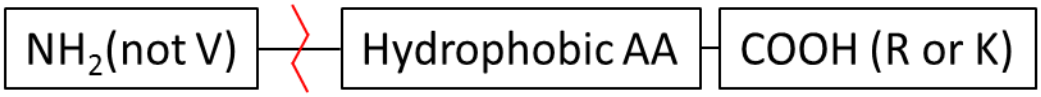

Figure 1-6 Possible structure of peptide resulting from hydrolysation of a polypeptide by papain

Because papain is not a highly specific protease, the peptides that result from papain hydrolysis are likely to be diverse. However, there are a number of statements that can be made about peptides generated from papain:

- Valine will not be at the N-terminus or the C-terminus: If valine is present in the peptide it will be mid sequence. Valine is hydrophobic so it can be next to the C-terminus.
- Arginine and lysine are likely to be at the C-terminus; other amino acids that may be at the C-terminus are glutamic acid, histidine, glycine, tyrosine, and alanine.
- The amino acid immediately upstream of the C-terminus will be a hydrophobic residue

1.11 Rationale of Study

The methodology of the studies that look into the bioactivity of peptides generally follow a similar trajectorary: Separate the hydrolysate; assay the fractions; isolate indivdual peptides in active fractions; synthesise the peptides, and repeat the assay. The aims of this project were, 1) to identify the host proteins that were hydrolysed to produce the peptides and 2) to identify, using *in silico* methods, peptides that would likely be produced by the particular enzyme used in the hydrolysis. The resultant peptides could then be anaylsed for the likelyhood of bioactivity, then manufactured and used in assays. The method described by Cheung et al. could also be applied to different enzymes, in doing so it would

be possible to identify peptides before hydrolysis. For this project however, papain was the target enzyme because of its use by Biofac in the manufacture of its products.

The data from the studies discussed in this review indicates the possibilities for the Biofac peptides to show bioactivity. Some of the studies discussed have made direct links to the structure and sequence of peptides to their bioactivity while looking at derivatives of larger proteins (Himaya et al., 2012, Jang and Lee, 2005, Lassoued et al., 2015). It is clear that the amino acid sequence is important to the relative bioactivity. Moreover, if similar sequences can be identified within peptides from different sources, such as meat waste, and plants, it suggests that there are a many potential bioactive peptides in the hydrolysates produced by Biofac.

CHAPTER 2 **Materials and General Methods**

2.1 Materials

2.1.1 Biofac hydrolysates

The hydrolysates were produced by Biofac at their manufacturing site in Copenhagen, Denmark. Over the course of the study a number of batches, of each type of hydrolysate were used. This study was an industrially funded project, which meant that the changing requirements of the company had to be taken into account. The products that they produce changed over this period, and so their interests in some of the hydrolysates lessened. An important factor relating to this was the introduction of an additional filtration step in the production of the liver, and placenta hydrolysates. Another change was that after the first stage of the project, the heart hydrolysate was deemed to be less of a priority. It is for this reason the investigation focused on the liver and placenta hydrolysates, and that not all the batches were analysed using the same techniques. Throughout this thesis the hydrolysates are referred to the abbreviations reported in **Table 2-1**.

Table 2-1 Description, batch number, and abbreviated form for the Biofac hydrolysates used in this study

Description	Batch number	Abbreviation
Heart hydrolysate	150601-1000	H1
Liver hydrolysate	150615-1900	L1
Liver hydrolysate	160126-0700	L2
Liver hydrolysate	170127-0815	L3
Placenta hydrolysate	0-150625-1700	P1
Placenta hydrolysate	0-160330-1500	P2

2.1.2 Synthetic peptides

The synthetic peptides that were used in this project (**Table 2-2**) are referred to as their sequence of amino acids (single letter code). The peptides were synthesised by Peptide Protein Research, 10 mg of each peptide were provided.

Table 2-2 Sequences of the synthetic peptides derived from amino acid sequences found in the Biofac hydrolysates

Description	Supplier
FFNDA	Peptide Protein Research Ltd (Fareham, UK)
FWG	Peptide Protein Research Ltd (Fareham, UK)
SDPPLVFVG	Peptide Protein Research Ltd (Fareham, UK)
MFLG	Peptide Protein Research Ltd (Fareham, UK)
LG	Sigma Aldrich (Gillingham, UK)

2.1.3 Equipment

The specialist equipment used to analyse the hydrolysates, and the synthetic peptides for this project are listed in **Table 2-3**.

Table 2-3 Specialist Equipment

Description	Name	Supplier
Analytical column	Ascentis® Express Peptide ES-C18	Sigma Aldrich (Gillingham, UK)
Prep column	Dynamax C18 -60A	Agilent (Cheadle, UK)
HPLC pumps	System Gold 125 Solvent Module	Beckman Coulter (Palo Alta, USA)
HPLC detector	System Gold Programmable Detector Module 166	Beckman Coulter (High Wycombe, UK)
Prep HPLC pumps	Model 303, and Model 305	Gilson (Dunstable, UK)
Prep HPLC detector	HM Holodrone UV-Vis	Gilson (Dunstable, UK)
Prep HPLC printer	Kipp and Zonen BD40	Gilson (Dunstable, UK)
Fluorescent microplate reader	Fluostar Optima microplate reader	BMG Labtech (Aylsbury, UK)
Microplate reader	Infinite F50	Tecan (Männedorf, He)
Wet laser diffraction particle size analyser	Mastersizer	Malvern Panlytical (Malvern, UK)
Dry powder laser diffraction particle size analyser	Helos	Sympatec (Bury, UK)
SECMALS (Size Exclusion Chromatography coupled to Multi-Angle Laser Light Scattering	DAWN HELIOS-II (light scattering detector) & rEX (refactive index detector)	Wyatt Technologies (Santa Barbara, USA)
Shear cell apparatus	RST-XS	Dietmar Schulze (Wolfenbüttel Germany)
SEM	Quanta250 FEG	FEI Instruments (Hillsboro, USA)
Light microscope	E24 HD	Leica (Wetzlar, Germany)

2.1.4 General materials

All general laboratory reagents and materials used in this project were supplied by Sigma Aldrich (Gillingham, UK), Sarsedt (Nümbrecht, Germany), and Thermo Scientific (Loughborough, UK). Specific materials and reagents are recorded in **Table 2-4**.

Table 2-4 Specific materials and reagents

Description	Supplier
FluoroNunc™/LumiNunc™ 96-Well Plate	Thermo Scientific
Nunc™ F96 MicroWell™ Black	Thermo Scientific

2.1.5 Cell line

The cell line used for the entirety of the cell culture for this project was mouse 3T3 fibroblasts (p12) (NIH 3t3 cells, LGC, Middlesex, UK).

2.2 General Methods

The analytical methods used in this project were used over multiple chapters, with slightly different procedures. This section describes the basic mechanisms of the methods, and rationale behind their use. For more detailed procedures, see the methods sections in the results chapters (3, 4, and 5).

2.2.1 Microscopy

Microscopy was used to analyse the physical structure of the hydrolysate particles. This information was used to build up a profile on each sample, which could provide information on how the hydrolysate powders flow.

2.2.1.1 Light Microscopy

Light microscopy (LM) was used to investigate the structure of the particles under visible light, thus allowing the colour of the samples to be analysed. A Leica E24 HD was used for LM; samples were taken from P1, L1, and H1, and pictures taken.

2.2.1.2 Scanning Electron Microscopy

Scanning electron microscopy (SEM) was used to analyse the structure of the particles to a greater magnification than is possible using LM. Samples were analysed using a FEI Instruments, Quanta250 FEG SEM (full details in section 3.2.1).

2.2.2 Particle Size Analysis

The particle size distributions of the hydrolysates were analysed using three methods. Pharmaceutical sieves were used to separate the powders into fractions of different sizes. The fractions generated were used in the particle flow analysis to understand how the different sizes of particles, and their distribution influenced the flow of the product. Alongside the sieves, two methods of laser diffraction were used to

analyse the particle size distribution, wet laser diffraction using a Malvern Mastersizer 2000, and dry laser diffraction using a HELOS (Hi209) laser diffraction sensor with RODOS dispersion unit. The laser diffraction methods are useful to analyse particles that are rounded, and are able to separate particles that are agglomerated (a limitation with the pharmaceutical sieves).

2.2.3 Particle Flow Analysis

The ability of the particles, that make up the hydrolysate, to flow is an important factor to consider in the manufacturing process. To analyse the flow properties of the hydrolysates, a RST-XS shear cell apparatus was used. The data outputted from this device indicates how well the samples flow as a flow function (10 is free flowing and 1 is cohesive). The fractions generated through the molecular sieving were used, alongside the full hydrolysates in the flow analysis.

2.2.4 Size Exclusion Chromatography Multi-Angle Light Scattering

The hydrolysates were analysed using Size Exclusion Chromatography Multi-Angle Light Scattering (SEC-MALS) to assess the molecular weight profile of the peptides. SEC-MALS is a method that separates the molecules in a sample by size, before analysing them using multi-angle light scattering, which is used to determine the molecular weight of the molecules in solution.

2.2.5 Phenol-Sulphuric Acid Assay

The production method used to make the hydrolysates is intended to produce a powder that is made up of peptides derived from the specific starting material. The analysis of the bioactivity of the hydrolysates is directed towards bioactive peptides, however, there could be other active molecules within the samples. Therefore, the total carbohydrate content of the hydrolysates was assessed using the phenol-sulphuric acid assay. This colourimetric assay can determine the concentration of reducing sugars in solution, when mixed with phenol and sulphuric acid, by measuring the optical density at 490 nm (orange/red) (DuBois et al., 1956). This assay can be used to estimate the carbohydrate content of a sample in relation to a standard. In this case, glucose was used as the standard.

2.2.6 Antioxidant Assays

2.2.6.1 DPPH Radical Scavenging Activity (RSA)

1, 1-Diphenyl-2-Picrylhydrazyl (α,α-Diphenyl-β-Picrylhydrazyl (DPPH) is a stable free radical that is utilised in a simple assay that can be used to determine the radical scavenging capacity of an antioxidant. When mixed with a proton donating substance, DPPH is reduced from the purple radical to produce the pale yellow to clear non-radical form. The change in colour is used to evaluate the ability of an antioxidant to scavenge radicals through proton donation (Alam et al., 2013). The inexpensive, and simple nature of this assay makes it an ideal method to rapidly screen antioxidants. The limitations of this assay are that the test sample solutions must be miscible with alcohol, and that the mechanism of reduction demonstrated is not limited to antioxidants; other substances that exhibit no antioxidant activity, such as hydrogen peroxide, can reduce the radical form of DPPH to the non-radical form (Amorati and Valgimigli, 2015).

2.2.6.2 Oxygen Radical Absorbance Capacity Assay (ORAC)

The ORAC assay, is one of the more prevalent methods in the literature to determine the level of activity of antioxidants. The ORAC method is an example of an assay that utilises a fluorescent probe that can be oxidised by free radical generating compounds such as 2,2′-Azobis(2-methylpropionamidine) dihydrochloride (AAPH) (Amorati and Valgimigli, 2015). The assay measures the ability of antioxidants to protect the probe by absorbing oxygen radicals, and is detected by measuring the fluorescence of the probe at specific time points over a set period of time. The antioxidant capacity is measured by comparing the area under the curve of the experimental samples to that of a known antioxidant standard, in this case the vitamin E analogue Trolox, and is reported as Trolox equivalence (TE) (where a TE of 1 indicates that 1 g of the experimental sample is equivalent to 1 g of Trolox).

2.2.6.3 Lipid Peroxidation Inhibition

To assess the ability of the hydrolysates to reduce or inhibit lipid peroxidation, the linoleic acid/ ferric thiocyannate assay (FTC) method was used. This assay is based on the production of lipid peroxyl fatty

acid radicals through autoxidation. The linoleic acid model is used as an approximation of phospholipid bilayers that make up cell membranes. This assay is an inexpensive, and relatively rapid (in comparison to cell culture assays) method to determine the effect of antioxidants on oxidative stress caused through the autoxidation of non-conjugated polyunsaturated lipids (Nazeer et al., 2013).

2.2.6.4 Cellular Antioxidant Activity Assay

While the use of chemical *in-vitro* assays to assess the antioxidant capacity compounds is an important element in antioxidant screening, there are a number of issues associated with these methods. Some of these methods are not carried out under biologically relevant conditions, such as pH, and they do not account for the biological mechanisms *in-vivo*, that could affect the compounds such as them being metabolised, and their bioavailability. They also use molecules that are not found *in-vivo* such radicals like DPPH, or oxygen radical generators like AAPH (Liu and Finley, 2005). The most relevant assays would therefore be *in-vivo* methods that use animal models, and detect the effects of the antioxidant through experiments on serum samples (Onoja et al., 2014), however, the cost and ethical considerations make these methods less attractive. Cell-based assays are therefore a viable alternative to both chemical *in-vitro*, and *in-vivo* assays because they take into account physiological conditions. The method used in this study exploited the intracellular oxidation of 2′, 7′-dichlorodihydrofluorescein (DCFH) into the fluorescent dichlorfluorescein (DCF). In the case of the assay, AAPH is used as a source of oxygen radicals, to differentiate from oxidative stress that would occur naturally with the cells. The ability of antioxidant to reduce the oxidation of DCFH to DCF (and therefore produce lower fluorescence) is measured by comparing the experimental groups with that of a negative control. The percentage reduction in oxidation can be calculated from this data (Wolfe and Liu, 2007).

2.2.7 Cell Proliferation

The ability of the hydrolysates to influence cell proliferation (negativity or positively) were analysed to assess if the samples could have an impact on wound healing. Two methods were used to determine the level of proliferation of treated cells in relation to a control group of untreated cells.

2.2.7.1 Cell Counting

This method used cell counts derived from a haemocytometer to determine the number of cells in culture for each test sample, and to generate population doubling level (PDL), and doubling time (DT) data. PDL is a measure of how many times a population of cells have doubled over the time that they have been in culture, while DT measures the average time taken for the population to double. These two figures are an important measure of the health of cells in culture. A greater PDL indicates that the cells are proliferating a higher rate, while a lower PDL indicates that the teat samples are having a negative effect on the cells.

2.2.7.2 3-(4,5-Dimethylthiazol-2-yl)-2,5-diphenyltetrazolium bromide (MTT) Assay

3-(4,5-Dimethylthiazol-2-yl)-2,5-diphenyltetrazolium bromide (MTT) is a yellow tetrazole that when reduced by enzymes present in mitochondria, forms purple formazan crystals that are soluble in organic solvents. Measuring the absorbance of the dissolved formazan crystals is used to determine metabolic activity of the cell population. This can be used as an indirect measure of cell viability and proliferation (Liu et al., 1997). In this study, the MTT assay is used by generating standard curves with known numbers of cells, which the test samples were measured against. In this way the assay could be used to estimate cell number directly.

2.2.8 Wound Healing Assay (Scratch Assay)

The scratch wound assay is a convenient method to test the ability of the peptides in aiding cell migration. The simulation of a wound on a confluent monolayer, by creating a 'scratch' is easy to prepare, quick, and is low cost; this makes it an ideal preliminary assay for wound healing (Liang et al., 2007). This method is used as a measure of cytotaxis, therefore the antimitotic compound Mitomycin C was added to the cell culture media to arrest cell proliferation.

2.2.9 High Performance Liquid Chromatography (HPLC)

2.2.9.1 Analytical HPLC

Reverse phase HPLC was used to analyse the composition of the hydrolysates, to isolate individual peaks for use in identification, and to test the purity of the collected fractions. All HPLC used in this study used an analytical C18 column specifically designed for peptides and small proteins (Ascentis® Express Peptide ES-C18 (length 100 mm, ID 4.6 mm). All HPLC used UV at 220 nm for detection except HPLC used in the ACE assay (228 nm).

2.2.9.2 Preparative HPLC

Preparative HPLC (prep HPLC) was used to fractionate the hydrolysates, which could then be recovered by lyophilisation. The recovered fractions were then analysed for physical appearance, and bioactivity using the assays established for the analysis of the full hydrolysates. The method used to fractionate the hydrolysates with the preparative column was produced by scaling up the method used for the analytical HPLC.

2.2.10 Lyophilisation

Peptides in the fractions generated from preparative HPLC were recovered by lyophilisation. This method was used because it is relatively simple, and because the method is unlikely to alter the molecular compositions of the peptides, because it does not use high temperatures as the drying method. The powders resulting from the freeze drying process were then reconstituted in the appropriate buffers for the required assay.

2.2.11 ACE Inhibition Assay

The prevalence of bioactive peptides, which have been reported to inhibit ACE was the reason the hydrolysates anti-ACE activity were assessed. The method used in this study uses the substrate HHL, which ACE will metabolise to produce HA. The digestions were separated by HPLC using UV to detect the levels of HHL, and HA (detection at 228 nm). Inhibition of ACE would lead to a reduction in the

levels of HA. This method was selected because HPLC is able to separate the product from the substrate, leading to a sensitive detection method.

2.2.12 De-Novo Peptide Sequencing Using MS/MS

De-Novo peptide sequencing was outsourced to the Metabolomics & Proteomics Lab at the University of York. This method was used to determine the sequences of the isolated peptides derived from the hydrolysates. These sequences were used to identify the probable host protein from in which the peptides originated.

2.2.13 In silico Analysis of Bioactive Peptides

In silico analysis was used to analyse the likelihood of certain peptides being present in the hydrolysates, and the possibility of those sequences being bioactive. The digestion of the host proteins derived from the *De-Novo* sequencing, and their comparison to known bioactive peptides were performed using tools on the BIOPEP website (Minkiewicz et al., 2008). The likelihood of the peptides being bioactive were assessed using the Bioware Peptide Ranker tool (Mooney et al., 2012).

CHAPTER 3 **Physicochemical analysis of possible bioactive hydrolysates derived from porcine hydrolysates**

3.1 Introduction

The initial work carried out on the evaluation of the three Biofac hydrolysates (liver (L1), placenta (P1), and heart (H1)) supplied, was focused on their physicochemical properties. This included the morphological characteristics of the peptide samples, the particle size distribution, and their solubility. The rationale for investigating these properties at the beginning of the project was that these data are important parameters, which may provide useful information with regards manufacturing processes. The physicochemical properties of the individual hydrolysates will be affected by both their molecular composition, and the manufacturing process used to produce them. An example of a property that can be affected is flowability. For instance, lyophilised samples will demonstrate a reduced ability to flow because of their planer morphology, compared to spray dried samples which produces more spherical particles (Singh et al., 2013, Febriyenti et al., 2014). The drying process therefore, will alter the final physical make-up (size and shape of the particles) of the powders, which in turn, will affect certain physical properties. These include flowability, compaction behaviour, and dissolution (Rajinikanth et al., 2012), therefore identifying the basic morphology of the powders was an important first step as this also affects how the hydrolysates are further processed into formats that can be consumed, such as tableting and capsule filling. The solubility of the hydrolysates is important to the bioavailability of any potential bioactive peptides within the powder. Solubility is the ability of a substance to dissolve into solution. The fundamental parameters of solubility are dependent on the molecular composition of the solute, and therefore not necessarily affected by the drying process, however, if the temperature used in a process such as spray drying is too high, then this could have an effect on the molecular composition of peptides in the hydrolysates (Mujumdar et al., 2014).

The average molecular mass of the peptides within the hydrolysates was analysed using size exclusion chromatography coupled with multi-angle light scattering detection (SEC-MALS). This procedure was

used on the original hydrolysates (L1, P1, and H1) as well as further batches received from Biofac (L2, and P2). L2 and P2 were produced in a similar fashion to L1 and P1, but with an added filtration step to remove particles with a molecular weight (MW) greater than 5 kDa.

The hydrolysates were analysed using a phenol-sulphuric acid assay. This was used to determine the concentration of reducing sugars in the hydrolysates, when mixed with phenol and sulphuric acid, by measuring the optical density at 490 nm. A series of glucose standards were prepared and assayed alongside the hydrolysates. Carbohydrates can also illicit bioactivity, so it was important to assess the proportion of carbohydrates in each sample (Hu et al., 2016). All liver, and placenta hydrolysates used in this project were analysed using this method (L1, L2, L3, P1, and P2).

This section of the study is dedicated to the physical properties of the hydrolysates. This information was gathered to gain an understanding of how the individual products behave as solids and in solution. This information was aimed at the producing data that can be used in the optimisation of the production process for Biofac.

3.2 Materials and methods

3.2.1 Microscopy of peptide samples

The size and shape the particles from each sample were analysed using LM (Leica E24 HD), and SEM (FEI Instruments, Quanta250 FEG). The samples were prepared for SEM by coating in a gold and platinum alloy (3 nm) using a 7920 Sputter coater (Quorum Instruments) for a period of 45 seconds. The samples were mounted on an aluminium stub (50 nm diameter). The SEM was operated in high vacuum mode with an accelerating voltage of 20 kV. The images were taken using Back Scattered Electron Image (BSEI), and an Everheart Thornley Detector (ETD) for secondary electrons. The images generated by SEM were used to compare the microstructure of the samples and the light microscopy provided information regarding the macroscopic size and shape.

3.2.2 Particle size analysis

To determine the particle size distribution of the samples three methods were used: Wet laser diffraction, dry powder laser diffraction, and pharmaceutical sieving. The hydrolysate samples were analysed by wet laser diffraction using a Malvern Mastersizer 2000. The samples were dispersed in hexane and particle size distribution was measured. Individual samples were measured four times to assess the reproducibility of the data.

The hydrolysate samples were analysed in the dry powder form using a HELOS (Hi209) laser diffraction sensor with RODOS dispersion unit, this method of sizing is particularly beneficial for moisture-sensitive materials.

To assess the range of particles present and to assess a cheap and simple approach to sizing pharmaceutical sieves were used. The samples were passed through a series of sieves with an aperture range of 250-180 µm, 180-125 µm, 125-75 µm, 75-38 µm, and less than 38 µm. Particles that were retained by each sieve were collected and weighed as a percentage of the total weight (assuming that the density was equal) of the hydrolysates added to the sieves. The mass of each hydrolysate loaded onto the sieves were, 135 g of H1, 85 g of L1, and 78 g P1.

3.2.3 Particle flow analysis

To assess the followability of each of the crude hydrolysate, and the fractions generated by pharmaceutical sieving, a RST-XS shear cell apparatus was used. The flowability of each fraction was expressed as a flow function (FFC), where 10 is free flowing and 1 is cohesive. The individual fractions were loaded into the annular shear cell. Vertical force (measured as vertical load F_N) was applied to the sample through a loading rod connected to the annular lid. Torque (measured as shear forces F_1 and F_2) was then applied to the cell through horizontal tie and push rods. Torque was applied until the powder contained in the cell began to shear. The forces applied to the cell were computer-controlled through a program with pre-set parameters (RST-CONTROL 95). The flow properties were calculated from multiple measurements.

3.2.4 Solubility and saturation point

The saturation point over a pH range between 1.2 and 7.2, for each hydrolysate was investigated as this information can potentially relate to the bioavailability of the hydrolysates if taken orally. The saturation point for each hydrolysate was obtained by adding the samples to 10 mM phosphate buffer (at pH 1.2, 5.8, and 7.2) at room temperature until the solution was saturated (powder remained in suspension, which was 1.5 g in 5 mL of buffer for L1, and 1 g in 5 mL for P1). The samples were placed in a shaking water bath, at 37 °C and 100 oscillations per minute, and left for 24 hours. The samples were then centrifuged at 3.0 x g for 6 minutes, and the supernatant removed. The supernatant was then filtered through filter paper to remove any residual particulates. The samples were then diluted accordingly with the relevant buffer to enable analysis by UV-Vis (ultra violet/visible light spectrophotometry). The concentration of the hydrolysate in solution was calculated from a standard curve derived from known concentrations (0 – 80 µg/mL) of the same hydrolysate (**Figure 3-1, and Figure 3-2**); the concentrations calculated for each sample were then multiplied by the relevant dilution factor to give the saturation concentration.

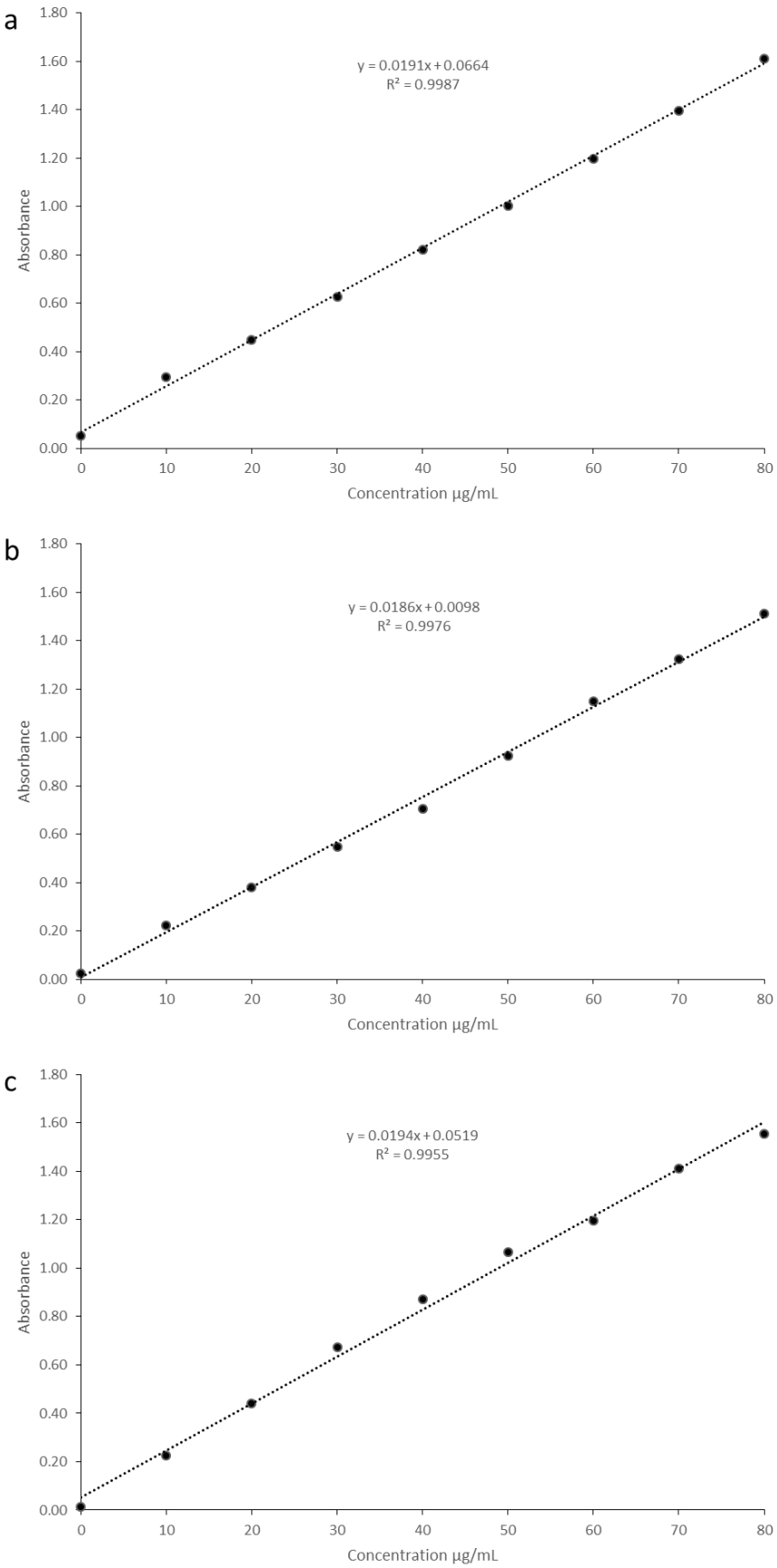

Figure 3-1 Standard curve using different concentrations of liver 150615-1900 (L1) to determine the concentration of 150615-1900 (L1) at the saturation point at pH 1.2 (a), pH 5.8 (b), and pH 7.2 (c)

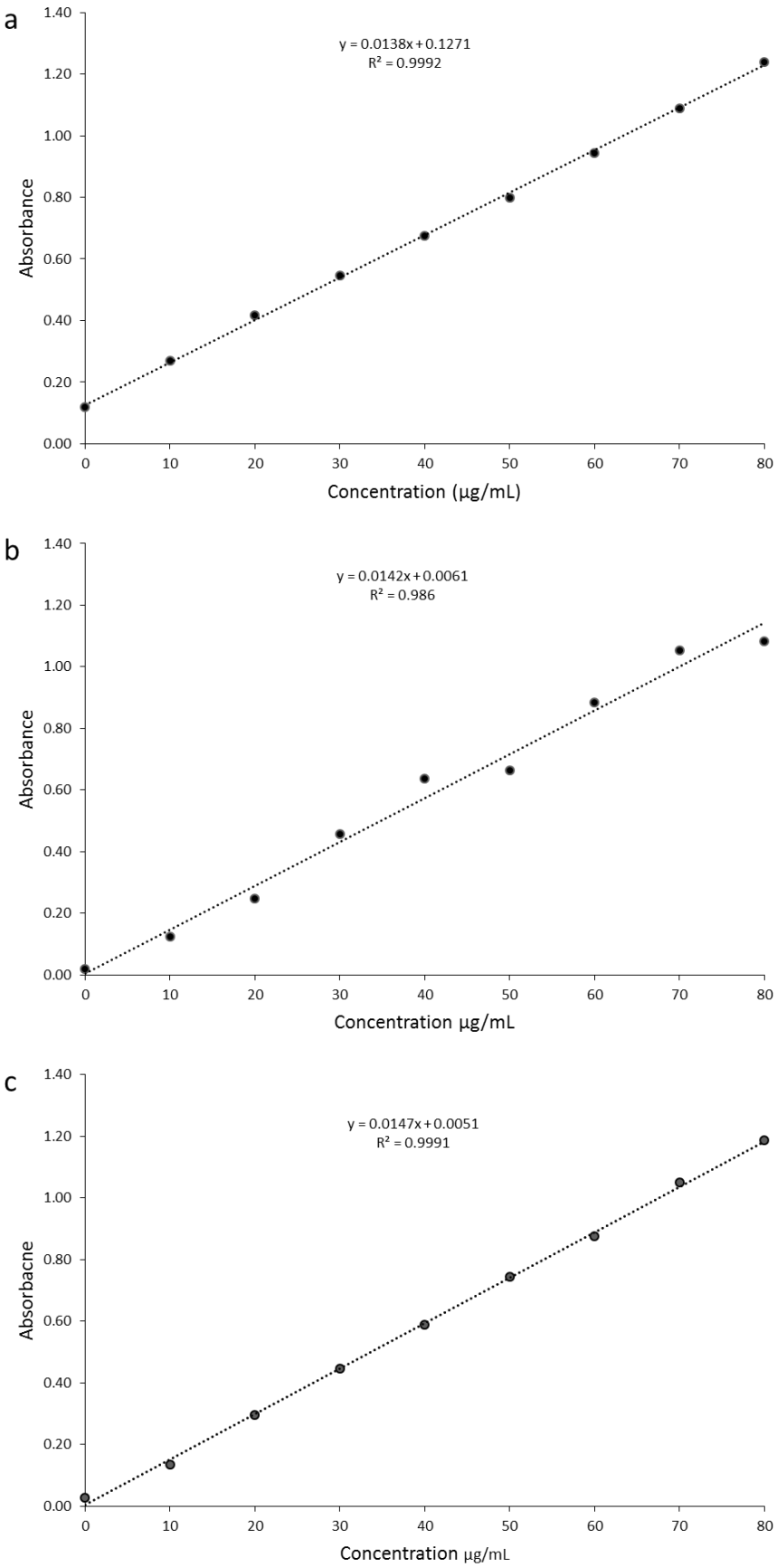

Figure 3-2 Standard curve using different concentrations of heart 150615-1900 (H1) to determine the concentration of heart 150615-1900 (H1) at the saturation point at pH 1.2 (a), pH 5.8 (b), and pH 7.2 (c)

The standard curves were generated by preparing a stock solution for each individual hydrolysate, (1.0 mg/mL). This was prepared by adding the relevant hydrolysate (100 mg) to a 100 mL buffer solution in a volumetric flask. A series of dilutions was then prepared in triplicate for all samples.

The dilutions were analysed by UV-Vis to determine the absorbance of each concentration. The wavelength range used was 300 nm to 190 nm because peptide bonds absorb UV between 190-230 nm, and the UV active amino acids (tryptophan, tyrosine, and phenylalanine) absorb UV between 257 and 280 nm. The samples were analysed in silica cuvettes, and run on a fast scan mode. The average peak absorption (λ_{max}) of each sample was plotted against concentration to produce standard curves. Standard curves were not produced for placenta peptide at pH 5.8, and pH 1.2. This was because of the high solubility of this peptide at pH 7.2.

3.2.5 SEC MALS analysis

SEC-MALS was used to determine the molecular weight of the hydrolysates. Heart (H1), two batches of liver (L1, and L2) and two batches of placenta (P1, and P2) hydrolysates were analysed. The hydrolysates were first dissolved in 0.1 M sodium nitrate before being passed through a 0.2 µm (polyrthersulphone) filter. High performance size exclusion chromatography (HPSEC) was performed at room temperature on a system consisting of a PL aquagel guard column (Polymer Labs, Amherst, U.S.A.) followed by in series (PL aquagel-OH 60, PL aquagel-OH 50 and PL aquagel-OH 40) eluted with 0.1 M sodium nitrate containing 0.02 % sodium azide as an antibacterial agent at a flow rate of 0.7 mL/min. The eluent was detected on-line by a DAWN EOS light scattering (LS) detector and a rEX differential refractometer (RI) (both supplied by Wyatt Technology, Santa Barbara, U.S.A.). The refractive index increment, *dn/dc* was taken to be 0.185 mL/g.

3.2.6 Determination of Total Sugars Using the Phenol-Sulphuric Acid Assay

Calibration solutions were prepared (D-glucose in deionised water) at the following concentrations: 200 µg/mL, 160 µg/mL, 120 µg/mL, 80 µg/mL, 40 µg/mL, and 20 µg/mL. The final concentrations, when combined with the 5% phenol in 0.1 M HCl were 100 µg/mL, 80 µg/mL, 60 µg/mL, 40 µg/mL, 20

µg/mL, and 10 µg/mL). The test samples were prepared in triplicate at a concentration of 1 mg/mL in deionised water. 5% phenol in 0.1 M hydrochloric acid (HCl) was prepared by adding phenol (0.5 g) to 0.1 M HCl (9.5 mL). The assay was performed by combining the glucose calibration solution or test samples (0.5 mL) with 5% phenol in 0.1 M HCl (0.5 mL), and concentrated sulphuric acid (2.5 mL). The vials were shaken vigorously then left at room temperature for 10 minutes. A blank solution was also prepared in a similar fashion that replaced the sample solution with deionised water. The vials were then placed in a water bath set at 25-30°C for 20 minutes. The absorbance of the samples was measured at a wavelength of 490 nm using a UV-Vis spectrophotometer. A standard curve was generated (**Figure 3-3**) from the glucose standards (0 - 100 µg/mL) which was then used to calculate the carbohydrate contents of the peptide hydrolysates (**Table 3-2**).

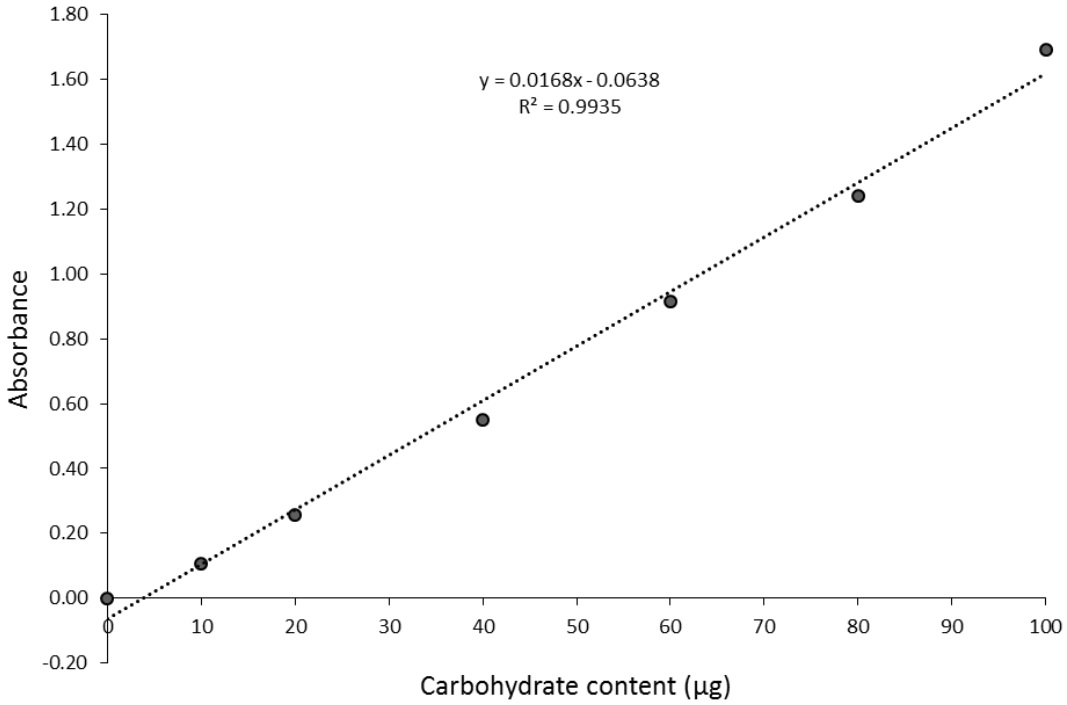

Figure 3-3 Standard curve using different concentrations of glucose (0 - 100 µg/mL) to determine the carbohydrate content of the peptide hydrolysates

3.2.7 Statistical analysis

Data were analysed using ANOVA, and t-tests. The ANOVA was single factor, where the null hypothesis stating that there is no significant difference in the data points analysed. The t-tests used were one-tailed t-tests with equal variances assumed. Statistical analyses were performed on data (n =

6) using Microsoft Excel. A p value of < 0.05 was considered significant and standard deviation derived from the mean values were indicated with error bars.

3.3 Results

3.3.1 Microscopy of peptide samples

The LM, and SEM images (**Figure 3-4**) indicate that there is a major difference in morphology between the H1 hydrolysate, and the L1 and P1 hydrolysates. The LM and SEM images of the H1 sample (**Figure 3-4 a and d**) are more angular and in general smaller than the images for the L1 and placenta samples (**Figure 3-4 b and e, and c and f**). The particles that make up the P1, and the L1 samples are also appear to be more uniform in their size distribution.

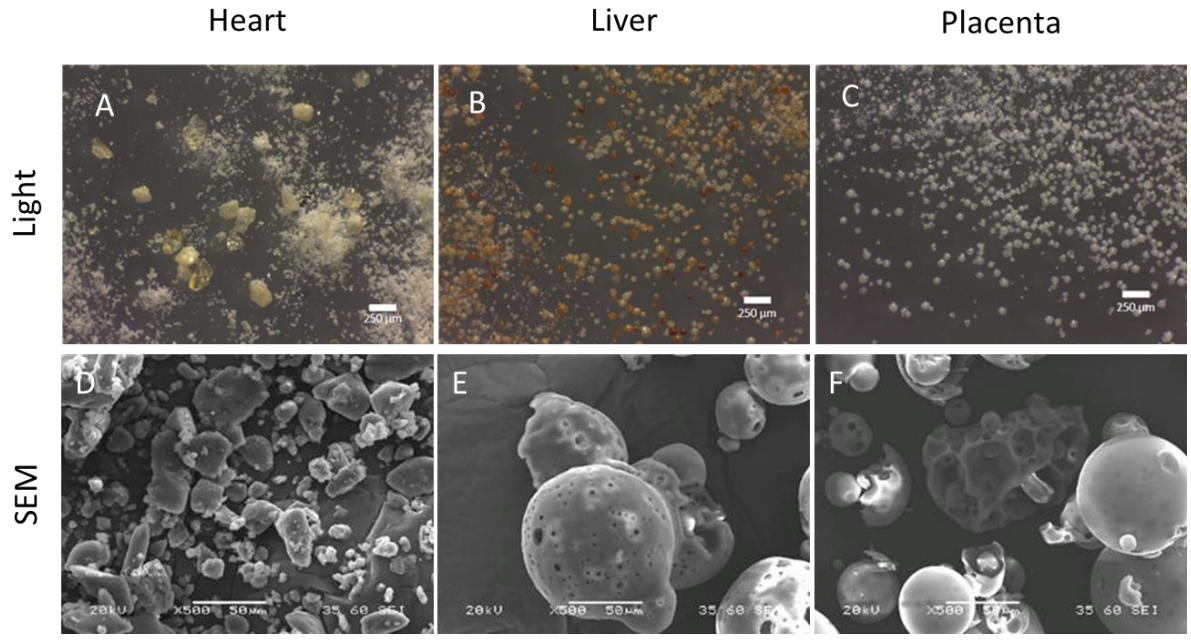

Figure 3-4 : Microscopy images of hydrolysates heart 150615-1900 (H1) (A and D), liver 150615-1900 (L1) (B and E), and placenta 0-150625-1700 (P1) (C and F) by light microscopy A-C and scanning electron microscopy (SEM) D-F

3.3.2 Particle size and distribution

The three methods used for the size distribution (wet laser diffraction, dry laser diffraction and pharmaceutical sieves) were compared by converting the data ranges to be similar to the sieves. The mass of the fractions generated from sieving the hydrolysate are shown in table **Table 3-1**. The percentages of particle sizes for each method are shown in **Figure 3-7**. The percentages of particle size distribution were calculated by identifying the fractions that fall within the size range of each of the sieves and then working out the value as a percentage of the total. The particle size distribution generated using the Malvern Mastersizer (**Figure 3-5**), and the HELOS (Hi209) (**Figure 3-6**) show a

similar pattern of size distribution. The heart hydrolysate had the greatest uniformity in particle size (the majority of the particles were under 75 µm) while the liver, and placenta samples had similar size distribution. The most uniform distribution of particle size groups was observed in the liver hydrolysate.

Table 3-1: Mass of fractions generated from sieving the hydrolysates heart 150615-1900 (H1), liver 150615-1900 (L1) and placenta 0-150625-1700 (P1).

Size range (µm)	H1 mass (g)	L1 mass (g)	P1 mass (g)
>250	0.00	1.02	1.01
250-180	0.95	6.12	3.98
180-125	4.05	25.59	20.98
125-75	11.07	25.59	22.00
75-38	61.43	22.53	29.02
≤38	57.38	4.08	1.01

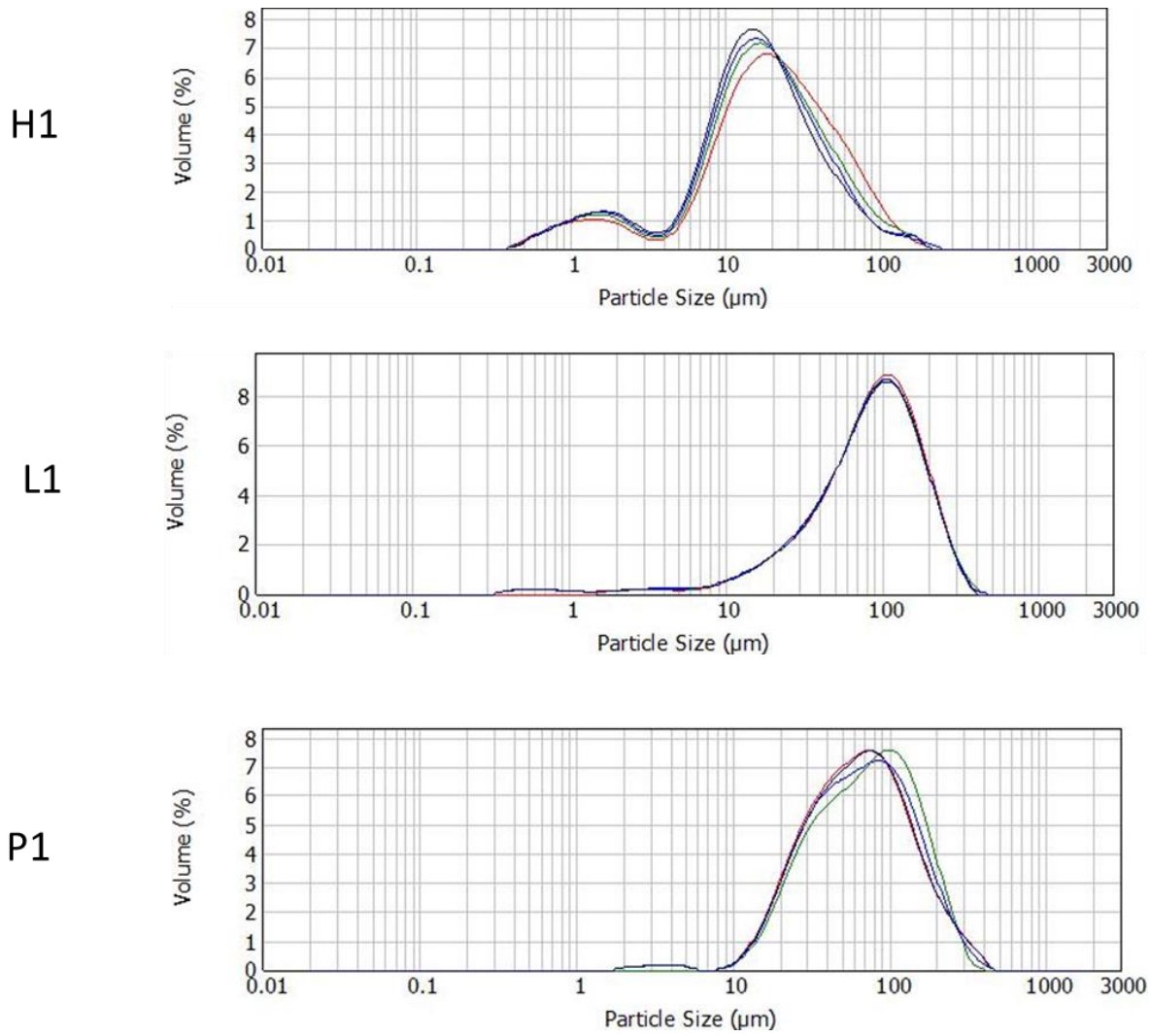

Figure 3-5 Particle size distributions using wet laser diffraction for heart 150615-1900 (H1), liver 150615-1900 (L1) and 0-150625-1700 (P1) hydrolysate samples

H1

L1

P1

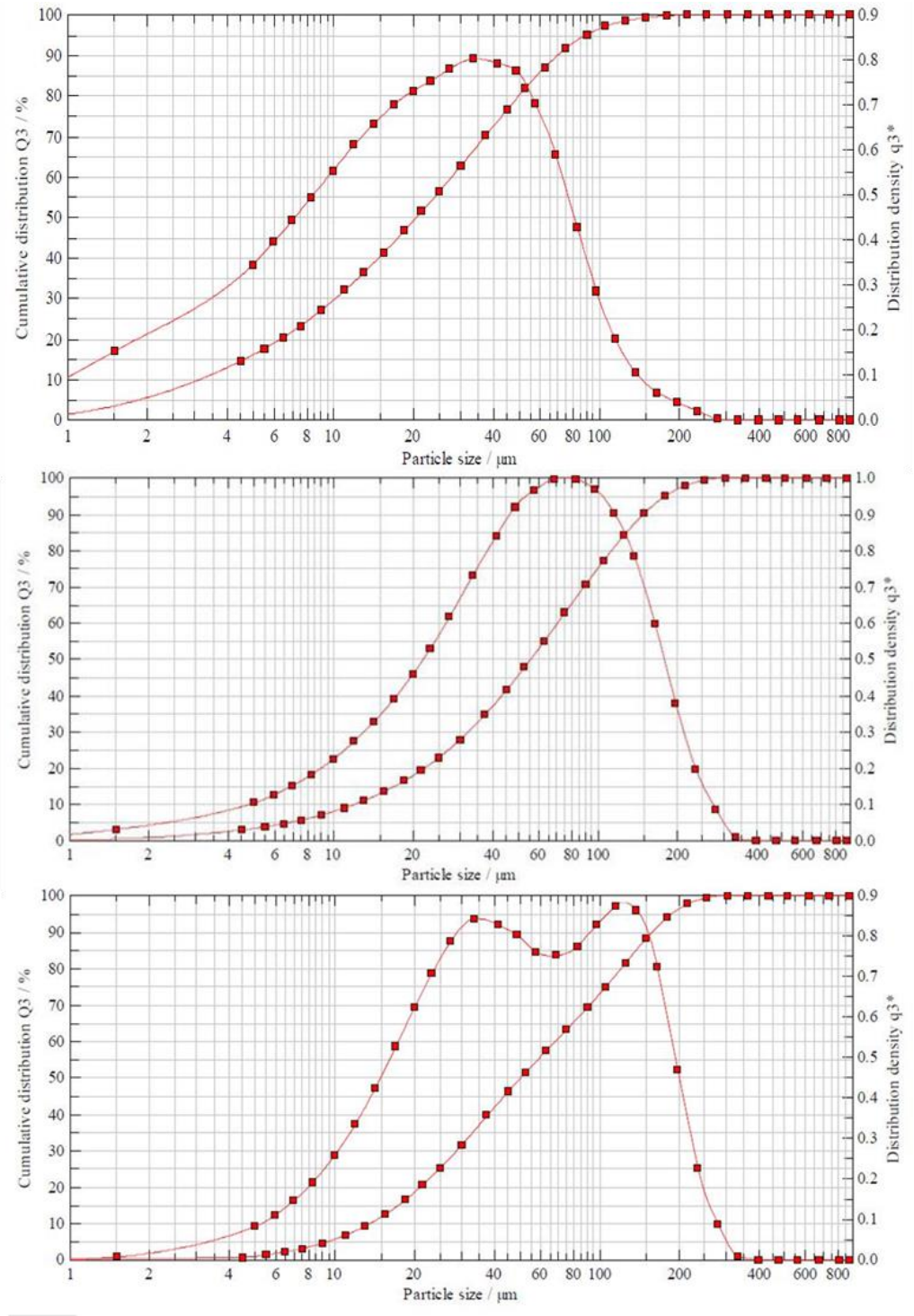

Figure 3-6 Particle size distributions using dry powder laser diffraction for heart 150615-1900 (H1), liver 150615-1900 (L1) and placenta 0-150625-1700 (P1) hydrolysate samples. Where the distribution density is represented on the right y-axis and the cumulative distribution is represented on the left y-axis

In general, the data for the pharmaceutical sieves shows a similar size distribution pattern as the laser diffraction methods, however, it was apparent that smaller particle sizes resulted in less uniform data. The data does indicate that there is a greater proportion of smaller particles in the heart hydrolysate than the liver, and placenta hydrolysate (**Figure 3-7**).

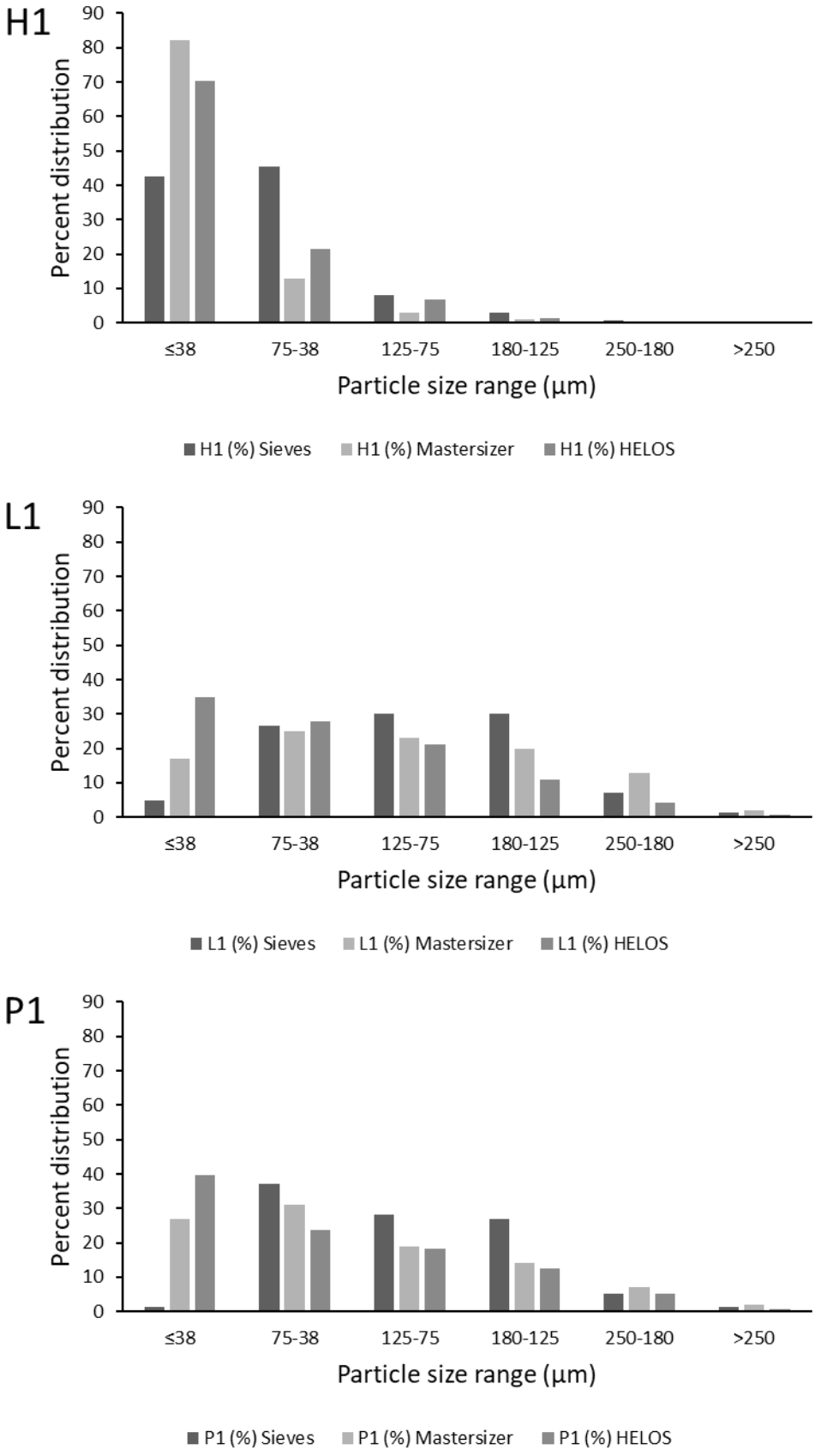

Figure 3-7 Comparison of the three methods of particle size analysis, wet laser diffraction, dry powder laser diffraction, and sieve fractionation for heart 150615-1900 (H1), liver 150615-1900 (L1) and placenta 0-150625-1700 (P1) hydrolysate samples

3.3.3 Particle flow analysis

The fractions generated from the mechanical sieving, along with the crude peptide samples were used in flowability analysis using a RST-XS shear cell apparatus. The ability of each peptide sample to flow was first assessed, before the fractions generated from the sieving were analysed. The FFC values obtained from the shear cell are represented in **Figure 3-8**. The data is incomplete for the particle flow analysis because some of the fractions generated for the liver and placenta hydrolysates, and all the fractions generated from the heart hydrolysates became too compact and therefore adhesive when the force required for this method was applied to the samples. The results that were gathered indicated that the placenta hydrolysate (FFC ~ 8.5) had a greater flowability than the liver (FFC < 3). Both were greater than the heart, which could not be successfully analysed using this method.

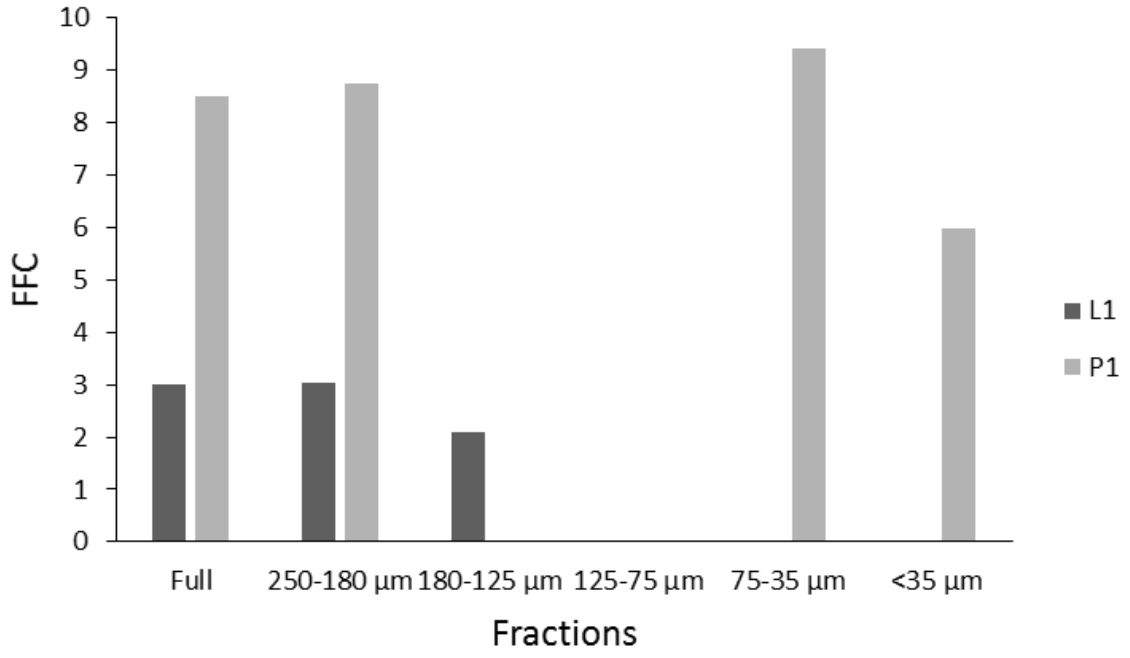

Figure 3-8 Flow factor values for fractions generated from pharmaceutical sieves. Data could not be generated for the heart 150615-1900 (H1) peptide fractions

3.3.4 Saturation point

The solubility of the hydrolysates was measured at varying pH levels to simulate the conditions of various parts of the gastrointestinal tract. The calculated saturation points of each peptide tested are shown in **Figure 3-9**. The calculated saturation point presented represents the mean of 6 readings ±

SD. The placenta hydrolysate did not reach saturation using this method. This hydrolysate was highly soluble, which resulted in a viscous solution at high concentrations. This in turn hindered the dissolution of more peptide to reach the saturation point. The liver hydrolysate was more soluble than the heart over the full pH range. The pattern of solubility for the two hydrolysates tested were similar in that they were both more soluble at pH 5.8. The reduced solubility of the heart hydrolysate at pH 7.2 was significantly different to the heart samples tested at pH 1.2, and 5.8 ($p = 0.068$, and 0.055 respectively).

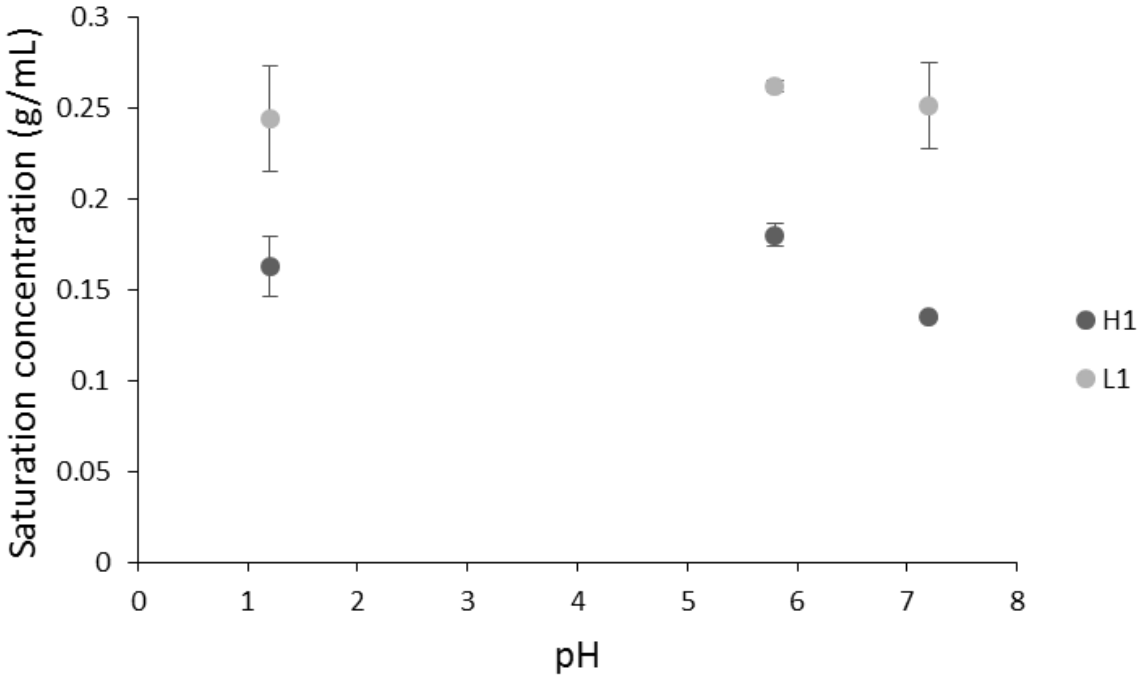

Figure 3-9 Mean saturation point concentrations for hydrolysate samples heart 150615-1900 (H1), and liver 150615-1900 (L1) (n=6)

3.3.5 SEC MALS analysis

The variability of the data generated from SEC MALS (**Figure 3-10, and Figure 3-11**was judged too great to assign an accurate MW, but all the samples fell in between 2 and 14 kDa, which is what would be expected for peptides.

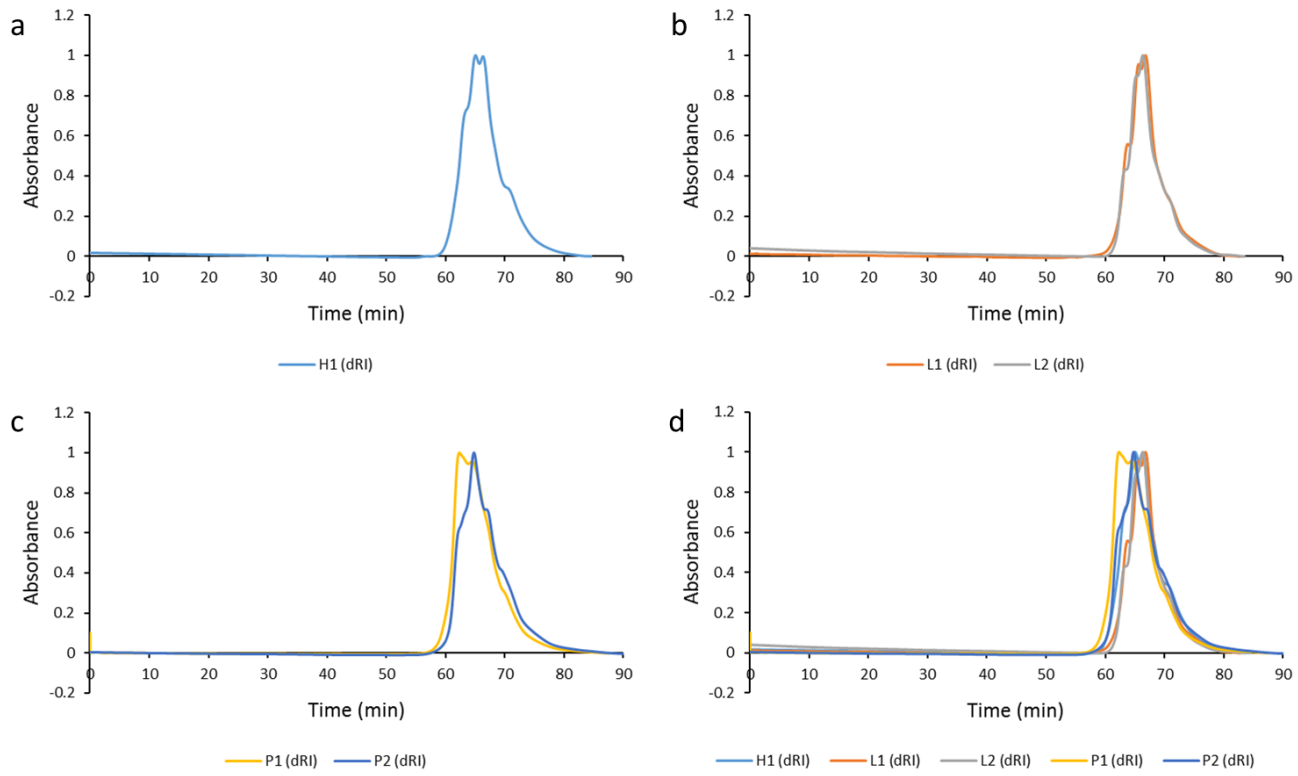

Figure 3-10 Chromatograms for the size exclusion chromatography coupled with multi-angle light scattering (SEC-MALS) for heart 150615-1900 (H1) (a), liver 150615-1900 (L1) and liver 160126-0700 (L2) (b being L2) (b), placenta 0-150625-1700 (P1) and placenta 0-160330-1500 (P2) (b being P2) (c), and the combined graphs (d).

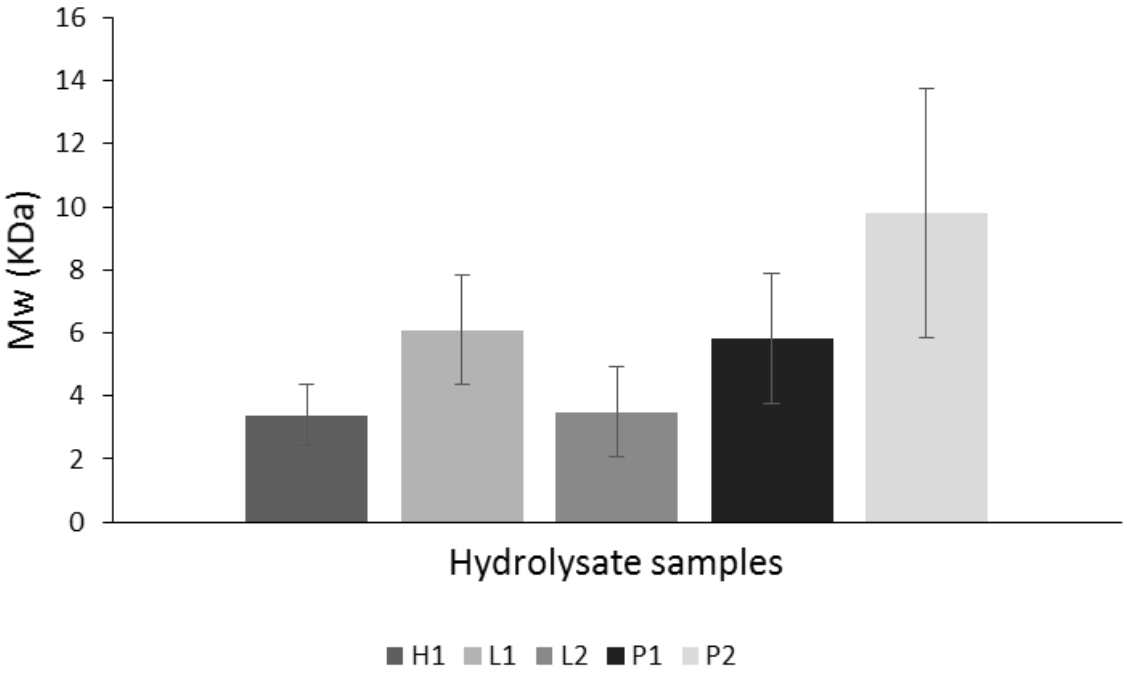

Figure 3-11 Molecular weight for the size exclusion chromatography coupled with multi-angle light scattering (SEC-MALS) for the Biofac hydrolysates

3.3.6 Determination of Total Sugars Using the Phenol-Sulphuric Acid Assay

The data generated from the phenol-sulphuric acid assay indicated that while there was carbohydrate present in all of the hydrolysates, the concentrations were low. The greatest proportion of total carbohydrate was found in L1 (4.32%) followed by L3 (3.62%) (no significant difference between the two p = 0.13). P2 and L2 (p = 0.49) showed similar amounts of sugars (2.53% and 2.51% respectively). P1 had the lowest amounts of carbohydrate of all hydrolysates tested (0.62%) (significantly less than all other hydrolysates except P2, p = 0.051) (**Table 3-2**)

Table 3-2 Total carbohydrate content (in relation to glucose) for the peptide hydrolysates

	P1	P2	L1	L2	L3
Abs	0.12	0.28	0.43	0.27	0.37
µg	3.09	12.64	21.58	12.55	18.11
mg/g	6.19	25.28	43.15	25.10	36.23
% total	0.62	2.53	4.32	2.51	3.62

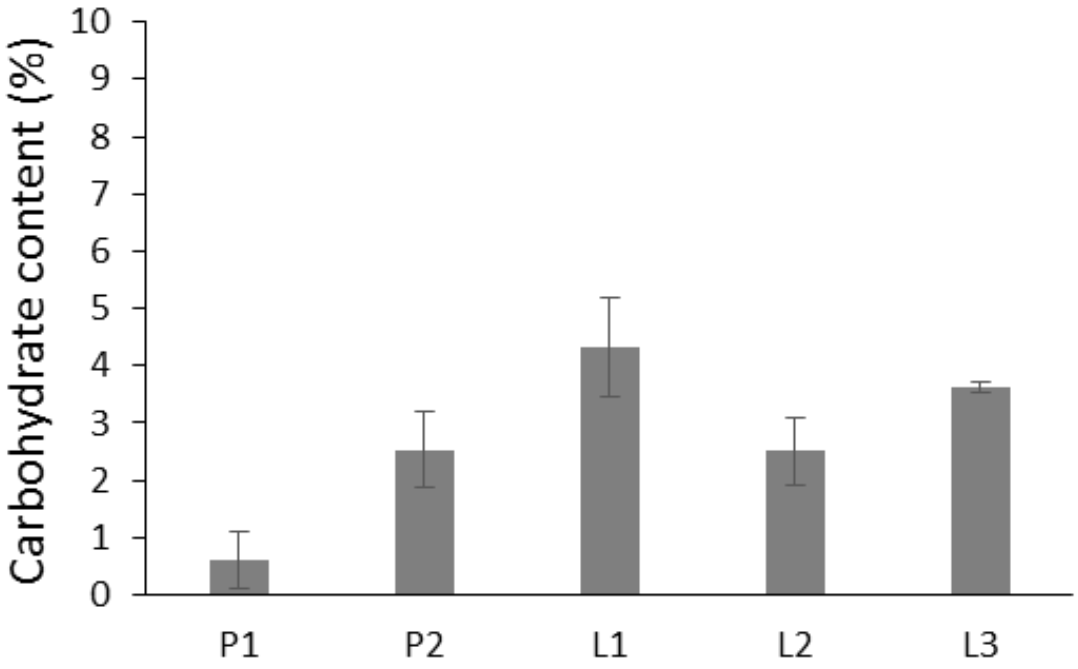

Figure 3-12 Total carbohydrate content (in relation to glucose) for the peptide hydrolysates

3.4 Discussion

The most striking difference between the samples was the morphology of the heart hydrolysate (H1) in comparison with the liver (L1) and placenta (P1) hydrolysates. The heart hydrolysate appears much smaller than the liver and placenta hydrolysates, which have a similar size range to each other (**Figure 3-4 A-C**). The heart sample (H1) also had irregular shaped particles unlike the liver and placenta samples, which were uniform and spherical. The SEM images (**Figure 3-4 D-E**) highlight further differences on a microstructural level as the liver and placenta hydrolysates appeared to contain large porosities within the particles and H1 showed flattened plate-like structures with the smaller particles forming aggregates. The holes on the surface of the particles are likely to have arisen from the vacuum applied during the SEM analysis. The morphology of the heart hydrolysate is noticeably different, being more irregular, with the general particle size being smaller. The spherical honeycomb like structures of the spray-dried liver, and placenta hydrolysates contrasted with the angular crystalline structures of the freeze-dried heart hydrolysate. The images generated from these methods indicated that the morphology of the particles was determined by the production method used to generate the hydrolysates. The methods of production are also likely to have had an effect on the particle size distribution of each sample. L1 and P1 samples had a similar size distribution with the majority of particles between 10 and 300 µm, whereas the heart peptide sample had a size range between 5 and 100 µm in addition to a significant population of particles below 3 µm (**Figure 3-5 and Figure 3-6**). Examining the heart peptide hydrolysate SEM and light microscopy images show the particles to have planar layers, and rough edges. Again, this is likely down to the particle preparation method. Importantly however, this may affect the flowability and tableting behaviour of the heart peptide sample. An interesting feature of the hydrolysate samples was the variation in colour (**Figure 3-4 A-C**).

The fact that the sieve data was different to the laser diffraction data is not too surprising after the fractions were analysed under microscopy, which provides shape information. All three hydrolysate samples showed that there was a lower proportion of particles < 38 µm, collected from the sieves than what was measured in the other two methods. Analysis of the images of the heart hydrolysate (**Figure**

3-4 A and **D**) suggests that the smaller particles aggregated. Particles less than 100 µm become more cohesive and below 10 µm resist flow under gravity and are extremely cohesive, and therefore are unable to pass through smaller meshes (Lu et al., 2015). This property was also observed for the liver, and placenta hydrolysates (figures not shown).

The differences between the wet laser diffraction (Mastersizer) and the dry powder laser diffraction (HELOS) appear to be comparable with one another considering the polydisperse nature of the samples. The shear cell method used to determine the flowability of the hydrolysates was unable to determine the FFC for all the fractions. Some of the samples reported FFC values well above 10 (placenta 180-125 µm, and 125-75 µm), whereas the FFC could not be calculated for other samples (all liver fractions less than 125 µm, and all heart samples). The lack of results for the heart samples can be explained by the extremely cohesive nature of the particles. The SEM images clearly show irregular crystalline structures that are generally small. The smaller liver fractions seem to have been affected by the 'sticky' nature of the particles. The results of the placenta fractions do show that the shape of the particle has had a direct effect on the flowability of the hydrolysates. The placenta fractions were also significantly less 'sticky' than the liver peptide fractions.

The flowability of the hydrolysates was not further investigated in an attempt to attain a complete data set because this data was not deemed vital to the investigations on bioactivity. The flowability of the hydrolysates could however, have an impact on the further processing and manufacturing procedures. Because the initial aim of this study was to evaluate the peptide hydrolysates for bioactive properties, the solubility in physiological conditions is important for this activity to be translated *in vivo* (Savjani et al., 2012). The solubility of each peptide sample at different pH levels was therefore investigated to evaluate the limits of solubility. The method used in this study calculated the saturation point of each hydrolysate as the solubility limit.

The data shown in **Figure 3-9** indicated that both H1, and L1 were more soluble at pH 5.8 than pH 1.2 and pH 7.2, and that the liver hydrolysate is more soluble than the heart hydrolysate. The placenta hydrolysate was not analysed using this method because the saturation point could not be reached. The extremely high solubility of the placenta peptide is an interesting property that could be utilised by potential customers of Biofac. The ability of the hydrolysate to produce viscous solutions could be exploited in the production of topical formulations for example. These could either be a method of administering the hydrolysate as it is, or with other active compound mixed in with it.

Statistical analysis using ANOVA (single factor, null hypothesis being that there is no difference in solubility at different pH levels) indicated that there was a significant difference in solubility at different pH levels in the heart hydrolysate (p-value < 0.02), but not for the liver hydrolysate (p-value > 0.05). Further statistical analysis of the H1 hydrolysate solubility data using t-tests identified that the data point at pH 7.2 was significantly different to the data points at pH 1.2, and pH 5.8. There was no significant difference between the data points at pH 1.2, and pH 5.8.

Concerning the total carbohydrate assay, the proportion of carbohydrate in each hydrolysate sample was measured using glucose as a reference. Glucose was selected as the standard because of its importance to biological systems, and therefore may be present in the samples. It is interesting that there was a difference between the placenta samples (**Figure 3-12**). P1 (no filtration) gave a value of 0.62%; P2 (< 5 kDa) gave a value of 2.53%. There was also a difference between the values for the liver samples; here L1 (no filtration) gave a value of 4.32%, L2 (< 5 kDa) gave a value of 2.51%, and L3 (< 5 kDa) batch 2 gave a value of 3.62%. The fact that there are differences in total carbohydrate content between samples from the same source material indicates that there are differences between the batches. However, the differences are small, and considering the source of the material, the presence of some carbohydrate is to be expected (Gupta et al., 2015).

3.5 Summary

The investigation into the physicochemical properties of the Biofac hydrolysates highlighted that the production method has an important impact on their physical properties. The size distribution and morphology of the particles were directly linked to the method of drying (either lyophilisation or spray drying). This subsequently, affects properties such as flowability, the lyophilised H1 for example did not flow at all compared to the spray-dried L1and P1 samples. In contrast to the size distribution and morphology, the solubility is not directly linked to the production method (although dissolution rate may be linked). Solubility is dependent upon the molecular composition of the hydrolysates, though the high temperatures used in spray drying could be responsible for the differences between the spray dried and the freeze dried samples.

CHAPTER 4 **Bioactive properties of whole and fractionated hydrolysates**

4.1 Introduction

The investigation into the hydrolysates supplied by Biofac initially centred on the analysis of the physicochemical properties of the hydrolysates L1, P1, and H1 (see chapter 3). This work highlighted how the manufacturing process had a major impact on the physical properties. With regards to bioactivity, the physical properties of the hydrolysates relate to the bioavailability of the peptides within the samples. The solubility at various pH levels is an example where the physical properties affect the bioactivity; if the hydrolysates do not dissolve easily at biologically relevant buffers at certain pH levels, then they will not be biologically available.

The hydrolysates that were analysed in the bulk of the physicochemical study (chapter 3) were the original samples from Biofac, these were liver 150615-1900 (L1), placenta 0-150625-1700 (P1), and heart 150615-1900 (H1) (All hydrolysates were analysed using the total carbohydrate assay, and L2 and P2 were analysed along with H1, L1, and P1 using SEC-MALS). It was decided that the work would concentrate on the placenta and liver hydrolysates because these were more interesting to Biofac. As well as the original placenta (P1), and liver (L1) hydrolysates, newer batches were supplied by Biofac. These were generated using similar processes but with an added step to remove particles with a greater molecular weight than 5 kDa. The majority of the data generated was from these newer batches denoted as L2 (liver 160126-0700), L3 (liver 170127-0815), and P2 (placenta 0-160330-1500).

The specific examples of bioactivity used to assay the Biofac hydrolysates for this study were selected because they were commonly used in relatable studies on bioactive peptides found in the literature. The main areas of interest for this study were antioxidant activity, cell proliferation and wound healing, and anti-hypertension. Of these three bioactivities, antioxidant, and anti-hypertension activity have been researched extensively in relation to peptides, whereas cell proliferation and wound healing properties of peptides have not been investigated to the same extent, but there are examples of studies into these properties (Ryaby et al., 2006, Demidova-Rice, 2011).

The antioxidant assays used to assess the hydrolysates were the DPPH assay, ORAC assay, the linoleic acid/ FTC assay, and the CAA assay. The DPPH assay is a radical scavenging assay that assesses to what degree a compound can protonate the stable radical DPPH· to the non-radical DPPH. The ORAC assay is a relatively simple assay, and is widely used in similar studies that investigate the antioxidant activity of bioactive peptides. The mechanism of the ORAC assay is the degradation of the fluorescent probe sodium fluorescein when exposed to reactive oxygen species generating compound (in this case AAPH). The antioxidant activity of compounds is assessed by their ability to reduce or stop the degradation of the fluorescent probe. The DPPH, and ORAC assays are two non-cell based assays that are used to investigate two different mechanisms of antioxidant activity. While they are widely used in the literature, they have faced criticism on their lack of biological relevance (Wolfe and Liu, 2007). For this reason, the linoleic acid/FTC assay was used to investigate the ability of the hydrolysates to reduce autoxidation in lipids. The final assay used was the CAA assay. This assay was used to assess how well the hydrolysates could reduce the oxidative stress to a cell when external oxidative stress is applied, in this case with the application of AAPH to the cells. This assay was selected because of its biological relevance (Wolfe and Liu, 2007). Antioxidant assays that use cells are performed under physiological pH and temperature, but most importantly, they take metabolism and intracellular transport under consideration.

The effects on cell proliferation were investigated using a simple cell counting method, with the data generated used to calculate cell DT, and PDL, and using the MTT assay. The potential effect of the hydrolysates on wound healing was assayed using the scratch wound assay. Using PDL and DT to analyse the effects of the hydrolysates on the cells is a good way to gather initial data related to the health of the cell population. Healthy cells will routinely divide within a certain time range depending on the cell line. If the cells are affected either positively (increased proliferation) or negatively, the number of times the population doubles (PDL) and the doubling time (DT) will differ from that of the control group. Major deviations from a normal DT is an indication that the cells have been affected by the sample being tested. The PDT is measured against the control group. If a sample group PDL is significantly different to the control, the compound being tested is likely to be the cause. These assays

are preliminary tests; if significant results are generated then a more in depth, investigation can be undertaken.

Bioactivity of peptides is directly linked to their structure (Nardo et al., 2018). Understanding the structure activity relationships of compounds is a powerful tool in the analysis of bioactivity. Analysis of the composition of the hydrolysates is therefore an interesting, and important element of this study. The first steps in analysing the composition of the hydrolysates were carried out using RP-HPLC with a C-18 analytical column specifically designed for peptide analysis. The L2 hydrolysate was also selected to be further analysed using prep HPLC. The fractions generated from the prep HPLC were recovered by lyophilisation before reconstitution in relevant buffers. This work led onto the investigation into peptide sequencing (using *de novo* sequencing), which was used to create novel synthetic peptides (described in chapter 5).

The possible effects of peptide degradation on the bioactivity of the hydrolysates was also investigated in this section of the study. It was noted in chapter 1, that bioactive peptide sequences can be found in longer peptide chains, or within host proteins. With this in mind, the stability of the hydrolysates in solution was investigated over a seven-day period. This was undertaken using HPLC, with the activity of the samples tested using the MTT assay.

The aim of this section of work was to discover if the Biofac hydrolysates demonstrate certain bioactivities, namely antioxidant activity, cell proliferation and chemotaxis, and to assess fractions of the hydrolysates generated from HPLC, for bioactivity. The information on the crude hydrolysates are of particular importance to Biofac because the data generated can be used in the promotion of their products.

4.2 Materials and methods

4.2.1 DPPH Radical Scavenging Activity (RSA)

4.2.1.1 DPPH Method 1

The DPPH assay is an inexpensive, and relatively simple assay that can be used to ascertain the antioxidant capacity of a given substance. The assay is based on the stable radical DPPH·**,** which is purple in colour, being converted to the pale yellow DPPH. This requires molecules that act as proton donators (**Figure 4-1**). The method used in this assay was developed from various protocols used in the literature (Ahmed et al., 2015, Shen et al., 2010, Romano et al., 2009, Szabo et al., 2007).

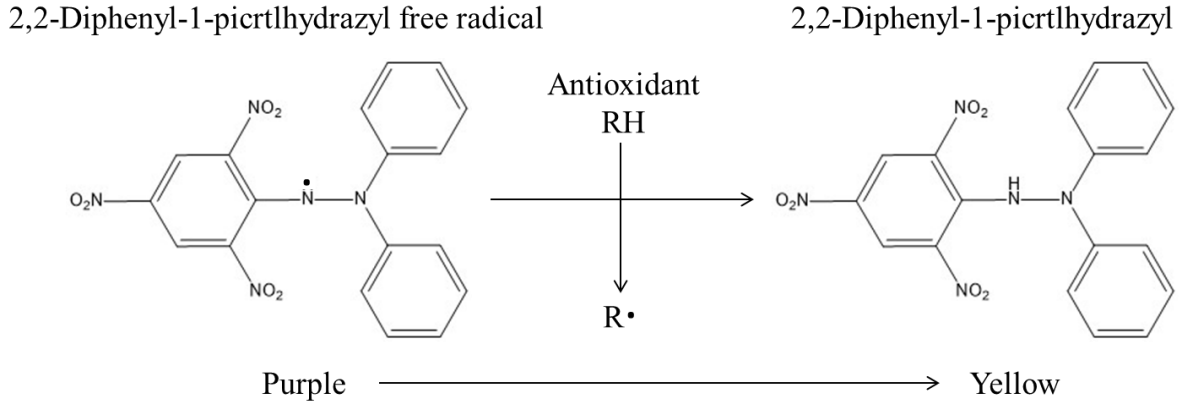

Figure 4-1 Conversion of the purple 1, 1-diphenyl-2-picrylhydrazyl (α,α-diphenyl-β-picrylhydrazyl radicl (DPPH·) to the yellow 1, 1-diphenyl-2-picrylhydrazyl (α,α-diphenyl-β-picrylhydrazyl (DPPH) by protonation

DPPH (0.1 mM) in 100 % ethanol was prepared immediately before use. DPPH (3.9 mg) was added to a 10 mL volumetric flask then made up to 10 mL with 100 % ethanol to produce a stock solution. The working solution was prepared by diluting the stock DPPH solution (3 mL) with 100% ethanol (27 mL). Both DPPH solutions were wrapped in foil and stored at 3-8 °C until required.

Hydrolysates and L-Ascorbic acid (control) solutions (500 µg/mL) were prepared by adding 50 mg of sample to deionised water in a 100 mL volumetric flask. All samples were prepared in triplicate and wrapped in foil. Each sample was shaken vigorously before being left to incubate at room temperature for 30 minutes. Blank solutions were prepared for each sample by adding 100 % ethanol (0.75 mL) to the sample (2.25 mL). A negative control was prepared by combining DPPH working solution (0.75

mL) with deionised water (2.25 mL). Hydrolysate samples and positive controls were prepared by combining DPPH working solution (0.75 mL) with the relative sample solution (2.25 mL). The samples were measured using a UV-VIS spectrophotometer at 517 nm. The UV-VIS spectrophotometer had the baseline adjusted, and blanked by the relative blank solution prior to use. Antioxidant activity of the samples were determined using **equation 4.1**:

$$RSA\ (\%) = [1-(Abs_1 \div Abs_0)] \times 100 \qquad \textbf{(Eq. 4.1)}$$

Where RSA is Radical Scavenging Activity, Abs_1 is the absorbance of the sample at 517 nm and Abs_0 is the absorbance of negative control at 517 nm

4.2.1.2 DPPH Method 2: 96 well plate DPPH RSA assay

A DPPH assay using 96 well plates was developed to increase the throughput, and to make the assay more statistically robust. DPPH solution was prepared as stated previously in section 4.2.1.1. Hydrolysate solutions were prepared by adding the relevant sample to 10 mM potassium phosphate buffer in a volumetric flask (buffer at a higher concentration forms precipitation with the addition of ethanol).

The hydrolysate solutions (225 µL) were added to the relevant wells in row b of the plates, and the relative solvent (112.5 µL) being added to the other wells. A 1:1 dilution series was created by removing 112.5 µL of the peptide solution and mixing with the next row, this was continued until the lowest concentration. The negative control was 112.5 µL of the relevant solvent. For each dilution, a blank was also prepared in the same manner. To each of the sample wells, DPPH solution (37.5 µL) was added. To each of the blank wells ethanol (37.5 µL) was added. The plates were covered with a plate cover, and incubated in the dark at room temperature for 30 minutes.

The plates were read using a Tecan Infinite F50 plate reader. The wavelength was set to 540 nm (this is the closest wavelength possible to 517 nm on this apparatus; DPPH still absorbs well at this wavelength). The results were generated form the plate reader data by subtracting the mean blank value of a particular concentration form the individual values of the samples. The RSA was calculated using **equation 1**.

4.2.2 ORAC Assay

The Oxygen Radical Absorbance Capacity of the Biofac hydrolysates were analysed using the ORAC assay. The assay was based on work carried out by Boxin et al (2001), and Huang et al (2002) with minor changes (Boxin Ou 2001, Huang et al., 2002).

AAPH solution (153 mM) was prepared fresh by adding AAPH (0.414 g) to 10 mM potassium phosphate buffer (pH 7.4) (made up to 10 mL).

Sodium fluorescein stock solution (4 µM) was prepared by adding sodium fluorescein (15 mg) to 10 mM potassium phosphate buffer (pH 7.4) (made up to 100 mL) to produce a concentration of 0.4 mM. This was then diluted with 75 mM potassium phosphate buffer (pH 7.4) 1:1000 to reach the required concentration. The stock solution was stored at 2-5°C. Working sodium fluorescein solution (4 µM) was prepared fresh by diluting the stock with buffer 1:1000.

The synthetic vitamin E analogue Trolox is a widely used standard for antioxidant assays. Trolox was used to generate a standard curve against which the experimental samples could be measured. The Trolox standard solution (200 µM) was prepared by adding 10 mg of Trolox to 10 mM potassium phosphate buffer (pH 7.4) (made up to 50 mL). Trolox was dissolved using a magnetic stirring hot plate set to 50°C and left until the Trolox had fully dissolved.

Hydrolysate samples (800 µg/mL) were prepared by dissolving the specific sample in 10 mM potassium phosphate buffer (pH 7.4). The stock solutions were used to prepare a concentration gradient ranging from 100 µg/mL to 0.78 µg/mL.

Black 96 well plates (Thermo Scientific™ Nunc™ FluoroNunc™/LumiNunc™ 96-Well Plate) were set up with the outside wells (rows A and H, and columns 1 and 12), and wells in columns 9, 10, and 11, rows b to g, filled with deionised water (200 µL). The plates were covered and warmed to 37°C. Sample dilution series were created by adding sodium fluorescein working solution (300 µL) to sample wells with either a sample stock solution, or the Trolox standard (50 µL) in a single row. Sodium fluorescein working solution (175 µL) was added to all other sample wells. 175 µL was removed from the first set of wells and added to the next, and so on until the final well after which the 175 µL removed was discarded. A negative control was prepared with buffer replacing the sample. Blanks were prepared by adding 10 mM potassium phosphate buffer (pH 7.4) (175 µL) to the plate in triplicate. The plates were incubated at 37°C for 30 minutes.

Following incubation, the plates were placed in the Fluostar Optima microplate reader using the plate mode for slow kinetics. The fluorescence was measured every minute for 5 cycles. After 5 cycles, the

plate was removed and 153 mM AAPH solution (25 µL) was added to each experimental well. The plate was returned to the plate reader where the fluorescence was measured every minute for 115 minutes. The fluorescence of each sample, at each time point were blank corrected to remove background fluorescence. The data from the plate reader were plotted onto graphs so that the area under the curve (AUC) could be calculated. The ORAC value (**equation 4.3)** was calculated from the (AUC) (**equation 4.2**).

$$AUC = \sum [(a + b) \div 2] + [(b + c) \div 2] \ldots\ldots\ldots\ldots + [(y + z) \div 2] \quad \textbf{(Eq. 4.2)}$$

$$\textit{Relative ORAC value} = [(AUC_{sample} - AUC_{blank}) \div (AUC_{Trolox} - AUC_{blank})] \; X \; (mol_{Trolox} \div mol_{sample})] \quad \textbf{(Eq. 4.3)}$$

4.2.3 Lipid peroxidation inhibition

Lipid peroxidation inhibition followed the method used in previous studies with some modifications (Nazeer et al., 2013, Chen et al., 1996, Osawa and Namiki, 1985). Linoleic acid emulsion was used as the lipid peroxidation model with the FTC assay used to quantify the peroxidation. All samples were prepared in triplicate as follows: Solution A: Test samples (Trolox/hydrolysates) were dissolved in 0.1 M pH 7.0 phosphate buffer (1.0 mL). The negative control was prepared with buffer alone. Deionised water (0.5 mL) was added to bring final volume to 1.5 mL. Solution B: 50 mM linoleic acid (16 µL) was added to 1.0 mL 100 % ethanol. Solutions A and B were then combined to produce an emulsion. A 50 µL aliquot was removed immediately for the first time point of the FTC assay. The vial was then sealed and placed in an incubator at 40°C and 50 µL samples were taken every 24 hours and analysed using the FTC assay.

FTC solution was prepared by adding 30% ammonium thiocyanate (50 µL), and 20 mM ferrous chloride solution in 3.5% HCl (50 µL) to 75% ethanol (2.35 mL). The linoleic acid emulsion system (50 µL) was added to the FTC preparation and left to incubate at room temperature for 3 minutes. The absorbance was read at 500 nm to determine the level of peroxidation. To obey the Beer-Lambert law absorbance values of the samples generally need to be below 2.0.

The last FTC assay was performed 24 hours after the negative control exceeded 2.0 on the absorbance scale; the end-point of the assay was taken at the time point before the absorbance reached 2.0. The level of peroxidation inhibition is relative to the negative control. **Equation 4.4** was used to calculate percentage of inhibition of lipid peroxidation:

$$\textit{Inhibition (\%)} = (1 - \textit{Abs. of sample} \div \textit{Abs. of negative control}) \times 100\ \% \qquad \textbf{(Eq. 4.4)}$$

4.2.4 Cellular antioxidant activity assay (CAA)

The CAA assay was based on the method developed by (Wolfe and Liu, 2007). The other antioxidant assays performed for this project are directed at specific mechanisms (one for each assay); they also do not involve biological systems. The CAA assay performed in this research used 3T3 fibroblasts. The mechanism for the assay is described in **Figure 4-2, and Figure 4-3**.

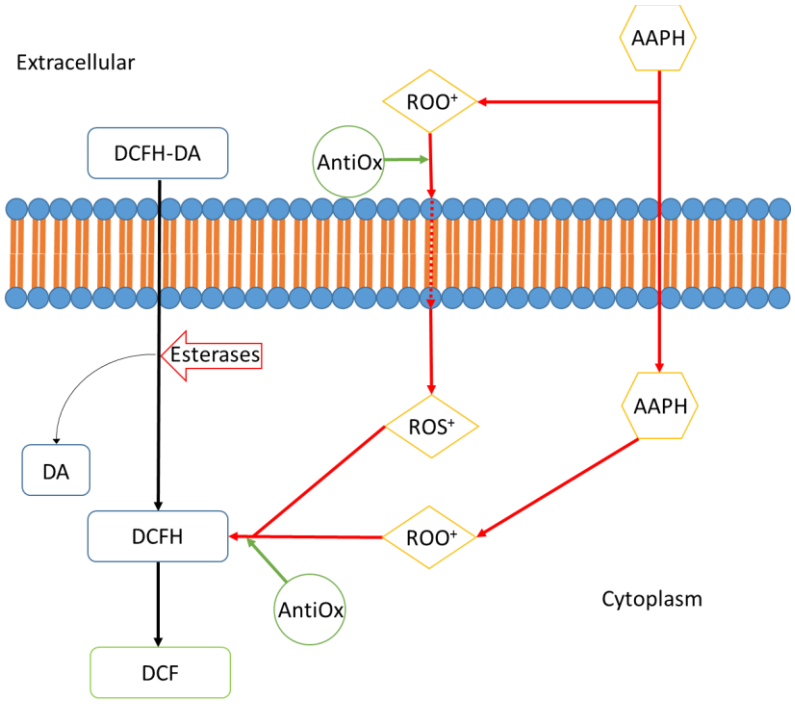

Figure 4-2 Mechanism for the cellular antioxidant assay. 2'-7' dichloro-dihydro-fluorescein diacetate (DCFH-DA) (non-polar) crosses the cell membrane where it is cleaved to form the more polar 2'-7' dichloro-dihydro-fluorescein (DCFH); DCFH cannot then diffuse out of the cell.

Briefly, the non-polar DCFH-DA crosses the cell membrane where it is cleaved into the polar DCFH; DCFH cannot then diffuse out of the cell. AAPH can diffuses into the cell where it generates peroxide radicals (ROO^+) by spontaneously decomposing; these radicals can also attack the cell membrane,

which in turn generates other radical (ROS^+). The radicals oxidise the DCFH to the fluorescent DCF. The introduction of antioxidants to the system will reduce the levels of DCF in the cell by interacting with the ROO^+ and ROS^+, and by preventing the generation of ROS^+ from the breakdown of the membrane.

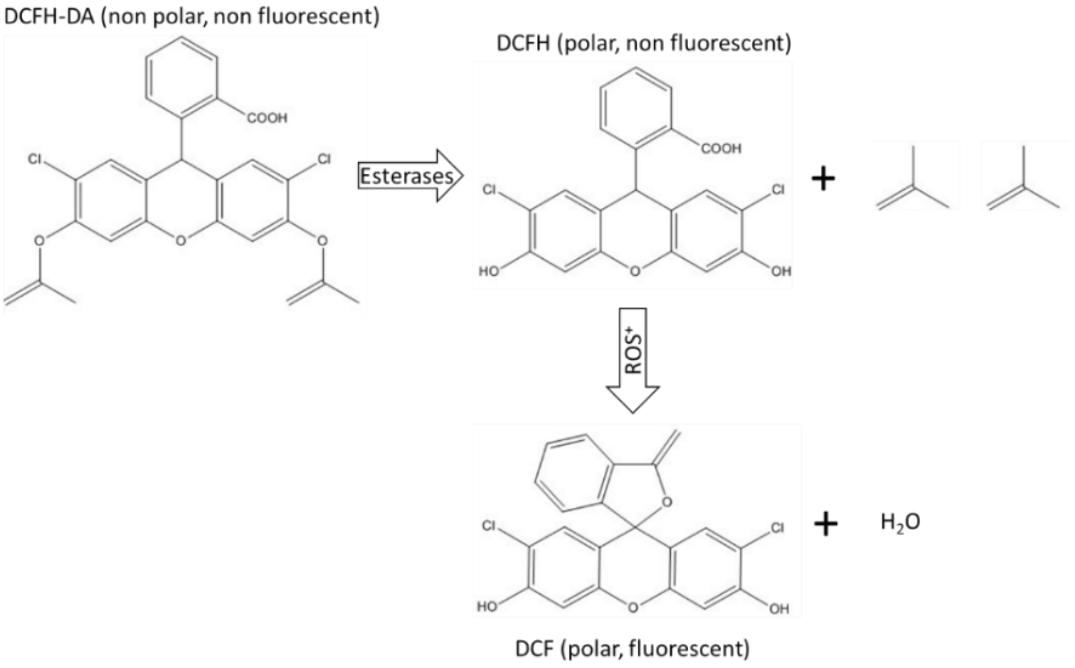

Figure 4-3 The nonpolar 2'-7' dichloro-dihydro-fluorescein diacetate (DCFH-DA) is converted into the polar 2'-7' dichloro-dihydro-fluorescein (DCFH) by cellular esterases. DCFH can then be oxidised into the fluorescent form of 2'-7' dichloro-dihydro-fluorescein (DCF) by (reactive oxygen species (ROS+) and peroxide radicals (ROO+).

3T3 fibroblast cells were seeded in triplicate at cell density of 3 x 10^4/well on a 96 well plate (3 x 10^5/mL) using Dulbecco's Modified Eagle Medium (DMEM) supplemented with L-glutamine, HEPES buffer, and PenSrep. The cells were incubated for 24 hours at 37°C, 5% CO_2. After 24 hours the media was aspirated and the cells washed with PBS (0.01 M). To the relevant wells, hydrolysates dissolved in 100 µL of supplemented DMEM (containing DCFH-DA (5 µM)) were added. The concentrations of hydrolysates in the sample media were 8, 4, and 2 mg/mL. The plates were returned to the incubator for a further 1 hour. After 1 hour the sample media was removed and the cells were washed with PBS (0.01 M). AAPH (120 µM) in Hank's balanced salt solution (HBSS) (100 µL) was added to each experimental well before the plate was placed into the Fluostar Optima microplate reader (set to 37ºC, excitation at 485 nm, emission at 520 nm, readings taken every 5 minutes for 45 minutes). All plates

included control, and blank wells. Control wells contained no experimental sample and blank wells contained no AAPH and no sample.

The values from the blank wells were subtracted from the experimental, and control wells. The fluorescence was plotted against time, and the AUC (**equation 4.2**) for each sample was calculated. The AUC of the control (no sample) was used to calculate the cellular CAA (**equation 4.5**.), which was expressed as a percentage. Positive figures indicated that a particular sample showed antioxidant properties in relation to this assay, whereas negative figures would suggest that the sample increased the production of DCF, and therefore were causing oxidative stress.

$$CAA\ unit = 100 - (\int SA \div \int CA) \times 100 \qquad \textbf{(Eq. 4.5)}$$

∫SA is the integrated area under the curve of the sample fluorescence versus time and ∫CA is the integrated area from the control curve.

4.2.5 Cell proliferation

The hydrolysates were assayed for potential wound healing properties. One aspect of wound healing is cell proliferation (Gonzalez et al., 2016). Two methods were used to discover if the hydrolysates had an effect on the proliferation of fibroblasts *in vitro*.

4.2.5.1 Cell counting method

Hydrolysate solutions were prepared by dissolving 360 mg in 30 mL of PBS (pH 7.4). This was then sterile filtered, and used to produce the following dilutions: 12 mg/mL, 6 mg/mL, and 3 mg/mL. Six well plates were seeded with 3T3 fibroblasts at 3 x 10^5 cells/well (2.95 mL) in DMEM supplemented with FBS (10%), 1 M HEPES (2%), 220 mM L-glutamine (2%), and penicillin-streptomycin (1%). 50 µL of the relevant dilutions were added to make the total volume 3 mL. The plates were incubated for 48 hours at 37 °C, 5 % CO_2. The cells were counted using a haemocytometer and staining with trypan blue to evaluate cell proliferation. From the cell count data, the average PDL (**equation 4.6** (Roth, 1974)), and DT (**equation 4.7**) were calculated. Any significant effect of the peptides on the cells would be indicated by a deviation in the PDL and DT when compared to the control.

$$PDL = 3.321 \times \log (b \div c) \quad \textbf{(Eq. 4.6)}$$

$$DT = T \times \log 2 \div \log (b \div c) \quad \textbf{(Eq. 4.7)}$$

Where T = time in culture (hours), b = end cell number (total), and c = start cell number (total)

4.2.5.2 MTT (3-(4,5-Dimethylthiazol-2-yl)-2,5-diphenyltetrazolium bromide) assay

To identify and quantify cell proliferation an MTT assay was performed, whereby the tetrazolium ring of MTT is cleaved by the mitochondrial dehydrogenases in living cells, producing purple formazan crystals. Dissolving these crystals and measuring the absorbance is an indication of the cell population metabolic activity. A growth curve was generated by seeding 3T3 cells at various densities (5×10^2 to 1×10^5 cells) in a 96 well plate. They were left for 22 hours before a MTT assay was performed. The resultant absorbance data was then used to generate growth curves, which were used to calculate cell number. A 96 well plate was seeded at 2×10^3 cells/well with 3T3 cells and left to incubate overnight to allow cell adhesion. A dilution series was produced from the hydrolysate solutions prepared for the cell counting assay. The range was from 600 µg/mL to 25 µg/mL. 50 µL of each dilution was added to the relevant wells in triplicate. The final concentrations of each ranged from 200 µg/mL to 8.3 µg/mL. The plate was then returned to the incubator and after 48 hours, the cells were assayed using MTT. The subsequent absorbance values were used to calculate the proliferation of the cells by using **equation 4.8**.

$$\text{Percentage proliferation} = [(a \div b) \times 100) - 100] \quad \textbf{Eq. 4.8}$$

Where a = mean absorbance of control group, and b = absorbance of experimental sample.

4.2.6 HPLC analysis of hydrolysates and fractionation of liver hydrolysate

The hydrolysates were analysed using HPLC to gather information on the composition of the hydrolysates. The hydrolysates were first analysed using analytical HPLC, which was then scaled up to prep HPLC to generate fractionated samples for further investigation. UV at 220 nm was used for detection.

4.2.6.1 Reverse phase HPLC

The initial chromatography work on the samples utilised HPLC using an analytical C18 column specifically designed for peptides and small proteins (Ascentis® Express Peptide ES-C18 (length 100 mm, ID 4.6 mm). Hydrolysate samples were dissolved in the aqueous mobile phase (acetonitrile (0.2%), TFA (0.01%), made up to required volume using HPLC grade water) and then 100 µL of the reconstituted hydrolysates were injected onto C18 column for analysis using a flow rate of 1 mL/min. The concentration gradient of acetonitrile for all samples went from 5% to 29% in the first 10 minutes followed by from 29% to 95% in the following 5 minutes.

4.2.6.2 Preparative HPLC

To accurately quantify the activity of each fraction generated by HPLC, a greater mass was required. To generate more of the fractionated samples a Gilson prep HPLC system was used with a Dynamax-60A C18 (length 250 mm, ID 21.4 mm) column. The difference in size between the analytical column and the prep column has to be taken into account. **Equation 4.9**, and **Equation 4.10** were used to alter the method used for the analytical column, to scale up for the prep column:

$$Fp = [Fa \times (D^2p \div D^2a)] \div (PSp \div PSa) \qquad \textbf{(Eq. 4.9)}$$

$$Vp = Va \times [(D^2p \div D^2a) \times (Lp \div La)] \qquad \textbf{(Eq. 4.10)}$$

Where Fp = Flow rate of prep column (13.5 mL/min), Fa = Flow rate of analytical column (1 mL/min), D^2p = Internal diameter of column squared of prep column (457.96 mm), D^2a = Internal diameter of column squared of analytical column (21.16 mm), PSp = Particle size of prep column (0.008 mm), PSa = Particle size of analytical column (0.0027 mm), Vp = injection volume for prep column (2.2 mL), Va = injection volume for analytical column (0.04 mL), Lp = Length of prep column (250 mm), and La = Length of analytical column (100 mm).

The prep HPLC was only carried out on the <5 kDa liver hydrolysate (L2). For each run 1 mL of dissolved hydrolysate (50 mg/mL) was loaded onto the column.

4.2.6.3 Freeze drying fractions

The collated fractions were divided up into smaller aliquots for freeze-drying (approximately 10 mL into 50 mL tubes). The aliquots were covered with Parafilm then flash frozen using liquid nitrogen so that the samples coated the sides of the tubes (to increase the surface area of the frozen sample). The aliquots were stored on dry ice until required. The samples were freeze dried for 25 hours. Freeze dried samples of the same fractions were combined then stored at -20°C.

4.2.6.4 HPLC analysis of fractions generated form prep HPLC

The fractions generated from the prep HPLC were further analysed using an analytical C18 column (Ascentis® Express Peptide ES-C18). The parameters were the same as described in section *4.2.6*.

4.2.7 Assays performed on prep HPLC fractions

The lyophilised samples generated from the HPLC fractions were assayed along with the full liver hydrolysate (L2) to test for bioactivity. The assays performed were the MTT assay, to identify any increase or decrease in cell proliferation, a scratch assay to identify any increase or decrease in chemotaxis, and a radical scavenging assay utilising DPPH.

4.2.7.1 MTT assay

The cell plates for the MTT assay were prepared according to section *4.2.5.2*. Liver hydrolysate fraction preparations (concentration gradient from 200 – 50 µg/mL) were added to the plate and incubated at 37°C at 5% CO_2 for 46 hours. 20 µL of MTT in PBS (5 mg/mL) was then added to each well and the plate was then incubated at 37°C at 5% CO_2 for 4 hours after which, the media was aspirated and 150 µL of dimethyl sulfoxide (DMSO) was added. The plate was read at 540 nm on a plate reader utilising a 5 second shake. The data was generated using **equation 4.8**.

4.2.7.2 Scratch Assay

The scratch assay was adapted from the method used by Travan et al (2016) (Travan et al., 2016). 12 well plates were seeded with 3T3 fibroblasts at a cell density of 1.5×10^5 cells/mL (2.25×10^5 cells/well)

two days prior to the assay and were cultured until confluent. Peptide fractions were weighed out, and used to produce sample preparations using complete growth media (CGM). Each sample preparation was then sterile filtered using 0.22 µM syringe filters. The target concentration for the preparations was 400 µg/mL. It should be noted that there was not enough of sample F2R1 to produce a concentration of 400 µg/mL in the volume required (the maximum concentration of this sample was 50 µg/mL). Mitomycin C in PBS (1mg/mL) was added to each preparation along with control media (CGM only) to achieve a concentration of 15 µg/mL. Mitomycin C was added to inhibit mitosis therefore, preventing the proliferation of cells without inhibiting chemotaxis (Schreier et al., 1993).

Using sterile 20 µL pipette tips, a scratch was made in the confluent monolayer of each well to produce a wound. The wells were then washed using PBS before the sample preparations were added. Each well was marked in a suitable place and micrographs were taken to record the area of each wound. This was repeated until the wounds were healed.

The first micrograph taken was assigned as 0% closed (**Figure 4-4 a**) and the area of the wound was used as a reference for all other micrograph images taken at the proceeding time points to calculate the percentage of wound closure. The assay ended when the cells had migrated to fill in the wound gap (**Figure 4-4 b**). The area of each wound was calculated using Image J (version 1.51j8, National Institute of Health Bethesda, U.S.A.) (Schindelin et al., 2012). Wound closure rate ($\mu m^2/h$) was calculated using **Equation 4.11**: Percentage wound closure was calculated using **equation 4.12**.

$$Wound\ closure\ rate\ (\mu m^2/h) = (W_n - W_0) \div T_n \qquad \textbf{(Eq. 4.11)}$$

$$\%\ wound\ closure = [1 - (W_n \div W_0)] \times 100 \qquad \textbf{(Eq. 4.12)}$$

Where W_n = Area of wound at the end time point, W_0 = Area of wound at time zero, and T_n is the number of hours of the end time point.

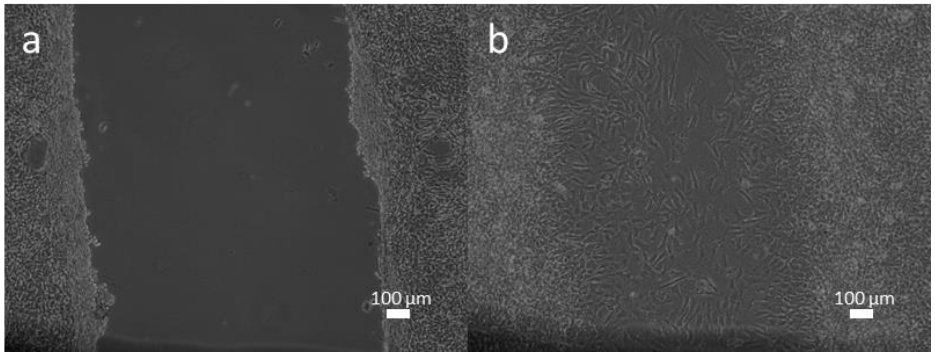

Figure 4-4 An example of a wound created in a confluent monolayer of 3T3 fibroblasts (a), and the 'healed' wound (b)

4.2.7.3 DPPH Radical Scavenging Assay

The collated liver hydrolysate fractions from the prep HPLC were used in a quantitative DPPH assay using the 96 well format that was previously described in section *4.2.1*. The samples were prepared in pH 7.4 potassium phosphate buffer to a concentration of 0.8 mg/mL. A serial dilution was then performed on the plate to produce a concentration gradient.

4.2.8 Stability studies

Whole hydrolysates were prepared in supplemented DMEM to the concentrations of 0.8, 0.4, and 0.2 mg/mL. The specific media were then separated into eight aliquots each, before being stored at -20°C for 24 hours. After 24 hours one of each of the placenta (P2), and liver hydrolysate (L2) media were removed from the freezer and stored at 5°C. This was performed every 24 hours until all aliquots had been removed. The thawed aliquots were then used in MTT assays (set up described in section *4.2.5.2*, concentrations as in *4.2.10.1*), and analysed using HPLC (parameters described in *4.2.6*) to determine whether the peptides contained in the hydrolysates were stable at 5°C. The aliquot taken for the 0 h sample was used immediately after it had thawed.

4.2.9 ACE inhibition assay

ACE from rabbit lung was (purchased form Sigma Aldrich 2U equal to 1 mg of protein) reconstituted in milli-q water (1 mL) to produce the ACE stock solution (1 U/mL, 500 µg/mL of protein). ACE working solution (200 mU/mL, 100 µg/mL of protein) was prepared by diluting the stock solution 1:5. ACE stock solution was stored at -20°C and the ACE working solution was prepared when required,

and stored at -20°C. HHL solution was prepared by adding HHL (2.15 mg) to TRIS buffer (pH 8.3) (10 mL) containing NaCl (300 mM), and $ZnSO_4$ (10 µM) (10 mL). Peptide hydrolysate preparations were prepared by dissolving either liver 57061850 (L1), liver 58063636 (L2) or placenta 5338 3617 (P1) hydrolysates into milli-q water. Milli-q water or experimental sample (40 µL) and 0.5 mM HHL (145 µL) were added to 1.5 mL micro-centrifuge tubes and incubated in a water bath at 37°C for 3 minutes then 200 mU/mL ACE (15 µL) was added to each tube, which were then incubated in a water bath at 37°C for 30 minutes. After 30 minutes 1 M HCl (200 µL) was added to the tubes to stop the reaction. **Table 4-1** represents how the samples were set up, where column A indicates experimental samples, column B control 1, and column C control 2. Captopril was used as a known ACE inhibitor.

Table 4-1 Sample preparation for angiotensin II converting enzyme (ACE) inhibition assay

Reagents	Volume (µL)		
	A	B	C
Milli-Q Water	-	40	15
Inhibitor/Peptide	40	-	40
0.5 mM HHL	145	145	145
Incubate 37°C for 3 min			
200 mU/mL ACE	15	15	-
Incubate 37°C for 30 min			
1M HCl	200	200	200

The samples were analysed by HPLC (Beckman Coulter) using an Ascentis® Express Peptide ES-C18, 2.7 µm column, to determine the anti-ACE activity of the analytes. The HPLC was setup as follows: 0.4 mL/min flow rate, isocratic (mobile phase 50% methanol, 50% water containing trifluoroacetic acid (TFA) (0.2%). The substrate and the product were detected using UV at 228 nm. The ability of each peptide to inhibit ACE was measured by comparing the reduction of HA (the product of ACE digested HHL) in relation to the positive control (no inhibitor or peptide present). **Equation 4.13** was used to calculate the inhibition.

$$ACE\ inhibition\ (\%) = (1-(B \div A)) \times 100 \qquad \textbf{(Eq. 4.13)}$$

Where A is area of HA peak in control 1 and B is the area of HA peak in experimental sample.

4.3 Results

4.3.1 DPPH Radical Scavenging Activity (RSA)

Data generated is represented in (**Figure 4-5 a**). Due to the very low levels of activity of P1 at 375 µg/mL the activity was retested at 5 mg/mL and 50 mg/mL (**Figure 4-5 b**)

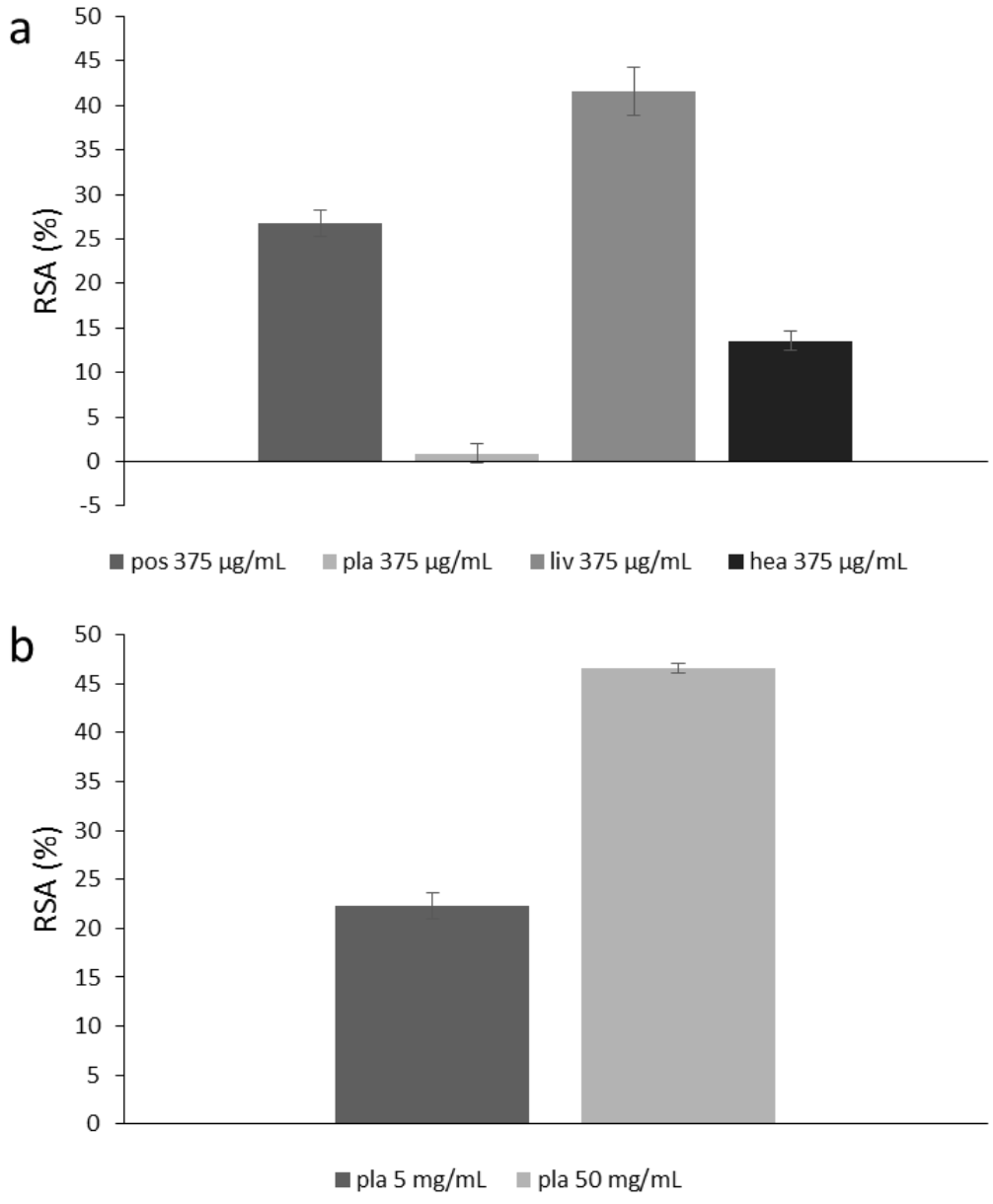

Figure 4-5 Radical scavenging activity (RSA) of 0-150625-1700 (P1) hydrolysate, liver 150615-1900 (L1) hydrolysate, and heart 150615-1900 (H1) hydrolysate compared with the positive control ascorbic acid at 375 µg/mL (a) 0-150625-1700 (P1) hydrolysate at 5 mg/mL, and 50 mg/mL (b)

The DPPH assay method used here was a useful way to assess whether the hydrolysate samples showed activity and it was shown that the activity related to the quantity of proton donors in the peptide and

followed the trend Liver > Heart > Placenta. As a quantitative measure of activity however, the method was not robust. The assay was therefore developed into a 96 well plate format, with the absorbance of the samples read on a plate reader.

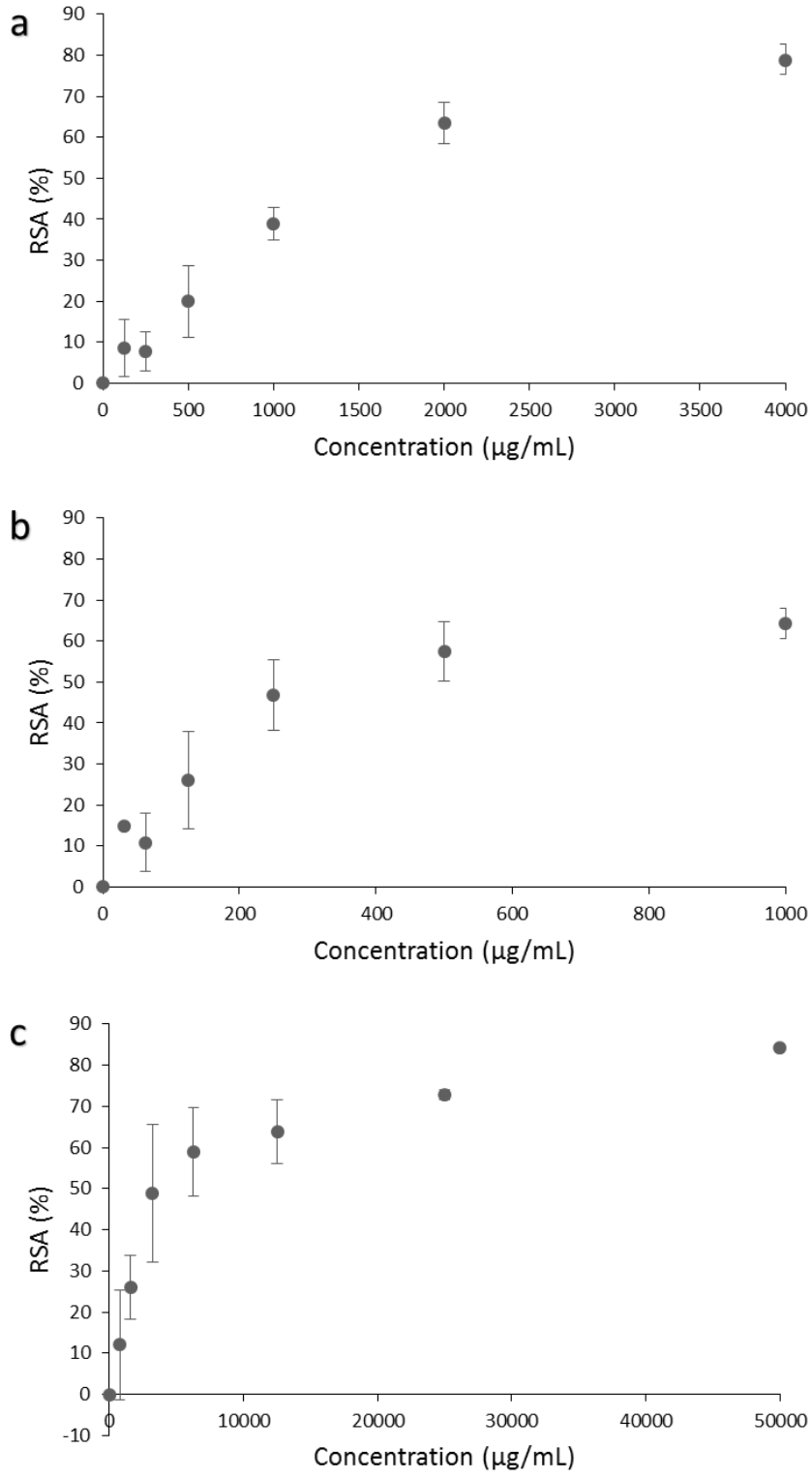

Figure 4-6 Radical scavenging activity (RSA) of heart 150615-1900 (H1) (a), liver 150615-1900 (L1) (b), and 0-150625-1700 (P1) (c) hydrolysates at different concentrations for 96 well plate assay

The results presented in **Figure 4-6** indicate that L1 has the higher radical scavenging activity, followed by H1, and then P1. This activity is also dependant on the concentration of the hydrolysate. It should

be noted that this activity is applicable to the mechanism of the DPPH assay only. The data generated from the 96 well plate assay was comparable to the data generated from the original method (**Figure 4-5**). The same trend was also observed in the assay performed on the samples L2, and P2 **Figure 4-7**.

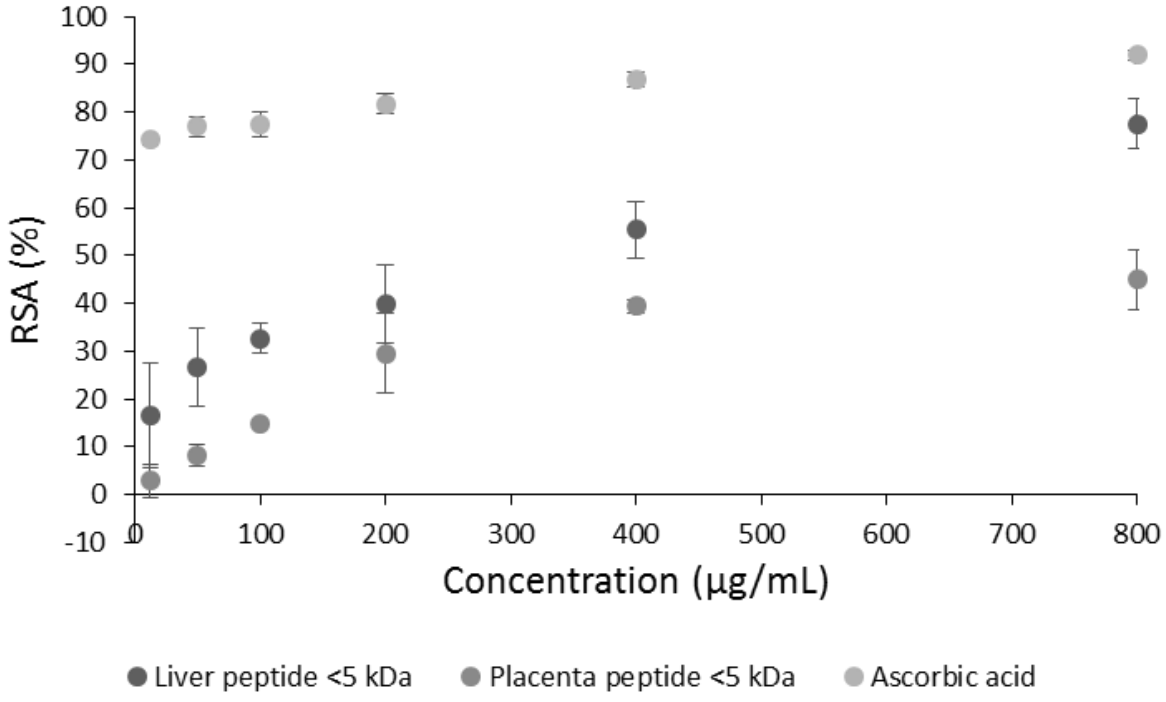

Figure 4-7 Radical scavenging activity (RSA) of liver 160126-0700 (L2), and placenta 0-160330-1500 (P2) for 96 well plate assay

4.3.2 ORAC Assay

The ORAC activities calculated for the first batch of hydrolysates (L1, and P1) were calculated from the data shown in **Figure 4-8**, and presented as trolox equivalents (TE) (**Table 4-2**), which represent the relative quantity of analyte required to achieve equivalent ORAC activity. The TE were calculated from the AUC of the Trolox standard curve (**Figure 4-9**).

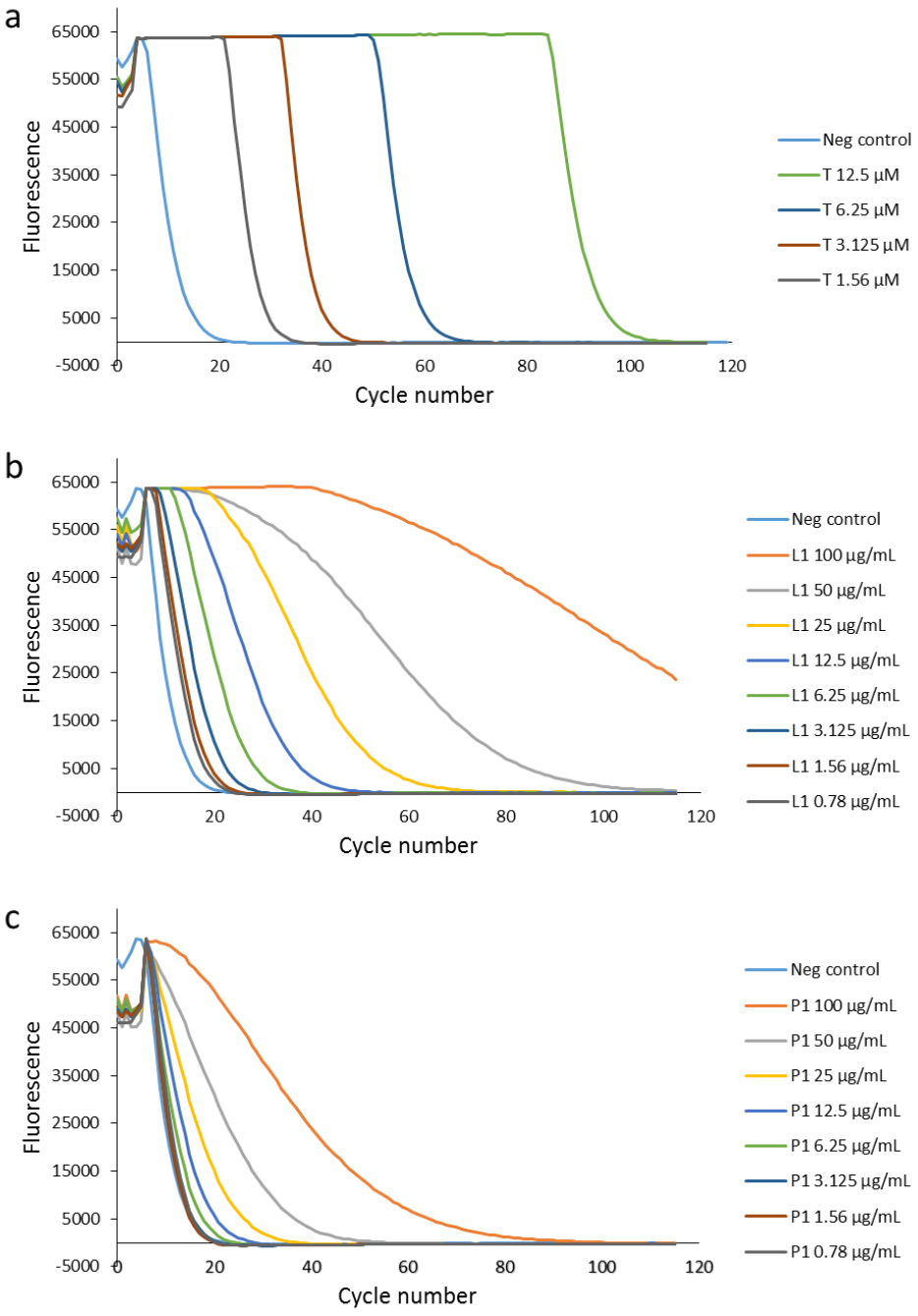

Figure 4-8 Data plots generated from the fluorescent plate reader used to calculate the area under the curve (AUC) of Trolox (a), liver 150615-1900 (L1) (b), and 0-150625-1700 (P1) (c) hydrolysates

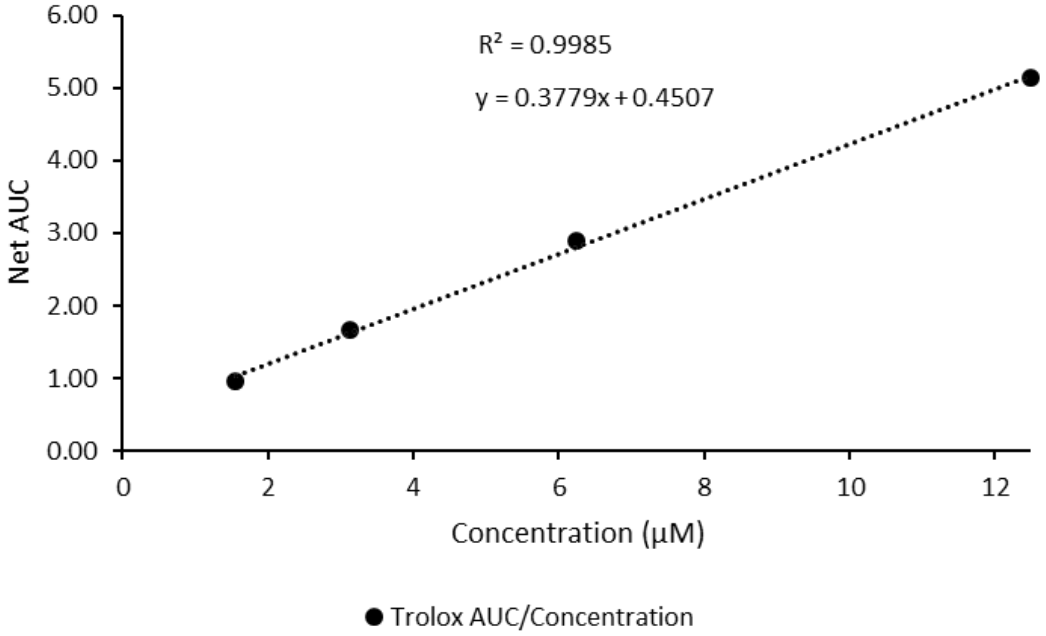

Figure 4-9 area under the curve (AUC) against the concentration of Trolox (run in conjunction with liver 150615-1900 (L1), and 0-150625-1700 (P1) hydrolysates) plotted to form a standard curve to calculate Trolox equivalents (TE)

The hydrolysates from the original batch (L1, P1) demonstrated markedly different ORAC activity. The TE for L1 was 30.5 (30.5 g of L1 wold be needed to achieve the same ORAC value as 1 g of Trolox), and the TE for P1 was 277.8.

Table 4-2 Trolox equivalents for liver 150615-1900 (L1), and placenta 0-150625-1700 (P1)

Trolox Equivalents (TE)	
L1	P1
30.5	277.8

The ORAC activities calculated for the L2, L3, and P2 were calculated from the data shown in **Figure 4-10**, and presented as Trolox equivalents (TE) (**Table 4-3**). The TE were calculated from the AUC of the Trolox standard curve (**Figure 4-11**).

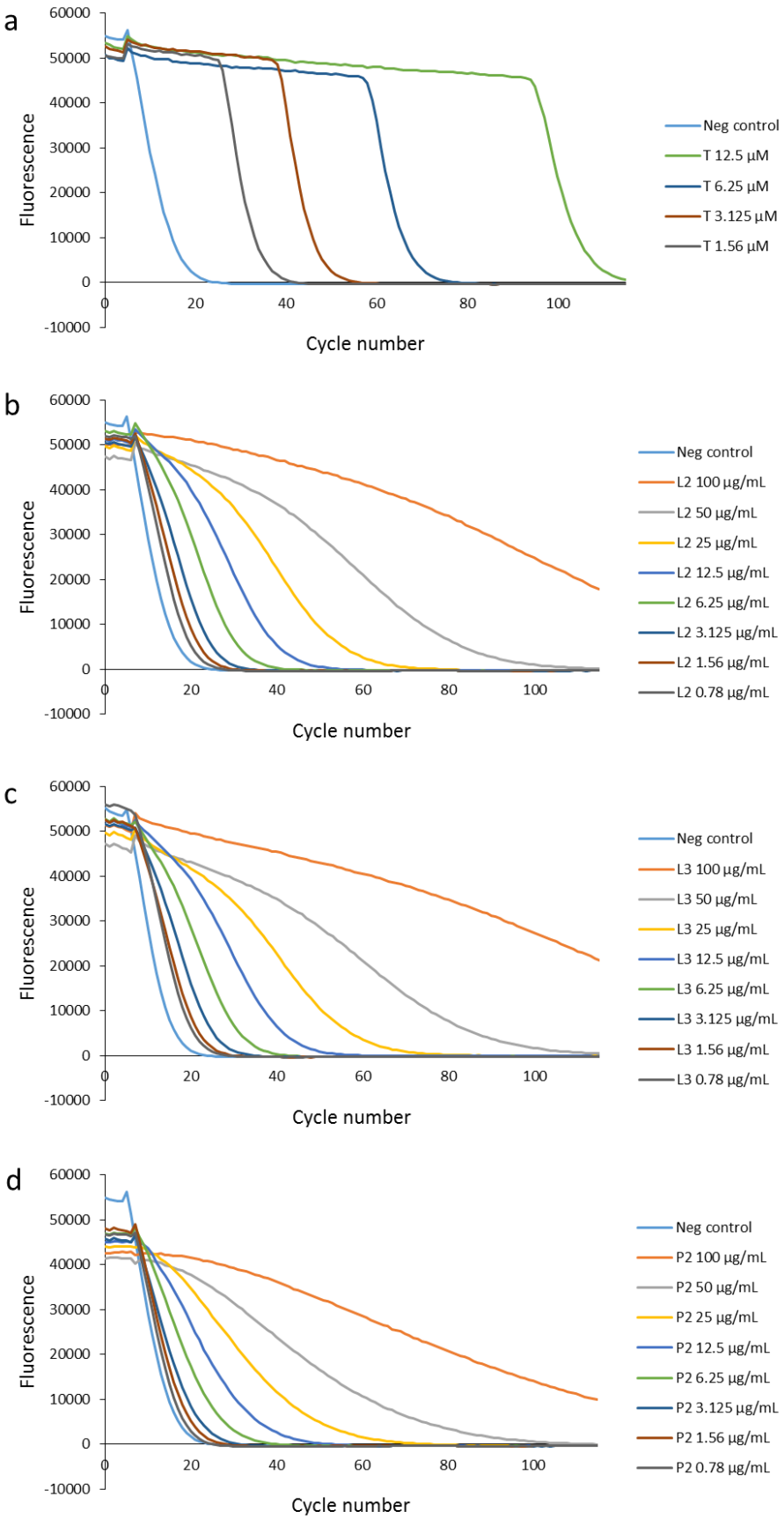

Figure 4-10 Data plots generated from the fluorescent plate reader used to calculate the area under the curve (AUC) of Trolox (a), and liver 160126-0700 (L2) (b), liver 170127-0815 (L3) (c), and placenta 0-160330-1500 (P2) (d) hydrolysates

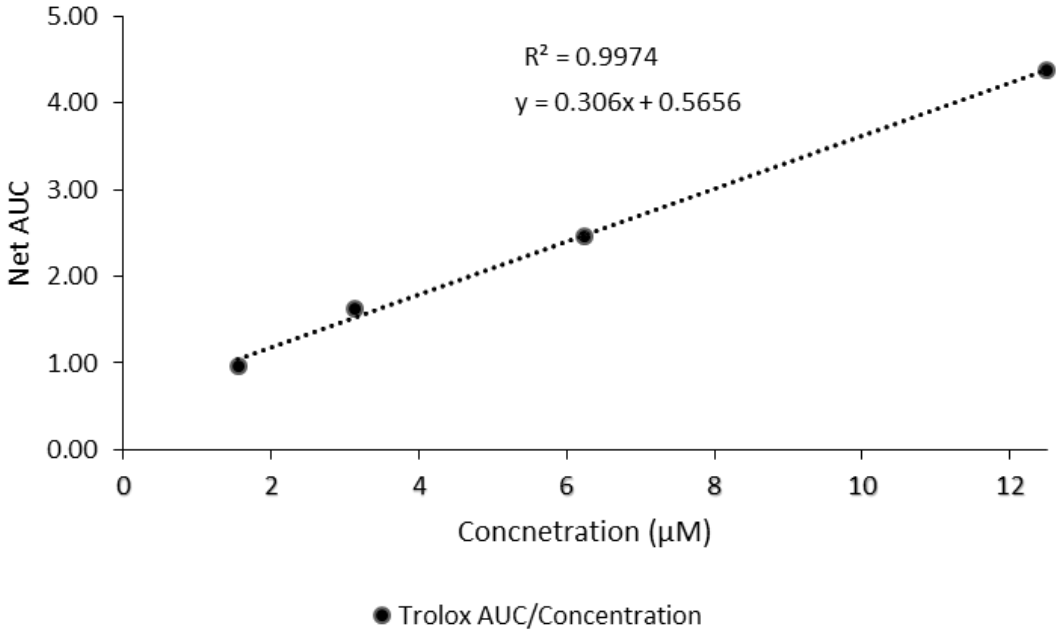

Figure 4-11 area under the curve (AUC) against the concentration of Trolox (run in conjunction with liver 160126-0700 (L2), liver 170127-0815 (L3), and placenta 0-160330-1500 (P2) hydrolysates) plotted to form a standard curve to calculate Trolox equivalents (TE)

The hydrolysates L1, and L2 demonstrated slightly different ORAC activity to L1, with L3 (TE = 50) requiring 40% more than L1 to achieve a similar TE, and L2 (TE = 38.3) 22% more. The TE for P2 was 71.4, this was approximately 75% less than the TE for P1.

Table 4-3 Trolox equivalents (TE) for liver 160126-0700 (L2), liver 170127-0815 (L3), and placenta 0-160330-1500 (P2)

Trolox Equivalents (TE)		
L2	L3	P2
38.3	50	71.4

4.3.3 Lipid peroxidation inhibition assay

The ability of the hydrolysates (L1, P1, and H1) to reduce lipid peroxidation was assessed using the lipid peroxidation assay. The assay measures the level of peroxidation by using the FTC assay, where an increase in peroxidation is by visualised by an increase in absorbance at 500 nm (**Figure 4-12**). The end-point of the assay was selected to be the time point before the absorbance of the negative control exceeded 2 AU.

The results showed that all the samples significantly reduced autoxidation in the linoleic acid system (**Figure 4-13**). There was no significant difference between the hydrolysates in this assay.

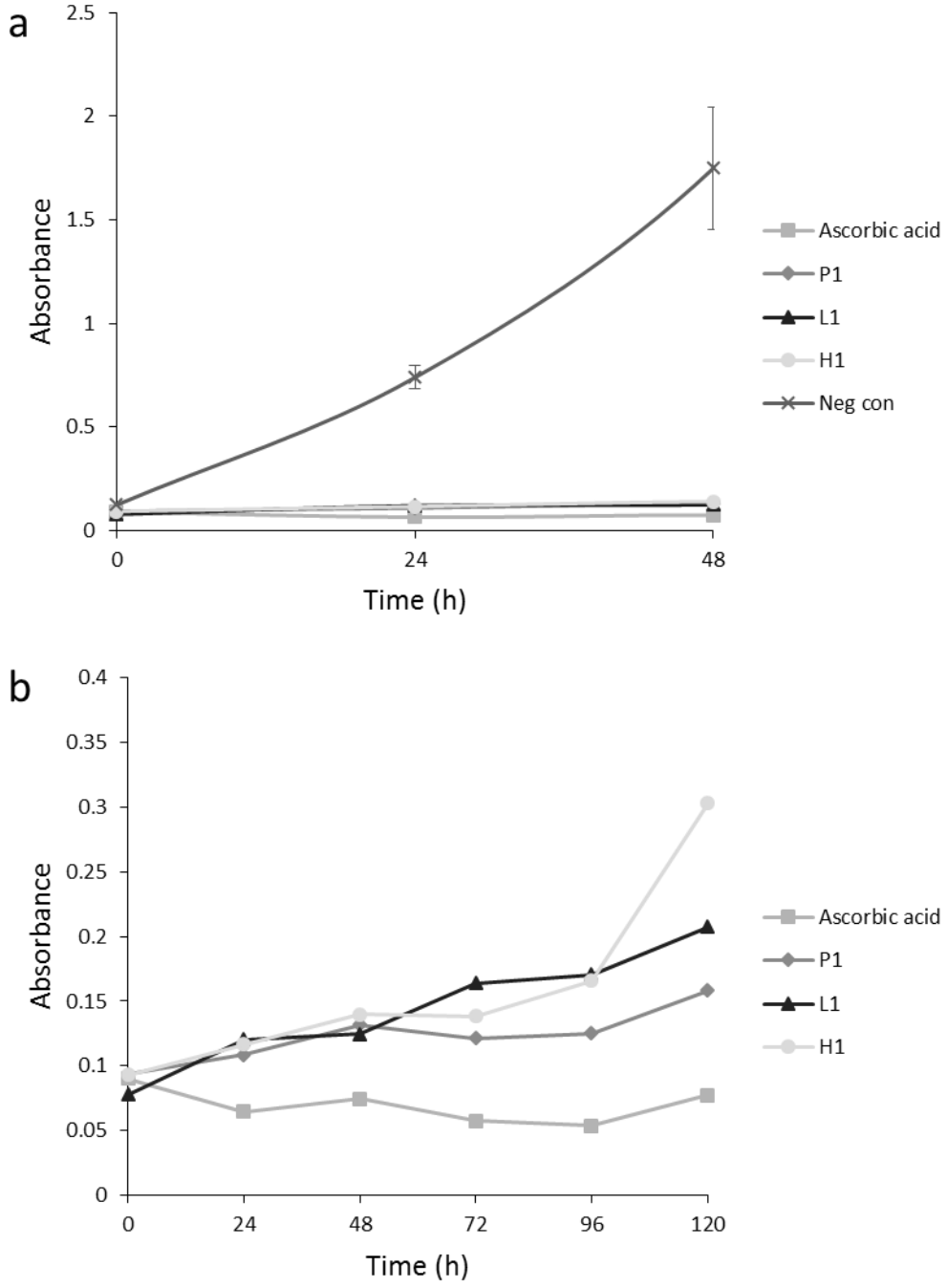

Figure 4-12 Absorbance at 500 nm as a result of the ferric thiocyannate assay (FTC) for liver 150615-1900 (L1), 0-150625-1700 (P1), and heart 150615-1900 (H1) plus ascorbic acid (positive control), and the negative control (a), with the traces for the hydrolysates and ascorbic acid show in greater detail (b).

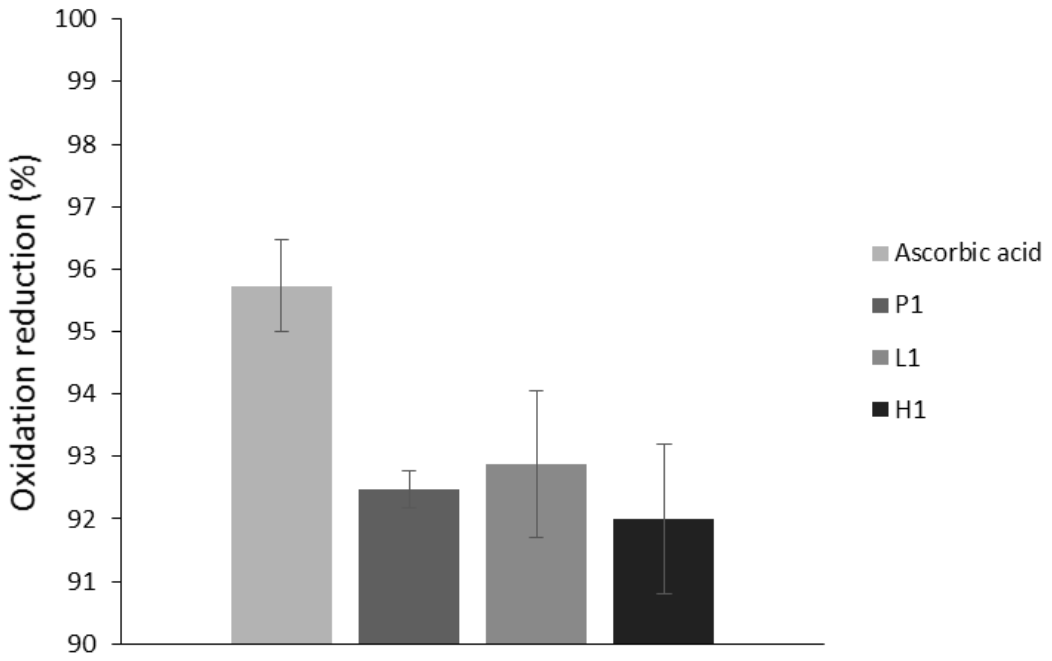

Figure 4-13 Percentage inhibition of lipid peroxidation at the reaction endpoint (48 h)

4.3.4 Cellular antioxidant activity assay (CAA)

The fluorescence of each sample at each time point was plotted to show the change in fluorescence over time. The CAA (percentage) (**Figure 4-15**) was calculated from the subsequent plots (**Figure 4-14**). Single factor Anova tests were carried out on the data to determine whether the results were significant. The data indicates that both peptide samples display antioxidant activity for most of the conditions assayed with values of 12.8% for liver, and 8% for placenta at 8 mg/mL, 8.7% for liver, and 13.8% for placenta at 4 mg/mL, and -2.9% for liver, and 14.3% for placenta at 2 mg/mL. The CAA (percentage) for Trolox were greater than the hydrolysates for all conditions. The statistical analysis of the data indicated that there was a significant difference ($p < 0.05$) between Trolox samples and the hydrolysates. There was no significant difference between the liver, and placenta samples at 8 and 4 mg/mL, a significant difference between liver, and placenta samples at 2 mg/mL, and that the data over the concentration gradient were not significant for the Trolox, and the placenta samples, but they were significant for the liver samples (**Figure 4-15**).

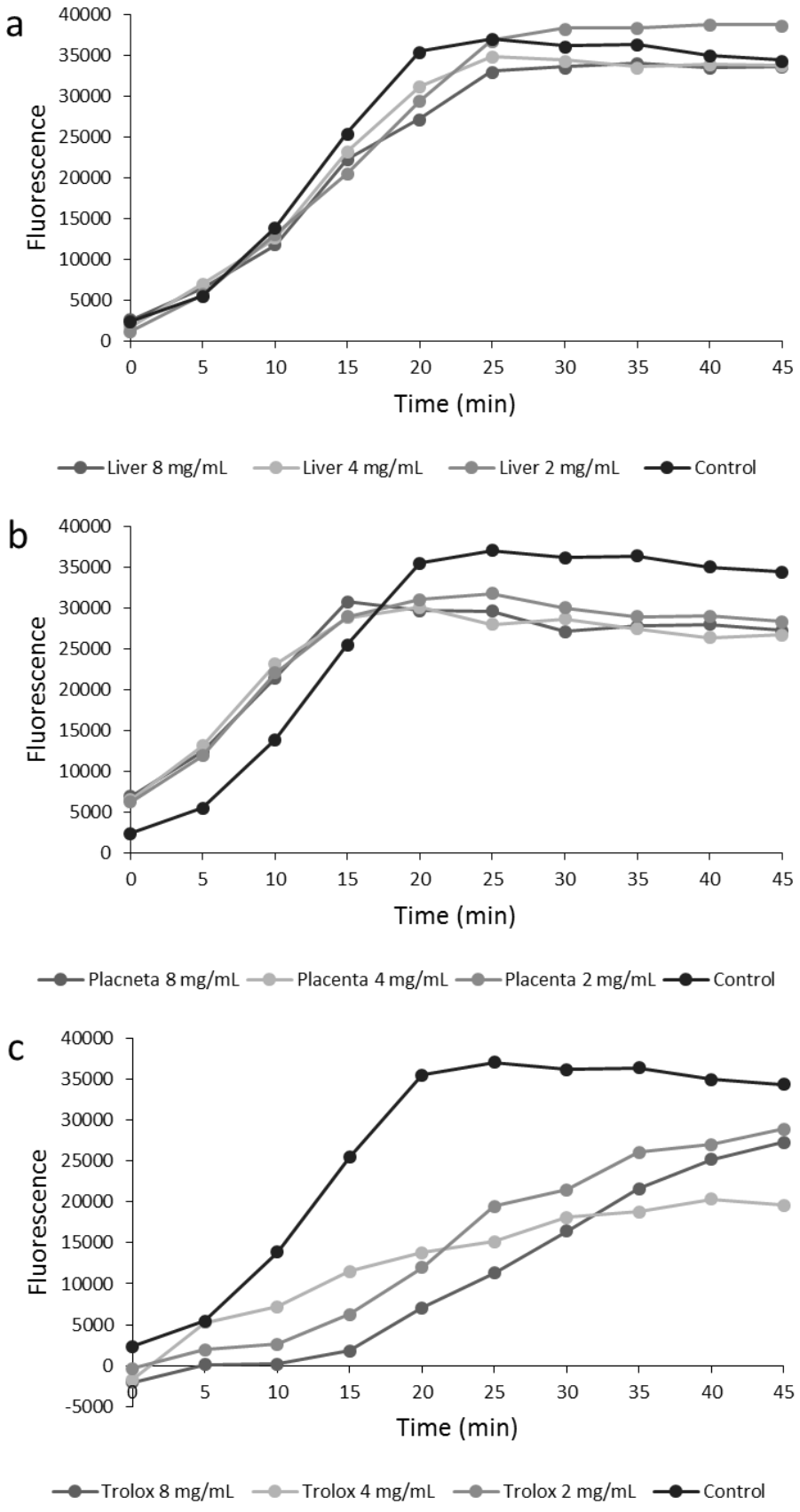

Figure 4-14 Fluorescence traces showing fluorescence against time (a-c) for liver 160126-0700 (L2) peptides (8 mg/mL, 4 mg/mL, and 2 mg/mL) (a), placenta 0-150625-1700 (P1) peptides (8 mg/mL, 4 mg/mL, and 2 mg/mL) (b), and Trolox (8 mg/mL, 4 mg/mL, and 2 mg/mL) (c).

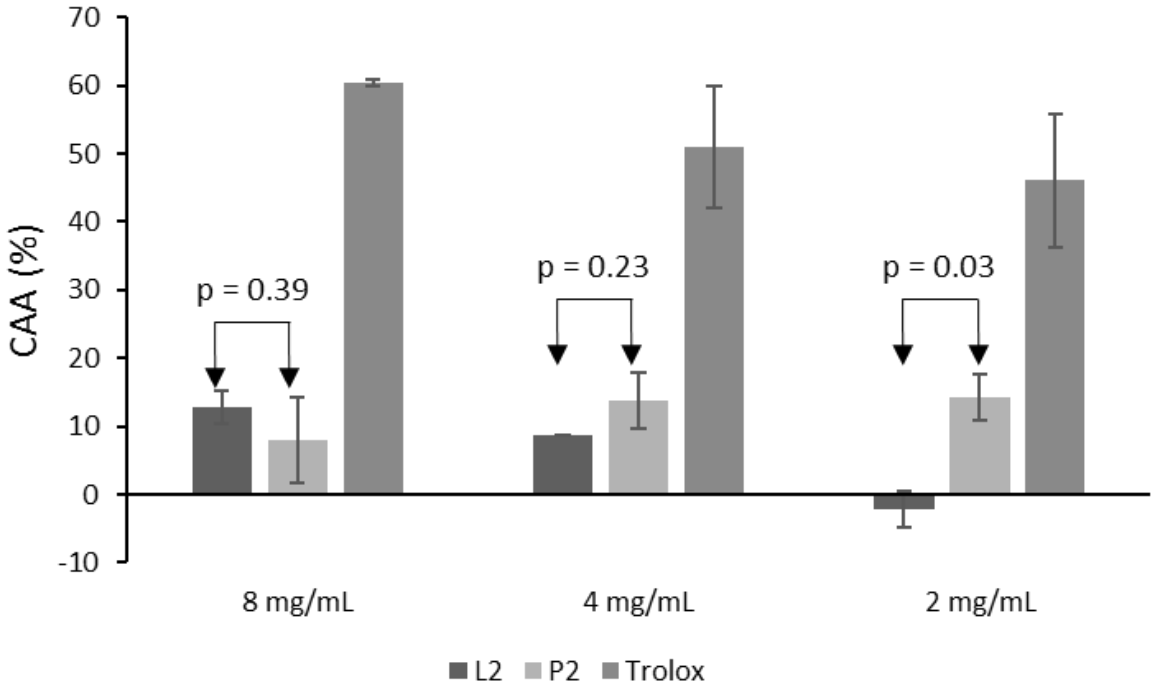

Figure 4-15 Cellular antioxidant activity (percentage) derived from the traces shown in figure 4-13

4.3.5 Cell proliferation

4.3.5.1 Cell counting method

The data for the cell counting method (**Figure 4-16**) indicates that there is no significant difference in cell proliferation between cells that were treated with L1, and P1 hydrolysates, and the control group (no hydrolysate).

4.3.5.2 MTT (3-(4,5-Dimethylthiazol-2-yl)-2,5-diphenyltetrazolium bromide) assay

The MTT assay indicated that in higher concentrations, the hydrolysates (L1, and P1) caused cell proliferation to be drastically reduced. However, at lower concentrations, both hydrolysates increased proliferation (**Figure 4-17**).

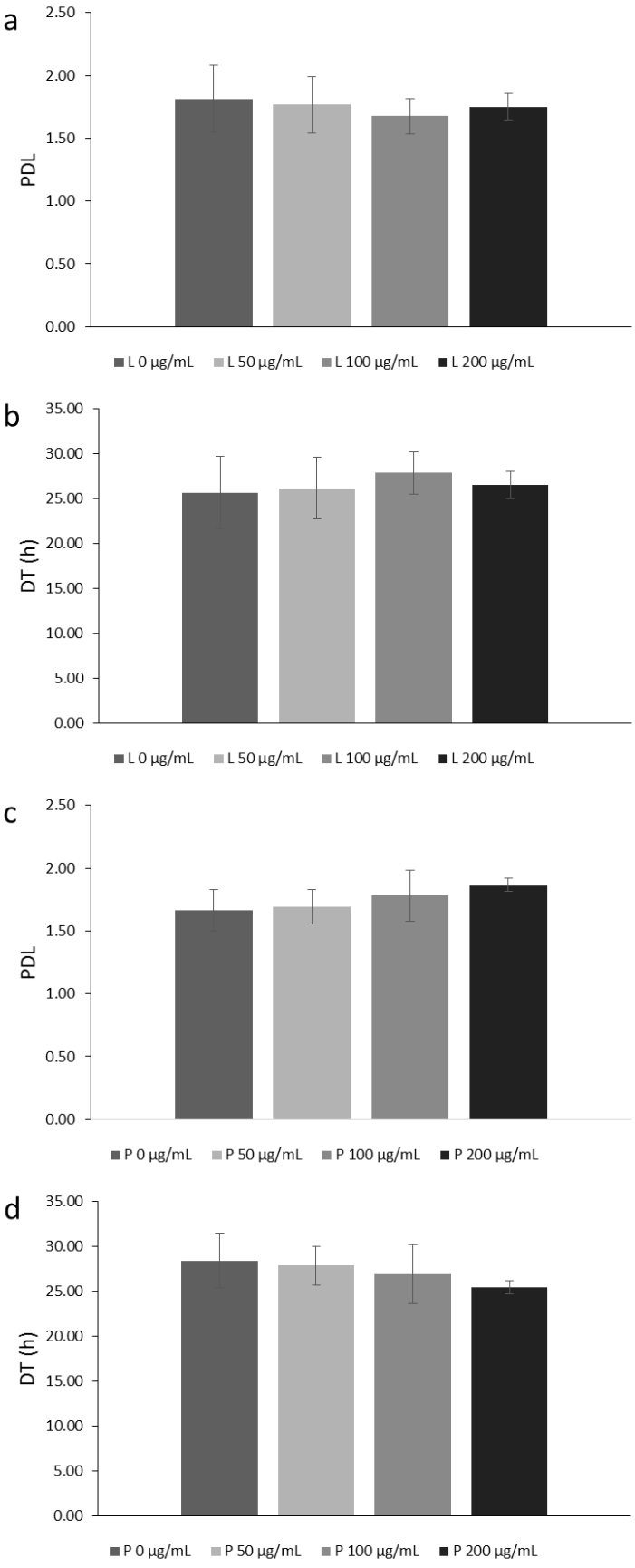

Figure 4-16 Cell doubling time (DT), and population doubling level (PDL) measured using cell counts for liver 150615-1900 (L1) (a, and b), and 0-150625-1700 (P1) (c, and d) at concentrations ranging from 0 -200 µg/mL

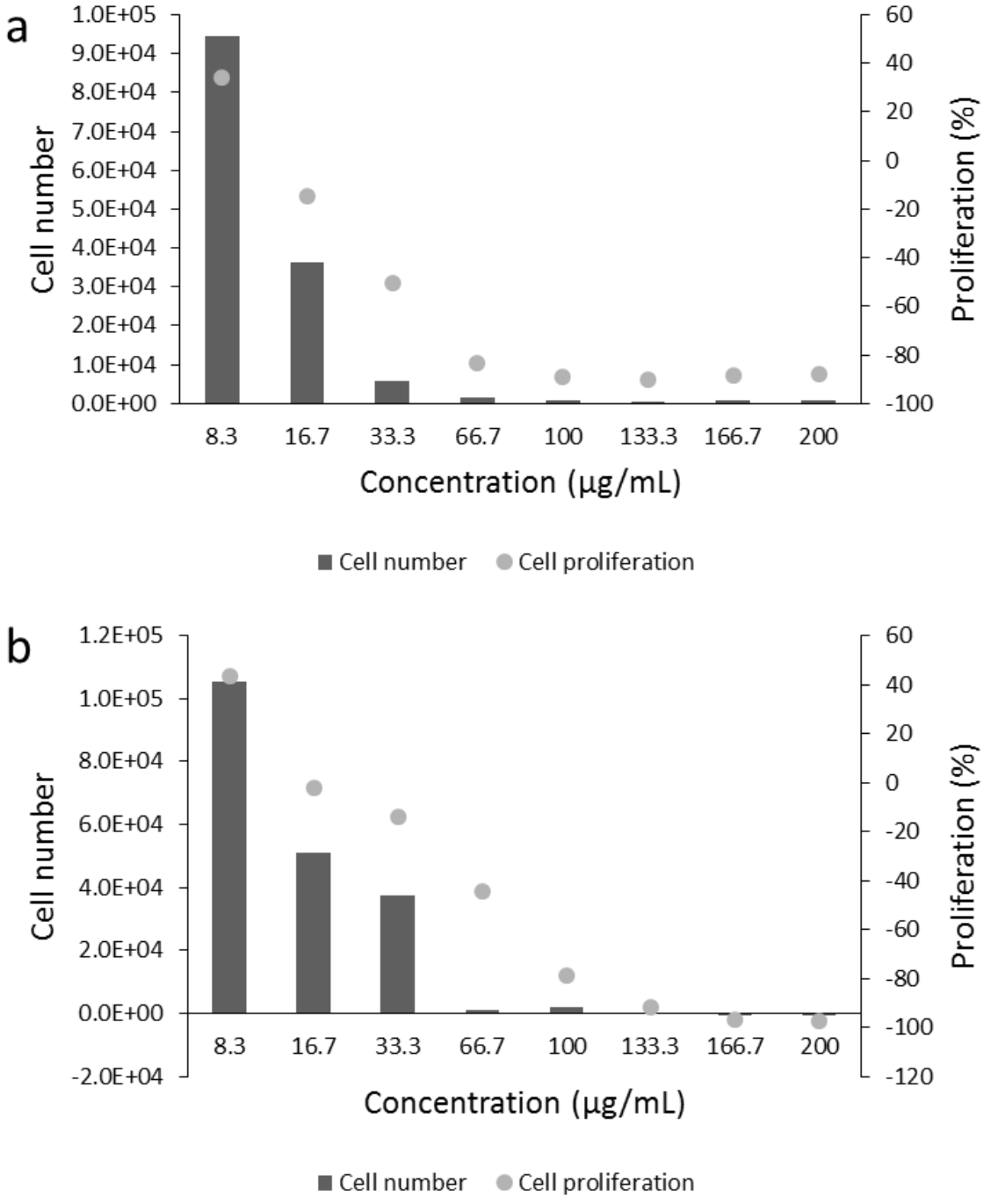

Figure 4-17 Cell number (bars), and cell proliferation (dots) using (3-(4,5-Dimethylthiazol-2-yl)-2,5-Diphenyltetrazolium Bromide) (MTT) assay in comparison to the control for cells treated with liver 150615-1900 (L1) (a) and placenta 0-150625-1700 (P1) (b)

4.3.6 HPLC analysis of hydrolysates and fractionation of liver hydrolysate

4.3.6.1 Reverse phase HPLC

The hydrolysates L2, and P2 were analysed using an Ascentis® Express Peptide ES-C18 column. The chromatograms for both hydrolysates both indicate that they are composed of multiple peptides, of varying sizes. The hydrolysate L2 (**Figure 4-18**) appears to be composed of peptides that fall into three different size ranges. The peaks between 1 and 3 minutes (**Figure 4-18 b**) are likely to consist of short peptides, and single amino acids. There is a significant peak at 5.6 minutes (**Figure 4-18 b**), which probably is made up of a group of similar longer peptides. The third significant group is between 22 and 28 minutes, which was likely to be aggregated product and therefore discounted (**Figure 4-18 d**). The hydrolysate P2 (**Figure 4-19**), like L2 is also composed of peptides that fall into three different size ranges. The peaks between 1 and 3 minutes (**Figure 4-19 b**) are likely to be made up of short peptides, and single amino acids. There are more peaks in this range than found in L2. There is a peak in a similar range as found in L2 at 5.78 minutes (**Figure 4-19 b**); this is also probably made up of a group of similar longer peptides. This peak is much smaller than found in L2. The third group of peak is very similar to the group found in L2 (**Figure 4-19** d).

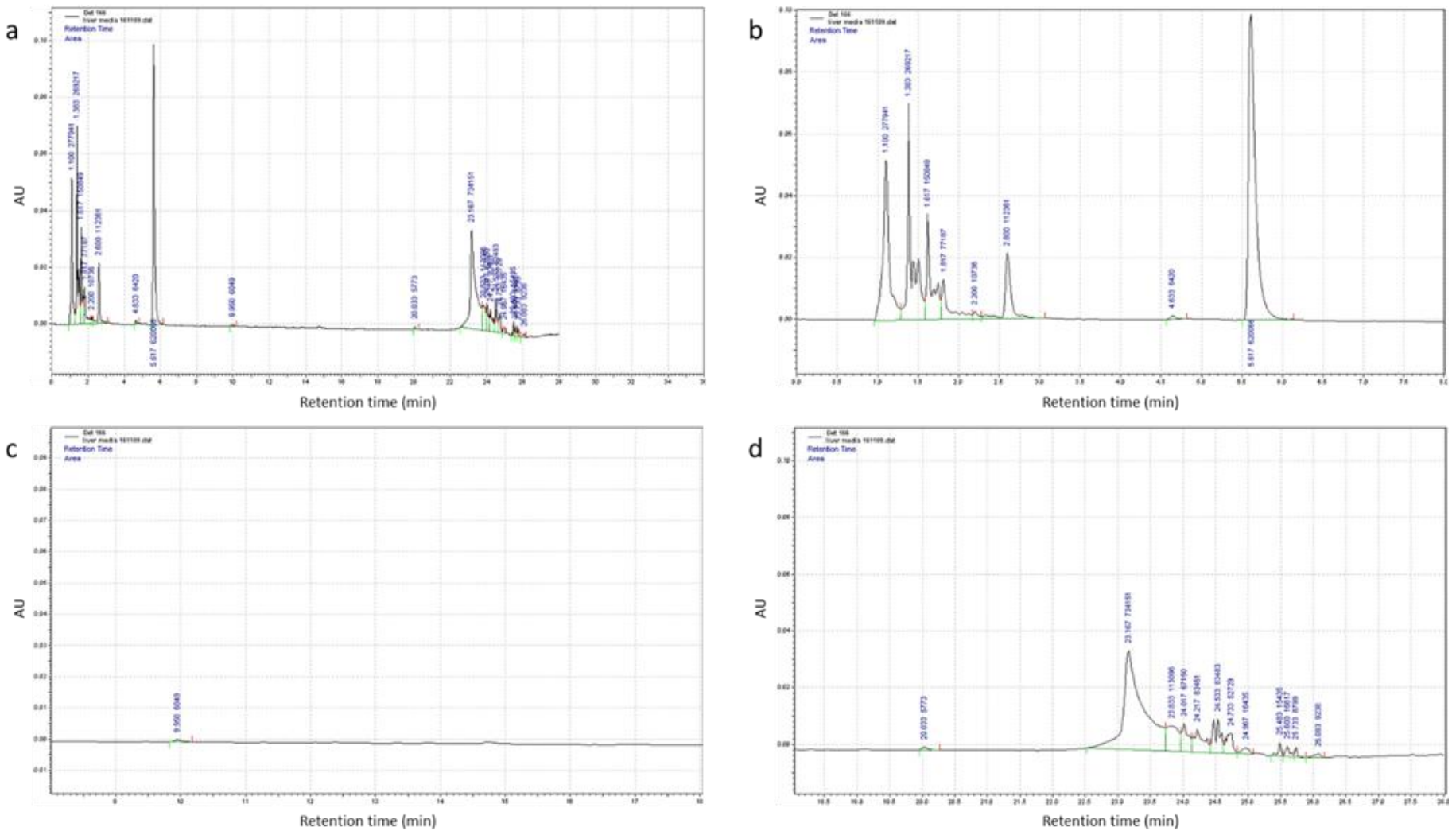

Figure 4-18 Analytical high performance liquid chromatography (HPLC) traces for liver 160126-0700 (L2) full chromatogram (a), with 0 – 8 minutes magnified (b), 8 – 18 minutes magnified (c), and 18 – 28 minutes magnified (d)

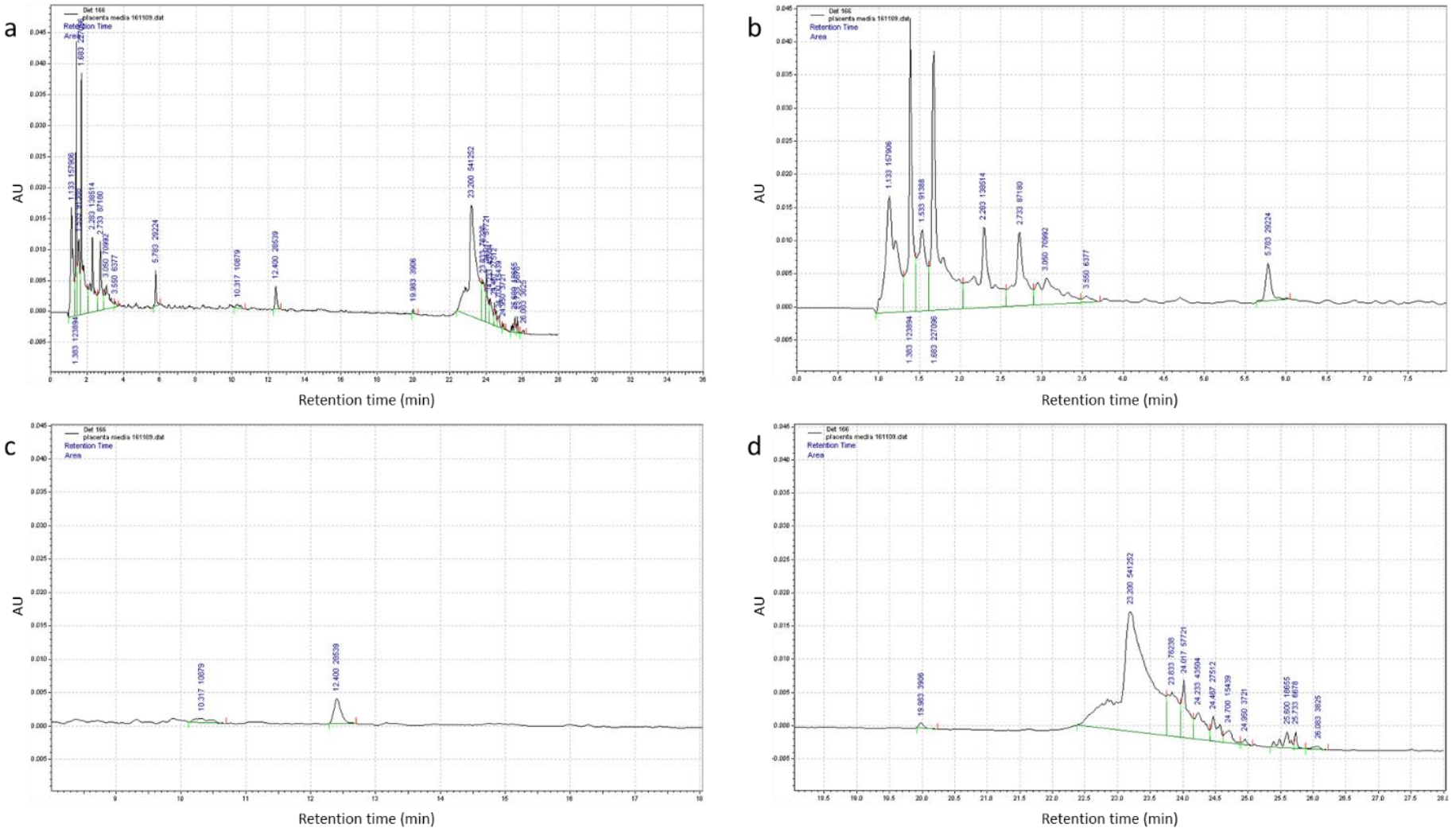

Figure 4-19 Analytical high performance liquid chromatography (HPLC) traces for placenta 0-160330-1500 (P2) full chromatogram (a), with 0 – 8 minutes magnified (b), 8 – 18 minutes magnified (c), and 18 – 28 minutes magnified (d)

4.3.6.2 Preparative HPLC (pHPLC) of liver hydrolysate

The liver hydrolysate (L2) was selected to be fractionated using preparative HPLC. The fractions that were collected (**Table 4-4**) over five runs were combined and retrieved by freeze-drying the fractions for reconstitution in different buffers for further analysis.

Table 4-4 Times at which each fraction was taken for runs 1 to 5 using liver 160126-0700(L2). Fractions from run 2 to 5 were collated. Fraction from run 1 were kept separate

	Run 1	**Run 2**	**Run 3**	**Run 4**	**Run 5**
Fraction 1	2.8-4.3 min	2.9-4.0 min	2.7-4.1 min	2.8-4.2 min	2.7-4.3 min
Fraction 2	4.3-5.6 min	4.0-5.8 min	4.1-5.6 min	4.2-5.8 min	4.3-6.2 min
Fraction 3	5.6-9.1 min	5.8-9.2 min	5.6-9.4 min	5.8-9.3 min	6.2-9.9 min
Fraction 4	9.1-13 min	9.2-13.2 min	9.4-13.3 min	9.3-13.5 min	9.9-13.5 min
Fraction 5	n/a	n/a	15-18 min	15-18 min	15.3-18.3 min

The chromatograms produced from the prep HPLC of the L2 hydrolysate (**Figure 4-20)** are quite different to the ones produced by the analytical HPLC column. The fractions obtained from run 2 to run 5 were collated (these were denoted as R2 fractions, e.g. F2R2 was a mixture of fraction 2 from run 2 to run 5). Fractions from run 1 were not mixed with other runs. The samples collected from the prep HPLC were labelled F1R1, F1R2, F2R1, F2R2, and F4R1. After freeze-drying, there was very little sample recovered from all F3, F5 fractions, or F4 fractions from run 2 - 5. Therefore, no analysis was carried out on these samples.

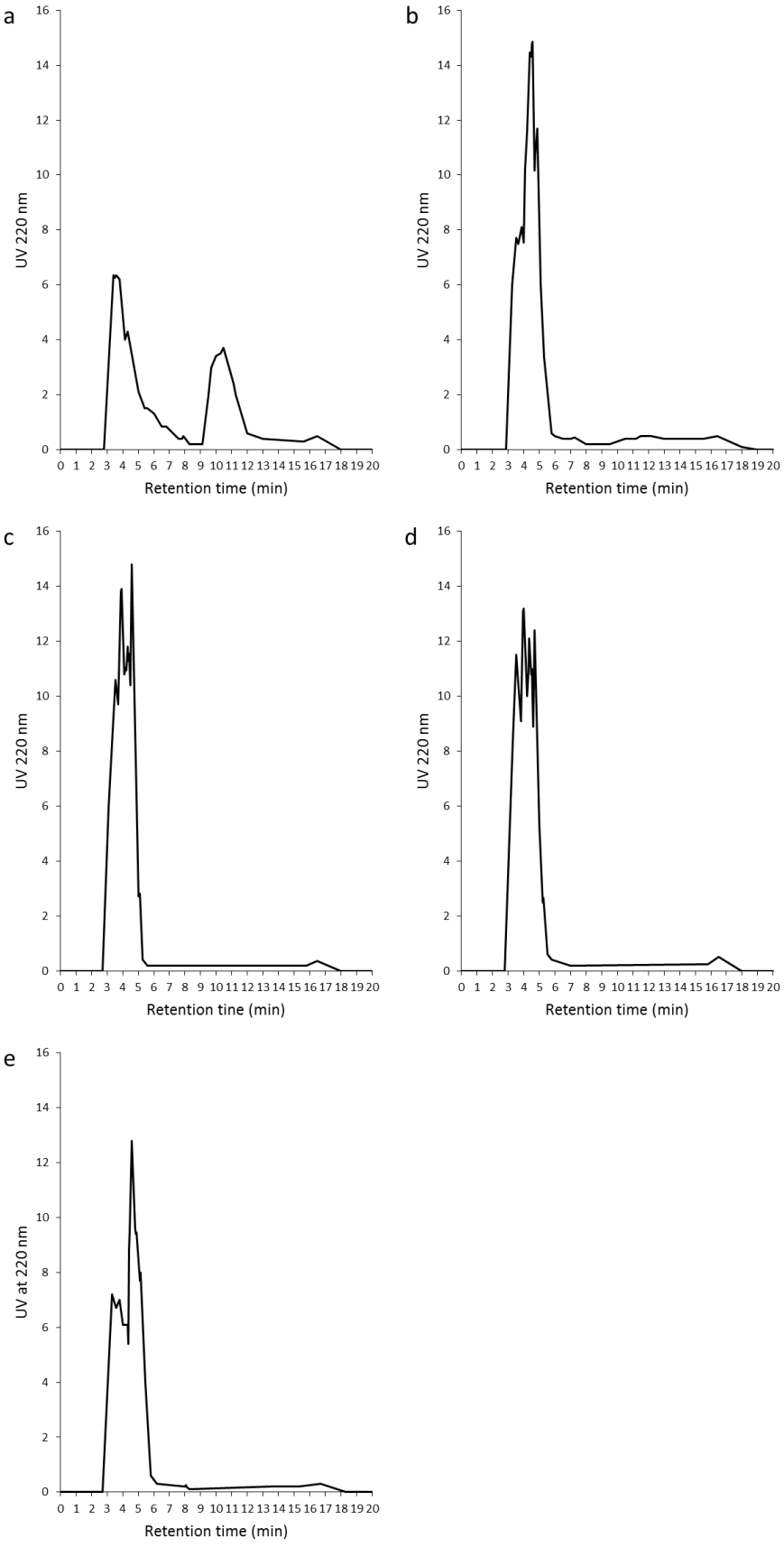

Figure 4-20 High performance liquid chromatography (HPLC) chromatograms derived from preparative HPLC of liver 160126-0700 (L2). Run 1-4 (a - d) were loaded with 50 mg/mL peptide sample (2.2 mL), run 5 (e) was loaded with 25 mg/mL peptide sample (4.4 mL)

4.3.7 HPLC analysis, and physical description of the fractions generated from prep HPLC

4.3.7.1 Physical appearance of lyophilised peptide fractions (liver)

The physical properties of the lyophilised fractions from run 1 and the collected samples from runs 2 to 5 showed some variation between the fractions. Fraction 1 for both samples appeared denser in that there was a greater mass to the pellet than the other fractions collected. The pellet was also noticeably more hygroscopic than the other fractions. The samples from fraction 2 appeared visually much less dense and paler in colour. It was noticeable that fraction 2 samples were charged which caused them to be attracted to the plastic container and made handling of this sample difficult. Fraction 4 from run 1 was extremely hygroscopic. The solid contents of this fraction quickly turned into a liquid when exposed to air. This was observable to the eye, the solid changed form a pale colour to a dark brown liquid. The volume of the sample also reduced in size considerably.

4.3.7.2 HPLC analysis of fractions

The fractions generated form the prep HPLC (section 4.3.6.2) were further analysed using an analytical C18 column specifically designed for peptides and small proteins (Ascentis® Express Peptide ES-C18). The gradients of acetonitrile, and flow rates used were scaled from the data gained from the prep HPLC.

The data shown in (**Figure 4-21**) highlight the difference between fractions F2R1 and F2R2. Fraction F2R2 had a prominent peak at 4.4 minutes, which was not present in F2R1. This peak is likely a result of the disappearance of the large peak that is present in the chromatogram for run 1, where the amplitude of the peaks that eluted between 3 and 5 minutes (**Figure 4-20 b to e**) are greater in comparison to the peaks at a similar retention time (**Figure 4-20 a**). There is also a difference in the composition of F1R1 and F1R2, though not quite so pronounced. The most obvious difference is the small peak at 4.117 minutes present in F1R2 (**Figure 4-22 b1/b2**). The larger peaks also show a difference. There appeared to be more compounds in F1R1 than F1R2. Maybe the same process that caused the disappearance of the peaks at 9.1 minutes in F1R4 is also responsible for this change.

Fraction F4R1 was analysed using the method used for the previous two (**Figure 4-23 a1/a2**), and with a method used to mimic the acetonitrile gradient profile of the prep column (**Figure 4-23 b1/b2**). This resulted in a different gradient (therefore concentration) of acetonitrile at any given time point. The chromatograms both have a very sharp peak at around 4.3 minutes. These peaks show similarities to the peak described in **Figure 4-20** (at 4.4 minutes). It cannot be determined if these are the same compound as of yet. These samples would have to be analysed with MS/MS to investigate this. What can be said about the peaks at 4.3 minutes in **Figure 4-23** is that they have similar retention times irrespective to the concentration of acetonitrile

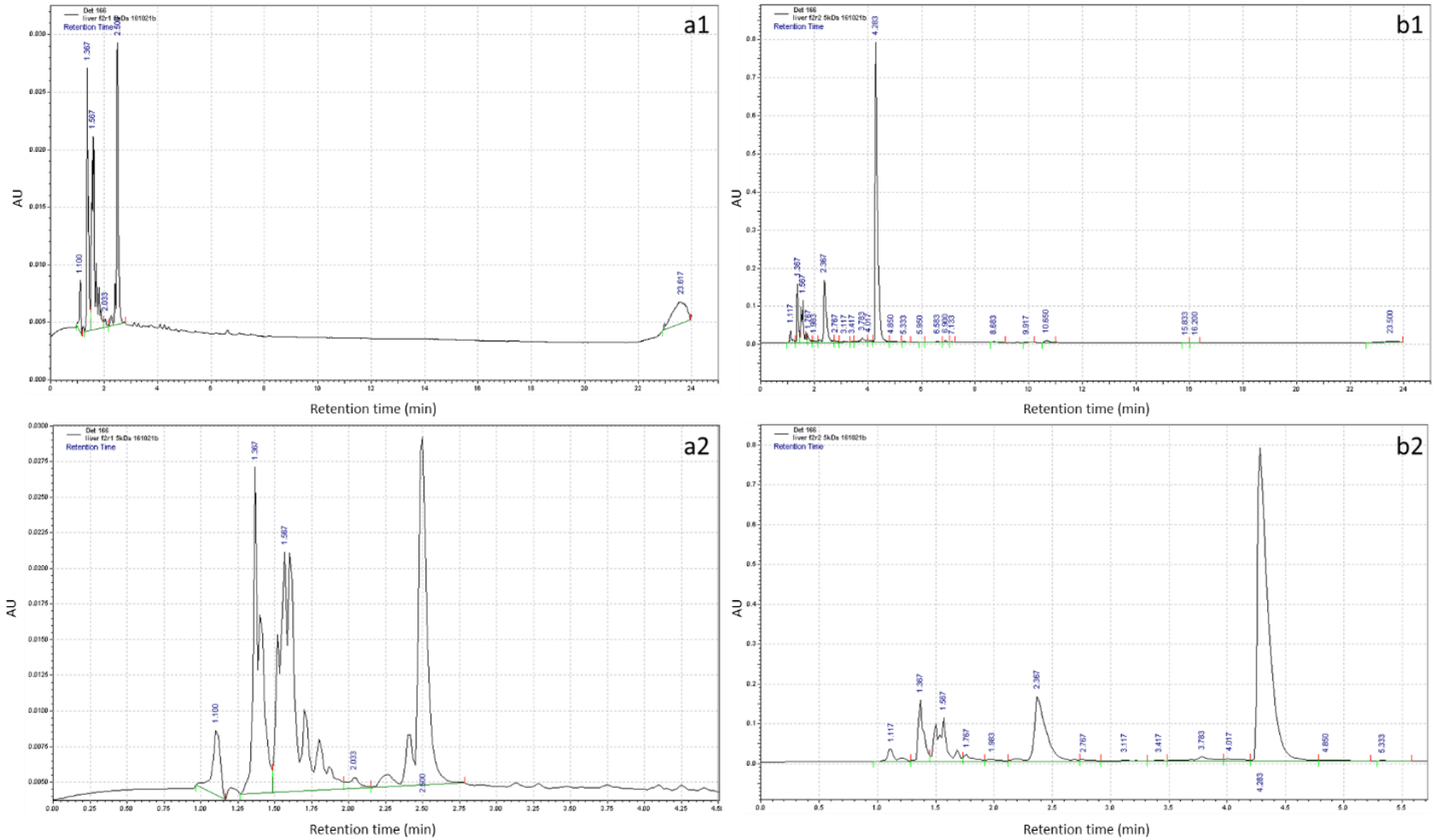

Figure 4-21 Comparison of analytical high performance liquid chromatography (HPLC) chromatograms of fractions F2R1 (a1), and F2R2 (b1) with areas of interest highlighted (F2R1 peaks indicated in a2, and F2R2 peaks indicated in b2)

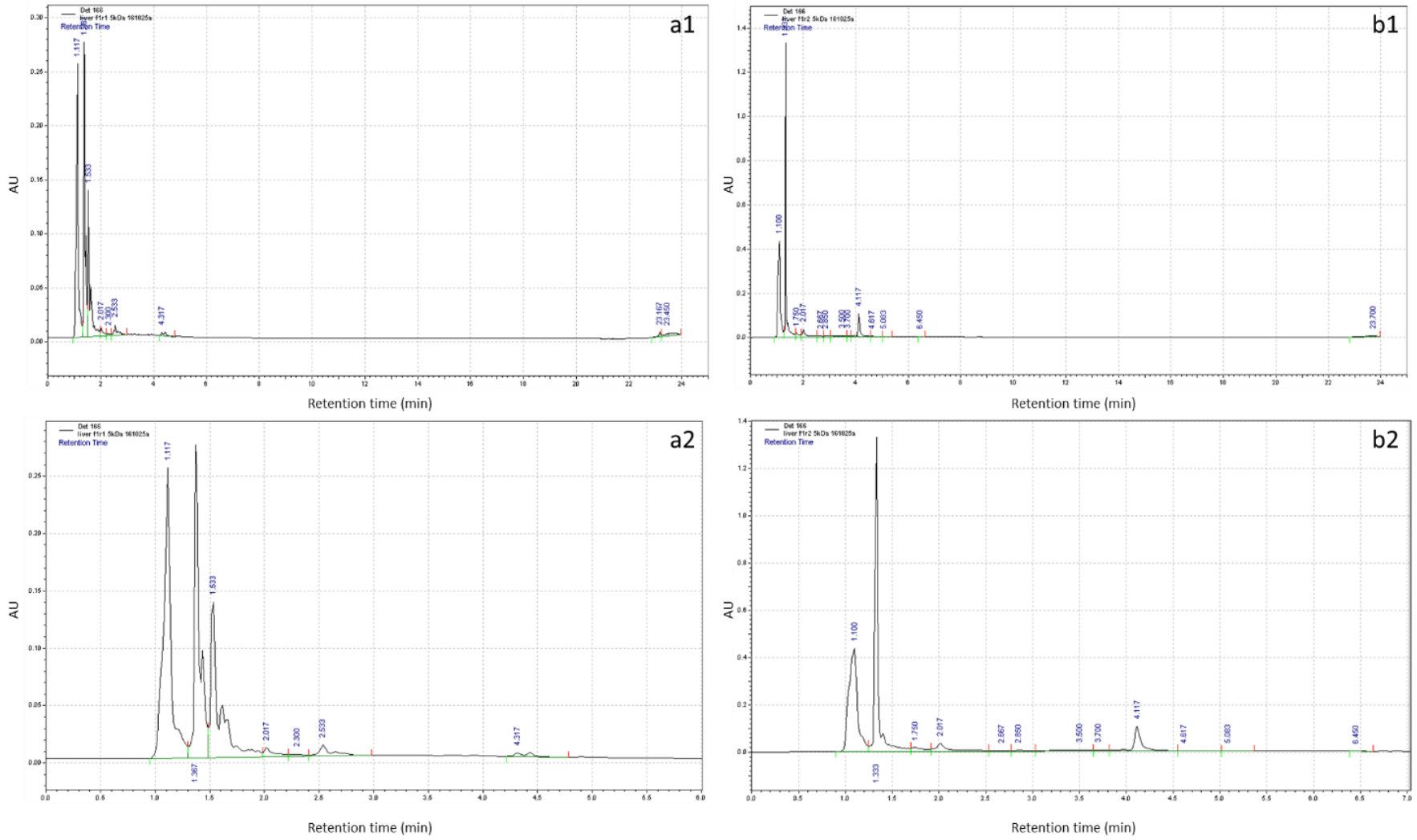

Figure 4-22 Comparison of analytical high performance liquid chromatography (HPLC) chromatograms of fractions F1R1 (a1), and F1R2 (b1) with areas of interest highlighted (F1R1 peaks indicated in a2, and F1R2 peaks indicated in b2)

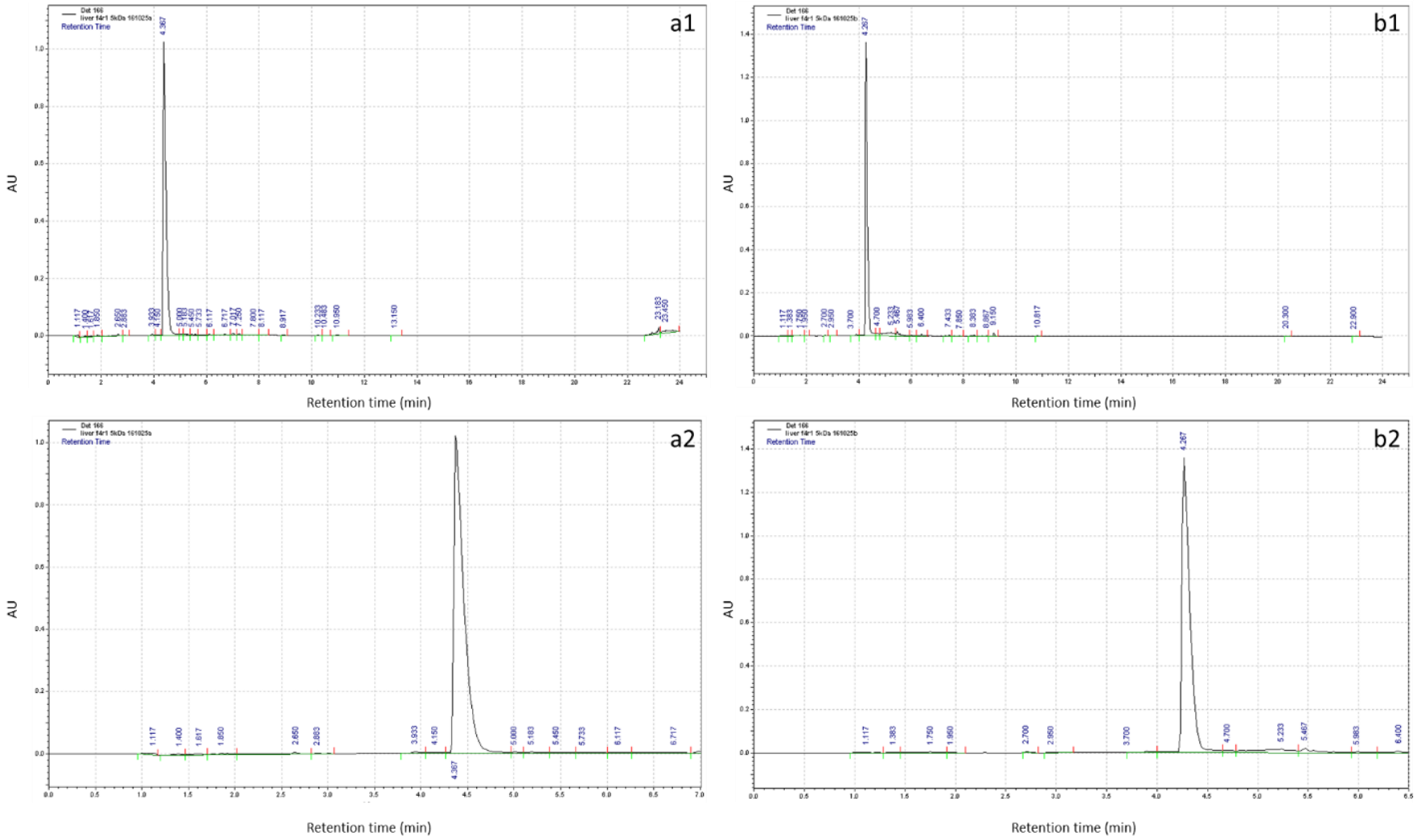

Figure 4-23 Comparison of analytical high performance liquid chromatography (HPLC) chromatograms of fractions F4R1a (a1), and F4R1b (b1) with areas of interest highlighted (F4R1a peaks indicated in a2, and F4R1b peaks indicated in b2)

4.3.7.3 MTT assay of lyophilised peptide fractions (liver)

The results for the MTT assay (**Figure 4-24 and Figure 4-25**) indicate the percentage of MTT metabolism by the cells in the presence of the different fractions, with the results for the control group used as the baseline. The data suggests that there is no significant difference between most of the fractions in regards to cell viability (P>0.05). The two results that show significant differences from the others are from fractions F1R2, and F2R2. F1R2 appears to result in a reduction in cell viability at 200 µg/mL, whereas F2R2 causes an increase (P<0.05).

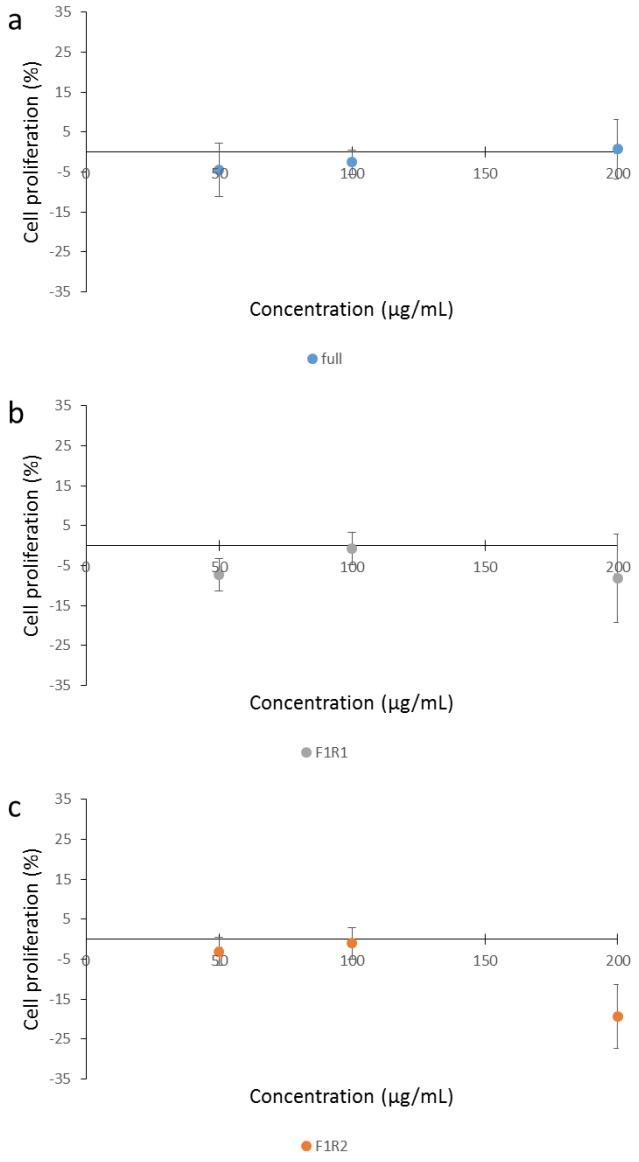

Figure 4-24 Cell proliferation data derived from (3-(4,5-Dimethylthiazol-2-yl)-2,5-Diphenyltetrazolium Bromide) (MTT) assay for the fractions collected from prep high performance liquid chromatography (HPLC): Liver hydrolysate (L2) (a), F1R1 (b), and F1R2 (c) (fractions described in section 4.3.6.2).

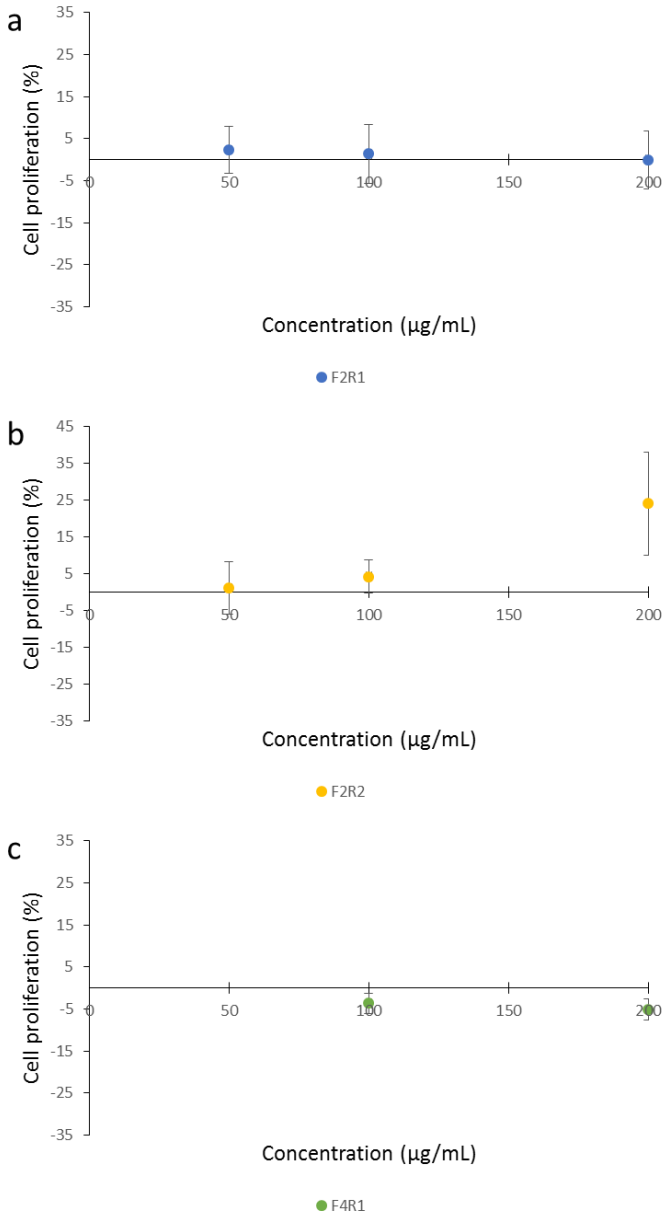

Figure 4-25Cell proliferation data derived from (3-(4,5-Dimethylthiazol-2-yl)-2,5-Diphenyltetrazolium Bromide) (MTT) assay for the fractions collected from prep high performance liquid chromatography (HPLC): F2R1 (a), F2R2 (b), and F4R1 (c)

4.3.7.4 Scratch Assay of lyophilised peptide fractions (liver)

The results of the scratch assay (**Figure 4-26 and Figure 4-27**) indicated that there was no significant difference in chemotaxis between the fractions. The full hydrolysate did show the greater closure overall however. When the rates of closure for the samples were analysed (**Figure 4-28**) it was found that there was no significant difference between the samples.

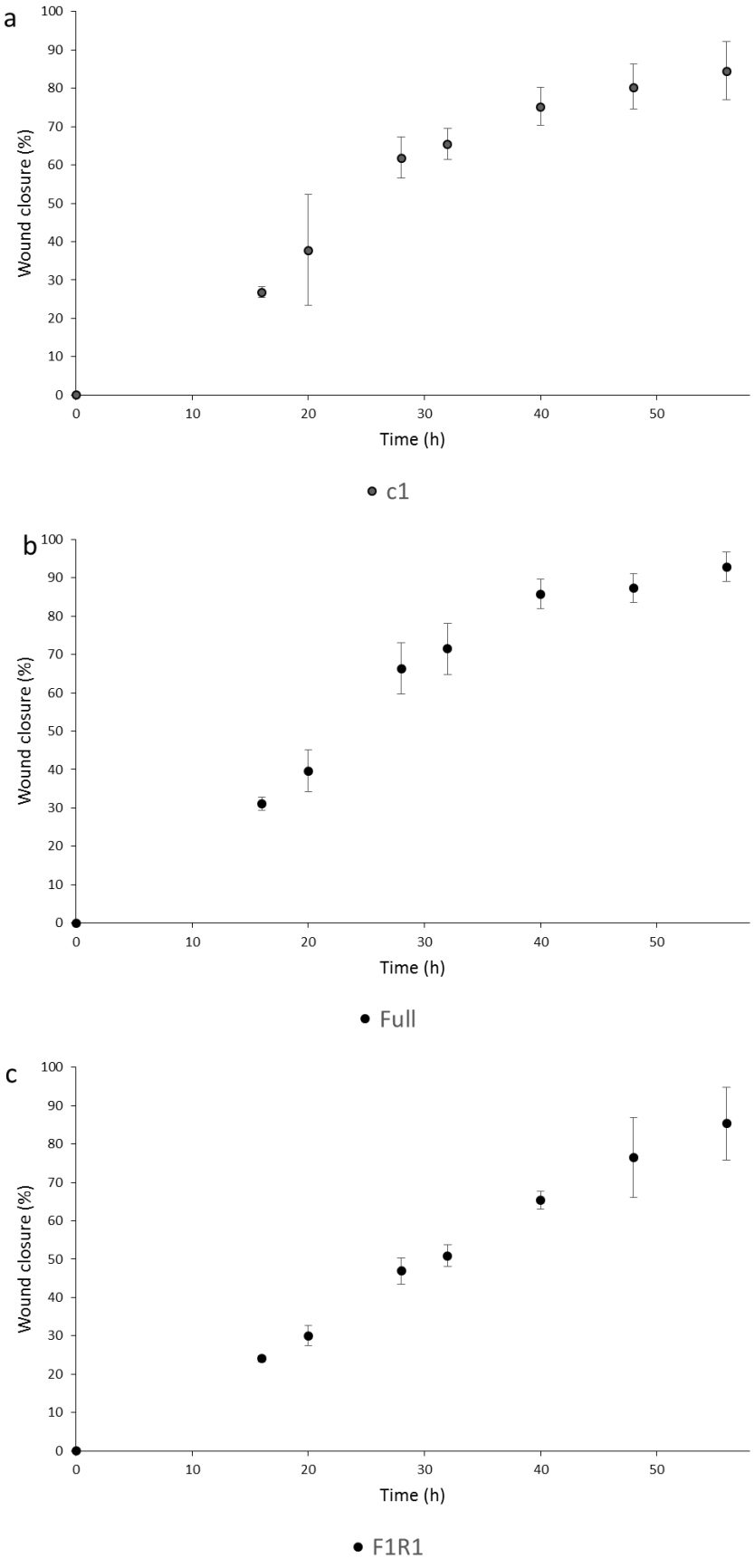

Figure 4-26 Percentage wound closure for each sample over time showing the error bars for no peptide (c1) (a), full hydrolysate (b), and F1R1 (c)

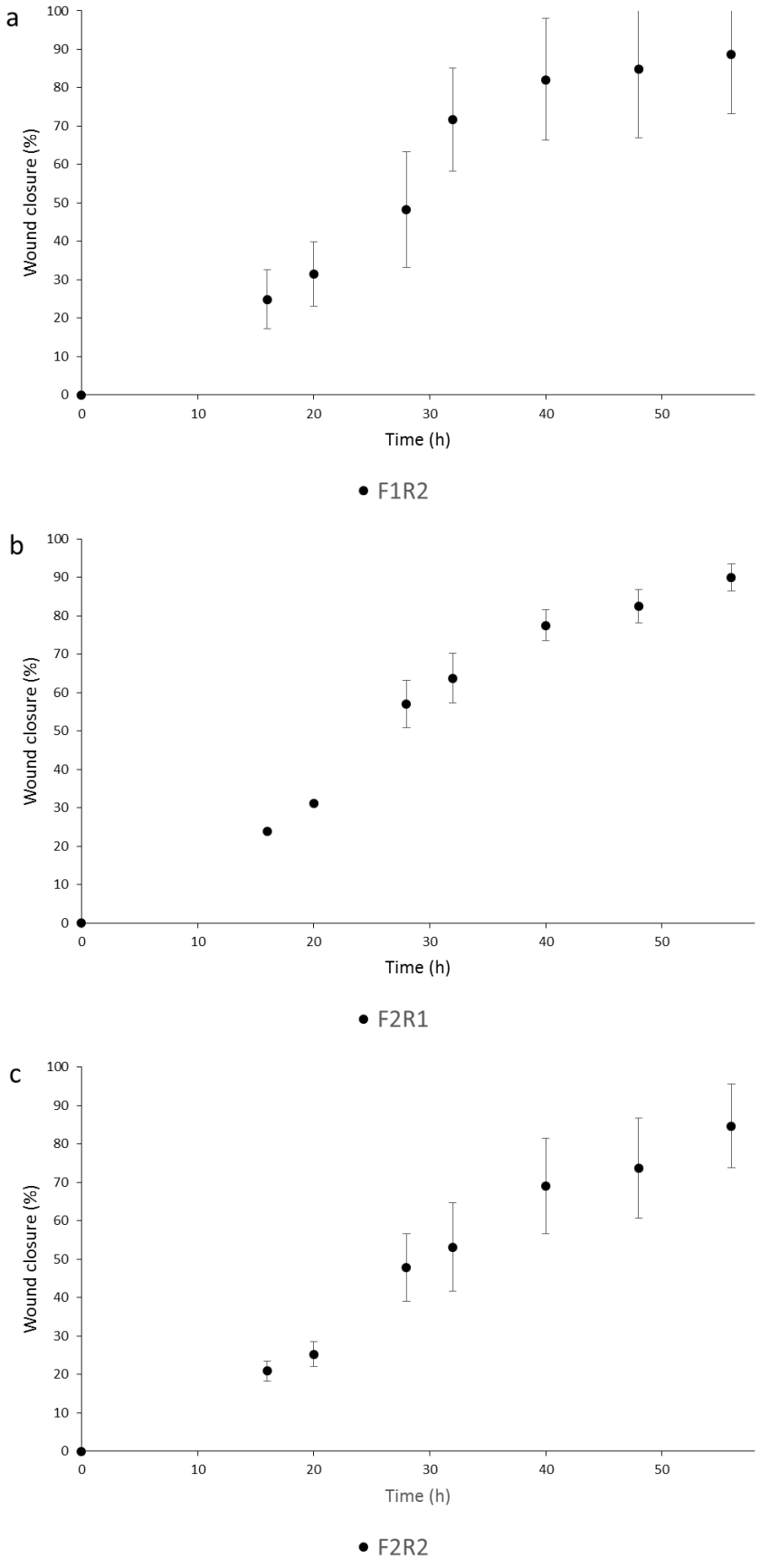

Figure 4-27 Percentage wound closure for each sample over time showing error bars for F1R2 (a), F2R1 (b), and F2R2 (c)

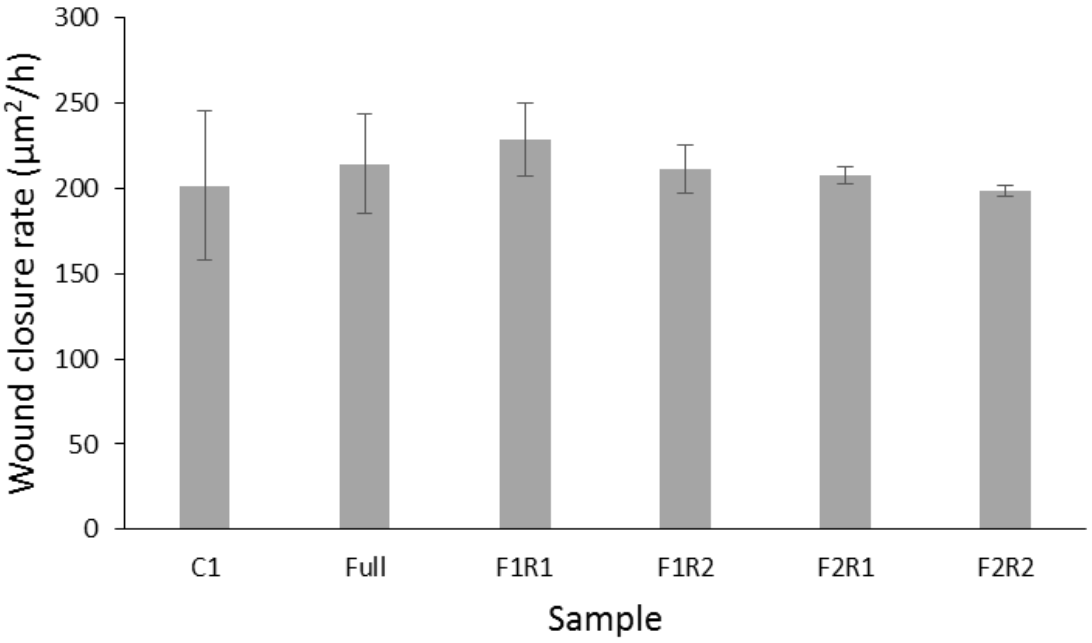

Figure 4-28 Rate (µm2/h) of wound closure for negative control (C1), liver hydrolysate (L2) (Full), and the fractions generated from preparative high performance liquid chromatography (prep HPLC) (F1R1, F1R2, F2R1, and F2R2).

4.3.7.5 DPPH Radical Scavenging Assay of lyophilised peptide fractions (liver)

For the samples prepared at 0.8 mg/mL the fraction with the greatest RSA was F2R2. A Tukey test (HDS = 5.71) indicated that F2R2 was significantly different to F1R1, F1R2, and F2R1, but not the full hydrolysate, and that the full hydrolysate was also significantly different to F1R1, and F1R2. For the samples prepared at 0.4 mg/mL, the fraction with the greatest RSA was F2R2. A Tukey test (HSD = 5.99) indicated that F2R2 was significantly different to all other samples in the group. For both the 0.8 and 0.4 mg/mL concentrations, the full hydrolysate showed the second greatest RSA. The fraction with the greatest RSA for the samples prepared at 0.2 mg/mL was the full hydrolysate, with F2R2 being second (no significant difference) (Tukey test HDS = 3.99). F1R2 showed a significant difference to the full hydrolysate but not F2R2. F1R1, and F2R1 both a significantly lower RSA than the other samples; there was no significant difference between these two samples. The RSA data for the lyophilised fractions showed a concentration dependence (**Figure 4-29)**.

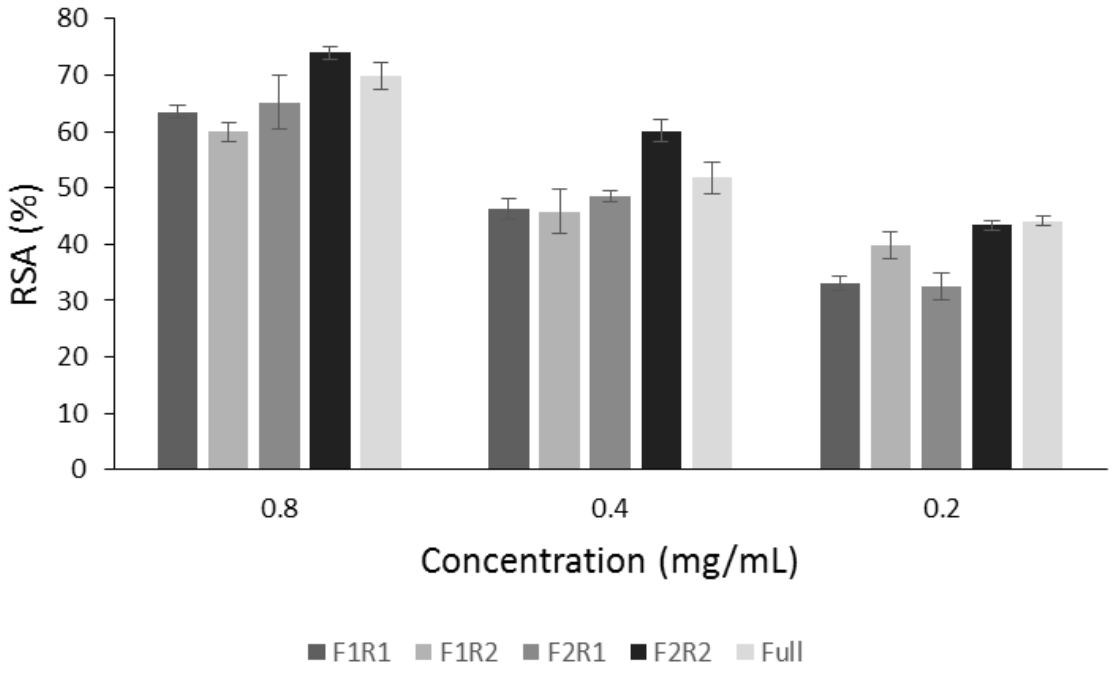

Figure 4-29 Radical Scavenging activity (RSA) of lyophilised liver peptide fractions measured by the 1, 1-diphenyl-2-picrylhydrazyl (α,α-diphenyl-β-picrylhydrazyl (DPPH) assay

4.3.8 Stability studies of full hydrolysates

The data for the stability studies are presented in **Figure 4-30 to Figure 4-33**. The MTT data is represented as cell proliferation with 0% being the control group. The data from the stability studies indicate that hydrolysates are stable in solution over the period of time that the study was performed. This can be seen in the chromatograms in **Figure 4-31, and Figure 4-33**, and the cell proliferation graphs in **Figure 4-30, and Figure 4-32**.

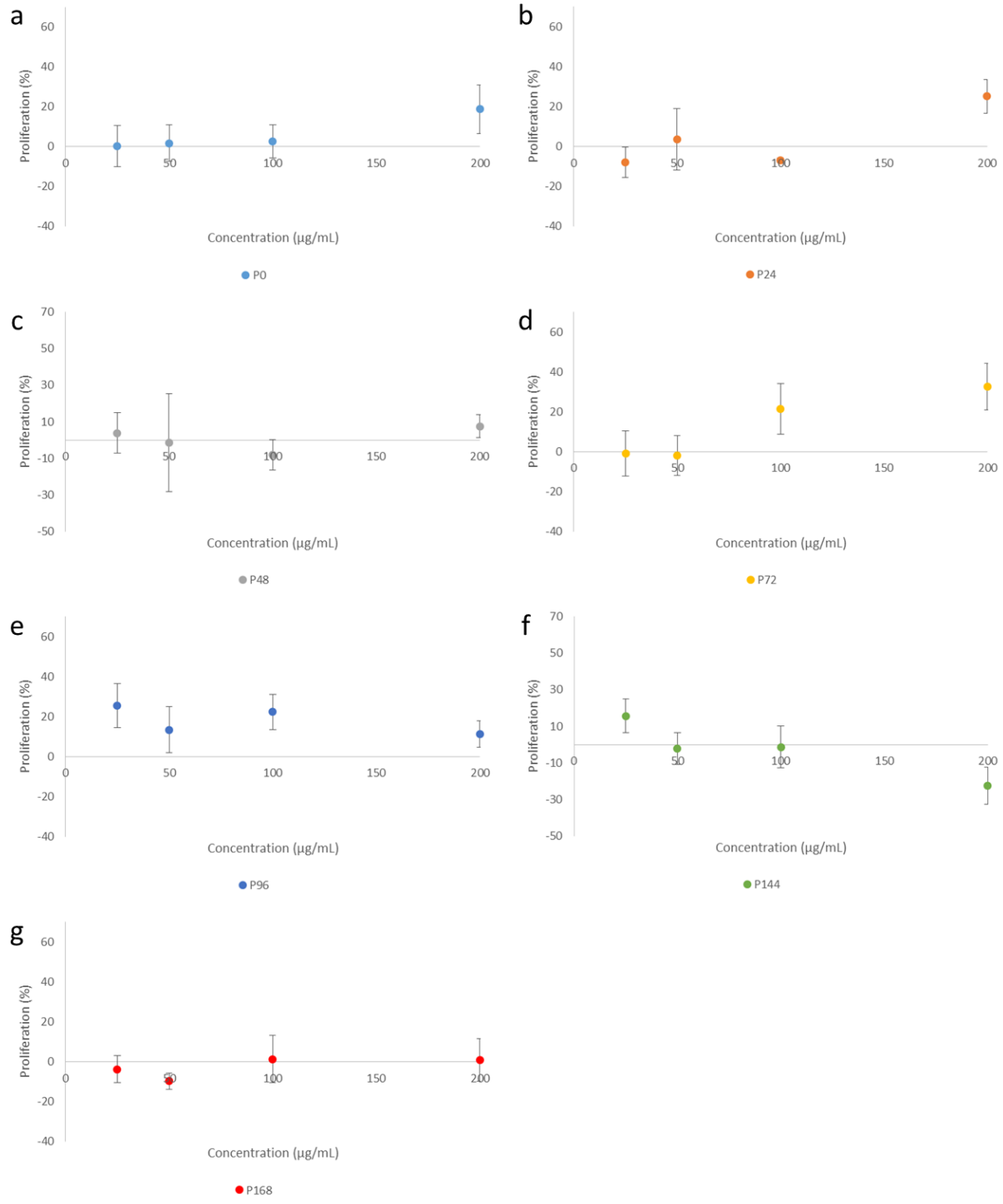

Figure 4-30 Cell proliferation data derived from 1, 1-diphenyl-2-picrylhydrazyl (α,α-diphenyl-β-picrylhydrazyl (MTT) assay: placenta 0-160330-1500 (P2) 0h after preparation (a), placenta 0-160330-1500 (P2) 24h after preparation (b), placenta 0-160330-1500 (P2) 48h after preparation (c), placenta 0-160330-1500 (P2)72h after preparation (d), placenta 0-160330-1500 (P2) 96h after preparation, placenta 0-160330-1500 (P2) 144h after preparation, and placenta 0-160330-1500 (P2) 168 h after preparation.

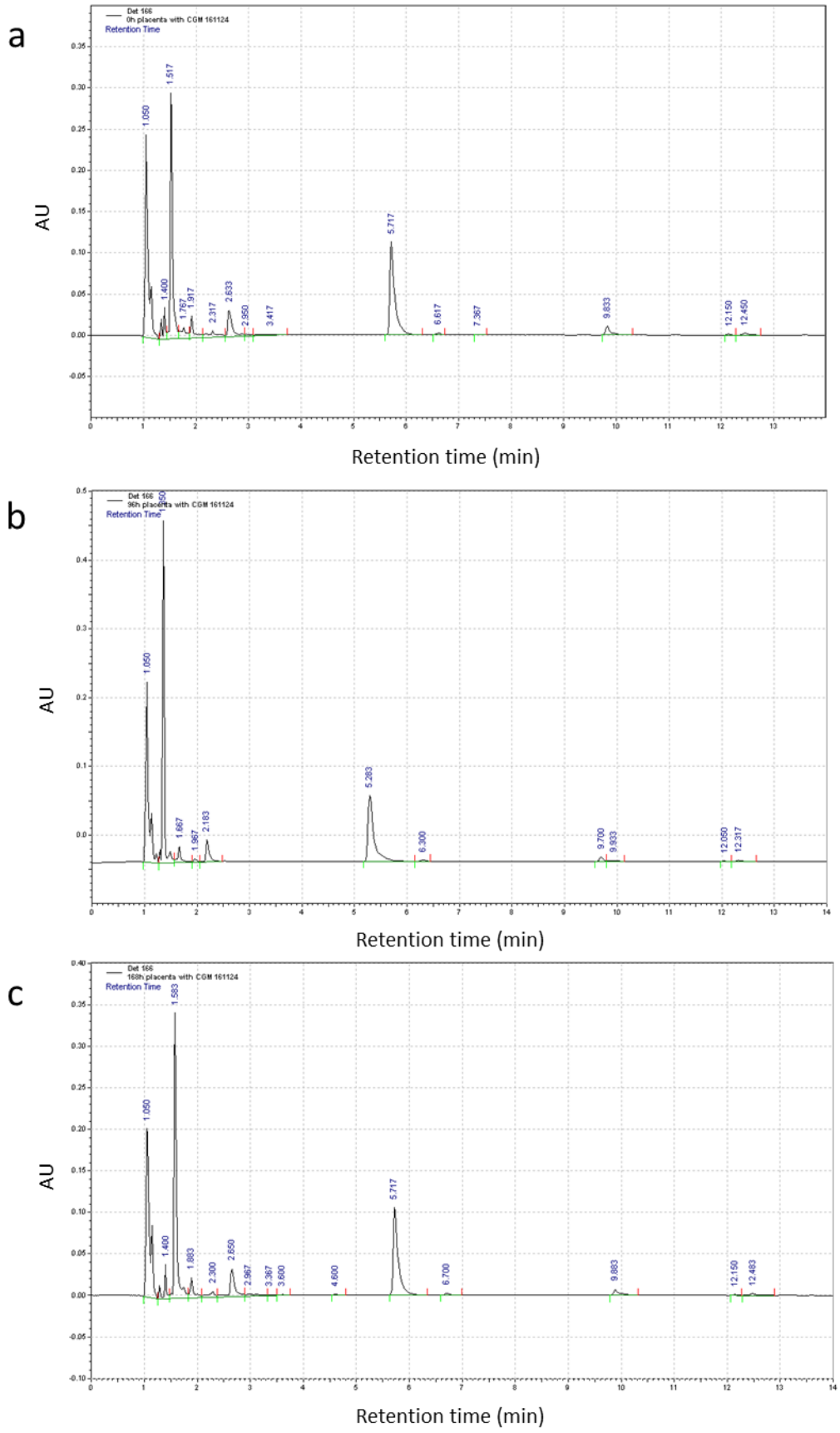

Figure 4-31 High performance liquid chromatography (HPLC) data obtained using an Ascentis® Express Peptide ES-C18, 2.7 Micron HPLC Column, showing data for placenta 0-160330-1500 (P2) in supplemented Dulbecco's Modified Eagle Medium (DMEM) 0h after preparation (a), 96h after preparation (b), and 168h after preparation (c)

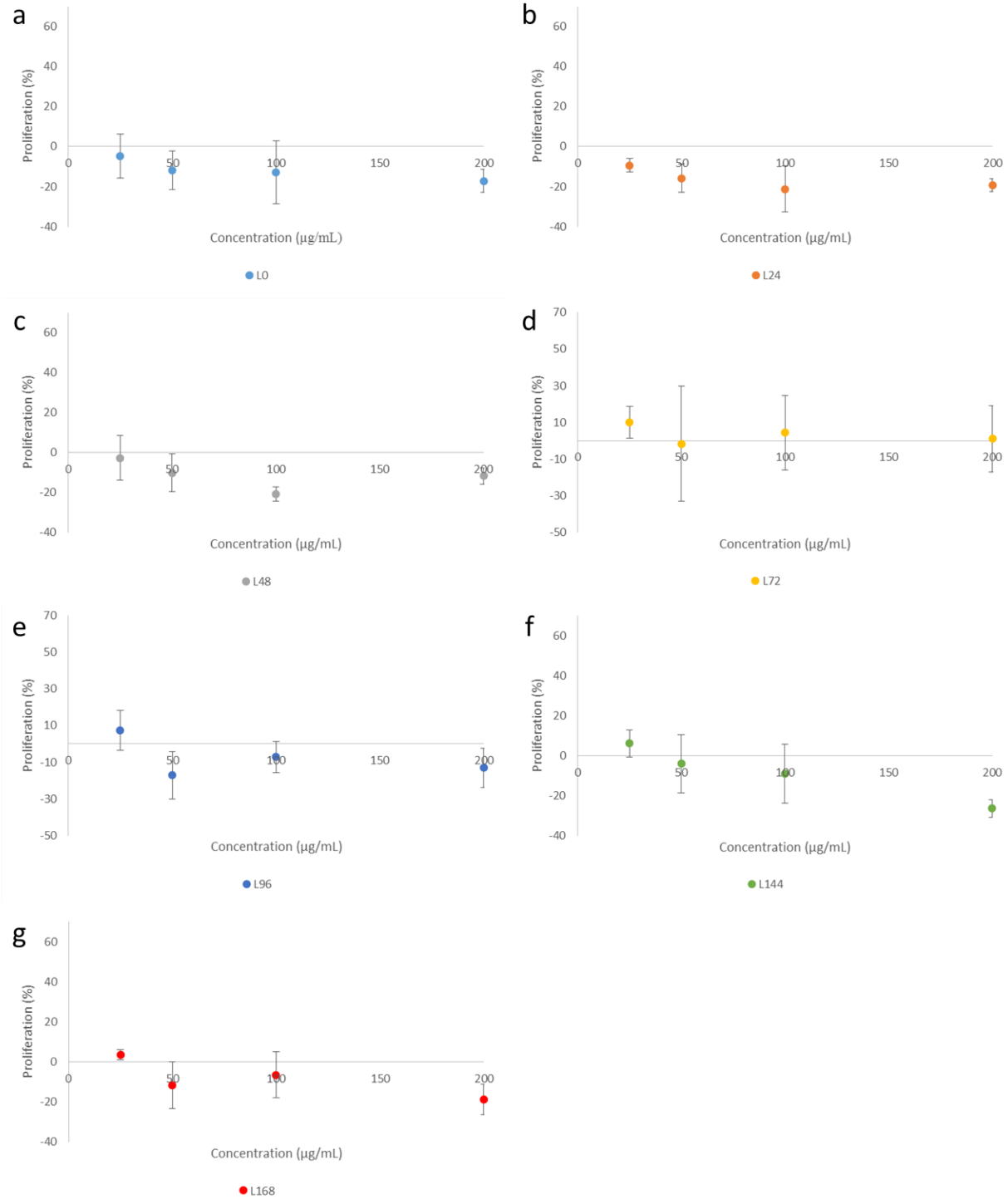

Figure 4-32 Cell proliferation data derived from 1, 1-diphenyl-2-picrylhydrazyl (α,α-diphenyl-β-picrylhydrazyl (MTT) assay: liver 160126-0700 (L2)0h after preparation (a), liver 160126-0700 (L2) 24h after preparation (b), liver 160126-0700 (L2) 48h after preparation (c), liver 160126-0700 (L2) 72h after preparation (d), liver 160126-0700 (L2) 96h after preparation, liver 160126-0700 (L2) 144h after preparation, and liver 160126-0700 (L2) 168 h after preparation.

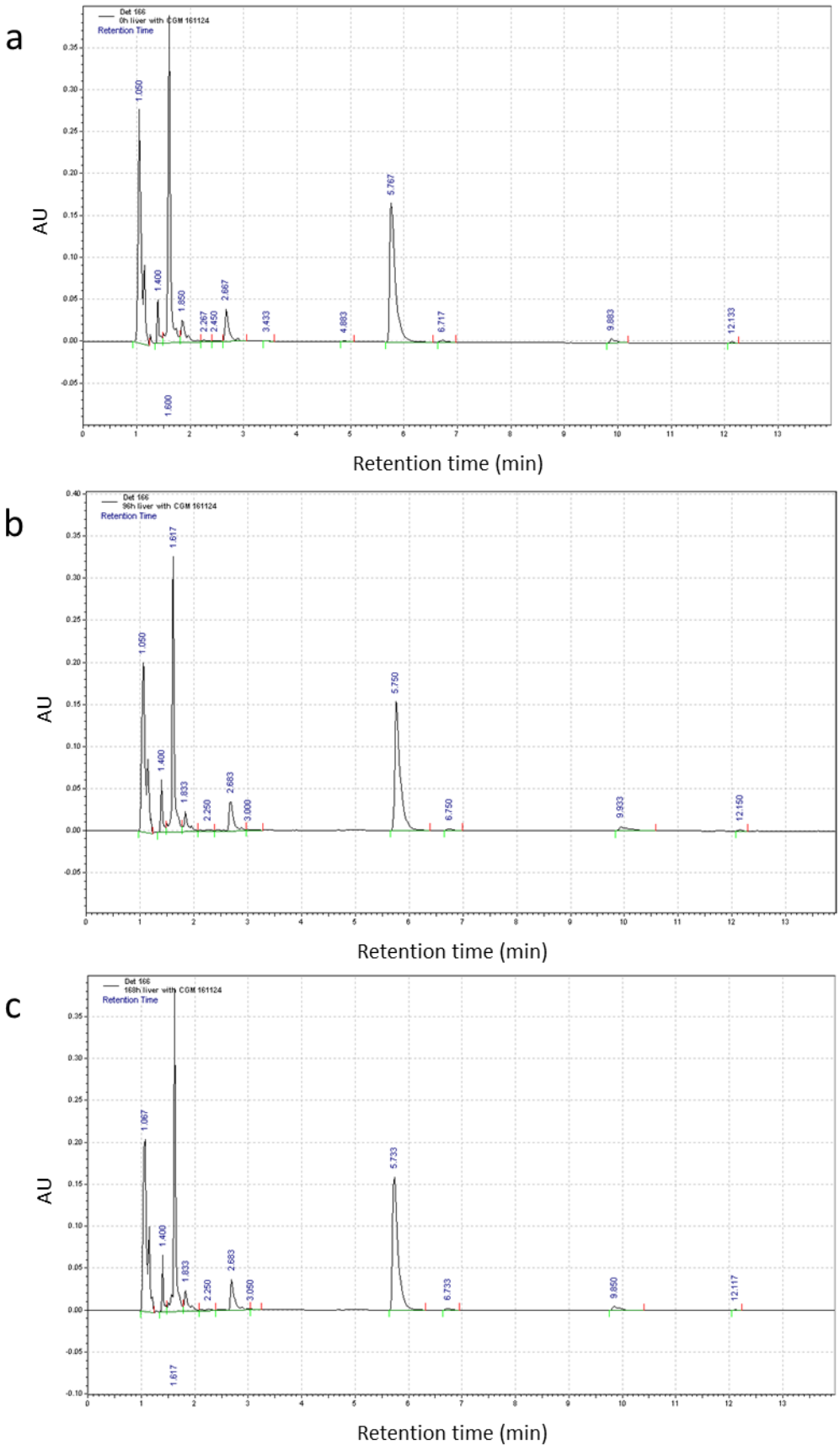

Figure 4-33 High performance liquid chromatography (HPLC) data obtained using an Ascentis® Express Peptide ES-C18, 2.7 Micron HPLC Column, showing data for liver 160126-0700 (L2) in supplemented Dulbecco's Modified Eagle Medium (DMEM) 0h after preparation (a), 96h after preparation (b), and 168h after preparation (c)

4.3.9 ACE inhibition assay

Three hydrolysates (Placenta (P2), Liver (L2), and Liver (L3)) were tested for anti-ACE activity. All the hydrolysate showed ACE inhibitory activity. P2 demonstrated the greatest activity with significantly more inhibition than either of the liver samples ($p<0.05$). There was no significant difference between the liver samples L2, and L3 (Error! Reference source not found.**)**. All peptides t ested showed significantly less ACE inhibition activity than captopril (0.02 µg/mL of captopril showed a percentage reduction of ACE activity of 98.7%; data not shown).

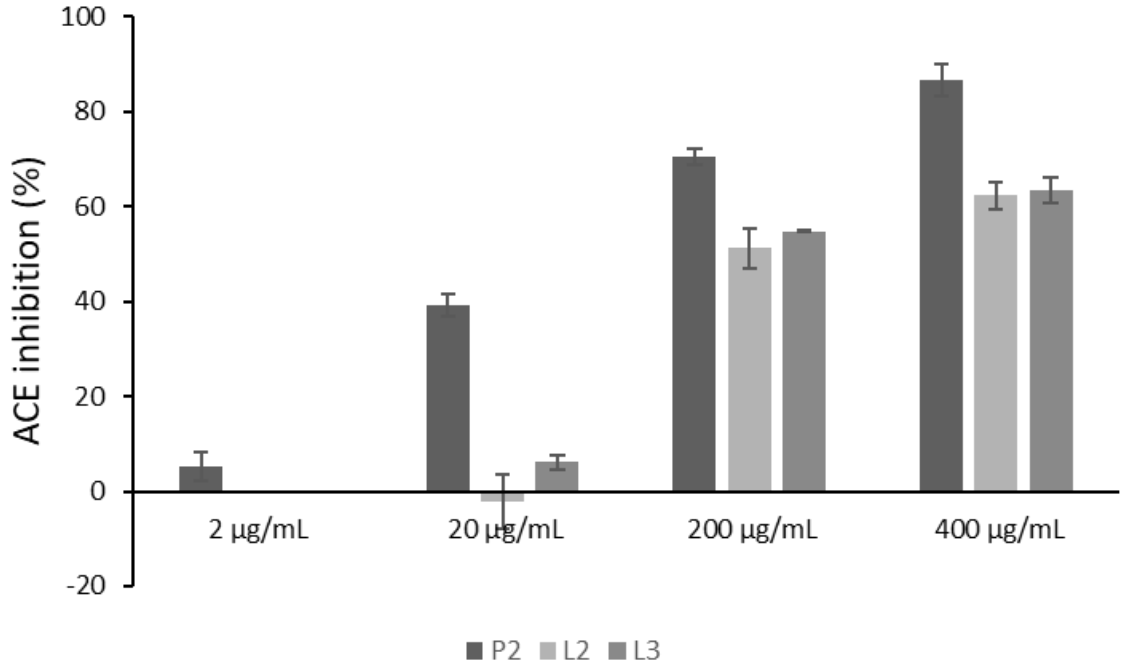

Figure 4-34: Percentage inhibition of angiotensin II converting enzyme (ACE) by the hydrolysates placenta 0-160330-1500 (P2), liver 160126-0700 (L2), and liver 170127-0815 (L3)

4.4 Discussion

4.4.1 Antioxidant activities of the whole hydrolysates

The investigation into the possible bioactivity of the hydrolysates began with researching their antioxidant activity in relation to four different antioxidant assays. The antioxidant assays were chosen because they each concentrate on a different mechanism of action. Testing the samples using different types of assays is important to gain a more complete picture of antioxidant activity exhibited by the hydrolysates.

The DPPH assay works by the protonation of the stable radical DPPH·, into DPPH therefore the greater the proportion of proton donors present in a sample being analysed, the greater the radical scavenging activity. The Biofac hydrolysates are composed of a mixture of peptides, which are themselves composed of various examples of amino acids with charged side chains. Amino acids with charged side chains can be either proton donors or proton acceptors. The proton donating amino acids are glutamic acid and aspartic acid; the proton accepting amino acids are arginine, lysine, and histidine. Histidine is not charged at values above pH 6, therefore under the assay conditions (pH 7.2) histidine is neutral, and has no bearing on the RSA of the hydrolysates. The pK_a values for the charged amino acids (not histidine) are Aspartic acid 3.9, glutamic acid 4.2, lysine 10.5, and arginine 12.5. This value will affect the radical scavenging activities of the peptides at pH values lower than 4.2 and at values greater than pH 10.5, only positively charged side chains will be available. This would likely lead to no radical scavenging activity for this particular assay. This limits the pH range in which this assay is useful. The proportion of charged amino acids in the hydrolysates (

Table 4-5) can be used to explain the RSA performance of each hydrolysate. The RSA results as a whole demonstrated that the liver hydrolysates exhibited the greatest antioxidant activity, followed by heart, with the placenta hydrolysates exhibiting the least activity.

Table 4-5 Percentage of net proton donors present in the Biofac hydrolysates

	Net Proton Donors (%)					
	H1	L1	L2	L3	P1	P2
With His	8.2	11	10.8	10.3	5.7	5.7
Without His	10.3	13.8	13.4	13	6.8	6.8

The net proton donating groups found in the liver hydrolysates (L1, L2, and L3) are comparable, with each other (L1 10.8, L2 10.8, L3 10.3) and the placenta hydrolysates (P1, and P2) both exhibit 5.7 % (for full amino acid composition data see appendix I). The net proton donor groups in the liver hydrolysates are 49.3 - 52.3% greater than both placenta hydrolysates and 20.8 - 25.4 % greater than H1. The distribution of the charged amino acids that make up the hydrolysates can be related to their relative RSA. This explains most of the results, however there is a large difference in the RSA of the two placenta hydrolysates (P1, and P2) with P1 exhibiting the lowest RSA of all the tested hydrolysates (over 100 fold lower than L1). P2 exhibits a RSA that is approximately 2 fold lower than L2 (which is similar to the difference in the proportion of net proton donors). This large difference cannot be just based on the relative proportion of charged side chains because the proportion of net proton donors present in P1 and P2 is the same. There must be another property of P1 that causes it to perform much worse than the other hydrolysates, including P2. The production method to generate P2 utilises a step to remove components of the hydrolysates that are > 5 kDa in molecular weight. It is suggested in this study (see chapter 5), and in the literature that small peptides (especially dipeptides) are likely to exhibit bioactivity, including antioxidant activity. It was also noted that the placenta hydrolysates had in general a greater proportion of small peptides than those of the liver. Therefore, the molecular cut-off of the P2 hydrolysate relative to P1 would increase the proportion of smaller peptides, and therefore increase the antioxidant activity.

The ORAC assay was selected as a means to determine the oxygen radical absorbing activities of the hydrolysates because it is a relatively simple assay that is widely used in related literature. The ORAC assay uses the water-soluble azo compound AAPH as the source of reactive oxygen species, and sodium fluorescein as the fluorescent probe. The ability of experimental samples to protect the fluorescent

probe (or absorption of oxygen radicals) is directly measured by comparing the fluorescence of a control with no sample with that of the experimental sample. AAPH is a commonly used in antioxidant assays as a free radical generator because it will decompose into molecular nitrogen, and two carbon radicals through thermal decomposition, with the majority of the carbon radicals then reacting with oxygen, resulting in the production of peroxyl radicals (Niki, 1990).

The general trend of the data from the ORAC assays performed on all of the hydrolysate samples follow that of the DPPH assay, in that the liver hydrolysates (L1, L2, and L3) show slightly more activity than the low molecular weight placenta hydrolysate (P2), with the original placenta hydrolysate (P1) being significantly less antioxidant than all the other samples. The significant lack of activity demonstrated by P1 in comparison to the other hydrolysates in relation to the DPPH, and the ORAC assay are likely to be related. The pattern of antioxidant activities exhibited by the liver hydrolysates in the ORAC assay follow that of the DPPH assay, where L1 had the greatest activity, followed by L2, and then L3. The proportion of proton donating groups in the hydrolysates may interact with the carbon radicals produced from the decomposition of AAPH, this in turn would inhibit the production of peroxy radicals. The hydrolysates may also interact with the peroxy radicals directly to reduce the oxidation of the fluorescent probe.

The data generated for lipid peroxidation reduction showed that all the samples significantly reduced autoxidation in the linoleic acid system. There was no significant difference between the hydrolysates used in this assay (L1, H1, and P1). The reduction in lipid peroxidation is interesting because the same mechanism of oxidative stress demonstrated with this model could be related to the oxidative damage caused to cell membranes. Lipid peroxidation occurs when oxidants attack lipids, which contain carbon double bonds. The presence of carbon double bonds found in phospholipids that make up the cell membrane, means that lipid peroxidation is biologically relevant (Ayala, 2014). In the lipid peroxidation assay performed for this study, linoleic acid was used as a model for lipids found in cell membranes. This assay was only performed on L1, H1, and P1 because it was decided that developing a cell-based assay would be more biologically relevant, and give an indication of how these samples

affect the whole cell instead of just one mechanism, and that the L2, L3, and P2 batches were received from Biofac after this decision was made. However, the results of this assay were interesting because they did not follow the trend demonstrated by the DPPH, and the ORAC assays. This is because the mechanism of autoxidation of lipids, which drives this assay, is not relevant to the DPPH and ORAC assays.

The hydrolysates analysed using the lipid peroxidation assay (L1, H1, and P1) all exhibited relatively good antioxidant activity, whereas when L1, and P1 were analysed using the DPPH, and ORAC assay L1 demonstrated greater activity. This is likely because the mechanisms of the assays are different and therefore relate to different mechanisms of antioxidant activity. The ability of P1 to reduce lipid peroxidation in the linoleic acid system is unrelated to its lack of activity for the DPPH, and the ORAC assay. Because P2 shows a relatively large increase in activity over P1 in the DPPH, and ORAC assays, it was decided to discontinue the analysis of P1 in further studies.

The hydrolysates assayed using the CAA assay were samples L2, and P2. The antioxidant activity was significantly less than the Trolox control used for this assay, but there was some activity. The mechanism of this assay is the conversion of DCFH to DCF through oxidation by the initial oxidation by AAPH. DCFH is formed by the cleavage of DCFH-DA by cellular enzymes and because DCFH cannot pass through the membrane and out of the cell, any production of DCF will be intracellular. This would suggest that some of the peptides present in the hydrolysates are either entering the cell, where they can counter the oxidative action of AAPH, or interacting with the membrane thus preventing some of the oxidation of the membrane lipids by AAPH. Any reactive oxygen species that are produce through normal cell metabolism can be discounted because the activity is calculated from the negative control.

What these data do indicate is that the assay is a useful one in relation to bioactivity. Whereas the non-cell based assays also showed robust data, they utilised pathways that are not necessarily biologically relevant. This assay also indicates the bioavailability of the samples being tested. Compounds may

demonstrate good antioxidant properties, but if they cannot get to the target site of action, then this activity may not be useful (Sánchez-Rivera et al., 2014). The samples L2, and P2 do therefore contain elements that have antioxidant properties that are biologically available. Bearing in mind that the crude hydrolysates may contain potent antioxidant peptides, just in low concentration, a pure sample of one of a synthesised peptide derived from the hydrolysates could show high activity.

In general, the hydrolysates assayed all showed antioxidant activity, over a number of assays, which are based on different mechanisms. These different methods demonstrated that an example of a high activity in one assay does not indicate that a similar result will be seen in another assay. P1 prevented the autoxidation of linoleic acid as well as L1, and H1, but it was significantly less active in the DPPH, and ORAC assays. This reinforces the need to use multiple antioxidant assays when assessing antioxidant activity.

4.4.2 Cell proliferation and wound healing

Potential wound healing properties of the hydrolysates were initially investigated using two methods; a cell counting method that compared the DT, and the PDL, and the MTT assay where absorbance values related to the metabolism of MTT were used to quantify cell number. 3T3 fibroblasts were selected as the cell model due to the important role fibroblasts play in the wound healing process. 3T3 cells are frequently used in wound healing models because they undergo chemotaxis when a simulated wound is created in a cell monolayer. As well as exhibiting chemotaxis, they also deposit collagen, which is important in the wound healing process (Fronza et al., 2009, Lipton et al., 1971, Peterkofsky, 1972). Fibroblasts migrate to the area of a wound between 16 and 24 hours post damage, and express COL1A1. Over the next 6 days the expression of this gene, and subsequent production of type I collagen increases, this contributes to the formation of granulation tissue at the wound site (Scharffetter, 1989). The use of 3T3 cells for the cell proliferation assays centred on whether the addition of hydrolysate samples would increase, decrease, or have no effect on the proliferation of cells.

The results for the proliferation assays performed on the hydrolysates (L1, and P1) varied greatly between the two different methods. The cell counting method showed very little difference in the proliferation of cells, whereas the MTT assay showed that in high concentrations, the peptides caused cell proliferation to be drastically reduced. However, at lower concentrations, both peptides significantly increased proliferation. The initial hypothesis for this event suggested that this could have be caused by the decomposition of longer peptide chains, releasing smaller active peptides. The idea that decomposition was responsible arose because the same hydrolysate preparations were used for both assays, however, there was a week between the assays (with the week old preparations used in the MTT assay, and the fresh preparations used in the cell counting method). This hypothesis is supported in the literature, where there are multiple references to active sequences bound within longer chains (Ahmed et al., 2015, Corrêa et al., 2014). This lead onto work investigating the stability of the peptides, within the hydrolysates (discussed later in chapter 5), which indicated that the peptides were in fact stable over a longer period than seven days. The data collected from analysis of the hydrolysates from later batches would indicate that the apparent change in bioactivity was either related to a lack of stability within the peptides contained within L1, and P1, or that there was some other element present within the samples that had an effect on the cell proliferation.

Further investigation into the original hydrolysates (L1, and P1) was not carried out as priority was given to the newer batches L2 and P2, which had added filtration step during production to remove particles with molecular weights (MW) greater than 5 kDa. Whilst the investigation into the first batch was progressed further, it did provide important data, which influenced the direction of the research. The apparent break down of the peptides to release shorter bioactive sequences was the basis for the *in silico* work described in chapter 5.

4.4.3 HPLC analysis of hydrolysates and fractionation of liver hydrolysate L2

The method of producing the hydrolysates uses the cysteine enzyme papain to hydrolyse the raw material. The fact that papain is a relatively unspecific enzyme (see chapter 1) with regards to where it hydrolyses peptide bonds means that it is likely that there will be multiple peptides of different

sequences and length. This will result in a complex mixture of peptides, and amino acids that constitutes the hydrolysates. This complex nature is a problem when it comes to analysing the hydrolysates for bioactive properties as it is possible to identify if the samples show activity but it is difficult identify particular peptides responsible. To analyse the activity in the hydrolysates further, two methods were used. The first method used analytical reverse phase HPLC to separate the peptides in the samples to the greatest resolution possible, before the using the method developed to scale up the fractionation by prep HPLC. The fractions were then collected and freeze-dried prior to use in bioactivity assays. The only hydrolysate sample to be analysed using this method was L2. The second method concentrated on the identification of peptides in the hydrolysates using *de novo* sequencing and *in silico* analysis (described in chapter 5).

The initial analytical HPLC analysis of the hydrolysates L2, and P2 (**Figure 4-18**, and **Figure 4-19**) indicated that the hypothesis that the samples were made up of a complex mixture of peptides was correct. The majority of peptides eluted from the column in the first 4 minutes. The column used to analyse the samples was C-18 reverse phase, this means that compounds are separated through hydrophobic interactions, and size of the molecule. It can therefore be said that the majority of the peptides eluting from the column, for both L2, and P2 were small, though there are a greater number of peaks in the P2 sample in the fraction eluted before 4 minutes. There was a significant peak present in the L2 samples at 5.6 minutes, and it appears like there is a smaller corresponding peak in the P2 sample at 5.78 minutes. The similarities between the samples could be because of the unspecific nature of papain, which would result in many small peptides, however, the exact composition of these small peptides found in each sample could differ greatly. The significant group of peaks present in both L2 and P2 samples that eluted from the column between 22 and 28 minutes, (using a high proportion of acetonitrile in the mobile phase), were likely to be conjugates of peptides and other impurities that have stuck onto the column, and elute in bulk with the polar conditions.

The liver hydrolysate sample L2 was selected for further analysis using prep HPLC. This was chosen because the liver hydrolysate samples generally had greater bioactivity, and the HPLC data (**Figure 4-18**) suggested that there was a greater heterogeneity in peaks.

In total, five prep HPLC runs of L2 were performed. There was a clear difference between the chromatogram for liver peptide run 1 compared to runs 2 to 5. The significant peaks present in fraction 4 (9.1-13 min) are not evident in the chromatograms for subsequent runs (**Table 4-4, and Figure 4-20**). Another obvious difference between the chromatograms is the magnitude of the peaks represented in fractions 1 and 2. The peaks from run 1 have approximately half the absorbance as the peaks from runs 2 to 5. In addition to this observation, the peaks from run 5 appear different to the ones form previous runs, though it could be argued that runs 2 and 5 are more similar. A possible explanation for the differences between the chromatograms could be that the peptides hydrolysed in the time between the first run and the subsequent runs. This could be the reason for the disappearance of the peaks with a greater retention time, and the doubling in intensity for the peaks with a lower retention time (larger peptides breaking down to smaller ones). There was, however, no evidence of this in the stability studies (section 4.3.10). Therefore, the most likely explanation was that the peptides were aggregating and then dispersing, which would affect the chromatography of the peptides.

The fractions from runs 2 to 5 generated from the prep HPLC were combined whereas the fractions from run 1 were kept separate. The fractions were then lyophilised resulting in solid samples. While the fractions taken from the prep HPLC were from poorly resolved peaks (this being an apparent limitation of the column used), they did exhibit markedly different physical properties. The samples from fraction 1 (F1R1, and F1R2) appeared to be much denser than those samples from fraction 2 (F2R1, and F2R2), which were much less dense, and were obviously charged with clearly visible static electrical interactions with plastic containers. The high density of peaks that eluted from the analytical column for both L2, and P2, could be the reason that lyophilised samples were denser than the fractions taken after 4 minutes (where the density of peaks is much lower). The sample derived from fraction 4

(F4R1) was stated as being extremely hygroscopic. The physical properties of this sample could not be analysed because the sample quickly liquified within seconds of exposure to the air.

The samples generated from the lyophilised fractions (F1R1, F1R2, F2R1, F2R2, and F4R1) were dissolved in the aqueous running buffer for analysis using the Ascentis® Express Peptide ES-C18 column. Equivalent fractions from each run were compared to assess the differences between the runs. The chromatograms for F2R1, and F2R2 (**Figure 4-21**) demonstrated a noticeable difference between the two runs for this fraction. All of the significant peak in F2R1 eluted from the column before 2.75 minutes, and the peaks had significantly lower areas than those found in the F2R2 fraction. There was a significant peak at 4.28 minutes found in F2R2, which is completely absent from F2R1. Considering that there was a considerable peak that eluted from run 1 that was not present in runs 2 to 5, the peak at 4.28 minutes in F2R2 is likely related to this fact. This is corroborated by the chromatograms of F4R1 (**Figure 4-23**). When this sample was analysed there was only one peak observed, which eluted at similar times (4.37, and 4.27 minutes) to the peak found in F2R2 (**Figure 4-21b1/b2**). It is likely that the difference between the two fractions can be explained by the absence of a peak in fraction 4 for runs 2 to 5. The chromatograms for F1R1, and F2R1 (**Figure 4-22**) follow a similar pattern to the fraction 2 samples in that they the peaks have a greater amplitude in the samples from runs 2 to 5. The peaks themselves are more similar to each other in comparison to the chromatograms representing fraction 2 peaks. The fact that the peaks in F1R2 have a greater amplitude (with a similar fold change) is probably related to the peak found in F4R1.

The fractions generated from the prep HPLC were analysed using the MTT assay, scratch assay, and their radical scavenging activity was analysed using the DPPH assay. The results presented in **Figure 4-24** are the percentage of MTT metabolism by the cells in the presence of the different fractions with the results of the control group used as the baseline. These data suggest that on the whole there is no significant difference between most of the fractions in regards to cell metabolism . The two results that showed significant differences from the others were from fractions F1R2, and F2R2. F1R2 appeared to result in a reduction in metabolism at 200 µg/mL, whereas F2R2 caused an increase. Both these

results were significant according to the data. The fact that it is fraction F2 from the second run that showed the greatest positive result is interesting. Maybe there is a peptide, or multiple peptides that were present in this fraction generated from the breakdown, or de-aggregation of the fraction F4 from run 1. The increase/decrease in metabolism over the full peptide could be explained by the peptides in the fractions are at a greater concentration than in the full liver hydrolysate. It should also be noted that the peaks found in the fractions from run 2 had a greater amplitude, suggesting that they contained more peptides than those found in the fractions from run 1.

The results of the scratch assay indicated that there was no significant difference between the fractions in regards to a change in chemotaxis in both the percentage wound closure over time (**Figure 4-26**), and the rate of wound closure (**Figure 4-28**). These data taken alongside the MTT data for the fractions derived from L2 indicate that there is likely to be no wound healing properties exhibited by either the full hydrolysate, or the fractions. This follows on from the earlier cell proliferation data generated from samples L1, and P1, where proliferation was not affected in either a negative or positive manner. It can therefore be surmised that the Biofac hydrolysates do not show bioactivity related to wound healing. This does not necessarily mean that there will not be any potential peptides that influence wound healing in the samples, just that they are in too low a concentration (if they are there at all) to show an effect. This is further analysed using the synthetic peptides in chapter 5.

The results of the DPPH assay on the fractions (**Figure 4-29**) showed a similar relationship between activity and concentration as the assays performed on the full hydrolysates (the greater the concentration, the greater the radical scavenging activity). The activity of F2R2 at 0.8 mg/mL and 0.4 mg/mL were both significantly greater than the other fractions. The greater activity in comparison to the full sample at these concentrations could be due to more active components in the full sample being in a greater concentration in this fraction, however, this does not explain the equalisation of the activities at 0.2 mg/mL. The mechanism for the DPPH assay relies on the availability of proton donors. It would appear that the fractionation of the L2 hydrolysate did not drastically alter the proportion of charged amino acids.

4.4.4 Stability Studies

The data from the stability studies indicated that hydrolysates were stable in solution over the period of time that the study was performed. This can be seen in the chromatograms presented in **Figure 4-31, and Figure 4-33**, and the cell proliferation graphs in **Figure 4-30, and Figure 4-32**. These data show that the peptides that are present in the hydrolysates were stable in solution up to 168 hours. This discounts theories that more active peptides are released from larger peptides over time.

4.4.5 ACE inhibition assay

A large proportion of bioactive peptides that have been reported in the literature show anti-angiotensin converting enzyme (ACE) activity. It was this reason the anti-ACE activity of the hydrolysates was investigated. The method used was developed based on the synthetic ACE substrate HHL, using the known ACE inhibitor Captopril as the positive control. The ability of the enzyme to cleave HHL was determined by the decrease in the product HA.

The placenta hydrolysate (P2) demonstrated significantly more anti-ACE activity than the liver hydrolysates (L2, and L3) (Error! Reference source not found.). Looking at bioactive peptide d atabases, a common feature of peptides that show anti-ACE activity is that they are di-peptides. The data generated from HPLC analysis of the P2 hydrolysate indicated that there was a greater proportion of di-peptides in the sample than the liver hydrolysates. The majority of known bioactive peptides that exhibit anti-ACE activity are di-peptides. This would explain why the placenta hydrolysate showed significantly greater activity than the liver samples.

4.5 Summary

The assays performed on the Biofac hydrolysates indicated that there are bioactive peptides present in the samples. The antioxidant assays showed that there was a wide range of antioxidant activity in all the samples assayed, except for P1, which only showed significant activity (relative to the other samples), in the lipid peroxidation assay. Batch to batch variation (L1, L2, L3, and P1, P2.) was also apparent. This was clearly evident in the dramatic difference observed in the DPPH assay for the liver

hydrolysates, and the ORAC activity demonstrated by the both the placenta and liver hydrolysates. These batch-to-batch variations can be attributed to the production method used. The data generated from the ACE inhibition assay highlights interesting possibilities in the discovery of potent anti-hypertension peptides present in the hydrolysates. This data was encouraging, highlighting the possibility of discovering novel bioactive peptides, which was further explored in chapter 5.

CHAPTER 5 **Generation of and bioactivity analysis of synthetic peptides derived from hydrolysates**

5.1 Introduction

As discussed in previous chapters, bioactive peptides can be released from precursor proteins by proteolytic enzymes. Some common proteases that are used in the hydrolysis of proteins include digestive enzymes that can be found in the gastrointestinal tract, these include trypsin, and pepsin, while others can be derived from microorganisms and plants. Papain, and bromelain are two widely used proteases, used in meat tenderisation that are derived from plants (papain from papaya, and bromelain from pineapple) (Rawlings and Barrett, 1994, Zatul et al., 2014). The hydrolysates generated from these protein digests can be further processed using techniques such as FPLC, and RP-HPLC; the fractions generated can then be assayed for any bioactive properties. Active fractions identified through assays are then further separated using HPLC to isolate individual peptides, and sequenced using MS/MS and *de-novo* sequencing (Ahmed et al., 2015) (Corrêa et al., 2014). Sequences that are identified through *de-novo* sequencing can be cross checked with a number of databases that act as a depository of known bioactive peptides. Multiple studies have been undertaken where sequence data is obtained in this manner. The desired result is to discover new bioactive peptides, and determine what biological function they affect. This approach can be structured as follows: Digestion – separate – assay – separate – sequence – synthesis - assay.

HPLC coupled with MS/MS and *de-novo* sequencing can be used to identify peptides that show bioactivity, but data generated from this process can also be used to identify the host protein from which particular peptides was derived. Identifying a host protein from samples such as those produced by Biofac is a useful method to understand the composition of the hydrolysates. The raw material for each product is known, but it is not known exactly what proteins, and in what proportion they contribute to the bulk hydrolysates. Having an understanding of the source proteins can be used to perform *in silico*

digests, using online tools such as BIOPEP (Minkiewicz et al., 2008) to generate a list of peptides that could be released as a result of the production method.

In the case of the Biofac hydrolysates papain digestion was used, however, different proteases have differing specificity concerning where they cleave a protein. Therefore, it is possible to perform *in silico* digests of the target protein with various proteases, that will cleave at different sites producing multiple peptide fragments, that demonstrate different modes of bioactivity (Jang and Lee, 2005). The theoretical peptides generated using this method can then be analysed for possible bioactivity. This method will produce a large amount of theoretical peptides. To identify peptides that could be bioactive, the structures require analysis to single out interesting peptides, which not only have a high chance of demonstrating bioactivity, but also are novel peptides, in that they have not been previously reported in the literature. For this study the online bioactivity prediction tool Peptide Ranker, developed by Bioware was used (Mooney et al., 2012). This program assigns a rank to the likelihood of a peptide sequence being bioactive (0.0 being highly unlikely, 1.0 being highly likely). The Peptide Ranker tool works by analysing the sequence of peptides, and relating them to known bioactive peptides. Mooney et al (2012) noted that bioactive peptides that demonstrate different functional classes have certain attributes alike. Therefore, these similarities can be used to predict if a peptide is likely to be bioactive, without indicating what sort of bioactivity will be displayed. In developing the tool, they noted that elements that confer bioactivity differs in relation to the size of the peptide. For example, it was reported that short peptides (< 20 amino acids) that scored highly were likely to contain phenylalanine (F). The difference in the physical attributes that confer bioactivity between large, and small peptides is likely to be the ability of longer peptides to form tertiary structures (Mooney et al., 2012).

This project was based on investigating the bioactive properties of hydrolysates of porcine liver, and placenta provided by the company Biofac, which were generated through papain hydrolysis. Therefore, the focus of this section of work was on peptides generated through *in silico* hydrolysis with papain. However, this method could also be applied to different enzymes, in doing so it would be possible to identify peptides generated from different production methods prior to hydrolysis. To demonstrate this

it was decided to perform *in silico* digestion on the precurser proteins using the gastic enzymes trypsin and pepsin at pH 1.3 (levels found in the stomach), and the pineapple derived enzyme bromelain. The rationale behind using these particlar enzymes is that they have all been used in similar projects (Lafarga et al., 2014, Chatterjee et al., 2015), and that they are commerically available from companies such as Merck/Sigma-Aldrich. These enzymes are also more specific than papain, so it is likely that they will generate larger peptides from the digestion (Minkiewicz et al., 2008).

As has been mentioned, the methodology of the studies investigating the bioactivity of peptides generally follow a similar stratergy: Separate the peptides in the hydrolysate; assay the fractions; isolate indivdual peptides in active fractions; synthesis of the peptides and repeat the assay. The work carried out for this chapter focused on using *in silico* methods for identification of the host proteins that were hydrolysed to produce the peptides and identification of the peptides that would likely be produced by the particular enzyme used in the hydrolysis. These peptides could then be analysed for the likelyhood of bioactivity and then manufactured and used in assays.

This chapter will primarily investigate four synthetic peptides derived from hydrolysates of porcine liver, and placenta, supplied by Biofac. These peptides were selected after *in silico* analysis of sequence data derived from the hydrolysates that had been separated using HPLC. The synthetic peptides selected were predicted through *in silico* digestion by papain.

5.2 Materials and methods

5.2.1 Isolation of individual fractions for MS analysis

L2, and P2 hydrolysate solutions (5 mg/mL) were prepared in the aqueous HPLC running buffer (ultrapure water, acetonitrile (0.2 %), TFA (0.01 %)) and filtered using 0.2 µm syringe filters. This was loaded onto an analytical HPLC column (Ascentis® Express Peptide ES-C18) using a 20 µL loading loop at a flow rate of 1 mL/min. The concentration gradient of acetonitrile for all samples went from 5% to 29% in 10 minutes followed by 29% to-95% in 5 minutes. Samples were collected manually and tested by running the collected peak through the same HPLC setup to ensure that they only contained the desired peak. Sample L2a was derived from the liver hydrolysate L2 and was collected from the fraction containing the peak at 6.017 minutes. Sample L2b was collected from a similar fraction, from the same hydrolysate (L2) but on a different run. This was done to evaluate the reproducibility of the method. Sample P2a was derived from the placenta hydrolysate P2 and was collected from the fraction containing the peak at 6.1 minutes. The concentration of the peptides in the samples isolated from the peak at 6.1 minutes were estimated using a standard curve. Liver peptide solutions (80, 40, 20, and 10 µg/mL) were prepared using the aqueous buffer with 5% acetonitrile. The samples were analysed using a UV-Vis spectrophotometer at 220 nm that was blanked with the same buffer. This method estimates the concentration of the peptide in relation to the amount of peptide bonds.

5.2.2 Peptide Sequencing Using MS/MS

The three samples that were collected (L2a, L2b, and P2a), were shipped on dry ice to the Metabolomics & Proteomics Lab at the University of York for peptide sequencing using LC-MS/MS using a Bruker maXisHD mass spectrometer interfaced to a 50 cm PepMap column with a Bruker CaptiveSpray ion source. Peptides were eluted from the column over a 35 min gradient at 300 nL/min. Eluting peptides were selected for MS2 fragmentation using top speed data dependent acquisition, a dynamic 7-25 Hz acquisition rate and 1 s cycle time. Product ion spectra were searched against the porcine subset of the UniProt database (The UniProt Consortium, 2017) using Mascot, with no enzyme specificity. Search

results were filtered to require expect scores of 0.05 or lower, this means that sequence matches have a equal to or less than a 1 in 20 chance of being a false positive, and therefore incorrect.

5.2.3 In silico digestion, and activity prediction

In silico enzyme digestion were carried out on the protein sequences derived from the UniProt searches (cytosol aminopepsidase, haemoglobin subunit alpha, and type VI collagen alpha-1 chain), using the analysis tool available on the BIOPEP website (Minkiewicz et al., 2008). Sequences were generated using papain, bromelain, pepsin (pH 1.3), and trypsin. Generated sequences were then cross-referenced against a number of bioactive peptide databases to find any active sequences that have been previously reported. Peptide sequences that had not been reported were then analysed using the Peptide Ranker tool by Bioware (Mooney et al., 2012). Peptide Ranker predicts the likelihood of a peptide sequence being bioactive (0.0 being highly unlikely, 1.0 being highly likely).

5.2.4 Peptide synthesis and preparation

Based on the *in silico* activity prediction, four synthetic peptides were ordered from Peptide Synthetics (Protein Peptide Research Ltd. Bishops Waltham, UK). They were supplied as 10 mg aliquots of lyophilised powder. The synthetic peptides were dissolved in deionised water to produce 10 mM stock solutions:

- FWG: In 10 mg/mL = 0.024 M = 24.48 mM. 10 mM = 10 mg/2.448 mL
- MFLG: In 10 mg/mL = 0.021 M = 21.43 mM. 10 mM = 10 mg/2.143 mL
- SDPPLVFVG: In 10 mg/mL = 0.011 M = 10.75 mM. 10 mM = 10 mg/1.075 mL
- FFNDA: In 10 mg/mL = 0.016 M = 16.32 mM. 10 mM = 10 mg/1.632 mL

The dissolved peptides were aliquoted and stored at -20°C.

5.2.5 ORAC Assay

The Oxygen Radical Absorbance Capacity of the synthetic peptides were analysed using the ORAC assay as described in section 4.2.2 with some alterations. The synthetic peptides were used to generate stock solutions (100 µM) by diluting the specific synthetic peptide sample (10 mM) in 10 mM potassium

phosphate buffer (pH 7.4). The stock solutions were used to prepare a concentration gradient ranging from 12.5 µM to 3.25 µM. An off the shelf dipeptide Leucine-Glycine (LG) was used as another example of a synthetic peptide. It was prepared in the same concentrations as the other peptides.

5.2.6 Cellular Antioxidant Activity Assay

The CAA assay used to assess the antioxidant activity of the synthetic peptides followed the same method that was described in section *4.2.4*. Sample media used in the CAA was prepared by adding DCFH-DA to supplemented DMEM (10% FBS, 2% L-Glutamine (220 mM), 1% PenStrep) to a concentration of 5 µM. The synthetic peptides were added to the sample media to generate concentrations of 25 and 50 µM. Negative controls contained only DCFH-DA.

5.2.7 MTT assay

A 96 well plate was seeded at 5 x 10^4 cells/mL (5 x 10^3 cells/well) using 3T3 fibroblasts cultured in supplemented DMEM (10% FBS, 2% L-Glutamine (220 mM), 1% PenStrep) approximately 24 hours prior to the addition of the synthetic peptides. Peptide preparations (containing 100 – 3.25 µg/mL of synthetic peptide) were added to the plate and incubated at 37°C at 5% CO_2 for 46 hours before 20 µL of MTT in PBS (5 mg/mL) was then added to each well. The plate was then incubated at 37°C at 5% CO_2 for a further 4 hours, after which, the media was aspirated and 150 µL of DMSO was added. The absorbance was then measured at 540 nm using a plate reader (applying a 5 second shake to ensure the samples were suitably mixed prior to the measurement). Data were displayed as percentage proliferation, where the mean data for the control group was used as the base line for the experimental groups. Therefore, less proliferation than the control is displayed as a negative value, and more proliferation than the control is displayed as a positive value. The percentage proliferation was calculated using **equation 4.8**.

5.2.8 Scratch assay

To investigate potential wound healing activity of the synthetic peptides a scratch wound assay was performed. Briefly, 6 well plates were prepared as reported in section 4.2.10.2. Synthetic peptides were

added to CGM (10 mL) to produce sample preparations. Each sample preparation was then sterile filtered using 0.22 µm syringe filters. The concentration for the preparations was 100 µM. The procedure from this point followed that of section 4.2.10.2. Wound closure rate ($\mu m^2/h$) was calculated using **equation 4.11** and percentage wound closure was calculated using **equation 4.12**.

5.2.9 Angiotensin converting enzyme (ACE) inhibition assay

To assess the anti-ACE activity of the synthetic peptides, they were analysed using the ACE inhibition assay as described in section 4.2.12. Synthetic peptide samples were prepared by diluting the 10 mM stock solutions using milli-q water to produce samples at 2 mM, 1 mM, and 0.1 mM.

5.2.10 Statistical analysis

Data were analysed using one-tailed t-tests with equal variances assumed. Statistical analyses were performed on triplicate data using Microsoft Excel with a p value < 0.05 considered significant. Standard deviation derived from the mean values were indicated with error bars. Where relevant, p-values obtained in t-tests were included in the data to highlight significant differences, or where there was no significant difference.

5.3 Results

5.3.1 Isolation of individual peaks for MS analysis

Three samples from fractions eluted from individual peaks were collected; L2a (**Figure 5-1a**) and L2b (data not shown) from the liver hydrolysate (L2) (peak at 6.017 minutes), and P2a (**Figure 5-2a**) from the placenta hydrolysate (P2) (peak at 6.1 minutes). Samples of the collected fractions were analysed using HPLC using the same method used in the initial separation to check the purity of the aliquots (**Figure 5-1b,** and **Figure 5-2b**). The chromatograms in **Figure 5-1b, and Figure 5-2b** indicate that the aliquots were pure. The small peak at 1.117 minutes can be attributed to the solvent peak.

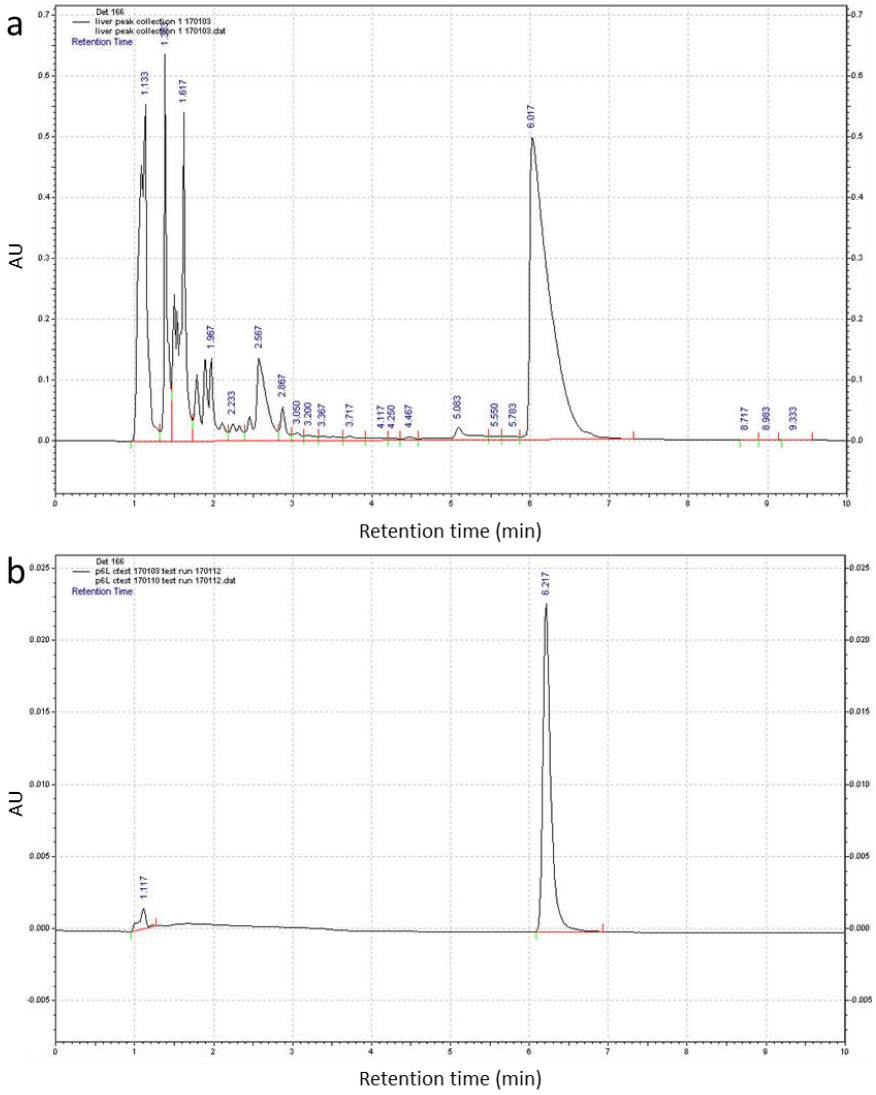

Figure 5-1 Chromatograms indicating the fraction that was collected for Liver 160126-0700 (L2) (peak at 6.017 min) (a), and the collected fraction loaded onto the column again to check for purity (peak at 6.217 min) (b)

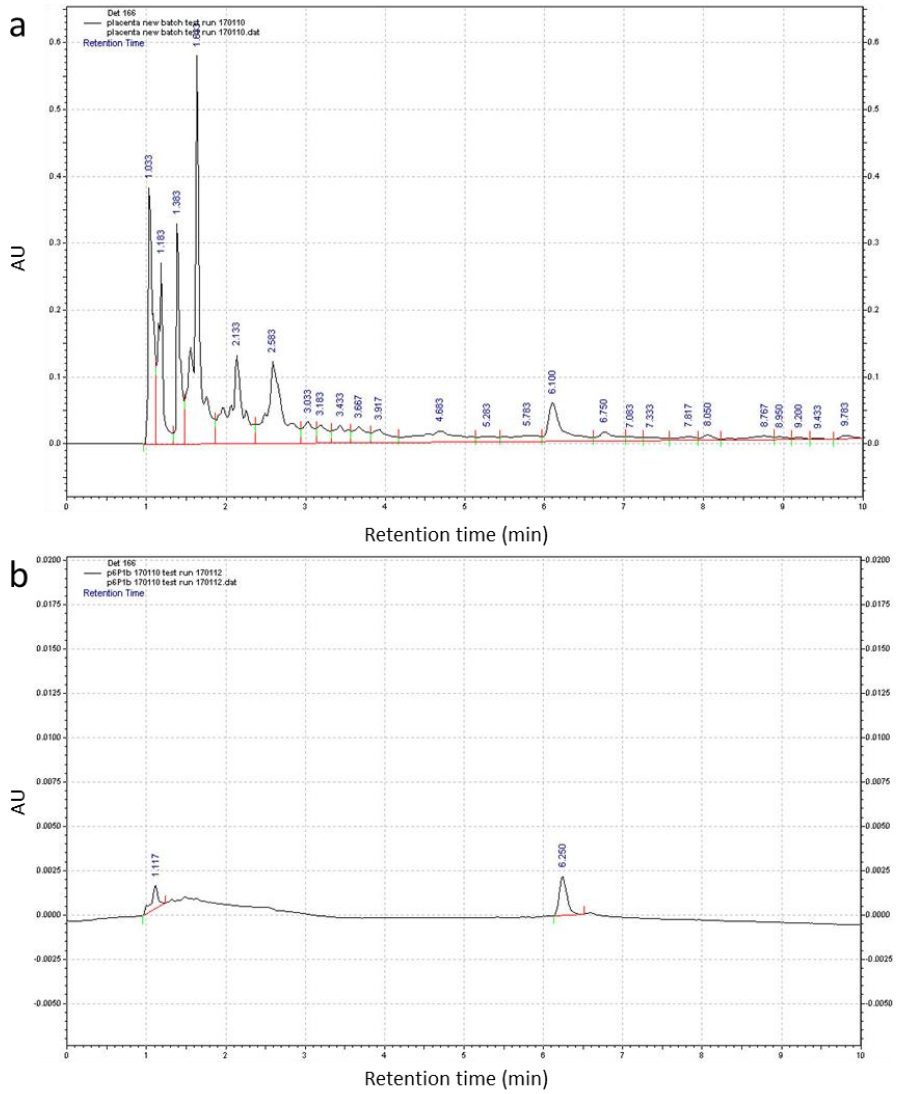

Figure 5-2 Chromatograms indicating the fraction that was collected for placenta 0-160330-1500 (P2) (peak at 6.100 min) (a), and the collected fraction loaded onto the column again to check for purity (peak at 6.250 min) (b)

5.3.2 Peptide Sequencing Using MS/MS

The following peptides were identified in the samples:

L2a: **TPANE<u>M</u>TPTR** + Oxidation (M) – expect = 0.0033, mass error = 0.45 ppm

L2b: **SAADKANVKAA** – expect = 0.01, mass error = -0.43 ppm

P2a: **YSGTGQQQPER** – expect = 0.00048, mass error = -1.98 ppm, and **NVINGGSHAGNK** – expect = 0.0034, mass error = -0.02

The predicted peptides were cross-referenced using the UniProt database to find the host protein. The structure of the peptides are shown in **Figure 5-3 to Figure 5-6**.

TPANEMTPTR + Oxidation (M)

Thr – Pro – Ala – Asn – Glu – Met – Thr – Pro – Thr – Arg

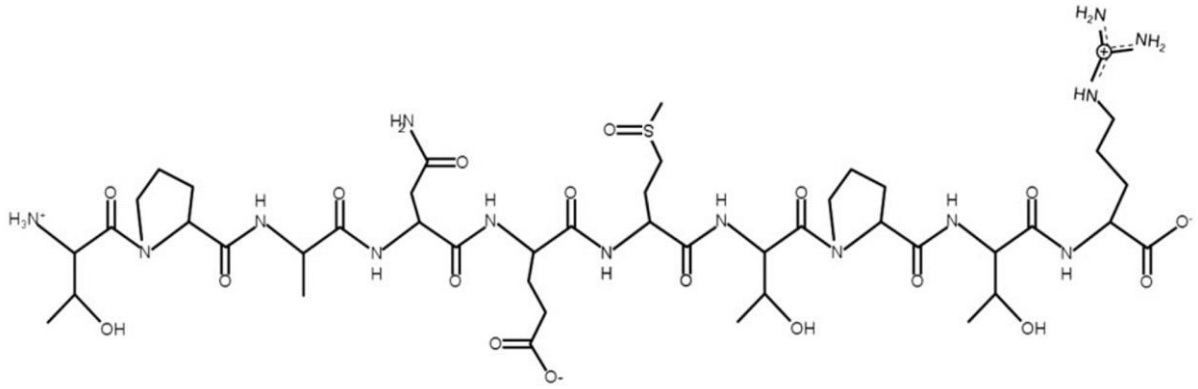

Figure 5-3 Structure of the peptide TPANEMTPTR with methionine sulfoxide

The host protein of this peptide was determined as cytosol aminopeptidase; an enzyme that can be found in the liver of mammals that facilitates the removal of N-terminal amino acid from peptides. It can also cleave the N-terminal of amides and arylamides. The peptide sequence is highlighted within the host protein sequence below:

Amino Acid Sequence of Cytosol aminopeptidase (Sus scrofa)

1 mfllplpaaa rvavrqlsvr rfwgpgpdaa nmtkglvlgi yskekeddap qftsagenfd

61 klvsgklrei lnisgpplka gktrtfyglh edfssvvvvg lgkkgagvdd qenwhegken

121 iraavaagcr qiqdleipsv evdpcgdaqa aaegavlgly eydelkqkkk vvvsaklhgs

181 gdqeawqrgv lfasgqnlar hlmetpanem tptrfaevie knlksasskt dvhirpkswi

241 eeqemgsfls vakgseeppv fleihykgsp dasdpplvfv gkgitfdsgg isikasanmd

301 lmradmggaa ticstivsaa kldlpinlvg laplcenmps gkankpgdvv raknqktiqv

361 dntdaegrli ladalcyaht fnpkviinaa tltgamdial gsgatgvftn sswlwnklfe

421 asietgdrvw rmplfehytk qivdcqladv nnigkyrsag actaaaflke fvthpkwahl

481 diagvmtnkd evpylrkgma grptrtlief llrfsqdsa

SAADKANVKAA

Ser – Ala – Ala – Asp – Lys – Ala – Asn – Val – Lys – Ala – Ala

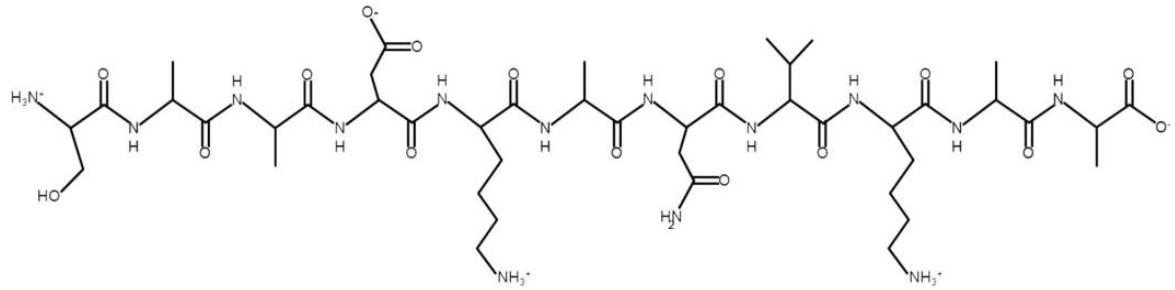

Figure 5-4 Structure of the peptide SAADKANVKAA

The host protein of this peptide was determined as haemoglobin subunit alpha. The peptide sequence is highlighted within the host protein sequence below:

Haemoglobin subunit alpha (Sus scrofa)

1 mvlsaadkan vkaawgkvgg qagahgaeal ermflgfptt ktyfphfnls hgsdqvkahg

61 qkvadaltka vghlddlpga lsalsdlhah klrvdpvnfk llshcllvtl aahhpddfnp

121 svhasldkfl anvstvltsk yr

YSGTGQQQPER

Tyr – Ser – Gly – Thr – Gly – Gln – Gln – Gln – Pro – Glu – Arg

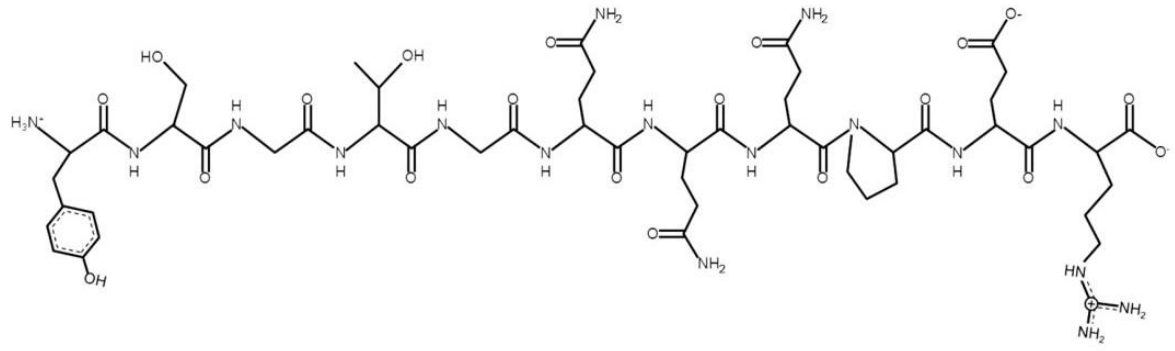

Figure 5-5 Structure of the peptide YSGTGQQQPER

The host protein of this peptide was determined as Type VI collagen alpha-1 chain. The peptide sequence is highlighted within the host protein below:

Type VI collagen alpha-1 chain, partial (Sus scrofa)

1 fsspaditil ldgsasvgsh nfdttkrfak rlaerfltag rtdpahdvrv avlqysgtgq

61 qqperaalqf lqnytvlast vdamgffnda tdvtdalgyv trfyreassg aakkkl

NVINGGSHAGNK

Asn – Val – Ile – Asn – Gly – Gly – Ser – His – Ala – Gly – Asn – Lys

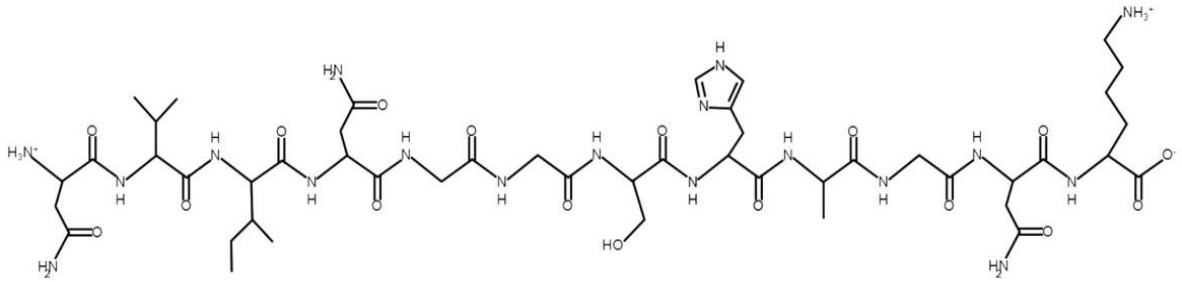

Figure 5-6 Structure of the peptide NVINGGSHAGNK

The host protein of this peptide was likely to be enolase. The peptide sequence is highlighted within the host protein below: This sequence was not analysed for this project because it was not identified until after the practical work was completed.

1 msiekiware ildsrgnptv evdlytakgl fraavpsgas tgiyealelr dgdkqrylgk

61 gvlkavdhin ttiapalvss glsvveqekl dnlmldldgt enkskfgana ilgvslavck

121 agaaerdlpl yrhiaqlagn sdlilpvpaf nvinggshag nklamqefmi lpvgaesfrd

181 amrlgaevyh tlkgvikdky gkdatnvgde ggfapnilen sealelvkea idkagyteki

241 vigmdvaase fyrdgkydld fkspadpsry itgdqlgaly qdfvrdypvv siedpfdqdd

301 waawskftan vgiqivgddl tvtnpkrier aveekacncl llkvnqigsv seaiqackla

361 qengwgvmvs hrsgetedtf iadlvvglct gqiktgapcr serlakynql mrieeelgde

421 arfaghnfrn psvl

5.3.3 In silico digestion, and activity prediction

5.3.3.1 Known bioactive peptides

All known bioactive peptides found using this method were dipeptides. They fell within the following categories: dipeptidyl peptidase IV inhibitors, ACE inhibitors, renin inhibitors, CaMPDE inhibitors, stimulating vasoactive substance release, regulating the stomach mucosal membrane activity, and antioxidant peptides. In total there were 34 dipeptides found in the databases (**Table 5-1 to Table 5-5**). These peptides were entered into the Peptide Ranker tool as a test to assess how it would report known active sequences. All the peptides were reported to have a high probability of bioactivity.

Table 5-1 Known bioactive peptides that were predicted from the in silico digest of cytosol aminopepsidase with papain. Data taken from the BIOPEP database

Sequence	Name	Function	Activity
PG	peptide regulating the stomach mucosal membrane activity	regulating the stomach mucosal membrane activity	regulating
	-	-	antithrombotic
	prolyl endopeptidase inhibitor	inhibitor of prolyl pndopeptidase (PEP) (EC 3.4.21.26) (MEROPS ID: S09.001)	antiamnestic
	ACE inhibitor	inhibitor of angiotensin-converting enzyme (ACE) (EC 3.4.15.1) (MEROPS ID: XM02-001)	ACE inhibitor
	dipeptidyl peptidase IV inhibitor (DPP IV inhibitor)	inhibitor of dipeptidyl peptidase IV (EC 3.4.14.5) (MEROPS ID: S09.003)	dipeptidyl peptidase IV inhibitor
VA	dipeptidyl peptidase IV inhibitor (DPP IV inhibitor)	inhibitor of dipeptidyl Peptidase IV (EC 3.4.14.5) (MEROPS ID: S09.003)	dipeptidyl peptidase IV inhibitor
MA	dipeptidyl peptidase IV inhibitor (DPP IV inhibitor)	inhibitor of dipeptidyl Peptidase IV (EC 3.4.14.5) (MEROPS ID: S09.003)	dipeptidyl peptidase IV inhibitor
FA	dipeptidyl peptidase IV inhibitor (DPP IV inhibitor)	inhibitor of dipeptidyl Peptidase IV (EC 3.4.14.5) (MEROPS ID: S09.003)	dipeptidyl peptidase IV inhibitor
IR	beta-lactokinin	inhibitor of angiotensin-converting enzyme (ACE) (EC 3.4.15.1) (MEROPS ID: XM02-001)	ACE inhibitor
	antioxidant peptide	oxygen radical scavenging	antioxidative
	renin inhibitor	inhibitor of renin (EC 3.4.23.15) (MEROPS ID A01.007)	hypotensive
	CaMPDE inhibitor	inhibitor of calmodulin-dependent phosphodiesterase 1 (abbrev. CaMPDE) (EC 3.1.4.17).	inhibitor
	dipeptidyl peptidase IV inhibitor (DPP IV inhibitor)	inhibitor of dipeptidyl peptidase IV (EC 3.4.14.5) (MEROPS ID: S09.003)	dipeptidyl peptidase IV inhibitor

Table 5-2 Known bioactive peptides that were predicted from the in silico digest of cytosol aminopepsidase with papain. Data taken from the BIOPEP database cont.

Sequence	Name	Function	Activity
LH	dipeptidyl peptidase IV inhibitor (DPP IV inhibitor)	inhibitor of dipeptidyl peptidase IV (EC 3.4.14.5) (MEROPS ID: S09.003)	dipeptidyl peptidase IV inhibitor
	ACE inhibitor	inhibitor of angiotensin-converting enzyme (ACE) (EC 3.4.15.1) (MEROPS ID: XM02-001)	ACE inhibitor
	peptide from soybean protein isolates: beta-conglycinin and glycinin	-	antioxidative
WA	-	activating ubiquitin-mediated proteolysis	activating ubiquitin-mediated proteolysis
	dipeptidyl peptidase IV inhibitor (DPP IV inhibitor)	inhibitor of dipeptidyl peptidase IV (EC 3.4.14.5) (MEROPS ID: S09.003)	dipeptidyl peptidase IV inhibitor
	ACE inhibitor	inhibitor of angiotensin-converting enzyme (ACE) (EC 3.4.15.1) (MEROPS ID: XM02-001)	ACE inhibitor
DA	ACE inhibitor	inhibitor of angiotensin-converting enzyme (ACE) (EC 3.4.15.1) (MEROPS ID: XM02-001)	ACE inhibitor
TR	dipeptidyl peptidase IV inhibitor (DPP IV inhibitor)	inhibitor of dipeptidyl peptidase IV (EC 3.4.14.5) (MEROPS ID: S09.003)	dipeptidyl peptidase IV inhibitor
SG	ACE inhibitor	-	ACE inhibitor
TG	ACE inhibitor	-	ACE inhibitor
	dipeptidyl peptidase IV inhibitor (DPP IV inhibitor)	inhibitor of dipeptidyl peptidase IV (EC 3.4.14.5) (MEROPS ID: S09.003)	dipeptidyl peptidase IV inhibitor
NG	ACE inhibitor	-	ACE inhibitor
	dipeptidyl peptidase IV inhibitor (DPP IV inhibitor)	inhibitor of dipeptidyl peptidase IV (EC 3.4.14.5) (MEROPS ID: S09.003)	dipeptidyl peptidase IV inhibitor
VR	ACE inhibitor from k-CN (fr. 67-68)	Inhibitor of angiotensin-converting enzyme (EC 3.4.15.1) (MEROPS ID: XM02-001)	ACE inhibitor
	dipeptidyl peptidase IV inhibitor (DPP IV inhibitor)	inhibitor of dipeptidyl peptidase IV (EC 3.4.14.5) (MEROPS ID: S09.003)	dipeptidyl peptidase IV inhibitor

Table 5-3 Known bioactive peptides that were predicted from the in silico digest of cytosol aminopepsidase with papain. Data taken from the BIOPEP database cont.

Sequence	Name	Function	Activity
QK	ACE inhibitor from pea vicilin	-	ACE inhibitor
NK	ACE inhibitor from wakame	-	ACE inhibitor
LY	peptide from soybean protein isolates: beta-conglycinin and glycinin	-	antioxidative
LK	antioxidative peptide	oxygen radical scavenging	antioxidative
SE	stimulating vasoactive substance release	-	stimulating
DR	dipeptidyl peptidase IV inhibitor (DPP IV inhibitor)	inhibitor of dipeptidyl peptidase IV (EC 3.4.14.5) (MEROPS ID: S09.003)	dipeptidyl peptidase IV inhibitor
IH	dipeptidyl peptidase IV inhibitor (DPP IV inhibitor)	inhibitor of dipeptidyl peptidase IV (EC 3.4.14.5) (MEROPS ID: S09.003)	dipeptidyl peptidase IV inhibitor
MG	dipeptidyl peptidase IV inhibitor (DPP IV inhibitor)	inhibitor of dipeptidyl peptidase IV (EC 3.4.14.5) (MEROPS ID: S09.003)	dipeptidyl peptidase IV inhibitor
	ACE inhibitor	-	ACE inhibitor
NE	dipeptidyl peptidase IV inhibitor (DPP IV inhibitor)	inhibitor of dipeptidyl peptidase IV (EC 3.4.14.5) (MEROPS ID: S09.003)	dipeptidyl peptidase IV inhibitor
PK	dipeptidyl peptidase IV inhibitor (DPP IV inhibitor)	inhibitor of dipeptidyl peptidase IV (EC 3.4.14.5) (MEROPS ID: S09.003)	dipeptidyl peptidase IV inhibitor
QA	dipeptidyl peptidase IV inhibitor (DPP IV inhibitor)	inhibitor of dipeptidyl peptidase IV (EC 3.4.14.5) (MEROPS ID: S09.003)	dipeptidyl peptidase IV inhibitor
QE	dipeptidyl peptidase IV inhibitor (DPP IV inhibitor)	inhibitor of dipeptidyl peptidase IV (EC 3.4.14.5) (MEROPS ID: S09.003)	dipeptidyl peptidase IV inhibitor
SK	dipeptidyl peptidase IV inhibitor (DPP IV inhibitor)	inhibitor of dipeptidyl peptidase IV (EC 3.4.14.5) (MEROPS ID: S09.003)	dipeptidyl peptidase IV inhibitor
TK	dipeptidyl peptidase IV inhibitor (DPP IV inhibitor)	inhibitor of dipeptidyl peptidase IV (EC 3.4.14.5) (MEROPS ID: S09.003)	dipeptidyl peptidase IV inhibitor

Table 5-4 Known bioactive peptides that were predicted from the in silico digest of Haemoglobin subunit alpha with papain. Data taken from the BIOPEP database

Sequence	Name	Function	Activity
VA	dipeptidyl peptidase IV inhibitor (DPP IV inhibitor)	inhibitor of dipeptidyl peptidase IV (EC 3.4.14.5) (MEROPS ID: S09.003)	dipeptidyl peptidase IV inhibitor
VG	ACE inhibitor	inhibitor of angiotensin-converting enzyme (ACE) (EC 3.4.15.1) (MEROPS ID: XM02-001)	ACE inhibitor
	dipeptidyl peptidase IV inhibitor (DPP IV inhibitor)	inhibitor of dipeptidyl peptidase IV (EC 3.4.14.5) (MEROPS ID: S09.003)	dipeptidyl peptidase IV inhibitor
TY	dipeptidyl peptidase IV inhibitor (DPP IV inhibitor)	inhibitor of dipeptidyl peptidase IV (EC 3.4.14.5) (MEROPS ID: S09.003)	dipeptidyl peptidase IV inhibitor
	antioxidant peptide		antioxidative
DA	ACE inhibitor	inhibitor of angiotensin-converting enzyme (ACE) (EC 3.4.15.1) (MEROPS ID: XM02-001)	ACE inhibitor
WG	dipeptidyl peptidase IV inhibitor (DPP IV inhibitor)	inhibitor of dipeptidyl peptidase IV (EC 3.4.14.5) (MEROPS ID: S09.003)	dipeptidyl peptidase IV inhibitor
	ACE inhibitor	inhibitor of angiotensin-converting enzyme (ACE) (EC 3.4.15.1) (MEROPS ID: XM02-001)	ACE inhibitor
	antioxidant peptide		antioxidative

Table 5-5 Known bioactive peptides that were predicted from the in silico digest of Type VI collagen alpha-1 chain, partial with papain. Data taken from the BIOPEP database

Sequence	Name	Function	Activity
LA	dipeptidyl peptidase IV inhibitor (DPP IV inhibitor)	inhibitor of dipeptidyl peptidase IV (EC 3.4.14.5) (MEROPS ID: S09.003)	dipeptidyl peptidase IV inhibitor
	ubiqitin-mediated proteolysis activating peptide	activator of ubiqitin-mediated proteolysis	activating ubiquitin-mediated proteolysis
	ACE inhibitor	inhibitor of angiotensin-converting enzyme (EC 3.4.15.1) (MEROPS ID: XM02-001)	ACE inhibitor
MG	ACE inhibitor		ACE inhibitor
	dipeptidyl peptidase IV inhibitor (DPP IV inhibitor)	inhibitor of dipeptidyl peptidase IV (EC 3.4.14.5) (MEROPS ID: S09.003)	dipeptidyl peptidase IV inhibitor
FA	dipeptidyl peptidase IV inhibitor (DPP IV inhibitor)	inhibitor of dipeptidyl peptidase IV (EC 3.4.14.5) (MEROPS ID: S09.003)	dipeptidyl peptidase IV inhibitor
FY	ACE inhibitor	inhibitor of angiotensin-converting enzyme (ACE) (EC 3.4.15.1) (MEROPS ID: XM02-001)	ACE inhibitor
SG	ACE inhibitor		ACE inhibitor
LG	ACE inhibitor	inhibitor of angiotensin-converting enzyme (EC 3.4.15.1) (MEROPS ID: XM02-001)	ACE inhibitor
SH	dipeptidyl peptidase IV inhibitor (DPP IV inhibitor)	inhibitor of dipeptidyl peptidase IV (EC 3.4.14.5) (MEROPS ID: S09.003)	dipeptidyl peptidase IV inhibitor
TG	ACE inhibitor		ACE inhibitor
	dipeptidyl peptidase IV inhibitor (DPP IV inhibitor)	inhibitor of dipeptidyl peptidase IV (EC 3.4.14.5) (MEROPS ID: S09.003)	dipeptidyl peptidase IV inhibitor

5.3.3.2 Predicted activity of peptides derived from simulated digests

The Peptide Ranker results for the peptides generated from the simulated papain digest of *cytosol aminopeptidase* are presented in (**Table 5-6 and Table 5-7**). The most potent peptide predicted was found to be FWG (1). This also is an example of a peptide that had not been previously described in the literature. The Peptide Ranker results for the peptides generated from the simulated papain digest of *Haemoglobin subunit alpha* are presented in **Table 5-8**. The dipeptide WG (0.98) showed the greatest predicted bioactivity and the greatest predicted activity from a peptide that had not been reported was shown by MFLG (0.98). The Peptide Ranker results for the peptides generated from the simulated papain digest of *Type VI collagen alpha-1 chain, partial* are represented in (**Table 5-9**). The reported dipeptide FY (0.98) demonstrated the greatest predicted bioactivity (Minkiewicz et al., 2008, Mooney et al., 2012). FFNDA (0.77) was the peptide that had yet to be reported that showed the greatest bioactivity.

The majority of the fragments from all the simulated digests were single amino acids, with glycine representing the greatest predicted bioactivity (0.89). Glycine is known to function in several roles as a neurotransmitter (Lopez-Corcuera et al., 2001). All the simulated digests had the same single amino acids present, these were G, R, Y, H, A, K, and E.

Simulated digests of the same protein were also carried out using the proteases trypsin, bromelain, and pepsin (at pH 1.3) (full data set in appendix IIa - IIl). Predicted peptides with a predicted rank > 0.5 for all the digests (proteases and proteins) are represented in **Table 5-10**. Selected peptides from this group, which have not been reported in the literature, were chosen to be synthesised.

Table 5-6 Peptide Ranker scores for predicted papain digestion of cytosol aminopeptidase (1)

Sequence	Score	Sequence	Score	Sequence	Score	Sequence	Score
FWG	1	LG	0.72	SPDA	0.36	A	0.21
WA	0.96	LG	0.72	MDIA	0.34	A	0.21
FA	0.96	MFLLPLPA	0.71	LH	0.34	A	0.21
MG	0.94	DMG	0.71	LH	0.34	A	0.21
G	0.89	TFY	0.7	VPY	0.33	A	0.21
G	0.89	MA	0.69	PK	0.33	A	0.21
G	0.89	NMDLMR	0.66	PK	0.33	A	0.21
G	0.89	PPLK	0.62	IR	0.33	A	0.21
G	0.89	PPVFLE	0.6	PDA	0.32	A	0.21
G	0.89	VDPCG	0.58	IY	0.32	A	0.21
G	0.89	LR	0.57	SFLSVA	0.31	A	0.21
G	0.89	LR	0.57	PTR	0.31	A	0.21
G	0.89	VFTNSSWLWNK	0.55	PQFTSA	0.31	A	0.21
G	0.89	R	0.55	LA	0.31	A	0.21
G	0.89	R	0.55	MTPTR	0.3	A	0.21
G	0.89	R	0.55	DR	0.29	A	0.21
G	0.89	R	0.55	FSQDSA	0.28	A	0.21
G	0.89	R	0.55	LILA	0.27	A	0.21
G	0.89	R	0.55	FVTH	0.25	A	0.21
G	0.89	LY	0.52	VLG	0.24	A	0.21
G	0.89	NMPSG	0.51	ITFDSG	0.24	A	0.21
G	0.89	LFE	0.51	CTA	0.24	A	0.21
G	0.89	VLFA	0.48	TPA	0.23	A	0.21
G	0.89	Y	0.44	QIVDCQLA	0.23	A	0.21
G	0.89	Y	0.44	LVLG	0.23	TG	0.19
PG	0.88	Y	0.44	LME	0.23	TG	0.19
PG	0.88	Y	0.44	H	0.23	QNLA	0.19
CR	0.87	TFNPK	0.42	H	0.23	LDIA	0.19
FLLR	0.86	SWIE	0.42	H	0.23	LK	0.17
WQR	0.84	PLCE	0.42	H	0.23	ILNISG	0.17
FLK	0.81	SG	0.41	NIR	0.22	NMTK	0.15
NWH	0.78	SG	0.41	DFSSVVVVG	0.22	SA	0.14
SDPPLVFVG	0.75	SG	0.41	IH	0.21	SA	0.14
MPLFE	0.75	LDLPINLVG	0.41	A	0.21	SA	0.14
VWR	0.73	NG	0.39	A	0.21	QLSVR	0.14
LCY	0.73	NFDK	0.39	A	0.21	QIQDLE	0.14

Table 5-7 Peptide Ranker scores for predicted papain digestion of cytosol aminopeptidase (2)

Sequence	Score	Sequence	Score
NLK	0.14	K	0.06
LVSG	0.14	K	0.06
TR	0.13	K	0.06
ISIK	0.13	K	0.06
DVNNIG	0.13	K	0.06
DDA	0.13	K	0.06
DA	0.13	K	0.06
DA	0.13	TLIE	0.05
QA	0.12	TDVH	0.05
VR	0.11	DQE	0.05
TLTG	0.11	VVVSA	0.04
IPSVE	0.1	VIE	0.04
VIINA	0.09	VDDQE	0.04
SSK	0.09	TIQVDNTDA	0.04
VMTNK	0.08	SE	0.04
TICSTIVSA	0.08	QE	0.04
SIE	0.08	DE	0.04
SK	0.07	DE	0.04
DVVR	0.07	TK	0.03
VA	0.06	NE	0.03
VA	0.06	E	0.02
QK	0.06	E	0.02
NK	0.06	E	0.02
K	0.06	E	0.02
K	0.06	E	0.02
K	0.06	E	0.02
K	0.06	E	0.02
K	0.06	E	0.02
K	0.06	E	0.02
K	0.06	E	0.02
K	0.06	E	0.02
K	0.06	E	0.02
K	0.06	E	0.02
K	0.06	E	0.02
K	0.06	E	0.02
K	0.06	E	0.02
K	0.06		

Table 5-8 Peptide Ranker scores for predicted papain digestion of Haemoglobin subunit alpha

Sequence	Score	Sequence	Score
WG	0.99	A	0.21
MFLG	0.96	A	0.21
FPH	0.94	A	0.21
G	0.89	A	0.21
G	0.89	A	0.21
G	0.89	A	0.21
G	0.89	A	0.21
G	0.89	A	0.21
FLA	0.89	A	0.21
LR	0.57	LLSH	0.2
R	0.55	VG	0.17
R	0.55	VG	0.17
PDDFNPSVH	0.5	LSA	0.17
Y	0.44	MVLSA	0.16
LDDLPG	0.44	SLDK	0.14
FNLSH	0.42	DA	0.13
VDPVNFK	0.41	QA	0.12
FPTTK	0.34	TY	0.11
LSDLH	0.27	SDQVK	0.11
H	0.23	LTK	0.07
H	0.23	VA	0.06
H	0.23	QK	0.06
H	0.23	NVSTVLTSK	0.06
H	0.23	LE	0.06
H	0.23	K	0.06
CLLVTLA	0.22	K	0.06
A	0.21	DK	0.06
A	0.21	NVK	0.04
A	0.21	E	0.02
A	0.21		

Table 5-9 Peptide Ranker scores for predicted papain digestion of Type VI collagen alpha-1 chain, partial

Sequence	Score	Sequence	Score
FY	0.98	A	0.21
FA	0.96	A	0.21
MG	0.94	A	0.21
G	0.89	A	0.21
FFNDA	0.77	TDPA	0.2
LG	0.72	TG	0.19
FSSPA	0.65	SH	0.16
LL	0.62	SVG	0.15
R	0.55	SA	0.14
R	0.55	VLQY	0.12
R	0.55	QQQPE	0.12
R	0.55	DVR	0.12
R	0.55	VA	0.06
R	0.55	TVLA	0.06
FLTA	0.51	STVDA	0.06
Y	0.44	K	0.06
SG	0.41	K	0.06
LQFLQNY	0.33	K	0.06
LA	0.31	K	0.06
SSG	0.25	VTR	0.05
H	0.23	TDVTDA	0.04
DITILLDG	0.23	E	0.02
NFDTTK	0.21	E	0.02
A	0.21		

Table 5-10 Predicted peptides with a predicted rank > 0.5 for all the digests (proteases and proteins). Green highlighted peptides were selected for synthesis, yellow highlighted peptides are repeats, and red highlighted peptides have been reported in the literature as bioactive peptides

Cytosol aminopepsidase derived peptides			
Papain	Bromelain	Pepsin	Trypsin
FWG (1)	WQRG (0.85)	WGPGPDAANMTKGL (0.89)	FWGPGPDAANMTK (0.86)
FLLR (0.86)	FLK (0.81)	MRADMGGAATICSTIVS AAKL (0.83)	SAGACTAAAFLK (0.74)
WQR (0.84)	SDPPLVFVG (0.75)	CYAHTF (0.73)	LDLPINLVGLAPLCENMP SGK (0.74)
FLK (0.81)	LCY (0.73)	YGL (0.72)	VWR (0.73)
NWH (0.78)	MFLLPLPA (0.71)	APL (0.7)	ASANMDLMR (0.72)
SDPPLVFVG (0.75)	DMG (0.71)	WNKL (0.69)	GMAGR (0.61)
MPLFE (0.75)	PPLK (0.62)	SVRRF (0.68)	
VWR (0.73)		NISGPPL (0.64)	
LCY (0.73)		HGSGDQEAWQRGVL (0.63)	
MFLLPLPA (0.71)		GKKGAGVDDQENWHEG KENIRAAVAAGCRQIQD L (0.63)	
DMG (0.71)		ADVNNIGKYRSAGACTA AAF (0.61)	
TFY (0.7)			
PPLK (0.62)			
PPVFLE (0.6)			
Haemoglobin subunit alpha derived peptides			
MFLG (0.96)	FLA (0.86)	PHF (0.94)	AAWGK (0.66)
FPH (0.94)	FPHFNLSHG (0.76)	ERMF (0.78)	
FLA (0.86)	LERMFLG (0.66)	PGAL (0.71)	
		DKF (0.66)	
		AAHHPDDF (0.64)	
		LSHCL (0.62)	
Type IV collagen alpha-1 chain partial derived peptides			
FFNDA (0.77)	RFA (0.87)	GYVTRF (0.64)	FYR (0.94)
FSSPA (0.65)	FFNDA (0.77)	ASTVDAMGF (0.6)	FAK (0.62)
	FSSPA (0.65)		

5.3.3.3 Synthesised peptides

The following peptides were selected to be synthesised and analysed (the host protein and the Peptide Ranker score are also reported): **FFNDA** type VI collagen alpha-1 chain (0.77) (**Figure 5-7**), **FWG** cytosol aminopeptidase (1.00) (**Figure 5-8**), **SDPPLVFVG** cytosol aminopeptidase (0.75) (**Figure 5-9**), and **MFLG** haemoglobin subunit alpha (0.96) (**Figure 5-10**). These peptides were chosen because they all elicit a relatively high score from the Peptide Ranker tool, and have not been reported in the literature as being bioactive.

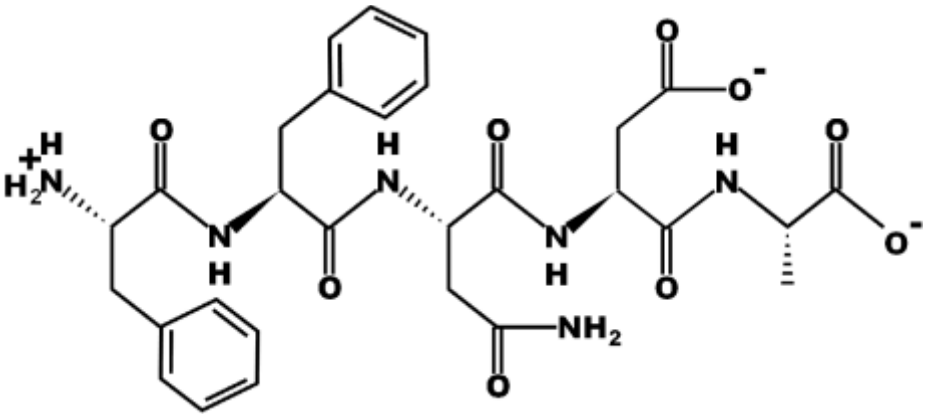

Figure 5-7 The molecular structure of the peptide FFNDA

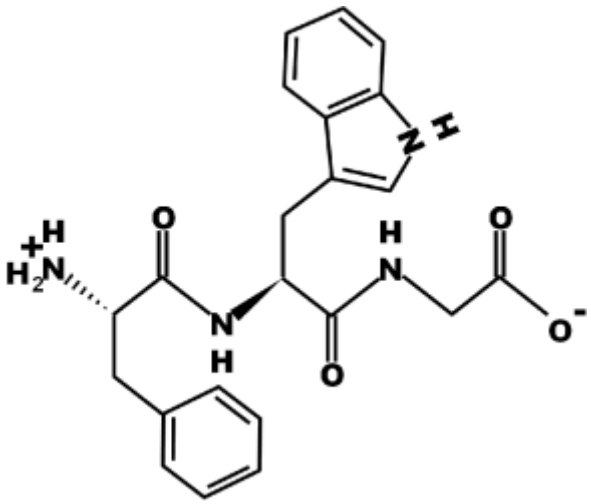

Figure 5-8 The molecular structure of the peptide FWG

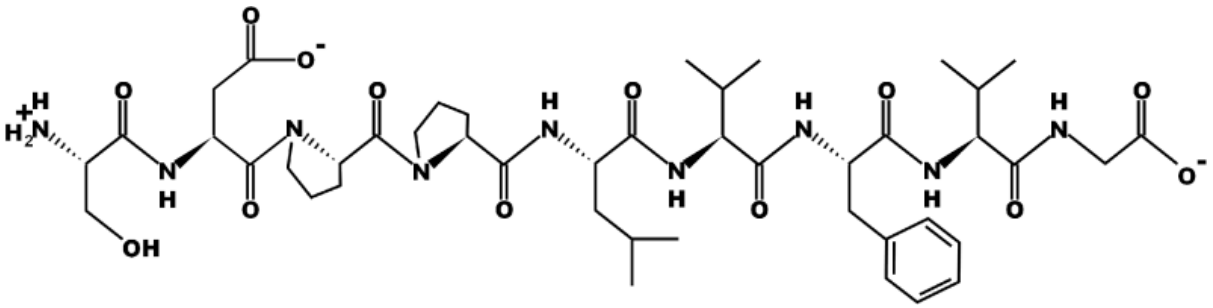

Figure 5-9 The molecular structure of the peptide SDPPLVFVG

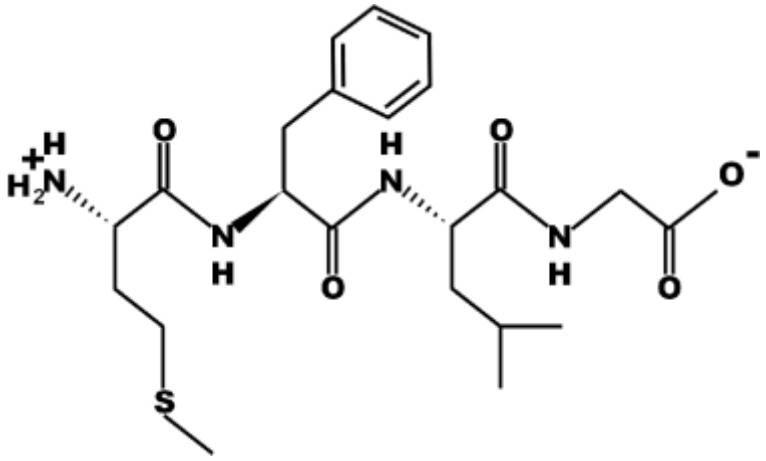

Figure 5-10 The molecular structure of the peptide MFLG

5.3.4 ORAC assay

The ORAC TE data for the synthetic peptides plus LG (**Figure 5-13**), that was derived from the data represented in the fluorescent traces (**Figure 5-11 and Figure 5-12**), indicated that FWG had a greater oxygen radical scavenging activity than Trolox (12.5 µM of FWG is equivalent to 19.2 µM of Trolox). For MFLG, 12.5 µM is equivalent to 6.47 µM of Trolox. Both these peptides were soluble in aqueous solutions. The other synthetic peptides plus LG gave a negative value at these concentrations; this indicated that at these concentrations they do not perform as oxygen radical scavengers. TE (**Table 5-11**) were calculated from these data.

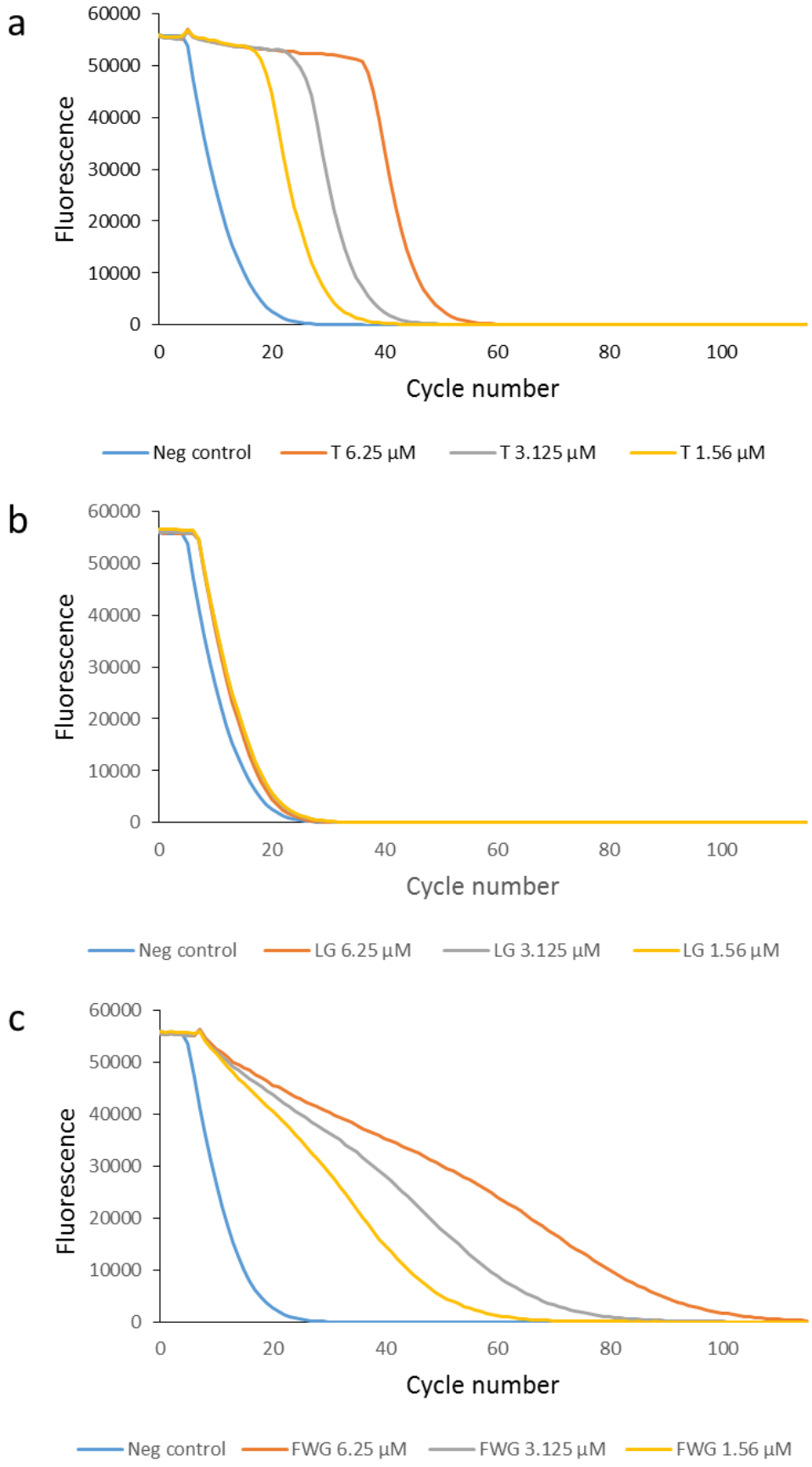

Figure 5-11 ORAC fluorescent traces for Trolox (a), LG (b), and FWG (c)

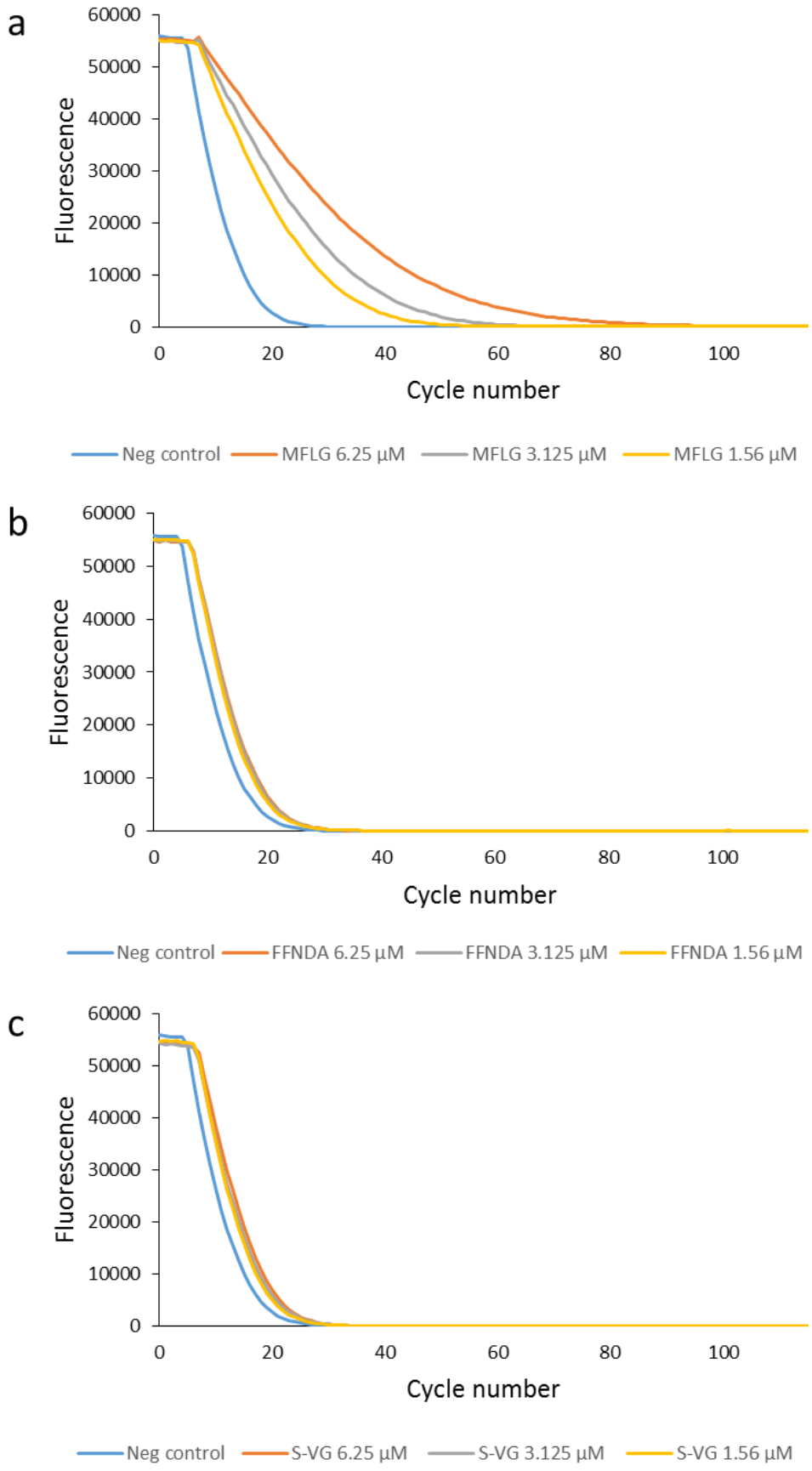

Figure 5-12ORAC fluorescent traces for MFLG (a), FFNDA (b), and SDPPLVFVG (c)

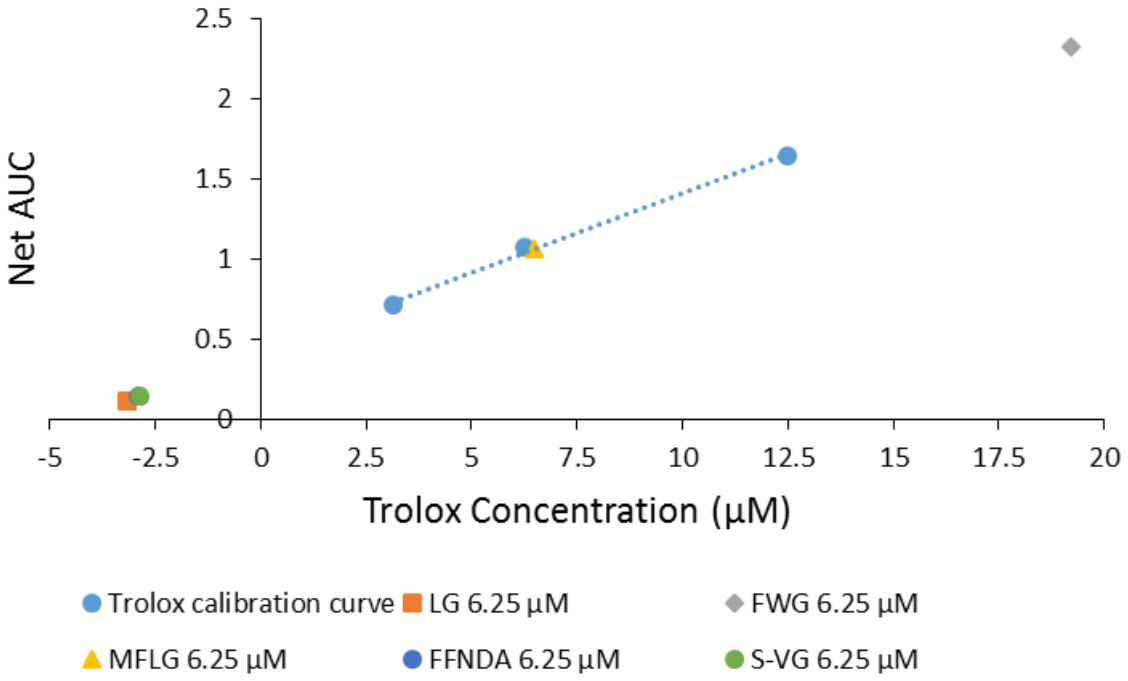

Figure 5-13 ORAC Trolox standard curve with the activity of the peptides at 12.5 µM plotted on the curve showing equivalence to Trolox concentration

Table 5-11 Trolox equivalent (TE) values for synthetic peptides

Peptides	TE
LG	9.09
FWG	0.43
MFLG	0.94
FFNDA	7.19
SDPPLVFVG	7.14

5.3.5 Cellular antioxidant activity assay (CAA)

The initial results for the CAA of the synthetic peptides indicated that they all demonstrated antioxidant activity, which is concentration dependant. All the test samples demonstrated some protection of the DCFH when oxidative stress was introduced (slower rate of fluorescence increase than the control) **(Figure 5-14)**. FWG demonstrated the greatest antioxidant activity at 50 µM, this was significantly greater than FFNDA, and SDPPLVFVG, however, the difference with MFLG was not significant. At 25 µM, there was no significant difference in antioxidant activity between the samples (**Figure 5-15**).

Trolox control was assessed alongside the hydrolysate samples (section 4.3.4). The concentration of Trolox was reported in mg/mL (data not shown). To compare it to the synthetic peptides, 50 µM of Trolox is equal to 12.5 µg/mL, 6.25 µg/mL (25 µM) gave a CAA of 34.1%. This is in a similar range as the synthetic peptides

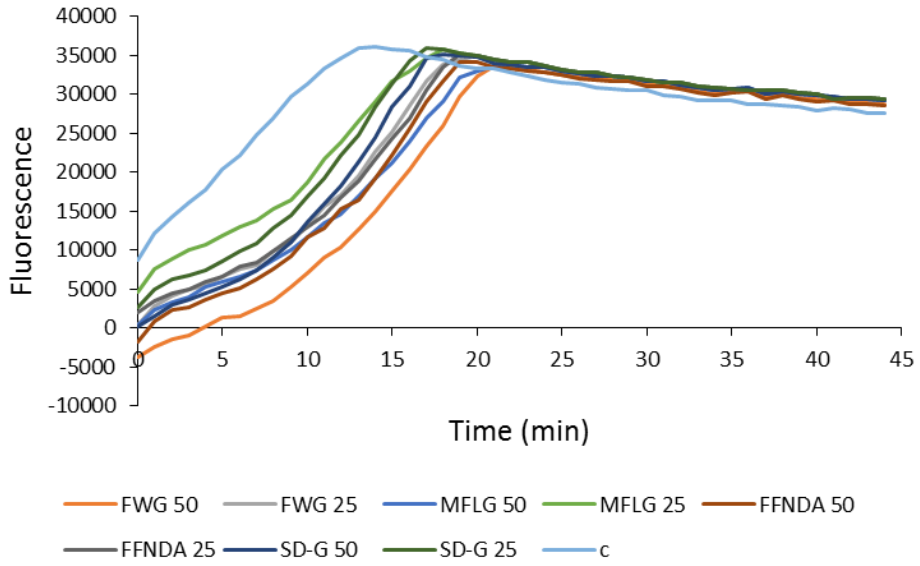

Figure 5-14 Fluorescence over time for synthetic peptides. The cellular antioxidant activity (CAA) of each sample is derived by comparing the area under the curve (AUC) of the samples to the AUC of the negative control (c)

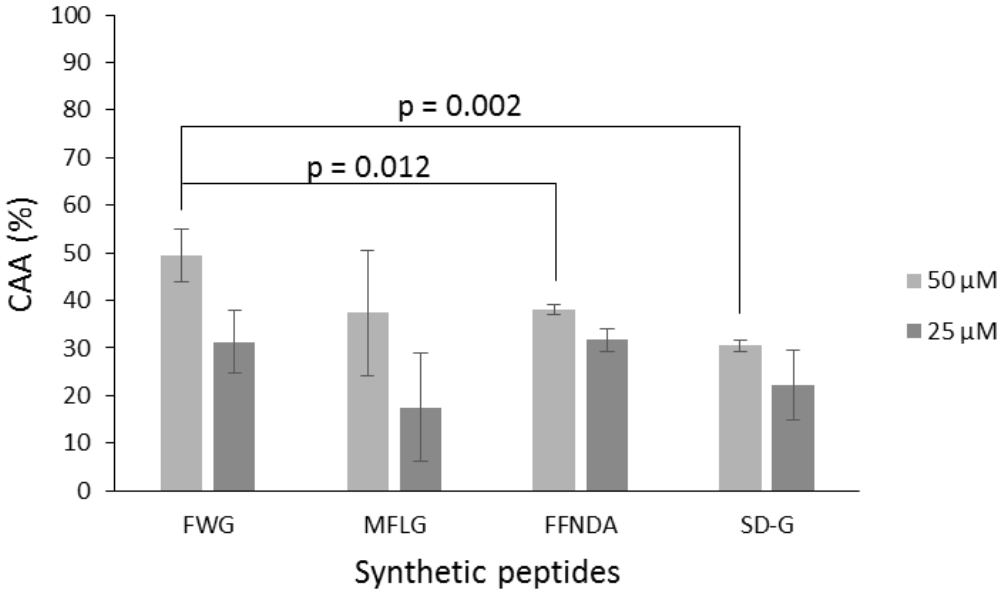

Figure 5-15 Cellular antioxidant activity (CAA) (%) of synthetic peptides with significant results highlighted

5.3.6 MTT Cell proliferation assay

The MTT results used to generate cell proliferation data indicated that there was no significant increase in cell proliferation for the peptide treated samples. Moreover, FWG, and SDPPLVFVG treated samples appeared to reduce proliferation at when treated at a concentration of 100 µM, **Figure 5-16 a, and c.**

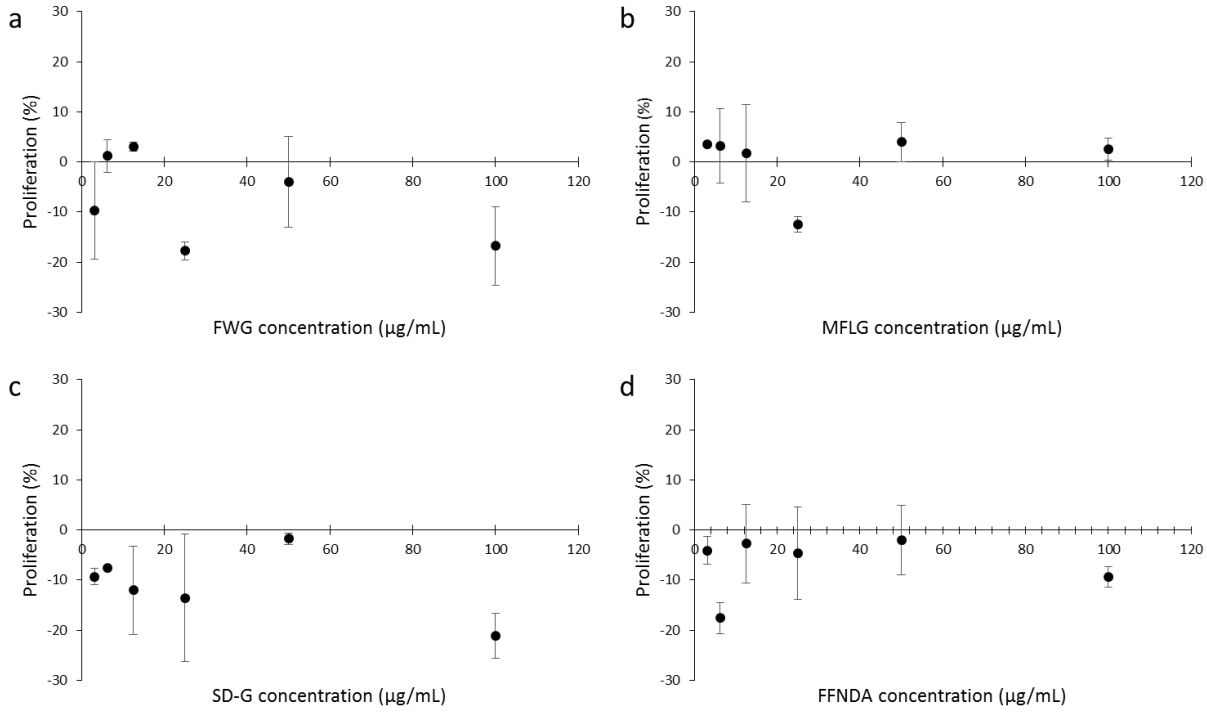

Figure 5-16 Cell proliferation data derived from (3-(4,5-Dimethylthiazol-2-yl)-2,5-Diphenyltetrazolium Bromide) (MTT) assay (percent proliferation relative to the control group) for synthetic peptides FWG (a), MFLG (b), SDPPLVFVG (c), and FFNDA (d)

5.3.7 Scratch assay

The potential wound healing properties of the peptides were investigated using the scratch assay. The data generated from the assay were used to calculate the rate of wound closure over 32 hours (all wounds had closed up by 38 hours). The rate of wound closure ($\mu m^2/h$) (**Figure 5-17**) for the samples treated with the synthetic peptides FWG, MFLG, and FFNDA were significantly less than the control groups. This indicates that at the concentrations used for this assay these peptides reduced cell taxis. SDPPLVFVG showed a significant increase in relation to the control group.

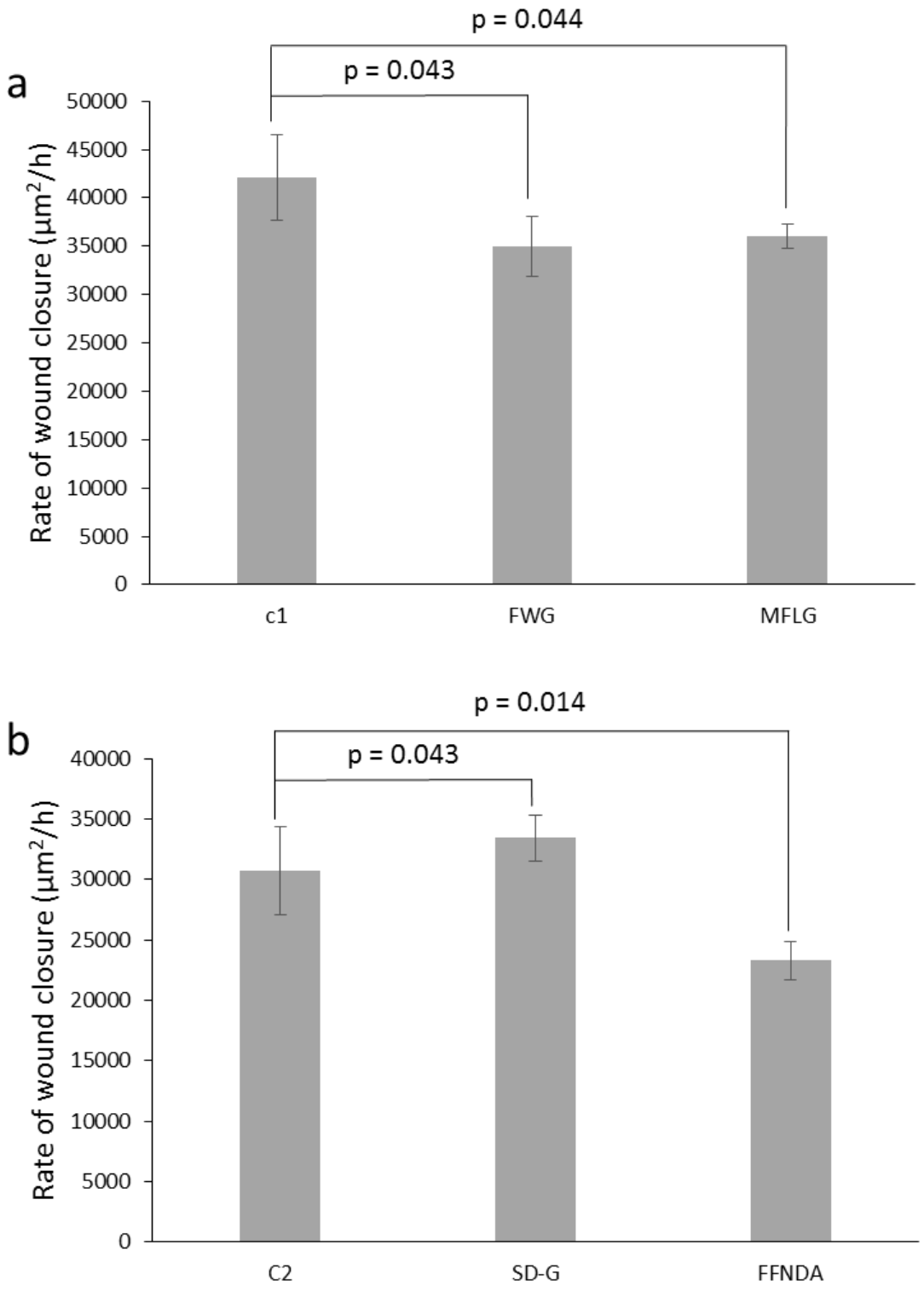

Figure 5-17 Rate of scratch wound closure over 32 hours with control groups (c1, and c2) (no peptide); FWG, and MFLG with control (c1) (a), and SDPPLVFVG, and FFNDA with c2 (b)

5.3.8 ACE inhibition assay

The synthetic peptides, and the hydrolysates had some inhibitory activity on ACE, which was concentration dependant. **Figure 5-18** shows the percentage inhibition on ACE of the synthetic peptides. MFLG, and FWG showed a greater inhibitory effect than SDPPLVFVG, and FFNDA. SDPPLVFVG, (FFNDA was not assayed at 2 mM because there was not enough sample to prepare this concentration). All synthetic peptides tested showed considerably less ACE inhibition activity than captopril (0.1 µM of captopril showed a percentage reduction of ACE activity of 98.7%, and 0.01 µM showed a percentage reduction of 88.7% data not shown).

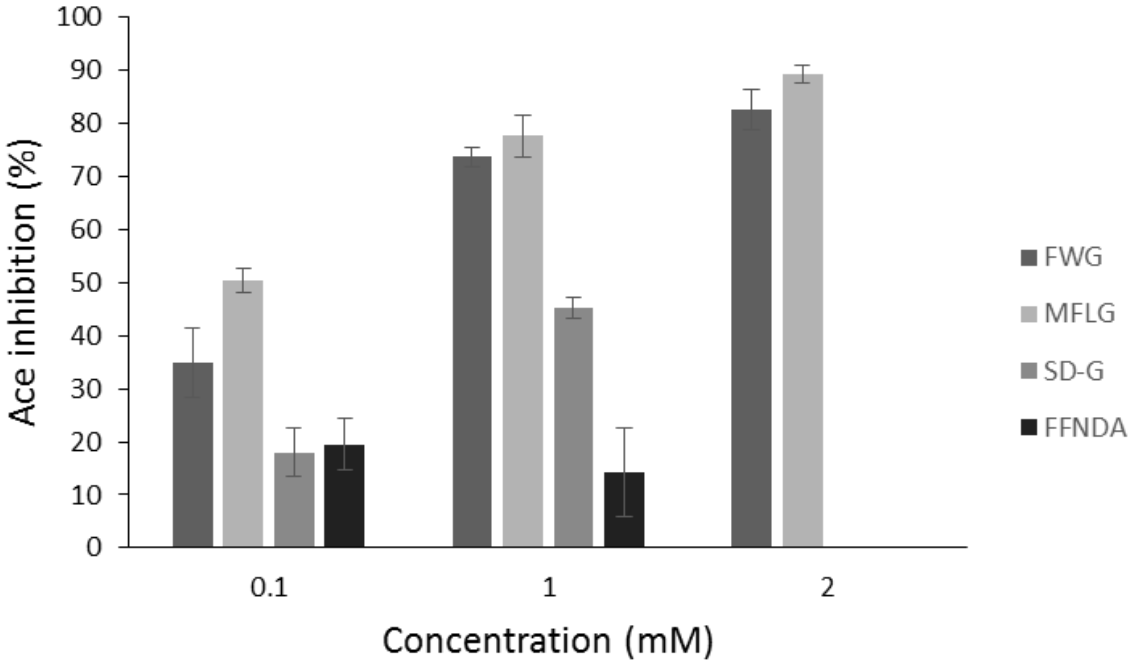

Figure 5-18 Percentage inhibition of angiotensin II converting enzyme (ACE) by the synthetic peptides FWG, MFLG, SDPPLVFVG, and FFNDA

5.4 Discussion

The aim of this section of the project was to develop a method that could identify bioactive peptides that were likely present within the Biofac porcine liver, and placenta hydrolysates. Other studies have used similar techniques to analyse bioactive peptides but they generally start from peptides that have been isolated from active fractions (Lassoued et al., 2015, Lafarga et al., 2014, Cheung et al., 2009). This method was designed as a more high-throughput approach. By sequencing straight after the initial separation, and using the BIOPEP database and Peptide Ranker utilities, it is possible to identify bioactive peptides before bioactivity assays are performed. That being said, it has been reported that there are significant differences in the predicted bioactive peptides, and actual peptides found using empirical methods (Chatterjee et al., 2015). This can be explained by the incomplete nature of these bioactive peptide databases, however, as the aim was to identify bioactive peptides that were not already in the databases, this was not a concern. There is therefore, a chance that the peptides released from experimental enzyme digestion could be different to the predicted peptides. This could be the result of miss-cleavage because of varying quality of the enzymes used (Burkhart et al., 2012). There is likely to be non-specific cleavage associated with the experimental process, therefore the complexity of the peptide profile of the hydrolysates cannot be just accreted to the specific enzyme used (in this case papain) (Picotti et al., 2007). However, if it is likely that a predicted peptide will be present, as in the case of this investigation, the overall complex nature of the hydrolysate is not a major concern.

The method of using the host protein as a starting point for *in silico* enzymatic cleavage was developed because the chance of identifying a bioactive peptide from the HPLC MS/MS process is slim. It does not appear to be an efficient way of uncovering bioactive peptides directly through HPLC, and sequencing. All the peptides that were reported from the MS/MS data when processed by the BIOPEP data base showed no similarities with reported bioactive peptides, and when they were analysed using the Peptide Ranker tool by Bioware all the peptides were predicted to have a low probability of being bioactive. While it was likely that no potential bioactivity was present in the peptides identified through MS/MS (section 5.3.2), the information about the host proteins was used in the *in silico* analysis in the

hunt for possible bioactive peptides. The Biofac hydrolysate are produced in a certain way using the same type of raw material. While it cannot be said that all the samples will be homogeneous, it is likely that a similar process will produce comparable results. By identifying the host protein, it can be argued that a particular bioactive peptide is likely to be present in the hydrolysate. Further analysis of the hydrolysates can then uncover further host proteins, ultimately generating a full-predicted profile for the product.

The assays used to analyse the synthetic peptides were selected because they were used for the analysis of the crude hydrolysates, however, this method could be used to tailor assays to the peptides/hydrolysates rather than blindly selecting an assay based on what may be useful. An example of this is the prevalence of ACE inhibitors identified in the hydrolysates. The basic structure of ACE inhibitors, and how they work are well known (Wu et al., 2006, Vulupala et al., 2018). This information therefore, can be used to select un-reported peptides that score highly on the peptide ranker tool, that have similar attributes to known ACE inhibitors.

The data generated from the antioxidant assays (ORAC, and CAA) indicated that the prediction of bioactivity using the peptide ranker tool could supply useful results. As mentioned previously, the group that developed Peptide Ranker discovered that in small peptides (< 20 amino acids), the presence of phenylalanine (F) was linked with bioactivity (Mooney et al., 2012). All the peptides selected to be synthesised contained phenylalanine. This could be related to the bioactivity demonstrated by FWG, and MFLG. The ORAC assay indicated that the two peptides that ranked the highest, FWG (1), and MFLG (0.96), were significantly more potent antioxidant compounds than FFNDA (0.77), and SDPPLVFVG (0.75). The Trolox equivalent value for FWG was 0.43. This means that for the peptide to exhibit the same ORAC value as 1 g of Trolox, 0.43 g of FWG would be required, indicating that FWG is a more potent antioxidant than Trolox. MFLG demonstrated a TE of 0.94, therefore, has a similar antioxidant capacity to Trolox. The TE for FFNDA, and SDPPLVFVG were 7.19, and 7.14 respectively. These scores are both relatively high, so they may exhibit some other bioactivity that is not related to the ORAC assay. This method does indicate that the bioactivity prediction for FWG and

MFLG is related to antioxidant activity, but this does not mean that these peptides could not demonstrate any other bioactivity. The CAA data showed that all the peptides demonstrated antioxidant activity that were similar to Trolox, with only FWG at 50 µM showing significantly more activity between the peptides. All other samples were not significantly different (**Figure 5-15**). The data from the antioxidant assays demonstrate that the predicted bioactivity is in some part related to antioxidant activity. The differences between the two antioxidant assays can be explained by the antioxidant mechanism of each assay. There is a great variety in mechanisms of oxidative stress, and antioxidant activity, and this is reflected in the types of *in vitro* assays used to for analysis. Two different assays may use completely different mechanisms, and compounds may generate different results. Therefore, compounds can only be determined as antioxidant in relation to a particular mechanism. For example, FWG and MFLG displayed potent antioxidant properties when measured using the ORAC assay, but all four of the synthetic peptides tested were potent antioxidant peptides when analysed using a more complex system. This would indicate that the mechanism of antioxidant activity is different for FWG and MFLF from FFNDA, and SDPPLVFVG. The CAA assay is therefore a good method to test antioxidant activity because it uses cells, and their entire metabolism to assess activity (López-Alarcón and Denicola, 2013).

All samples tested reduced the activity of ACE. There were significant differences between two groups of the synthetic peptides. FWG and MFLG showed greater activity than SDPPLVFVG, and FFNDA. At the lowest concentation tested (0.1 mM), MFLG showed significantly more activity than FWG, this was not shown in the other concentrations (1 mM and 2 mM). SDPPLVFVG and FFNDA were not assayed at 2 mM because there was not enough of these peptides to generate data at that concentration. Both FWG and MFLG were freely soluble in aqueous conditions whereas SDPPLVFVG and FFNDA were not as soluble. This may be linked with the lower anti-ACE activity demonstrated with these peptides. This could also be the reason that FFNDA, and SDPPLVFVG, did not show activity relative to FWG, and MFLG despite all of the peptides containing phenylalanine.

When the data from the synthetic peptides were compared to the anti-ACE activity of the hydrolysates from which they were derived (data not shown), it was clear that the placenta hydrolysate out performs the synthetic peptides in inhibition of ACE. It would appear that because the placenta hydrolysate contains a large proportion of di-peptides, it has a greater effect on ACE inhibition.

Captopril is by some margin a more potent ACE inhibitor than any of the samples tested here with 0.1 µM able to cause a reduction in ACE activity of 98.7%, and even at a concentration of 0.01 µM showed a percentage reduction of 88.7%. The fact that the synthetic peptides are less potent than captopril is not surprising when looking at the structure of the synthetic peptides in comparison to designed ACE inhibitors. The synthetic peptides were not selected because they were likely to be potent anti-ACE compounds, but due to potential bioactivity. It is clear that while they do show anti–ACE activity, it is not very high in comparison to other ACE inhibitors therefore the prediction of activity is unlikely to be associated with ACE inhibition. To compare the synthetic peptides used in this study to peptides used in similar investigations from the literature, the IC_{50} (Inhibitory Concentration at 50 %) values of each were calculated **(Table 5-12**). It is useful to express these data as IC_{50} because it can be difficult to determine the point at which a substance is 100 % effective.

Table 5-12 Inhibitory Concentration at 50 %(IC_{50}) values for the synthetic peptides

Peptide	ACE inhibition IC_{50} µM
FWG	470
MFLG	70
SDPPLVFVG	1160
FFNDA	830

The review by Vercruysse et al. (2005), aimed to investigate ACE inhibitory peptides derived from animal muscle protein. Selected data from this review (**Table 5-13**) shows the peptides that were generated from porcine muscle. The ACE inhibitory IC_{50} values of these peptides ranged from 34 to > 1000 µM. The peptides synthesised in the present study mostly fall within this range, with MFLG (70 µM) showing the greatest activity. Another example of an ACE inhibitory peptide reported in the

literature reviewed for this thesis was the study carried out by Himaya et al (2012). The peptide (LLMLDNDLPP) was derived from pacific cod skin gelatin. The IC_{50} value was reported to be 35.7 µM, with the authors suggesting that the prolines at the carboxyl end being important to the activity of the peptide.

Table 5-13 Examples of angiotensin II converting enzyme (ACE) Inhibitory Concentration at 50 % (IC_{50}) values for peptides derived from porcine muscle. Data in the review 'ACE Inhibitory Peptides Derived from Enzymatic Hydrolysates of Animal Muscle Protein' (Vercruysse et al., 2005)

Peptide	Parent Protein	Enzyme	ACE inhibition IC50 µM
ITTNP	myosin	thermolysin	549
MNPPK	myosin	thermolysin	945.5
MNP	myosin	synthesized	66.6
NPP	myosin	synthesized	290.5
PPK	myosin	synthesized	>1000
ITT	myosin	synthesized	678.2
TTN	myosin	synthesized	672.7
TNP	myosin	synthesized	207.4
RMLGQTPTK	troponin C	pepsin	34
RMLGQTP	troponin C	pepsin	503

The data sets reported here, from these two separate studies indicate that the peptide MFLG is comparable in terms of ACE inhibition. The method used to select the synthetic peptides could be used to focus on peptides that are more likely to have anti-ACE activity. The hydrolysate itself could be further investigated by using HPLC to create fractions, which could then be tested using this assay, as it is likely that there are potent anti-ACE peptides within the hydrolysate.

Data generated for the investigation into wound healing (cell proliferation (MTT), and chemotaxis (scratch assay)) indicated that the synthetic peptides show no effect. Both sets of data show that cells treated with the peptides did not propagate, or migrate differently to untreated cells. The predicted activity of these peptides is therefore, not likely to be related to wound healing.

5.5 Summary

The work carried out on the identification of potential bioactive peptides shows that it is possible to identify active peptides using the method developed in this study. The results indicated that the predicted bioactivity of the synthetic peptides would likely include antioxidant activity. FWG and MFLG showed activity better or comparable to Trolox in the ORAC assay, while all the peptides showed comparable activity to Trolox in the CAA assay. Of the other assays used in this project, the ACE assay demonstrated that the predicted bioactivity could be related to ACE inhibition, and that there is no evidence to support wound healing activity.

The information on the anti-ACE, and antioxidant activity of the peptides that were synthesised, and the examples of peptides that have been reported in bioactive peptide databases, indicate that there are multiple active peptides within the Biofac hydrolysates. Further analysis of the samples could lead to better profiling of the hydrolysates, so the approximate amounts of the active peptides can be predicted for the individual products. A good example is the large proportion of active dipeptides in the placenta hydrolysates. This could be then developed into a supplement that can be taken to reduce hypertension.

CHAPTER 6 **General Discussion, Future Work and Conclusions**

6.1 Original Project Aims

The original aim of this project was to investigate the physicochemical properties, and bioactivity of hydrolysates derived from porcine heart, liver, and placenta. These hydrolysates were produced by Biofac as commercial products to add monetary value to material that would otherwise be disposed of as waste. This not only generates income from the sales of the product, but also removes the cost of processing the waste. With a view to increasing the value of the hydrolysates, this project aimed to identify, and assign specific bioactivities of the peptides within the hydrolysates. The methods used to analyse the hydrolysates were selected because they represented common bioactivities investigated in other studies recorded in the literature, namely antioxidant activity, anti-ACE activity, and wound healing. Other potential bioactivities that have been previously reported in the literature for similar peptides that were not investigated in this study are antimicrobial, and immunomodulating activity. The assessment of these particular bioactivities would be a logical extension to the work carried out in this thesis.

The overall findings of the investigation into the bioactivity profiles of the hydrolysates were that the liver samples (L1, L2 and L3) demonstrated greater antioxidant activity than the placenta samples (P1 and P2) (section 4.4.1), and that the placenta samples outperformed the liver in anti-ACE activity (section 4.4.5). For reasons discussed previously, the investigation into the heart hydrolysate was not continued beyond the antioxidant activity (assayed using the DPPH, and lipid peroxidation method). The difference in antioxidant activity between the liver, and placenta hydrolysates was attributed to the greater proportion of proton donor residues within the liver hydrolysates compared to the placenta (section 4.4.1). The diverse mechanisms of antioxidant activity, as discussed, do not all rely on this particular facet but proportion of proton donors present is definitely a reason behind the difference. Despite the greater activity demonstrated by the liver samples overall, the placenta samples did perform similarly to the liver in the lipid peroxidation (section 4.3.3), and the CAA assays (section 4.3.4). Indeed, the results for the CAA assay indicated that the placenta samples (P2) performed better than the

liver (L2). The reason for this can be attributed to the greater proportion of smaller peptides within the placenta hydrolysates (section 4.3.6). One of the most important factors in bioactive peptides (and all pharmaceutics in general) is the ability of the target compound to be able to reach the desired area in the body (bioavailability). Where the chemical based assays do not have this limitation, the CAA assay does, whereby the peptides need to either interact with the membrane, or pass through the membrane into the cytoplasm. Large molecules such as peptides do not readily diffuse across cell membranes, but small, hydrophobic peptides should pass through more easily. An example of a cellular mechanism that allows small peptides (di, and tri-peptides) is the oligopeptide transporter PepT1 (Yang and Hinner, 2015).

The greater proportion of small peptides in the placenta hydrolysate (P2) can also be attributed to the greater anti-ACE activity demonstrated by P2 when compared to the liver hydrolysate L2 (section 4.3.9). The performance of P2 in the ACE inhibition assay suggests that it is the multitude of di-peptides that are likely to be present (section 4.3.7.2). The databases of known bioactive peptides, which have anti-ACE activity (such as BIOPEP) consist mainly of di-peptides. The *in silico* work carried out for this project identified a number of known di-peptides derived from the host proteins with anti-ACE activity (**Table 5-1, Table 5-2, Table 5-3, Table 5-4, and Table 5-5**), therefore, it is likely that similar sequences are present in the full hydrolysate.

6.2 High throughput screening method development

Over the course of this study, the analysis of the bioactivity of the hydrolysates shifted from screening the full hydrolysates to the identification of active components contained within the hydrolysates. This is a common theme in the literature where research is aimed at identifying specific sequences isolated from fractions of hydrolysates that were found to be bioactive. For this study a method that used a different tactic was developed, favouring a more theoretical approach that identified peptides that were both likely to be present in the hydrolysates and demonstrate some activity, rather than using empirical methods.

The rationale behind this was to develop a high throughput screening method that could be used to determine a good source of bioactive peptides without performing some or all of the steps reported in the literature. In the case of the Biofac hydrolysates, *de-novo* sequencing was performed to discover the host protein of an isolated peptide, but this step could be removed when analysing possible protein sources, of which the constituent protein is known (chickpeas for example, see section 6.4). The *de-novo* sequencing step could also be removed from subsequent analysis of the Biofac hydrolysates, however, this would require further work to confirm that common proteins found in the starting material (porcine organs) relate to the peptides found in the finished product.

The peptides that were synthesised from the data generated through this method were analysed using the same techniques that were applied to the full hydrolysates. The results indicate that the use of activity prediction algorithms did result in bioactive peptides. Like the full hydrolysates, only antioxidant activity, and anti-ACE activity were found in the peptides. FWG, and MFLG showed the greater antioxidant activity overall (FFNDA, and SDPPLVFVG performed poorly in the ORAC assay (section 5.2.5) but showed similar activity in the CAA assay (section 5.5.6)). They also showed the greater activity in the anti-ACE assay (5.3.7). It is likely that there is other activity, which these peptides will show, however, one of the limitations of the method is the inability of the Peptide Ranker algorithm to predict the specific type of activity. There are other algorithms that can be found that concentrate on specific activities, for example, AHTpin is an anti-ACE peptide predictor (Kumar et al., 2015), AntiCP is an anti-cancer peptide predictor (Tyagi et al., 2013), and AntiBP is an anti-microbial predictor (Lata et al., 2007). The use of these, alongside a robust range of assays that cover a wider range of bioactivities would be a way of improving the discovery of novel bioactive peptides.

6.3 Future Work

The investigation into the bioactivity of the hydrolysates supplied by Biofac began with researching the full hydrolysates along with the physicochemical properties of the powders. The study progressed onto the molecular make-up of selected peptides that constitute the hydrolysates and subsequently, led to the development of the method described in section 5.2.3. Future work that could be carried out following

on from this investigation would likely follow a similar direction as described in this thesis. This would likely involve the further investigation into the physicochemical attributes, the continuation of bioactivity assays on the full hydrolysates, and extending the work carried out on the screening methods developed in chapter 5. The method could also be applied to new sources of peptides, that could be of interest to Biofac.

The investigation into the physicochemical properties of the hydrolysates was performed to gain a basic understanding of the materials physical behaviour and was not designed to be a comprehensive study applied to a specific functionality. This therefore, leaves scope to investigate these properties in relation to production methods (are the drying processes the ideal methods), and maybe more interestingly formulation of potential dosage forms. If a certain bioactivity can be associated with the current or future products, understanding how they can be developed to successfully administer the products would also be worthwhile.

The range of bioactivities that were used during this study could be extended to include the study of activities not investigated for this project such as antimicrobial, and immunomodulation as discussed in chapter 1, and investigate activities such as antioxidative, and anti-ACE using different assays to gather a more complete picture of bioactivity of the hydrolysates.

The synthetic peptides that were derived from the work carried out for chapter 5 were analysed to a certain degree, but there are more assays that could be used to analyse bioactivity that have not been used in this study. An important factor that was not investigated in this study was the structure activity relationship (SAR) of the synthetic peptides in relation to their bioactivity. While the presence of phenylalanine in the peptides was an indication that they were bioactive, the relationship to the other amino acids in the sequence was not studied (Mooney et al., 2012). The SAR of bioactive peptides can be demonstrated by the activity of the peptide being compared with a mixture of its component amino acids. This was demonstrated by Chen et al (2015) where they analysed the antioxidant activity of peptides derived from defatted walnuts; when they analysed the amino acids that constituted these

peptides, no activity was found (Chen et al., 2015). This finding suggests that the sequence of amino acids in a peptide are vital to activity (Zou et al., 2016). The sequence of the amino acids in the peptides investigated in this project could explain the differences in activity in conjunction with other factors such as solubility, and the peptide being amphiphilic (Zou et al., 2016). Another important factor with sequence is how the amino acids interact with its adjacent partner. Bamdad et al (2015) demonstrated that if a glutamic acid is next to a tyrosine, the second carboxyl side chain can cause a proton to be released from the phenolic hydroxyl in tyrosine. This change in the the tyrosine residue, facilitated by its conjunction with glutamic acid increases the antioxidant activity of the peptide (Bamdad et al., 2015). Future investigation into the peptides generated in this project, and those that could be derived through *in silico* digests using different enzymes would benefit from studying possible SARs of said peptides.

The investigation into the theoretical bioactive peptides from the *in silico* protease digestions only used synthesised peptides that were the product of papain digestion, however, other enzymes were used (bromelain, trypsin, and pepsin). The data gathered from these enzymes could also be investigated using the same method. More importantly, this method could be applied to different sources of proteins such as the one described in section 6.4 that looks at the possibilities of using chickpeas as the protein source. Using a less complex hydrolysate, or isolating proteins from the raw material prior to hydrolysation, would be a logical step in proving the concept of the screening method. Finally, the use of more specific peptide activity prediction algorithms, like the ones discussed in section 6.2, after the initial use of Peptide Ranker could refine the method, and increase the chance of identifying a novel bioactive peptide.

6.4 Theoretical digestion of proteins found within chickpeas

Chickpeas are a prominent target for bioactive peptide research. Numerous studies have been undertaken on peptides isolated from chickpea hydrolysate, some of which have been discussed in this study (Xue et al., 2012, Xue et al., 2015). Three important globulin proteins present in chickpeas are legumin 11S, vicilin 7S, and convicilin 15S (Schwenke, 2001). For this demonstration of the method developed here, legumin 11S was selected as the protein of interest, and trypsin chosen as the enzyme.

The known sequences identified as bioactive by the BIOPEP database (**Table 6-1**) follow the trend found in the digestions performed for the proteins derived from the Biofac hydrolysates, namely being short (2 to 3 residues), and demonstrating anti-ACE activity. The peptides sequences that have not been reported on the BIOPEP database are represented in **Table 6-2**.

Table 6-1 Know bioactive peptides generated from trypsin digest of chickpea legumin 11S

Sequence	Name	Function	Activity
PR	ACE inhibitor	Inhibitor of Angiotensin-Converting Enzyme (ACE) (EC 3.4.15.1) (MEROPS ID: XM02-001)	ACE inhibitor
LHR	synthetic peptide		antioxidative
LR	ACE inhibitor	Inhibitor of Angiotensin-Converting Enzyme (ACE) (EC 3.4.15.1) (MEROPS ID: M02-001)	ACE inhibitor
GR	ACE inhibitor	Inhibitor of Angiotensin-Converting Enzyme (ACE) (EC 3.4.15.1) (MEROPS ID: XM02-001)	ACE inhibitor
VR	ACE inhibitor from k-CN (fr. 67-68)	Inhibitor of angiotensin-converting enzyme (EC 3.4.15.1) (MEROPS ID: XM02-001)	ACE inhibitor
VR	dipeptidyl peptidase IV inhibitor (DPP IV inhibitor)	Inhibitor of Dipeptidyl Peptidase IV (EC 3.4.14.5) (MEROPS ID: S09.003)	dipeptidyl peptidase IV inhibitor
FR	ACE inhibitor		ACE inhibitor
FR	dipeptidyl peptidase IV inhibitor (DPP IV inhibitor)	Inhibitor of Dipeptidyl Peptidase IV (EC 3.4.14.5) (MEROPS ID: S09.003)	dipeptidyl peptidase IV inhibitor
YK	ACE inhibitor from wakame		ACE inhibitor
YK	dipeptidyl peptidase IV inhibitor (DPP IV inhibitor)	Inhibitor of Dipeptidyl Peptidase IV (EC 3.4.14.5) (MEROPS ID: S09.003)	dipeptidyl peptidase IV inhibitor

Table 6-2 Un-reported peptides generated from trypsin digest of chickpea legumin 11S

Un-Reported Peptides from Tryptic Digest of Chickpea Legumin 11S	
MAAPPSMLWLLLLALLVLGVR	HIER
GEAE	VSQQR
EALSER	QQGQGLHIR
R	GQLDIPHPR
DACNR	GEESQQYYEPEYEEEEEEDEYK
LSNR	EEEEEYPCER
GIHPR	GSGNGVAEEGSCSMR
DPSQFPNR	QSLNR
SH	ADNADIYVR
GGTLQYASPADANMTDLDCAGVALLR	GAGR
EIIR	VNLANALK
PYSLSR	MPALQVVGLAADYVK
YSNAPHLLYVER	LER
GSGLLGIVTPGCPTTFR	GAMFAPSFVVNAHR
NPFATPSCPHR	IMYVTR
EEDR	IQIVDDK
PYDYESESER	VFSGEVR
ESEYEYEEEEEDEHETR	QGQFLLIPQNFAAVK
QR	EATAQIFEWVAFLTDGR
QQQEQEQGQEK	PLR
EGDTCQK	EQLVGR
VK	NSLIQSMPR
EGDLVVIFAGNTFWLDNDNPSQELR	QVVAATCGIR
LVAIVDVSNNQNQLDR	GNEAEQLIGSR
TFLVSGEAR	QQTVGPILTPPSSYYYSR
LESEEGGEEGGVSR	SSSSSR
GVLQGFSNDVLQR	TYPEDLDSTTESQTTETETK
ALDIGNTTILR	TEAETETEAEAQTETQPVT

The sequences generated from the *in silico* tryptic digest of chickpea legumin 11S, alongside MFLG, FFNDA, and SDPPLVFVG, were analysed using Peptide Ranker (Mooney et al., 2012), and the AHTpin tool (Kumar et al., 2015), which predicts the likelihood of a peptide sequence demonstrating anti-ACE activity. The predicted scores (**Table 6-3**) indicate that the peptide MAAPPSMLWLLLLALLVLGVR from legumin 11S would have a 98% chance of being bioactive, with a 72% chance of demonstrating anti-ACE activity. For comparison, the three synthetic peptides

tested that were made for this study ranked lower. Interestingly, MFLG ranked lower than FFNDA, which is a contradiction to the data generated in this study (the greater solubility of MFLG is the likely reason for this). This highlights the importance of empirically testing the peptides as well as running the simulation.

Table 6-3 The probability of general activity (using Peptide Ranker (Mooney et al., 2012)), and anti-angiotensin II converting enzyme (ACE) activity of Selected peptides from the tryptic digest of chickpea legumin 11S , and three of the synthetic peptides produced for this study (yellow highlighted) using the AHTpin is an anti-ACE peptide predictor (Kumar et al., 2015)

Peptide	Activity prediction	anti-ACE prediction
MAAPPSMLWLLLLALLVLGVR	0.98	0.72
GAGR	0.56	0.3
MFLG	0.98	0.61
FFNDA	0.77	0.69
SDPPLVFVG	0.75	0.58

This example demonstrates that in a relatively short period of time, a large amount of sequences can be identified, and screened. The use of the general ranking algorithm, Peptide Ranker indicated that MAAPPSMLWLLLLALLVLGVR is extremely likely to be bioactive. The type of activity has then been narrowed down using a more specific programme. The peptide of interest can then be synthesised, and assayed using an ACE inhibition assay such as the one described in this study.

6.5 Conclusions

The Biofac hydrolysates all exhibited antioxidant activity to a certain extent, depending on the mechanism of action of the assay used for analysis. All batches of hydrolysates tested with the lipid peroxidation assay for example reduced autoxidation in linoleic acid, there were however major differences between the batches demonstrated in the other antioxidant assays. In general, it can be said that liver hydrolysates performed better than placenta, the overall order being L1 > L2 > L3 > P2 > P1. The other significant area of bioactivity demonstrated in the hydrolysates was anti-ACE. Here the placenta hydrolysate P2 outperformed the liver hydrolysates L2, and L3, which had very similar activities. It should be noted that the levels of activity were much lower than that of the ACE inhibitor captopril, but the complex nature of the hydrolysates might lead to the active components (most likely dipeptides) being greatly diluted. These sets of data indicate that there is evidence that the hydrolysates, can be protective against oxidative stress, and hypertension, however, *in-vivo* studies would be required to ensure the peptides are bioavailable and to determine whether the activity was at therapeutic levels.

The data generated through the characterisation, and identification of the peptides within the hydrolysates indicate that there is a possibility to further refine the hydrolysates to isolate more active components. This information could be used to either extend the manufacturing process at Biofac to create a product with greater value, or be used by the customers of Biofac in their own use of the products.

Finally, the method used to predict the presence of bioactive peptides within hydrolysates utilising *de-novo* sequencing, and *in silico* analysis tools shows promise in the discovery of new bioactive peptides. This method could identify interesting potential targets before the time consuming process of discovering them empirically. The time constraints on this study led to only a small number of peptides being investigated in this fashion, but it is likely there are multiple undiscovered bioactive peptides present within the Biofac samples.

CHAPTER 7 **References**

AHMED, A. S., EL-BASSIONY, T., ELMALT, L. M. & IBRAHIM, H. R. 2015. Identification of potent antioxidant bioactive peptides from goat milk proteins. *Food Research International,* 74**,** 80-88.

ALAM, M. N., BRISTI, N. J. & RAFIQUZZAMAN, M. 2013. Review on in vivo and in vitro methods evaluation of antioxidant activity. *Saudi Pharmaceutical Journal,* 21**,** 143-152.

ALBERTS, B., JOHNSON, A., LEWIS, J., RAFF, M., ROBERTS, K. & WALTER, P. 2008. *Molecular Biology of the Cell,* New York, Garland Science.

AMORATI, R. & VALGIMIGLI, L. 2015. Advantages and limitations of common testing methods for antioxidants. *Free Radical Research,* 49**,** 633-649.

ANDREU, D. & RIVAS, L. 1998. Animal antimicrobial peptides: An overview. *Peptide Science,* 47**,** 415-433.

ARIHARA, K., NAKASHIMA, Y., MUKAI, T., ISHIKAWA, S. & ITOH, M. 2001. Peptide inhibitors for angiotensin I-converting enzyme from enzymatic hydrolysates of porcine skeletal muscle proteins. *Meat Science,* 57**,** 319-324.

AYALA, A. M., M, F. ARGUELLES, S 2014. Lipid Peroxidation: Production, Metabolism, and Signaling Mechanisms of Malondialdehyde and 4-Hydroxy-2-Nonenal. *Oxidative Medicine and Cellular Longevity,* 2014**,** 31.

BAMDAD, F., AHMED, S. & CHEN, L. 2015. Specifically designed peptide structures effectively suppressed oxidative reactions in chemical and cellular systems. *Journal of Functional Foods,* 18**,** 35-46.

BANGA, A. K. 2015. *Therapeutic peptides and proteins: formulation, processing, and delivery systems*, CRC press.

BEERMANN, C., EULER, M., HERZBERG, J. & STAHL, B. 2009. Anti-oxidative capacity of enzymatically released peptides from soybean protein isolate. *European Food Research and Technology,* 229**,** 637-644.

BHUYAN, B. J. & MUGESH, G. 2011. Effect of peptide-based captopril analogues on angiotensin converting enzyme activity and peroxynitrite-mediated tyrosine nitration. *Organic & Biomolecular Chemistry,* 9**,** 5185-5192.

BOWDISH, D. M. E., DAVIDSON, D. J., SCOTT, M. G. & HANCOCK, R. E. W. 2005. Immunomodulatory Activities of Small Host Defense Peptides. *Antimicrobial Agents and Chemotherapy,* 49**,** 1727-1732.

BOXIN OU , M. H.-W., AND RONALD L. PRIOR 2001. Development and Validation of an Improved Oxygen Radical Absorbance Capacity Assay Using Fluorescein as the Fluorescent Probe. *Journal of Agricultural and Food Chemistry,* 49**,** 4619-4626.

BROWN, K. L. & HANCOCK, R. E. W. 2006. Cationic host defense (antimicrobial) peptides. *Current Opinion in Immunology,* 18**,** 24-30.

BRUMMEL, K. E., PARADIS, S. G., BUTENAS, S. & MANN, K. G. 2002. Thrombin functions during tissue factor–induced blood coagulation. *Blood,* 100**,** 148-152.

BURKHART, J. M., SCHUMBRUTZKI, C., WORTELKAMP, S., SICKMANN, A. & ZAHEDI, R. P. 2012. Systematic and quantitative comparison of digest efficiency and specificity reveals the impact of trypsin quality on MS-based proteomics. *Journal of Proteomics,* 75**,** 1454-1462.

CAPRIOTTI, A. L., CARUSO, G., CAVALIERE, C., SAMPERI, R., VENTURA, S., CHIOZZI, R. Z. & LAGANÀ, A. 2015. Identification of potential bioactive peptides generated by simulated gastrointestinal digestion of soybean seeds and soy milk proteins. *Journal of Food Composition and Analysis,* 44**,** 205-213.

CARNEVALE, R., PIGNATELLI, P., NOCELLA, C., LOFFREDO, L., PASTORI, D., VICARIO, T., PETRUCCIOLI, A., BARTIMOCCIA, S. & VIOLI, F. 2014. Extra virgin olive oil blunt post-prandial oxidative stress via NOX2 down-regulation. *Atherosclerosis,* 235**,** 649-658.

CHANDRUDU, S., SIMERSKA, P. & TOTH, I. 2013. *Chemical Methods for Peptide and Protein Production*.

CHATTERJEE, A., KANAWJIA, S. K., KHETRA, Y. & SAINI, P. 2015. Discordance between in silico & in vitro analyses of ACE inhibitory & antioxidative peptides from mixed milk tryptic whey protein hydrolysate. *Journal of Food Science and Technology,* 52**,** 5621-5630.

CHEN, H.-M., MURAMOTO, K., YAMAUCHI, F. & NOKIHARA, K. 1996. Antioxidant Activity of Designed Peptides Based on the Antioxidative Peptide Isolated from Digests of a Soybean Protein. *Journal of Agricultural and Food Chemistry,* 44**,** 2619-2623.

CHEN, H., ZHAO, M., LIN, L., WANG, J., SUN-WATERHOUSE, D., DONG, Y., ZHUANG, M. & SU, G. 2015. Identification of antioxidative peptides from defatted walnut meal hydrolysate with potential for improving learning and memory. *Food Research International,* 78**,** 216-223.

CHEN, Y., MANT, C. T., FARMER, S. W., HANCOCK, R. E. W., VASIL, M. L. & HODGES, R. S. 2005. Rational Design of α-Helical Antimicrobial Peptides with Enhanced Activities and Specificity/Therapeutic Index. *Journal of Biological Chemistry,* 280**,** 12316-12329.

CHEUNG, I. W. Y., NAKAYAMA, S., HSU, M. N. K., SAMARANAYAKA, A. G. P. & LI-CHAN, E. C. Y. 2009. Angiotensin-I Converting Enzyme Inhibitory Activity of Hydrolysates from Oat (Avena sativa) Proteins by In Silico and In Vitro Analyses. *Journal of Agricultural and Food Chemistry,* 57**,** 9234-9242.

CORRÊA, A. P. F., DAROIT, D. J., FONTOURA, R., MEIRA, S. M. M., SEGALIN, J. & BRANDELLI, A. 2014. Hydrolysates of sheep cheese whey as a source of bioactive peptides with antioxidant and angiotensin-converting enzyme inhibitory activities. *Peptides,* 61**,** 48-55.

CUSHMAN, D. W. & CHEUNG, H. S. 1971. Spectrophotometric assay and properties of the angiotensin-converting enzyme of rabbit lung. *Biochemical Pharmacology,* 20**,** 1637-1648.

CUSHMAN, D. W. & ONDETTI, M. A. 1991. History of the design of captopril and related inhibitors of angiotensin converting enzyme. 17**,** 589-592.

DANQUAH, M. K. & AGYEI, D. 2012 Pharmaceutical applications of bioactive peptides. . *OA Biotechnology,* 5.

DAOUD, R., DUBOIS, V., BORS-DODITA, L., NEDJAR-ARROUME, N., KRIER, F., CHIHIB, N.-E., MARY, P., KOUACH, M., BRIAND, G. & GUILLOCHON, D. 2005. New antibacterial peptide derived from bovine hemoglobin. *Peptides,* 26**,** 713-719.

DE MEJIA, E. G. & DIA, V. P. 2010. The role of nutraceutical proteins and peptides in apoptosis, angiogenesis, and metastasis of cancer cells. *Cancer and Metastasis Reviews,* 29**,** 511-528.

DELACROIX, S. C., R.G AND WORTHLEY, S.G. 2014. Hypertension: Pathophysiology and Treatment. *J Neurol Neurophysiol,* 5.

DEMIDOVA-RICE, T. N., GEEVARGHESE, A. AND HERMAN, I. M. 2011. Bioactive peptides derived from vascular endothelial cell extracellular matrices promote microvascular morphogenesis and wound healing in vitro. . *Wound Repair and Regeneration,* 19**,** 59-70.

DI BERNARDINI, R., HARNEDY, P., BOLTON, D., KERRY, J., O'NEILL, E., MULLEN, A. M. & HAYES, M. 2011. Antioxidant and antimicrobial peptidic hydrolysates from muscle protein sources and by-products. *Food Chemistry,* 124**,** 1296-1307.

DOSTAL, D. E. & BAKER, K. M. 1999. The Cardiac Renin-Angiotensin System. Conceptual, or a Regulator of Cardiac Function? *Circulation Research,* 85**,** 643-650.

DUBOIS, M., GILLES, K. A., HAMILTON, J. K., REBERS, P. A. & SMITH, F. 1956. Colorimetric Method for Determination of Sugars and Related Substances. *Analytical Chemistry,* 28**,** 350-356.

EMING, S. A., KRIEG, T. & DAVIDSON, J. M. 2007. Inflammation in Wound Repair: Molecular and Cellular Mechanisms. *Journal of Investigative Dermatology,* 127**,** 514-525.

FEBRIYENTI, F., MOHTAR, N., MOHAMED, N., HAMDAN, M. R., NAJIB, S., SALLEH, M., BIN, S. & BAIE, B. 2014. Comparison of Freeze Drying and Spray Drying Methods of Haruan Extract. *International Journal of Drug Delivery,* 6**,** 286-291.

FRONZA, M., HEINZMANN, B., HAMBURGER, M., LAUFER, S. & MERFORT, I. 2009. Determination of the wound healing effect of Calendula extracts using the scratch assay with 3T3 fibroblasts. *Journal of ethnopharmacology,* 126**,** 463-467.

FU, Y., YOUNG, J. F. & THERKILDSEN, M. 2017. Bioactive peptides in beef: Endogenous generation through postmortem aging. *Meat Science,* 123**,** 134-142.

GAGNÉ, F. 2014. Chapter 6 - Oxidative Stress. *In:* GAGNÉ, F. (ed.) *Biochemical Ecotoxicology.* Oxford: Academic Press.

GEA-BANACLOCHE, J. 2006. Immunomodulation. *In:* RUNGE, M. & PATTERSON, C. (eds.) *Principles of Molecular Medicine.* Humana Press.

GIRIJA, A. R. 2018. 6 - Peptide nutraceuticals. *In:* KOUTSOPOULOS, S. (ed.) *Peptide Applications in Biomedicine, Biotechnology and Bioengineering.* Woodhead Publishing.

GÓMEZ-GUILLÉN, M. C., GIMÉNEZ, B., LÓPEZ-CABALLERO, M. E. & MONTERO, M. P. 2011. Functional and bioactive properties of collagen and gelatin from alternative sources: A review. *Food Hydrocolloids,* 25**,** 1813-1827.

GONZALEZ, A. C. D. O., COSTA, T. F., ANDRADE, Z. D. A. & MEDRADO, A. R. A. P. 2016. Wound healing - A literature review. *Anais Brasileiros de Dermatologia,* 91**,** 614-620.

GUPTA, A. J., WIERENGA, P. A., GRUPPEN, H. & BOOTS, J.-W. 2015. Influence of protein and carbohydrate contents of soy protein hydrolysates on cell density and IgG production in animal cell cultures. 31**,** 1396-1405.

HIMAYA, S. W. A., NGO, D.-H., RYU, B. & KIM, S.-K. 2012. An active peptide purified from gastrointestinal enzyme hydrolysate of Pacific cod skin gelatin attenuates angiotensin-1 converting enzyme (ACE) activity and cellular oxidative stress. *Food Chemistry,* 132**,** 1872-1882.

HONG, F., MING, L., YI, S., ZHANXIA, L., YONGQUAN, W. & CHI, L. 2008. The antihypertensive effect of peptides: A novel alternative to drugs? *Peptides,* 29**,** 1062-1071.

HOWELL, N. K. & KASASE, C. 2010. Bioactive Peptides and Proteins from Fish Muscle and Collagen. *Bioactive Proteins and Peptides as Functional Foods and Nutraceuticals.*

HU, S., YIN, J., NIE, S., WANG, J., PHILLIPS, G. O., XIE, M. & CUI, S. W. 2016. In vitro evaluation of the antioxidant activities of carbohydrates. *Bioactive Carbohydrates and Dietary Fibre,* 7**,** 19-27.

HUANG, D., OU, B., HAMPSCH-WOODILL, M., FLANAGAN, J. A. & PRIOR, R. L. 2002. High-Throughput Assay of Oxygen Radical Absorbance Capacity (ORAC) Using a Multichannel Liquid Handling System Coupled with a Microplate Fluorescence Reader in 96-Well Format. *Journal of Agricultural and Food Chemistry,* 50**,** 4437-4444.

HUANG, D., OU, B. & PRIOR, R. L. 2005. The Chemistry behind Antioxidant Capacity Assays. *Journal of Agricultural and Food Chemistry,* 53**,** 1841-1856.

JANG, A. & LEE, M. 2005. Purification and identification of angiotensin converting enzyme inhibitory peptides from beef hydrolysates. *Meat Science,* 69**,** 653-661.

KIMMEL, J. R. A. S., E. L 1954. Crystalline Papain I. Preparatlon, Specificity, and Activation. *The Journal of Biological Chemistry,* 207**,** 515-531.

KUMAR, R., CHAUDHARY, K., SINGH CHAUHAN, J., NAGPAL, G., KUMAR, R., SHARMA, M. & RAGHAVA, G. P. S. 2015. An in silico platform for predicting, screening and designing of antihypertensive peptides. *Scientific Reports,* 5**,** 12512.

LAFARGA, T., O'CONNOR, P. & HAYES, M. 2014. Identification of novel dipeptidyl peptidase-IV and angiotensin-I-converting enzyme inhibitory peptides from meat proteins using in silico analysis. *Peptides,* 59**,** 53-62.

LASSOUED, I., MORA, L., BARKIA, A., ARISTOY, M. C., NASRI, M. & TOLDRÁ, F. 2015. Bioactive peptides identified in thornback ray skin's gelatin hydrolysates by proteases from Bacillus subtilis and Bacillus amyloliquefaciens. *Journal of Proteomics,* 128**,** 8-17.

LATA, S., SHARMA, B. & RAGHAVA, G. 2007. Analysis and prediction of antibacterial peptides. *BMC Bioinformatics,* 8**,** 263.

LAU, J. L. & DUNN, M. K. 2018. Therapeutic peptides: Historical perspectives, current development trends, and future directions. *Bioorganic & Medicinal Chemistry,* 26**,** 2700-2707.
LIANG, C.-C., PARK, A. Y. & GUAN, J.-L. 2007. In vitro scratch assay: a convenient and inexpensive method for analysis of cell migration in vitro. *Nature Protocols,* 2**,** 329.
LIPTON, A., KLINGER, I., PAUL, D. & HOLLEY, R. W. 1971. Migration of mouse 3T3 fibroblasts in response to a serum factor. *Proceedings of the National Academy of Sciences,* 68**,** 2799-2801.
LIU, R., ZHENG, W., LI, J., WANG, L., WU, H., WANG, X. & SHI, L. 2015. Rapid identification of bioactive peptides with antioxidant activity from the enzymatic hydrolysate of Mactra veneriformis by UHPLC–Q-TOF mass spectrometry. *Food Chemistry,* 167**,** 484-489.
LIU, R. H. & FINLEY, J. 2005. Potential Cell Culture Models for Antioxidant Research. *Journal of Agricultural and Food Chemistry,* 53**,** 4311-4314.
LIU, Y., PETERSON, D. A., KIMURA, H. & SCHUBERT, D. 1997. Mechanism of Cellular 3-(4,5-Dimethylthiazol-2-yl)-2,5-Diphenyltetrazolium Bromide (MTT) Reduction. *Journal of Neurochemistry,* 69**,** 581-593.
LOFFREDO, L., PERRI, L., NOCELLA, C. & VIOLI, F. 2017. Antioxidant and antiplatelet activity by polyphenol-rich nutrients: focus on extra virgin olive oil and cocoa. *British Journal of Clinical Pharmacology,* 83**,** 96-102.
LÓPEZ-ALARCÓN, C. & DENICOLA, A. 2013. Evaluating the antioxidant capacity of natural products: A review on chemical and cellular-based assays. *Analytica Chimica Acta,* 763**,** 1-10.
LOPEZ-CORCUERA, B., GEERLINGS, A. & ARAGON, C. 2001. Glycine neurotransmitter transporters: an update. *Mol Membr Biol,* 18**,** 13-20.
LU, H., GUO, X., LIU, Y. & GONG, X. 2015. Effect of Particle Size on Flow Mode and Flow Characteristics of Pulverized Coal. *KONA Powder and Particle Journal,* 32**,** 143-153.
LUKIN, J. A., KONTAXIS, G., SIMPLACEANU, V., YUAN, Y., BAX, A. & HO, C. 2003. Quaternary structure of hemoglobin in solution. 100**,** 517-520.
MARR, A. K., GOODERHAM, W. J. & HANCOCK, R. E. W. 2006. Antibacterial peptides for therapeutic use: obstacles and realistic outlook. *Current Opinion in Pharmacology,* 6**,** 468-472.
MENG, Q. C., BALCELLS, E., DELL'ITALIA, L., DURAND, J. & OPARIL, S. 1995. Sensitive method for quantitation of angiotensin-converting enzyme (ACE) activity in tissue. *Biochemical Pharmacology,* 50**,** 1445-1450.
MINKIEWICZ, P., DZIUBA, J., IWANIAK, A., DZIUBA, M. & AND DAREWICZ, M. 2008. BIOPEP database and other programs for processing bioactive peptide sequences. *Journal of AOAC International,,* 91**,** 965-980.
MINUZ, P., VELO, G., VIOLI, F. & FERRO, A. 2017. Are nutraceuticals the modern panacea? From myth to science. *British Journal of Clinical Pharmacology,* 83**,** 5-7.
MIZUNO, A., MATSUI, K. & SHUTO, S. 2017. From Peptides to Peptidomimetics: A Strategy Based on the Structural Features of Cyclopropane. *Chemistry – A European Journal,* 23**,** 14394-14409.
MÖHLE, K. & HOFMANN, H.-J. 1998. Secondary structure formation in N-substituted peptides*. *The Journal of Peptide Research,* 51**,** 19-28.
MOONEY, C., HASLAM, N., POLLASTRI, G. & SHIELDS, D. 2012. Towards the Improved Discovery and Design of Functional Peptides: Common Features of Diverse Classes Permit Generalized Prediction of Bioactivity. *PLoS ONE 7,* (10): e45012.
MORA, L., REIG, M. & TOLDRÁ, F. 2014. Bioactive peptides generated from meat industry by-products. *Food Research International,* 65, Part C**,** 344-349.
MUJUMDAR, A., HAQUE, M. & ADHIKARI, B. 2014. Drying and Denaturation of Proteins in Spray Drying Process. *Handbook of Industrial Drying, Fourth Edition.*
NARDO, A. E., AÑÓN, M. C. & PARISI, G. 2018. Large-scale mapping of bioactive peptides in structural and sequence space. *PLOS ONE,* 13**,** e0191063.

NAZEER, R. A., PRABHA, K. R. D., KUMAR, N. S. S. & GANESH, R. J. 2013. Isolation of antioxidant peptides from clam, Meretrix casta (Chemnitz). *Journal of Food Science and Technology,* 50**,** 777-783.

NIKI, E. 1990. [3] Free radical initiators as source of water- or lipid-soluble peroxyl radicals. *Methods in Enzymology.* Academic Press.

ONOJA, S. O., OMEH, Y. N., EZEJA, M. I. & CHUKWU, M. N. 2014. Evaluation of the In Vitro and In Vivo Antioxidant Potentials of Aframomum melegueta Methanolic Seed Extract. *Journal of Tropical Medicine,* 2014**,** 6.

OSAWA, T. & NAMIKI, M. 1985. Natural antioxidants isolated from Eucalyptus leaf waxes. *Journal of Agricultural and Food Chemistry,* 33**,** 777-780.

OSMAN, A. O., MAHGOUB, S. A. & SITOHY, M. Z. 2013. Preservative action of 11S (glycinin) and 7S (β-conglycinin) soy globulin on bovine raw milk stored either at 4 or 25 °C. *Journal of Dairy Research,* 80**,** 174-183.

OTVOS, L. 2008. Peptide-Based Drug Design: Here and Now. *In:* OTVOS, L. (ed.) *Peptide-Based Drug Design.* Totowa, NJ: Humana Press.

PETERKOFSKY, B. 1972. Regulation of collagen secretion by ascorbic acid in 3T3 and chick embryo fibroblasts. *Biochemical and biophysical research communications,* 49**,** 1343-1350.

PICOTTI, P., AEBERSOLD, R. & DOMON, B. 2007. The Implications of Proteolytic Background for Shotgun Proteomics. *Molecular & Cellular Proteomics,* 6**,** 1589-1598.

POWERS, J. P. S. & HANCOCK, R. E. W. 2003. The relationship between peptide structure and antibacterial activity. *Peptides,* 24**,** 1681-1691.

PRUEKSARITANONT, T. & TANG, C. 2012. ADME of Biologics—What Have We Learned from Small Molecules? *The AAPS Journal,* 14**,** 410-419.

RAJINIKANTH, P. J., BALASUBRAMANIAM, M. & THILEK KUMAR, Y. V. R. 2012. Spray Drying as an Approach for Enhancement of Dissolution and Bioavailability of Raloxifene Hydrochloride. *2012,* 4**,** 11.

RAWLINGS, N. D. & BARRETT, A. J. 1994. [32] Families of cysteine peptidases. *Methods in Enzymology.* Academic Press.

RICARD-BLUM, S. 2011. The Collagen Family. *Cold Spring Harbor Perspectives in Biology,* 3**,** a004978.

ROMANO, C. S., ABADI, K., REPETTO, V., VOJNOV, A. A. & MORENO, S. 2009. Synergistic antioxidant and antibacterial activity of rosemary plus butylated derivatives. *Food Chemistry,* 115**,** 456-461.

ROTH, S. 1974. Tissue Culture. Methods and Applications. Paul F. Kruse, Jr. , M. K. Patterson, Jr. *The Quarterly Review of Biology,* 49**,** 150-151.

RYABY, J. T., SHELLER, M. R., LEVINE, B. P., BRAMLET, D. G., LADD, A. L. & CARNEY, D. H. 2006. Thrombin Peptide TP508 Stimulates Cellular Events Leading to Angiogenesis, Revascularization, and Repair of Dermal and Musculoskeletal Tissues. *The Journal of Bone & Joint Surgery,* 88**,** 132-139.

SÁNCHEZ-RIVERA, L., MARTÍNEZ-MAQUEDA, D., CRUZ-HUERTA, E., MIRALLES, B. & RECIO, I. 2014. Peptidomics for discovery, bioavailability and monitoring of dairy bioactive peptides. *Food Research International,* 63**,** 170-181.

SÁNCHEZ, A. & VÁZQUEZ, A. 2017. Bioactive peptides: A review. *Food Quality and Safety,* 1**,** 29-46.

SAVJANI, K. T., GAJJAR, A. K. & SAVJANI, J. K. 2012. Drug Solubility: Importance and Enhancement Techniques. *ISRN Pharmaceutics,* 2012**,** 195727.

SCHARFFETTER, K. K., M. STOLZ, W. LANKAT-BUTTGEREIT, B. HATAMOCHI, A. SÖHNCHEN, R. AND KRIEG, T. 1989. Localization of collagen alpha 1(I) gene expression during wound healing by in situ hybridization. *J. Invest. Dermatol.,* 93**,** 405-412.

SCHINDELIN, J., ARGANDA-CARRERAS, I., FRISE, E., KAYNIG, V., LONGAIR, M., PIETZSCH, T., PREIBISCH, S., RUEDEN, C., SAALFELD, S., SCHMID, B., TINEVEZ, J.-Y., WHITE, D. J., HARTENSTEIN, V., ELICEIRI, K., TOMANCAK, P. & CARDONA, A. 2012. Fiji: an open-source platform for biological-image analysis. *Nature Methods,* 9**,** 676.

SCHREIER, T., DEGEN, E. & BASCHONG, W. 1993. *Fibroblast migration and proliferation during in vitro wound healing. A quantitative comparison between various growth factors and a low molecular weight blood dialysate used in the clinic to normalize impaired wound healing*.

SCHWENKE, K. D. 2001. Reflections about the functional potential of legume proteins A Review. *Food / Nahrung,* 45**,** 377-381.

SEGURA CAMPOS, M. R., PERALTA GONZÁLEZ, F., CHEL GUERRERO, L. & BETANCUR ANCONA, D. 2013. Angiotensin I-Converting Enzyme Inhibitory Peptides of Chia (Salvia hispanica) Produced by Enzymatic Hydrolysis. *International Journal of Food Science,* 2013**,** 158482.

SHEN, Q., ZHANG, B., XU, R., WANG, Y., DING, X. & LI, P. 2010. Antioxidant activity in vitro of the selenium-contained protein from the Se-enriched Bifidobacterium animalis 01. *Anaerobe,* 16**,** 380-386.

SINGH, S. K., VUDDANDA, P. R., SINGH, S. & SRIVASTAVA, A. K. 2013. A Comparison between Use of Spray and Freeze Drying Techniques for Preparation of Solid Self-Microemulsifying Formulation of Valsartan and In Vitro and In Vivo Evaluation. *BioMed Research International,* 2013**,** 13.

STIERNBERG, J., NORFLEET, A. M., REDIN, W. R., WARNER, W. S., FRITZ, R. R. & CARNEY, D. H. 2000. Acceleration of full-thickness wound healing in normal rats by the synthetic thrombin peptide, TP508. *Wound Repair and Regeneration,* 8**,** 204-215.

STORER, A. C. & MÉNARD, R. 2013. Chapter 419 - Papain. *In:* RAWLINGS, N. D. & SALVESEN, G. (eds.) *Handbook of Proteolytic Enzymes (Third Edition).* Academic Press.

SZABO, M. R., IDIŢOIU, C., CHAMBRE, D. & LUPEA, A. X. 2007. Improved DPPH determination for antioxidant activity spectrophotometric assay. *Chemical Papers,* 61**,** 214-216.

TACCONELLI, E., CARRARA, E., SAVOLDI, A., HARBARTH, S., MENDELSON, M., MONNET, D. L., PULCINI, C., KAHLMETER, G., KLUYTMANS, J., CARMELI, Y., OUELLETTE, M., OUTTERSON, K., PATEL, J., CAVALERI, M., COX, E. M., HOUCHENS, C. R., GRAYSON, M. L., HANSEN, P., SINGH, N., THEURETZBACHER, U., MAGRINI, N., ABODERIN, A. O., AL-ABRI, S. S., AWANG JALIL, N., BENZONANA, N., BHATTACHARYA, S., BRINK, A. J., BURKERT, F. R., CARS, O., CORNAGLIA, G., DYAR, O. J., FRIEDRICH, A. W., GALES, A. C., GANDRA, S., GISKE, C. G., GOFF, D. A., GOOSSENS, H., GOTTLIEB, T., GUZMAN BLANCO, M., HRYNIEWICZ, W., KATTULA, D., JINKS, T., KANJ, S. S., KERR, L., KIENY, M.-P., KIM, Y. S., KOZLOV, R. S., LABARCA, J., LAXMINARAYAN, R., LEDER, K., LEIBOVICI, L., LEVY-HARA, G., LITTMAN, J., MALHOTRA-KUMAR, S., MANCHANDA, V., MOJA, L., NDOYE, B., PAN, A., PATERSON, D. L., PAUL, M., QIU, H., RAMON-PARDO, P., RODRÍGUEZ-BAÑO, J., SANGUINETTI, M., SENGUPTA, S., SHARLAND, M., SI-MEHAND, M., SILVER, L. L., SONG, W., STEINBAKK, M., THOMSEN, J., THWAITES, G. E., VAN DER MEER, J. W. M., VAN KINH, N., VEGA, S., VILLEGAS, M. V., WECHSLER-FÖRDÖS, A., WERTHEIM, H. F. L., WESANGULA, E., WOODFORD, N., YILMAZ, F. O. & ZORZET, A. 2018. Discovery, research, and development of new antibiotics: the WHO priority list of antibiotic-resistant bacteria and tuberculosis. *The Lancet Infectious Diseases,* 18**,** 318-327.

THE UNIPROT CONSORTIUM 2017. UniProt: the universal protein knowledgebase. *Nucleic Acids Research,* 45**,** D158-D169.

THOMAS, S., KARNIK, S., BARAI, R. S., JAYARAMAN, V. K. & IDICULA-THOMAS, S. 2010. CAMP: a useful resource for research on antimicrobial peptides. *Nucleic Acids Research,* 38**,** D774-D780.

TOLDRÁ, F., ARISTOY, M. C., MORA, L. & REIG, M. 2012. Innovations in value-addition of edible meat by-products. *Meat Science,* 92**,** 290-296.

TRAVAN, A., SCOGNAMIGLIO, F., BORGOGNA, M., MARSICH, E., DONATI, I., TARUSHA, L., GRASSI, M. & PAOLETTI, S. 2016. Hyaluronan delivery by polymer demixing in polysaccharide-based hydrogels and membranes for biomedical applications. *Carbohydrate Polymers,* 150**,** 408-418.

TYAGI, A., KAPOOR, P., KUMAR, R., CHAUDHARY, K., GAUTAM, A. & RAGHAVA, G. P. S. 2013. In Silico Models for Designing and Discovering Novel Anticancer Peptides. *Scientific Reports,* 3**,** 2984.

UHLIG, T., KYPRIANOU, T., MARTINELLI, F. G., OPPICI, C. A., HEILIGERS, D., HILLS, D., CALVO, X. R. & VERHAERT, P. 2014. The emergence of peptides in the pharmaceutical business: From exploration to exploitation. *EuPA Open Proteomics,* 4**,** 58-69.

VERCRUYSSE, L., VAN CAMP, J. & SMAGGHE, G. 2005. ACE Inhibitory Peptides Derived from Enzymatic Hydrolysates of Animal Muscle Protein: A Review. *Journal of Agricultural and Food Chemistry,* 53**,** 8106-8115.

VERMEIRSSEN, V., CAMP, J. V. & VERSTRAETE, W. 2007. Bioavailability of angiotensin I converting enzyme inhibitory peptides. *British Journal of Nutrition,* 92**,** 357-366.

VULUPALA, H. R., SAJJA, Y., BAGUL, P. K., BANDLA, R., NAGARAPU, L. & BENERJEE, S. K. 2018. Potent ACE inhibitors from 5-hydroxy indanone derivatives. *Bioorganic Chemistry,* 77**,** 660-665.

WOLFE, K. L. & LIU, R. H. 2007. Cellular Antioxidant Activity (CAA) Assay for Assessing Antioxidants, Foods, and Dietary Supplements. *Journal of Agricultural and Food Chemistry,* 55**,** 8896-8907.

WU, J., ALUKO, R. E. & NAKAI, S. 2006. Structural Requirements of Angiotensin I-Converting Enzyme Inhibitory Peptides: Quantitative Structure–Activity Relationship Study of Di- and Tripeptides. *Journal of Agricultural and Food Chemistry,* 54**,** 732-738.

XUE, Z., GAO, J., ZHANG, Z., YU, W., WANG, H. & KOU, X. 2012. Antihyperlipidemic and Antitumor Effects of Chickpea Albumin Hydrolysate. *Plant Foods for Human Nutrition,* 67**,** 393-400.

XUE, Z., WEN, H., ZHAI, L., YU, Y., LI, Y., YU, W., CHENG, A., WANG, C. & KOU, X. 2015. Antioxidant activity and anti-proliferative effect of a bioactive peptide from chickpea (Cicer arietinum L.). *Food Research International,* 77, Part 2**,** 75-81.

YANG, N. J. & HINNER, M. J. 2015. Getting Across the Cell Membrane: An Overview for Small Molecules, Peptides, and Proteins. *Methods in molecular biology (Clifton, N.J.),* 1266**,** 29-53.

ZATUL, I. M. A., AZURA, A., FARIDAH, Y., IRWANDI, J., KAUSAR, A. & SHOW, P. L. 2014. Bromelain: an overview of industrial application and purification strategies. *Appl Microbiol Biotechnol* 98**,** 7283–7297.

ZOU, T.-B., HE, T.-P., LI, H.-B., TANG, H.-W. & XIA, E.-Q. 2016. The Structure-Activity Relationship of the Antioxidant Peptides from Natural Proteins. 21**,** 72.

VII) Appendices

Appendix I: Amino Acid Composition of the Biofac Hydrolysates

Heart 150615-1900 (H1)		
Amino Acids	g	%
Serine	3.3	4.6
Glutamic Acid	10.7	14.8
Proline	4.1	5.7
Glycine	5.7	7.9
Alanine	5.3	7.3
Valine	4.3	5.9
Isoleucine	3.1	4.3
Leucine	6.5	9.0
Tyrosine	2.3	3.2
Phenylalanine	3.2	4.4
Threonine	3.3	4.6
Arginine	4.2	5.8
Lysine	6.1	8.4
Hydroxyproline	1.1	1.5
Histidine	1.5	2.1
Aspartic Acid	7.0	9.6
Ornitine	0.6	0.9
Total	72.1	100

Placenta 0-150625-1700 (P1)			Placenta 0-160330-1500 (P2)		
Amino Acids	g	%	Amino Acids	g	%
Serine	2.8	3.7	Serine	2.8	3.7
Glutamic Acid	9.18	12.0	Glutamic Acid	9.18	12.0
Proline	8.44	11.0	Proline	8.44	11.0
Glycine	15.4	20.1	Glycine	15.4	20.1
Alanine	7.17	9.4	Alanine	7.17	9.4
Valine	2.59	3.4	Valine	2.59	3.4
Isoleucine	1.42	1.9	Isoleucine	1.42	1.9
Leucine	3.5	4.6	Leucine	3.5	4.6
Tyrosine	0.887	1.2	Tyrosine	0.887	1.2
Phenylalanine	2.01	2.6	Phenylalanine	2.01	2.6
Threonine	1.92	2.5	Threonine	1.92	2.5
Arginine	5.77	7.5	Arginine	5.77	7.5
Lysine	3.43	4.5	Lysine	3.43	4.5
Hydroxyproline	5.93	7.7	Hydroxyproline	5.93	7.7
Histidine	0.906	1.2	Histidine	0.906	1.2
Aspartic acid	5.26	6.9	Aspartic acid	5.26	6.9
Ornitine	0.05	0.1	Ornitine	0.05	0.1
Total	76.663	100	Total	76.663	100.0

Liver 150615-1900 (L1)			Liver 160126-0700 (L2)			Liver 170127-0815/33155 (L3)		
Amino Acids	g	%	Amino Acids	g	%	Amino Acids	g	%
Serine	3.1	5.1	Serine	3.43	5.3	Cystein+Cystein	0.662	1.1
Glutamic Acid	8.61	14.1	Glutamic Acid	9.16	14.2	Methionin	1.46	2.5
Proline	3.52	5.8	Proline	3.54	5.5	Lysine	4.05	6.8
Glycine	4.05	6.6	Glycine	4.35	6.7	Threonine	3.15	5.3
Alanine	4.19	6.9	Alanine	4.54	7.0	Isoleucine	3.02	5.1
Valine	4.29	7.0	Valine	4.85	7.5	Leucine	5.25	8.8
Isoleucine	3.21	5.3	Isoleucine	3.49	5.4	Histidine	1.58	2.7
Leucine	6.04	9.9	Leucine	6.58	10.2	Phenylalanine	3.35	5.6
Tyrosine	0.812	1.3	Tyrosine	0.886	1.4	Tyrosine	0.825	1.4
Phenylalanine	3.12	5.1	Phenylalanine	3.58	5.6	Valine	4.48	7.5
Threonine	3.1	5.1	Threonine	3.45	5.4	Alanine	4.39	7.4
Arginine	1.38	2.3	Arginine	1.17	1.8	Arginine	0.808	1.4
Lysine	5.12	8.4	Lysine	5.11	7.9	Aspartic Acid	5.15	8.7
Hydroxyproline	0.326	0.5	Hydroxyproline	0.05	0.1	Glutamic Acid	7.42	12.5
Histidine	1.68	2.8	Histidine	1.75	2.7	Glycine	3.97	6.7
Aspartic Acid	6.3	10.3	Aspartic Acid	6.23	9.7	Hydroxyproline	0.193	0.3
Ornitine	2.11	3.5	Ornitine	2.31	3.6	Ornitine	2.16	3.6
Total	60.958	100	Tryptophane	1.06	1.6	Proline	3.19	5.4
			Cystein+Cystein	0.869	1.3	Serine	3.14	5.3
			Methionin	1.61	2.5	Tryptophane	1.19	2.0
			Total	64.476	100	Total:	59.438	100.0

Appendix IIa: In Silico Papain Digest of Cytosol Aminopepsidase Data

Sequence	Score
FWG	1
WA	0.96
FA	0.96
MG	0.94
G	0.89
G	0.89
G	0.89
G	0.89
G	0.89
G	0.89
G	0.89
G	0.89
G	0.89
G	0.89
G	0.89
G	0.89
G	0.89
G	0.89
G	0.89
G	0.89
G	0.89
G	0.89
G	0.89
G	0.89
G	0.89
PG	0.88
PG	0.88
CR	0.87
FLLR	0.86
WQR	0.84
FLK	0.81
NWH	0.78
SDPPLVFVG	0.75
MPLFE	0.75
VWR	0.73
LCY	0.73
LG	0.72
LG	0.72
MFLLPLPA	0.71

Sequence	Score
DMG	0.71
TFY	0.7
MA	0.69
NMDLMR	0.66
PPLK	0.62
PPVFLE	0.6
VDPCG	0.58
LR	0.57
LR	0.57
VFTNSSWLWNK	0.55
R	0.55
R	0.55
R	0.55
R	0.55
R	0.55
R	0.55
LY	0.52
NMPSG	0.51
LFE	0.51
VLFA	0.48
Y	0.44
Y	0.44
Y	0.44
Y	0.44
TFNPK	0.42
SWIE	0.42
PLCE	0.42
SG	0.41
SG	0.41
SG	0.41
LDLPINLVG	0.41
NG	0.39
NFDK	0.39
SPDA	0.36
MDIA	0.34
LH	0.34
LH	0.34
VPY	0.33
PK	0.33

Sequence	Score
PK	0.33
IR	0.33
PDA	0.32
IY	0.32
SFLSVA	0.31
PTR	0.31
PQFTSA	0.31
LA	0.31
MTPTR	0.3
DR	0.29
FSQDSA	0.28
LILA	0.27
FVTH	0.25
VLG	0.24
ITFDSG	0.24
CTA	0.24
TPA	0.23
QIVDCQLA	0.23
LVLG	0.23
LME	0.23
H	0.23
H	0.23
H	0.23
H	0.23
NIR	0.22
DFSSVVVVG	0.22
IH	0.21
A	0.21
A	0.21
A	0.21
A	0.21
A	0.21
A	0.21
A	0.21
A	0.21
A	0.21
A	0.21
A	0.21
A	0.21

Sequence	Score
A	0.21
A	0.21
A	0.21
A	0.21
A	0.21
A	0.21
A	0.21
A	0.21
A	0.21
A	0.21
A	0.21
A	0.21
A	0.21
A	0.21
A	0.21
A	0.21
TG	0.19
TG	0.19
QNLA	0.19
LDIA	0.19
LK	0.17
ILNISG	0.17
NMTK	0.15
SA	0.14
SA	0.14
SA	0.14
QLSVR	0.14
QIQDLE	0.14
NLK	0.14
LVSG	0.14
TR	0.13
ISIK	0.13
DVNNIG	0.13
DDA	0.13
DA	0.13
DA	0.13
QA	0.12
VR	0.11
TLTG	0.11
IPSVE	0.1
VIINA	0.09
SSK	0.09
VMTNK	0.08
TICSTIVSA	0.08

Sequence	Score
SIE	0.08
SK	0.07
DVVR	0.07
VA	0.06
VA	0.06
QK	0.06
NK	0.06
K	0.06
K	0.06
K	0.06
K	0.06
K	0.06
K	0.06
K	0.06
K	0.06
K	0.06
K	0.06
K	0.06
K	0.06
K	0.06
K	0.06
K	0.06
K	0.06
K	0.06
K	0.06
K	0.06
K	0.06
TLIE	0.05
TDVH	0.05
DQE	0.05
VVVSA	0.04
VIE	0.04
VDDQE	0.04
TIQVDNTDA	0.04
SE	0.04
QE	0.04
DE	0.04
DE	0.04
TK	0.03
NE	0.03
E	0.02
E	0.02
E	0.02
E	0.02

Sequence	Score
E	0.02
E	0.02
E	0.02
E	0.02
E	0.02
E	0.02
E	0.02
E	0.02
E	0.02
E	0.02

Appendix IIb: In Silico Bromelain Digest of Cytosol Aminopepsidase Data

Sequence	Score
WA	0.96
G	0.89
G	0.89
G	0.89
G	0.89
G	0.89
G	0.89
G	0.89
G	0.89
G	0.89
G	0.89
G	0.89
G	0.89
G	0.89
G	0.89
G	0.89
G	0.89
G	0.89
PG	0.88
PG	0.88
WQRG	0.85
FLK	0.81
SDPPLVFVG	0.75
LCY	0.73
LG	0.72
LG	0.72
MFLLPLPA	0.71
DMG	0.71
MA	0.69
PPLK	0.62
VFTNSSWLWNK	0.55
VRQLSVRRFWG	0.52
LY	0.52
NMDLMRA	0.51
VLFA	0.48
PLCENMPSG	0.47
SEEPPVFLEIHY	0.46
Y	0.44
LHG	0.43
SG	0.41
SG	0.41

Sequence	Score
SG	0.41
LDLPINLVG	0.41
NG	0.39
HTFNPK	0.38
DRVWRMPLFEHY	0.37
TRTFY	0.36
SPDA	0.36
LFEA	0.36
MDIA	0.34
SWIEEQEMG	0.33
NEMTPTRFA	0.33
PDA	0.32
IY	0.32
SFLSVA	0.31
PQFTSA	0.31
LA	0.31
RLILA	0.29
CRQIQDLEIPSVEVDPCG	0.28
VDDQENWHEG	0.27
LRK	0.26
VLG	0.24
ITFDSG	0.24
CTA	0.24
QIVDCQLA	0.23
LVLG	0.23
LHEDFSSVVVVG	0.22
A	0.21
A	0.21
A	0.21
A	0.21
A	0.21
A	0.21
A	0.21
A	0.21
A	0.21
A	0.21
A	0.21
A	0.21
A	0.21

Sequence	Score
A	0.21
A	0.21
A	0.21
A	0.21
A	0.21
A	0.21
A	0.21
A	0.21
A	0.21
A	0.21
RPTRTLIEFLLRFSQDSA	0.2
ENFDK	0.2
TG	0.19
QNLA	0.19
EFVTHPK	0.19
TDVHIRPK	0.18
HLDIA	0.18
RSA	0.16
NMTK	0.15
LREILNISG	0.15
DEVPY	0.15
SA	0.14
SA	0.14
RHLMETPA	0.14
NLK	0.14
LVSG	0.14
ISIK	0.13
DVNNIG	0.13
DA	0.13
DA	0.13
QA	0.12
TLTG	0.11
SIETG	0.11
ENIRA	0.1
EG	0.1
EG	0.1
VIINA	0.09
SSK	0.09
RVA	0.09
VMTNK	0.08

Sequence	Score
TICSTIVSA	0.08
DVVRA	0.08
SK	0.07
EY	0.07
DQEA	0.07
VA	0.06
QK	0.06
NK	0.06
K	0.06
K	0.06
K	0.06
K	0.06
K	0.06
K	0.06
K	0.06
K	0.06
K	0.06
K	0.06
K	0.06
K	0.06
K	0.06
K	0.06
K	0.06
K	0.06
K	0.06
EDDA	0.06
DELK	0.06
VVVSA	0.04
TIQVDNTDA	0.04
TK	0.03
EVIEK	0.03
EK	0.02

Appendix IIc: In Silico pepsin (pH 1.3) Digest of Cytosol Aminopepsidase Data

Sequence	Score
MF	1
F	1
F	1
F	1
RF	0.99
WGPGPDAANMTKGL	0.89
MRADMGGAATICSTIVSAAKL	0.83
VF	0.82
PL	0.81
GL	0.81
CYAHTF	0.73
YGL	0.72
APL	0.7
WNKL	0.69
SVRRF	0.68
NISGPPL	0.64
L	0.64
L	0.64
L	0.64
L	0.64
L	0.64
L	0.64
L	0.64
HGSGDQEAWQRGVL	0.63
GKKGAGVDDQENWHEGKENIRAAVA AGCRQIQDL	0.63
ADVNNIGKYRSAGACTAAAF	0.61
GSGATGVF	0.56
EASIETGDRVWRMPL	0.53
PINL	0.49
IEF	0.44
VTHPKWAHL	0.43
TNSSWL	0.43
DSGGISIKASANMDL	0.43
ARHL	0.42
IL	0.39
ASGQNL	0.38
RKGMAGRPTRTL	0.36
VGKGITF	0.34
HEDF	0.34

Sequence	Score
DL	0.33
ADAL	0.32
NPKVIINAATL	0.31
METPANEMTPTRF	0.31
KAGKTRTF	0.3
VGL	0.28
TGAMDIAL	0.28
PAAARVAVRQL	0.28
KEF	0.28
SVAKGSEEPPVF	0.26
EIHYKGSPDASDPPL	0.26
TSAGENF	0.24
SSVVVVGL	0.23
VSGKL	0.22
EIPSVEVDPCGDAQAAAEGAVL	0.2
YEYDEL	0.17
DKL	0.17
KQKKKVVVSAKL	0.16
GIYSKEKEDDAPQF	0.16
DIAGVMTNKDEVPYL	0.14
CENMPSGKANKPGDVVRAKNGKTIQ VDNTDAEGRL	0.14
VL	0.13
REIL	0.13
SQDSA	0.12
EHYTKQIVDCQL	0.1
AEVIEKNL	0.1
KSASSKTDVHIRPKSWIEEQEMGSF	0.03

Appendix IId: In Silico Trypsin Digest of Cytosol Aminopepsidase Data

Sequence	Score
FWGPGPDAANMTK	0.86
SAGACTAAAFLK	0.74
LDLPINLVGLAPLCENMPSGK	0.74
VWR	0.73
ASANMDLMR	0.72
GMAGR	0.61
LR	0.57
R	0.55
MFLLPLPAAAR	0.54
GSPDASDPPLVFVGK	0.54
YR	0.53
GSEEPPVFLEIHYK	0.51
AAVAAGCR	0.48
GVLFASGQNLAR	0.47
SWIEEQEMGSFLSVAK	0.41
QIVDCQLADVNNIGK	0.41
LILADALCYAHTFNPK	0.4
DEVPYLR	0.4
VIINAATLTGAMDIALGSGATGVFTNSSWLWNK	0.39
WAHLDIAGVMTNK	0.38
TLIEFLLR	0.38
MPLFEHYTK	0.35
PK	0.33
LHGSGDQEAWQR	0.33
GITFDSGGISIK	0.33
PTR	0.31
GAGVDDQENWHEGK	0.3
FSQDSA	0.28
EILNISGPPLK	0.28
TFYGLHEDFSSVVVVGLGK	0.27
EDDAPQFTSAGENFDK	0.26
AGK	0.24
ADMGGAATICSTIVSAAK	0.23
QIQDLEIPSVEVDPCGDAQAAAEGAVLGLYEYDELK	0.22
PGDVVR	0.22
NGK	0.19
EFVTHPK	0.19
LFEASIETGDR	0.18

Sequence	Score
GLVLGIYSK	0.17
QLSVR	0.14
NLK	0.14
HLMETPANEMTPTR	0.14
TR	0.13
FAEVIEK	0.13
TDVHIR	0.12
SASSK	0.11
LVSGK	0.11
ANK	0.1
AK	0.1
ENIR	0.08
VAVR	0.07
TIQVDNTDAEGR	0.07
QK	0.06
K	0.06
K	0.06
K	0.06
K	0.06
VVVSAK	0.04
EK	0.02

Appendix IIe: In Silico Papain Digest of Haemoglobin Sub-unit Alpha Data

Sequence	Score
WG	0.99
MFLG	0.96
FPH	0.94
G	0.89
G	0.89
G	0.89
G	0.89
G	0.89
FLA	0.89
LR	0.57
R	0.55
R	0.55
PDDFNPSVH	0.5
Y	0.44
LDDLPG	0.44
FNLSH	0.42
VDPVNFK	0.41
FPTTK	0.34
LSDLH	0.27
H	0.23
H	0.23
H	0.23
H	0.23
H	0.23
H	0.23
CLLVTLA	0.22
A	0.21
A	0.21
A	0.21
A	0.21
A	0.21
A	0.21
A	0.21
A	0.21
A	0.21
A	0.21
A	0.21
A	0.21
A	0.21
A	0.21
LLSH	0.2

Sequence	Score
VG	0.17
VG	0.17
LSA	0.17
MVLSA	0.16
SLDK	0.14
DA	0.13
QA	0.12
TY	0.11
SDQVK	0.11
LTK	0.07
VA	0.06
QK	0.06
NVSTVLTSK	0.06
LE	0.06
K	0.06
K	0.06
DK	0.06
NVK	0.04
E	0.02

Appendix IIf: In Silico Bromelain Digest of Haemoglobin Sub-unit Alpha Data

Sequence	Score
WG	0.99
G	0.89
G	0.89
FLA	0.89
FPHFNLSHG	0.76
LERMFLG	0.66
R	0.55
HLDDLPG	0.5
HG	0.49
HG	0.49
Y	0.44
LLSHCLLVTLA	0.37
LRVDPVNFK	0.36
HHPDDFNPSVHA	0.35
FPTTK	0.34
A	0.21
A	0.21
A	0.21
A	0.21
A	0.21
A	0.21
A	0.21
A	0.21
A	0.21
A	0.21
LSDLHA	0.2
VG	0.17
VG	0.17
LSA	0.17
MVLSA	0.16
SLDK	0.14
DA	0.13
QA	0.12
TY	0.11
SDQVK	0.11
HK	0.1
LTK	0.07
VA	0.06
QK	0.06
NVSTVLTSK	0.06
K	0.06
DK	0.06
NVK	0.04
EA	0.04

Appendix IIg: In Silico Pepsin (pH 1.3) Digest of Haemoglobin Sub-unit Alpha Data

Sequence	Score
GF	0.99
PHF	0.94
ERMF	0.78
PGAL	0.71
DKF	0.66
L	0.64
L	0.64
L	0.64
AAHHPDDF	0.64
LSHCL	0.62
MVL	0.41
RVDPVNF	0.39
SAADKANVKAAWGKVGGQAGAHGAEAL	0.32
SAL	0.3
NPSVHASL	0.29
NL	0.29
SHGSDQVKAHGQKVADAL	0.28
SDL	0.27
PTTKTYF	0.27
HAHKL	0.26
DDL	0.26
KL	0.23
TSKYR	0.14
ANVSTVL	0.14
TKAVGHL	0.11
VTL	0.06

Appendix IIh: In Silico Trypsin Digest of Haemoglobin Sub-unit Alpha Data

Sequence	Score
AAWGK	0.66
LR	0.57
MFLGFPTTK	0.54
YR	0.53
VDPVNFK	0.41
AVGHLDDLPGALSALSDLHAHK	0.36
VGGQAGAHGAEALER	0.31
LLSHCLLVTLAAHHPDDFNPSVHASLDK	0.29
TYFPHFNLSHGSDQVK	0.24
AHGQK	0.19
FLANVSTVLTSK	0.15
VADALTK	0.14
MVLSAADK	0.1
ANVK	0.07

Appendix IIi: In Silico Papain Digest of Type VI collagen alpha-1 chain Data

Sequence	Score
FY	0.98
FA	0.96
MG	0.94
G	0.89
FFNDA	0.77
LG	0.72
FSSPA	0.65
LL	0.62
R	0.55
R	0.55
R	0.55
R	0.55
R	0.55
R	0.55
FLTA	0.51
Y	0.44
SG	0.41
LQFLQNY	0.33
LA	0.31
SSG	0.25
H	0.23
DITILLDG	0.23
NFDTTK	0.21
A	0.21
A	0.21
A	0.21
A	0.21
A	0.21
TDPA	0.2
TG	0.19
SH	0.16
SVG	0.15
SA	0.14
VLQY	0.12
QQQPE	0.12
DVR	0.12
VA	0.06
TVLA	0.06
STVDA	0.06
K	0.06

Sequence	Score
K	0.06
K	0.06
K	0.06
VTR	0.05
TDVTDA	0.04
E	0.02
E	0.02

Appendix IIj: In Silico Bromelain Digest of Type VI collagen alpha-1 chain Data

Sequence	Score
MG	0.94
G	0.89
RFA	0.87
FFNDA	0.77
LG	0.72
FSSPA	0.65
LL	0.62
Y	0.44
VTRFY	0.41
SG	0.41
SHNFDTTK	0.35
RLA	0.35
LQFLQNY	0.33
SSG	0.25
DITILLDG	0.23
ERFLTA	0.22
A	0.21
A	0.21
A	0.21
TG	0.19
QQQPERA	0.18
SVG	0.15
RTDPA	0.15
SA	0.14
VLQY	0.12
HDVRVA	0.09
REA	0.07
TVLA	0.06
STVDA	0.06
K	0.06
K	0.06
K	0.06
K	0.06
TDVTDA	0.04

Appendix IIk: In Silico Pepsin (pH 1.3) Digest of Type VI collagen alpha-1 chain Data

Sequence	Score
F	1
F	1
QF	0.95
L	0.64
L	0.64
L	0.64
L	0.64
GYVTRF	0.64
ASTVDAMGF	0.6
AERF	0.57
SSPADITIL	0.53
DGSASVGSHNF	0.41
AKRL	0.33
QNYTVL	0.27
DTTKRF	0.27
YREASSGAAKKKL	0.25
TAGRTDPAHDVRVAVL	0.15
QYSGTGQQQPERAAL	0.14
NDATDVTDAL	0.11

Appendix III: In Silico Trypsin Digest of Type VI collagen alpha-1 chain Data

Sequence	Score
FYR	0.94
LL	0.62
FAK	0.62
R	0.55
R	0.55
FLTAGR	0.54
FSSPADITILLDGSASVGSHNFDTTK	0.28
TDPAHDVR	0.2
EASSGAAK	0.16
LAER	0.1
VAVLQYSGTGQQQPER	0.08
K	0.06
K	0.06
AALQFLQNYTVLASTVDAMGFFNDATDVTDALGYVTR	0.02